

Adenylyl cyclase isoforms as potential drug targets

Edited by

Tarsis Brust, Rennolds S. Ostrom and Val J. Watts

Published in

Frontiers in Pharmacology



FRONTIERS EBOOK COPYRIGHT STATEMENT

The copyright in the text of individual articles in this ebook is the property of their respective authors or their respective institutions or funders. The copyright in graphics and images within each article may be subject to copyright of other parties. In both cases this is subject to a license granted to Frontiers.

The compilation of articles constituting this ebook is the property of Frontiers.

Each article within this ebook, and the ebook itself, are published under the most recent version of the Creative Commons CC-BY licence. The version current at the date of publication of this ebook is CC-BY 4.0. If the CC-BY licence is updated, the licence granted by Frontiers is automatically updated to the new version.

When exercising any right under the CC-BY licence, Frontiers must be attributed as the original publisher of the article or ebook, as applicable.

Authors have the responsibility of ensuring that any graphics or other materials which are the property of others may be included in the CC-BY licence, but this should be checked before relying on the CC-BY licence to reproduce those materials. Any copyright notices relating to those materials must be complied with.

Copyright and source acknowledgement notices may not be removed and must be displayed in any copy, derivative work or partial copy which includes the elements in question.

All copyright, and all rights therein, are protected by national and international copyright laws. The above represents a summary only. For further information please read Frontiers' Conditions for Website Use and Copyright Statement, and the applicable CC-BY licence.

ISSN 1664-8714
ISBN 978-2-83251-128-2
DOI 10.3389/978-2-83251-128-2

About Frontiers

Frontiers is more than just an open access publisher of scholarly articles: it is a pioneering approach to the world of academia, radically improving the way scholarly research is managed. The grand vision of Frontiers is a world where all people have an equal opportunity to seek, share and generate knowledge. Frontiers provides immediate and permanent online open access to all its publications, but this alone is not enough to realize our grand goals.

Frontiers journal series

The Frontiers journal series is a multi-tier and interdisciplinary set of open-access, online journals, promising a paradigm shift from the current review, selection and dissemination processes in academic publishing. All Frontiers journals are driven by researchers for researchers; therefore, they constitute a service to the scholarly community. At the same time, the *Frontiers journal series* operates on a revolutionary invention, the tiered publishing system, initially addressing specific communities of scholars, and gradually climbing up to broader public understanding, thus serving the interests of the lay society, too.

Dedication to quality

Each Frontiers article is a landmark of the highest quality, thanks to genuinely collaborative interactions between authors and review editors, who include some of the world's best academicians. Research must be certified by peers before entering a stream of knowledge that may eventually reach the public - and shape society; therefore, Frontiers only applies the most rigorous and unbiased reviews. Frontiers revolutionizes research publishing by freely delivering the most outstanding research, evaluated with no bias from both the academic and social point of view. By applying the most advanced information technologies, Frontiers is catapulting scholarly publishing into a new generation.

What are Frontiers Research Topics?

Frontiers Research Topics are very popular trademarks of the *Frontiers journals series*: they are collections of at least ten articles, all centered on a particular subject. With their unique mix of varied contributions from Original Research to Review Articles, Frontiers Research Topics unify the most influential researchers, the latest key findings and historical advances in a hot research area.

Find out more on how to host your own Frontiers Research Topic or contribute to one as an author by contacting the Frontiers editorial office: frontiersin.org/about/contact

Adenylyl cyclase isoforms as potential drug targets

Topic editors

Tarsis Brust — aTyr Pharma, United States

Rennolds S. Ostrom — Chapman University, United States

Val J. Watts — Purdue University, United States

Citation

Brust, T., Ostrom, R. S., Watts, V. J., eds. (2023). *Adenylyl cyclase isoforms as potential drug targets*. Lausanne: Frontiers Media SA.
doi: 10.3389/978-2-83251-128-2

Table of contents

- 04 **Editorial: Adenylyl cyclase isoforms as potential drug targets**
Tarsis F. Brust, Rennolds S. Ostrom and Val J. Watts
- 06 **A Selective Adenylyl Cyclase 1 Inhibitor Relieves Pain Without Causing Tolerance**
Gianna Giacoletti, Tatum Price, Lucas V. B. Hoelz, Abdulwhab Shremo Msdi, Samantha Cossin, Katerina Vazquez-Falto, Tácio V. Amorim Fernandes, Vinícius Santos de Pontes, Hongbing Wang, Nubia Boechat, Adwoa Nornoo and Tarsis F. Brust
- 18 **Strategies to safely target widely expressed soluble adenylyl cyclase for contraception**
Jacob Ferreira, Lonny R. Levin and Jochen Buck
- 26 **Inhibition of adenylyl cyclase 1 by ST034307 inhibits IP₃-evoked changes in sino-atrial node beat rate**
Samuel J. Bose, Matthew J. Read, Emily Akerman, Rebecca A. Capel, Thamali Ayagama, Angela Russell, Derek A. Terrar, Manuela Zaccolo and Rebecca A. B. Burton
- 42 **Reduced activity of adenylyl cyclase 1 attenuates morphine induced hyperalgesia and inflammatory pain in mice**
Kayla Johnson, Alexis Doucette, Alexis Edwards, Aleeya Verdi, Ryan McFarland, Shelby Hulke, Amanda Fowler, Val J. Watts and Amanda H. Klein
- 56 **Protein-protein interaction-based high throughput screening for adenylyl cyclase 1 inhibitors: Design, implementation, and discovery of a novel chemotype**
Tiffany S. Dwyer, Joseph B. O'Brien, Christopher P. Ptak, Justin E. LaVigne, Daniel P. Flaherty, Val J. Watts and David L. Roman
- 81 **Ca²⁺-stimulated adenylyl cyclases as therapeutic targets for psychiatric and neurodevelopmental disorders**
Jiao Chen, Qi Ding, Lulu An and Hongbing Wang
- 94 **The evolutionary conservation of eukaryotic membrane-bound adenylyl cyclase isoforms**
Joachim E. Schultz
- 106 **The role of the type 7 adenylyl cyclase isoform in alcohol use disorder and depression**
Boris Tabakoff and Paula L. Hoffman
- 127 **Gα_s, adenylyl cyclase, and their relationship to the diagnosis and treatment of depression**
Jeffrey M. Schappi and Mark M. Rasenick



OPEN ACCESS

EDITED AND REVIEWED BY

Filippo Drago,
University of Catania, Italy

*CORRESPONDENCE

Tarsis F. Brust,
✉ tbrust@atyrpharma.com

SPECIALTY SECTION

This article was submitted to
Experimental Pharmacology and Drug
Discovery,
a section of the journal
Frontiers in Pharmacology

RECEIVED 14 November 2022

ACCEPTED 29 November 2022

PUBLISHED 09 December 2022

CITATION

Brust TF, Ostrom RS and Watts VJ
(2022), Editorial: Adenylyl cyclase
isoforms as potential drug targets.
Front. Pharmacol. 13:1098240.
doi: 10.3389/fphar.2022.1098240

COPYRIGHT

© 2022 Brust, Ostrom and Watts. This is
an open-access article distributed
under the terms of the [Creative
Commons Attribution License \(CC BY\)](#).
The use, distribution or reproduction in
other forums is permitted, provided the
original author(s) and the copyright
owner(s) are credited and that the
original publication in this journal is
cited, in accordance with accepted
academic practice. No use, distribution
or reproduction is permitted which does
not comply with these terms.

Editorial: Adenylyl cyclase isoforms as potential drug targets

Tarsis F. Brust^{1,2*}, Rennolds S. Ostrom³ and Val J. Watts⁴¹Department of Pharmaceutical Sciences, Lloyd L. Gregory School of Pharmacy, Palm Beach Atlantic University, West Palm Beach, FL, United States, ²ATyr Pharma, San Diego, CA, United States,³Department of Biomedical and Pharmaceutical Sciences, Chapman University School of Pharmacy, Irvine, CA, United States, ⁴Department of Medicinal Chemistry and Molecular Pharmacology, Purdue University, West Lafayette, IN, United States

KEYWORDS

adenylyl cyclase, cAMP, adenylate cyclase, G protein, cell signaling

Editorial on the Research Topic

Adenylyl cyclase isoforms as potential drug targets

Adenylyl cyclases (ACs) are important signaling enzymes that catalyze the conversion of adenosine triphosphate (ATP) into the second messenger, cyclic adenosine monophosphate (cAMP). cAMP has numerous cellular functions that translate to physiological outcomes. The ACs are diverse with 10 isoforms that are modulated through numerous different mechanisms (Ostrom et al., 2022). For instance, activation of G protein-coupled receptors (GPCRs), which are targeted by nearly one-third of all FDA-approved drugs, modulates the activity ACs directly through G protein subunits as well as through second messenger signaling pathways (Ostrom et al., 2022; Santos et al., 2017). Thus, it is surprising that although numerous drugs indirectly modulate AC activity, there are no drugs in the market that were designed to directly modulate AC isoforms. The goal of this Research Topic is to highlight and compile recent efforts implicating the development of therapeutic strategies that target AC isoforms.

The Research Topic has nine different articles. A common topic on all four original research articles is adenylyl cyclase 1 (AC1). Two of those articles highlight the role of AC1 in pain and nociception. Giacoletti et al. show that the selective AC1 inhibitor ST034307 (Brust et al., 2017) is efficacious in several different mouse pain models. Johnson et al. also use ST034307 and AC1 knockdown to show that both strategies for reducing AC1 activity lead to analgesic effects and a reduction of morphine-induced hyperalgesia in mice. These articles also show that inhibition/knockdown of AC1 does not cause analgesic tolerance or major disruptions of normal mouse behaviors. The article by Dwyer et al. focuses on novel strategies for the discovery of AC1 inhibitors. The authors report new small molecule scaffolds for AC1 inhibitors and also provide SAR information for tuning AC1/AC8 selectivity and inhibitory potency. The fourth original research article, by Bose et al., focuses on the role of AC1 in the sino-atrial node to regulate heart rate. The authors also use ST034307 and show that AC1 inhibition reduces the positive chronotropic effects of phenylephrine in tissue preparations from guinea pigs. These

articles highlight the therapeutic potential of small molecules that selectively target AC1, but also caution that possible adverse reactions should be thoroughly studied.

The reviews and perspectives published in the Research Topic cover diverse topics related to AC structure and function. A systematic review by [Shultz](#) provides a deep analysis of how membrane-bound ACs evolved to their present structural arrangement. The article compares the different isoforms and provides detailed discussion on each AC domain. The perspective article by [Ferreira et al.](#) details the structure and functions of the soluble AC. The article also informs on how that isoform can be targeted for contraception, including possible dosing regimens and routes of administration. Three review articles in the Research Topic centered on the role of ACs on neuropsychiatric disorders. The review by [Chen et al.](#) focuses on the calcium-stimulated group 1 ACs. The authors outline their functions and discuss the available literature that links those AC isoforms with neuropsychiatric and neurodevelopmental diseases, such as depression and schizophrenia, as well as the therapeutic potential of targeting them. [Tabakoff and Hoffman](#) review the role played by AC7 in alcohol use disorder and depression. The manuscript discussions range from the molecular regulation of AC7 to genetic associations with neuropsychiatric disorders. The authors also discuss potential strategies for selectively modulating AC7. The third review article, by [Schappi and Rasenick](#), centers on the relationship between G_{α_s} and depressive disorders. The authors provide comprehensive analyses of individual AC isoforms, cell signaling cascades, and the link between current antidepressant therapies and AC activity.

The articles in the topic present and discuss the latest findings and the different strategies being pursued and hypothesized for targeting AC isoforms to treat diseases. In addition to the different tools to study AC function that are identified and validated, the articles provide a framework for targeting individual AC isoforms and the contexts where AC modulation would be desired. Direct modulation of ACs

remains an attractive path for the development of new therapies, however, there are challenges related to isoform selectivity and possible adverse reactions that need to be overcome. Overall, the articles in the present Research Topic provide a positive outlook for targeting AC isoforms but also caution about isoform selectivity and off-target effects. Additionally, the original research articles provide preclinical proof-of-concept for the use of AC isoform modulators and a framework for the development of novel small molecules that selectively target AC isoforms. Finally, the editors would like to thank all contributors and reviewers that made this Research Topic possible.

Author contributions

TB wrote the first draft of the editorial, which was reviewed and edited by all authors.

Conflict of interest

TB was employed by the aTyr Pharma.

The remaining authors declare that the research was conducted in the absence of any commercial or financial relationships that could be construed as a potential conflict of interest.

Publisher's note

All claims expressed in this article are solely those of the authors and do not necessarily represent those of their affiliated organizations, or those of the publisher, the editors and the reviewers. Any product that may be evaluated in this article, or claim that may be made by its manufacturer, is not guaranteed or endorsed by the publisher.

References

- Brust, T. F., Alongkronrussmee, D., Soto-Velasquez, M., Baldwin, T. A., Ye, Z., and Dai, M., (2017). Identification of a selective small-molecule inhibitor of type 1 adenylyl cyclase activity with analgesic properties. *Sci. Signal* 10, eaah5381. doi:10.1126/scisignal.aah5381
- Ostrom, K. F., LaVigne, J. E., Brust, T. F., Seifert, R., Dessauer, C. W., and Watts, V. J., (2022). Physiological roles of mammalian transmembrane adenylyl cyclase isoforms. *Physiol. Rev* 102, 815–857. doi:10.1152/physrev.00013.2021
- Santos, R., Ursu, O., Gaulton, A., Bento, A. P., Donadi, R. S., and Bologa, C. G., (2017). A comprehensive map of molecular drug targets. *Nat. Rev. Drug Discov* 16 (1), 19–34. doi:10.1038/nrd.2016.230



A Selective Adenylyl Cyclase 1 Inhibitor Relieves Pain Without Causing Tolerance

Gianna Giacoletti¹, Tatum Price¹, Lucas V. B. Hoelz², Abdulwhab Shremo Msdi¹, Samantha Cossin¹, Katerina Vazquez-Falto¹, Tácio V. Amorim Fernandes^{2,3}, Vinícius Santos de Pontes², Hongbing Wang⁴, Nubia Boechat², Adwoa Nornoo¹ and Tarsis F. Brust^{1*}

¹Department of Pharmaceutical Sciences, Lloyd L. Gregory School of Pharmacy, Palm Beach Atlantic University, West Palm Beach, FL, United States, ²Laboratório de Síntese de Fármacos—LASFAR, Instituto de Tecnologia em Fármacos, Farmanguinhos—FIOCRUZ, Fundação Oswaldo Cruz, Rio de Janeiro, Brazil, ³Instituto Nacional de Metrologia, Qualidade e Tecnologia—INMETRO, Rio de Janeiro, Brazil, ⁴Department of Physiology, Michigan State University, East Lansing, MI, United States

OPEN ACCESS

Edited by:

Manuela Marcoli,
University of Genoa, Italy

Reviewed by:

Victor Ruiz-Velasco,
The Pennsylvania State University,
United States
J. Adolfo García-Sáinz,
Universidad Nacional Autónoma de
México, Mexico

*Correspondence:

Tarsis F. Brust
tbrust@atyrpharma.com

Specialty section:

This article was submitted to
Experimental Pharmacology and Drug
Discovery,
a section of the journal
Frontiers in Pharmacology

Received: 04 May 2022

Accepted: 20 June 2022

Published: 11 July 2022

Citation:

Giacoletti G, Price T, Hoelz LVB, Shremo Msdi A, Cossin S, Vazquez-Falto K, Amorim Fernandes TV, Santos de Pontes V, Wang H, Boechat N, Nornoo A and Brust TF (2022) A Selective Adenylyl Cyclase 1 Inhibitor Relieves Pain Without Causing Tolerance. *Front. Pharmacol.* 13:935588. doi: 10.3389/fphar.2022.935588

Among the ten different adenylyl cyclase isoforms, studies with knockout animals indicate that inhibition of AC1 can relieve pain and reduce behaviors linked to opioid dependence. We previously identified ST034307 as a selective inhibitor of AC1. The development of an AC1-selective inhibitor now provides the opportunity to further study the therapeutic potential of inhibiting this protein in pre-clinical animal models of pain and related adverse reactions. In the present study we have shown that ST034307 relieves pain in mouse models of formalin-induced inflammatory pain, acid-induced visceral pain, and acid-depressed nesting. In addition, ST034307 did not cause analgesic tolerance after chronic dosing. We were unable to detect ST034307 in mouse brain following subcutaneous injections but showed a significant reduction in cAMP concentration in dorsal root ganglia of the animals. Considering the unprecedented selectivity of ST034307, we also report the predicted molecular interaction between ST034307 and AC1. Our results indicate that AC1 inhibitors represent a promising new class of analgesic agents that treat pain and do not result in tolerance or cause disruption of normal behavior in mice. In addition, we outline a unique binding site for ST034307 at the interface of the enzyme's catalytic domain.

Keywords: adenylyl cyclase, pain, analgesia, AC1, tolerance

1 INTRODUCTION

Adenylyl cyclases (ACs) are the enzymes responsible for catalyzing the conversion of adenosine triphosphate (ATP) into cyclic adenosine monophosphate (cAMP) (Cooper and Crossthwaite, 2006; Dessauer et al., 2017). ACs integrate signaling from a large range of proteins and ions, including G protein-coupled receptors (GPCRs), protein kinases, and calcium, to name a few. There are ten different isoforms of ACs, nine of them are present in the cellular membrane and one is soluble. Each AC isoform has a specific expression pattern, which is related to a specific set of physiological functions (Ostrom et al., 2022). AC isoforms also display a unique set of regulatory properties that result in differences in how the isoforms are modulated by different types of G proteins, protein kinases, and ions (Cooper and Crossthwaite, 2006; Dessauer et al., 2017).

AC1 is part of the group of ACs that are activated by calcium through calmodulin (Masada et al., 2012). Additional regulatory properties of AC1 include inhibition by $G\alpha_{i/o}$ and $G\beta\gamma$ subunits of G proteins and activation by $G\alpha_s$ and the small molecule forskolin (Brust et al., 2017; Dessauer et al., 2017). AC1 has also been shown to undergo $G\alpha_{i/o}$ -coupled receptor-mediated superactivation (Cumbay and Watts, 2001; Brust et al., 2015; Brust et al., 2017). The expression pattern of AC1 is consistent with the physiological functions that have been associated with this AC isoform. AC1 transcripts are found in the dorsal root ganglion (DRG), spinal cord, and anterior cingulate cortex (ACC), and a role for this cyclase in pain and nociception has been suggested (Wei et al., 2006; Xu et al., 2008; Johnson et al., 2020). In fact, AC1 knockout (KO) mice display a reduction in typical behaviors that are induced by inflammatory and neuropathic pain, compared to wild-type mice (Wei et al., 2002; Vadakkan et al., 2006; Xu et al., 2008). These studies encouraged the pursuit and discovery of novel compounds that can selectively inhibit AC1 activity as potential novel pain-relieving therapeutics (Brand et al., 2013; Brust et al., 2017; Kaur et al., 2018).

AC1 transcripts are also found in the hippocampus, a brain region linked to learning and memory (Wong et al., 1999). Notably, AC8, another calcium/calmodulin-activated isoform, is also highly expressed in the hippocampus (Wang et al., 2003; Dessauer et al., 2017). Previous studies with single and double AC1/AC8 KO mice have indicated that some functions of AC1 and AC8 related to learning and memory are redundant (Wong et al., 1999). Specifically, AC1/AC8 double KO mice display impaired long-term memory in contextual learning and passive avoidance assays, whereas individual KO of each isoform separately results in wild-type-like behaviors (Wong et al., 1999). However, each isoform also appears to have specific functions. While less severe deficits are observed in AC1-KO mice compared to the AC1/AC8 double KO, the former still displays reduced long-term potentiation (LTP) in the hippocampus and impairments in certain recognition memory as well as spatial and avoidance learning tasks (Shan et al., 2008; Zheng et al., 2016). Those studies highlight the importance of selectivity for AC1 inhibition versus AC8 for a novel compound to treat pain, but do not exclude the possibility of adverse effects that may result from selective AC1 inhibition in the hippocampus.

We have recently reported the discovery of ST034307, a small molecule inhibitor of AC1 that is selective for AC1 inhibition versus all other membranous AC isoforms, including AC8 (Brust et al., 2017). Our previous study focused on the characterization of ST034307 at the molecular level, showing that the compound is a potent, highly selective, and direct AC1 inhibitor. Moreover, ST034307 was also analgesic in a mouse model of Complete Freund's Adjuvant (CFA)-induced allodynia (Brust et al., 2017). The present study represents a pre-clinical study with ST034307 to determine the potential of this class of compounds as novel analgesic agents. We compared the compound with morphine in mouse models of pain-induced and pain-depressed behaviors and also showed that the compound appears to be restricted to the periphery following subcutaneous injections and reduces cAMP

concentration in mouse DRG. Further, we showed that ST034307 does not induce analgesic tolerance or cross-tolerance with morphine. Finally, we expanded our previous mechanistic findings by modeling how the interaction of ST034307 with AC1 happens, this may aid future medicinal chemistry studies pursuing selective modulators of AC1.

2 MATERIALS AND METHODS

2.1 Experimental Design

The main goal of the present study was to determine the potency and efficacy of the AC1 selective inhibitor ST034307 in mouse models of pain and innate behavior. Male mice were used as research subjects and sample sizes for the different experiments were determined using power analyses from preliminary experiments following the guidelines of Palm Beach Atlantic University's Institutional Animal Care and Use Committee (IACUC) to attempt to minimize the numbers of animals used. Instances where the number of animals per group vary in an experiment were the result of additional animals being required for proper blinding when a drug dose was added. All animals were randomized to treatments and experimenters performing behavioral measurements and injections were blinded to all compound treatments and doses.

2.2 Materials

ST034307 (6-Chloro-2-(trichloromethyl)-4H-1-benzopyran-4-one) was purchased from Tocris Bioscience and morphine sulphate from Spectrum Laboratory Products. Acetic acid, lactic acid, Tween 80, and formaldehyde were from Sigma-Aldrich. Dimethyl sulfoxide (DMSO) and 0.9% sterile saline were from Fisher Scientific. ST034307 and morphine were prepared in a vehicle consisting of dimethyl sulfoxide (DMSO), Tween 80, and milli-Q water (1:1:8). Specifically, ST034307 was first dissolved in DMSO and sonicated in a 50°C water bath for 15 min. Next, Tween 80 was added, the solution was vortexed, and the sonication was repeated. Warm (37°C) milli-Q water was added and the solution was vortexed immediately before injections. While morphine is also soluble in aqueous solutions, such as saline, we chose to dilute it in the same vehicle as ST034307 to avoid having to add an additional vehicle control condition to our experiments. These procedures reduced the number of animals required in all *in vivo* experiments performed in the study. Acetic acid, lactic acid, and formalin were diluted in 0.9% sterile saline.

2.3 Study Approval

All experimental procedures involving mice adhered to the National Institutes of Health Animal Care guidelines and were approved by Palm Beach Atlantic University's IACUC (West Palm Beach, FL—protocol number 2020-01AMOUSE approved on 10 January 2020).

2.4 Animals

Male C57BL/6J mice were purchased from Charles Rivers Laboratories. This particular strain is commonly used in

studies related to analgesic agents (Brust et al., 2016; Grim et al., 2020; Pantouli et al., 2021) and provides a way of comparing the activity of ST034307 with other compounds, given that morphine was used as a positive control. AC1-KO mice were created as previously described and propagated using homozygous breeding using the C57BL/6J background (Zheng et al., 2016). Mice were housed in groups (2-5 per cage) in cages covered with filter tops (micro barrier top from Allentown), in a temperature-controlled room under a 12-h light/dark cycle. Animals had ad libitum access to water and food, as well as nesting material made from pulped virgin cotton fiber (nestlets from Lab Supply) for enrichment. Corn cob bedding (1/4") was used for bedding. Mice between 2 and 5 months of age were used for experiments and were dosed subcutaneously with 10 µl/g of ST034307, morphine, or vehicle solutions. After each experiment, mice were humanely euthanized via cervical dislocation under isoflurane anesthesia (open drop method).

2.5 Formalin-Induced Paw Licking

The formalin-induced paw licking assay was conducted similarly to previously described (Pantouli et al., 2021). Briefly, mice were acclimated to clear testing cylinders for 45 min. Next, mice were injected subcutaneously with compounds or vehicle solutions and returned to acrylic cylinders for 15 min. Mice were then injected into their right hind paw with 25 µl of 5% formalin using a 25 µl Hamilton syringe and a 30-gauge needle. Mice were immediately returned to the testing cylinders, and paw licking time was recorded in 5-min intervals for 40 min. The experiment was divided into two different phases. The first represents the time spent licking between 0 and 10 min, the second represents the time spent licking between 16 and 40 min.

2.6 Acid-Induced Writhing

For the acid-induced writhing assay, mice were acclimated to clear testing cylinders for 45 min. Next, mice were injected subcutaneously with compounds or vehicle solutions and returned to acrylic cylinders for 15 min. Mice were then injected intraperitoneally with 0.75% acetic acid (10 µl/g), returned to the testing cylinders, and the number of abdominal constrictions (stretching movements of the body as a whole, including the hind paws) was counted in 5-min intervals for 30 min as previously described (Tarselli et al., 2011). For the tolerance assay, mice were injected subcutaneously with either 100 mg/kg morphine or 30 mg/kg ST034307 (solubility issues prevented the use of higher doses) once a day for four or 8 days. Three hours after the last injection at day four or day eight, acid-induced writhing assays were performed.

2.7 Nesting

The mouse nesting assay was adapted from methods previously described (Negus et al., 2015). Mice were single housed and acclimated to their new home cage for 3 days. During the following 3 days, mice underwent one nesting session (as described below) per day to acclimate them to handling, the experimental procedure, and the testing room. The last acclimation session included a subcutaneous injection (for compound-inhibited nesting) or a subcutaneous injection and

an intraperitoneal injection (for acid-depressed nesting) with 0.9% saline. On the day after the third acclimation session, mice were injected subcutaneously with compounds or vehicle and returned to their respective home cages for 10 min. Mice were transferred to a transfer cage (<1 min) and nestlets were placed in each of the 6 different zones of the home cage as previously described (Negus et al., 2015). Mice were either returned to their home cages (compound-inhibited nesting) or injected intraperitoneally (10 µl/g) with 1% lactic acid (acid-depressed nesting) and returned to their home cages for nesting periods. Nesting was scored as the number of zones cleared over time.

2.8 Pharmacokinetic Studies

The disposition of ST034307 was studied in male C57BL/6J mice following a single subcutaneous injection (10 mg/kg). Mice were humanely euthanized via decapitation under isoflurane anesthesia (open drop method). Subsequently, brain and blood samples were collected at 5-, 25-, 45-, 60-, 120-, and 240-min post-injection. Blood was centrifuged, plasma collected and stored at -80°C. The analyses of the samples were conducted in the Drug Metabolism and Pharmacokinetics Core at Scripps Research. Brain samples were homogenized with water to form a slurry. ST034307 was extracted from plasma and brain slurry on solid-supported liquid-liquid extraction cartridges (HyperSep™, SLE, 1 g/6 ml, Thermo Scientific) and the resultant extract was assayed for ST034307 by tandem mass spectroscopy coupled to HPLC (SCIEX 6500). The lowest limits of quantitation were 10 ng/ml (34 nM) and 6 ng/ml (20 nM) for plasma and brain, respectively. A plot of plasma ST034307 concentration versus time was constructed and analyzed for non-compartmental pharmacokinetic parameters - half-life, volume of distribution and clearance (Phoenix, Pharsight, Certara Inc.).

2.9 Cyclic AMP Production in Mouse DRG

Male C57BL/6J mice were injected subcutaneously with 10 mg/kg ST034307 or vehicle. Mice were humanely euthanized *via* decapitation under isoflurane anesthesia (open drop method) 90 min after the injection. DRGs (approximately C5 to L3) were dissected as previously described (Sleigh et al., 2020), frozen in liquid N₂, and stored in a -80°C freezer until used. On assay day, DRGs from a ST034307-injected mouse and its vehicle-matched control were thawed on ice. Membrane buffer (50 mM HEPES, pH 7.4) was added and samples were homogenized using a tissue tearor. Next, samples were subjected to glass-on-glass dounce homogenization. Homogenates were centrifuged at 500 x g for 5 min at 4°C. The supernatant was collected and centrifugation was repeated until no visible pellet remained. Homogenates were plated in a low-volume 384 well plate at a protein concentration of 100 ng/well. Stimulation buffer (final well concentrations: 50 mM HEPES pH 7.4, 10 mM MgCl₂, 0.2 mM ATP, 10 µM GTP, 1% DMSO, 50 mM NaCl, 500 µM 3-isobutyl-1-methylxanthine, and 0.5 mg/ml bovine serum albumin) was added and the plate was incubated at room temperature for 45 min. cAMP concentrations were measured using Cisbio's dynamic 2 kit (Cisbio Bioassays) according to the manufacturer's instructions.

2.10 Molecular Docking

2.10.1 Construction of the AC1 Model

The AC1 model was constructed through ab-initio and threading methods on I-Tasser server, considering as input the sequences Phe291-Pro478 and Leu859-1058, registered under the UniProtKB ID Q08828 (Yang and Zhang, 2015; UniProt, 2021). The globular domain regions were identified using both Pfam and UniProtKB feature viewer, being selected for further refining (Mistry et al., 2021). Local sequence alignments with NCBI's BLAST+ were made between the Q08828 and those from Protein Data Bank (PDB) deposited structures to find experimentally solved structures with magnesium ions, ATP, and $G\alpha_s$ on their respective sites (Altschul et al., 1990; Berman et al., 2002). Thus, using molecular superpositions on VMD 1.9.3, the cofactors and ligands were extracted from the structure registered as 1CJK on PDB, while $G\alpha_s$ was extracted from the structure registered as 6R3Q, and positioned into the AC1 model (Humphrey et al., 1996). MODELLER 9.25-1 was then used to run 100 cycles of structural optimizations with molecular dynamics, simulated annealing, and conjugated gradient (Sali and Blundell, 1993). The generated structures were ranked by DOPE-Score and the best model was selected. To verify the structural quality of the best AC1 model built, the structure was submitted to the SAVES server, where two programs were selected, PROCHECK (Supplementary Figures. S1–S3) and VERIFY 3D (Supplementary Figure S4), and to the Swiss-PROT server, using QMEANDisCo algorithm (Supplementary Figure S5) (Colovos and Yeates, 1993; Laskowski et al., 1993; Studer et al., 2020).

2.10.2 Preparation of the ST034307 Structure

ST034307 was constructed and optimized with the HF/6-31G(d) level of theory using the SPARTAN'16 program (Wavefunction, Inc.).

2.10.3 Docking Using GOLD 2020.3.0 (Genetic Optimization for Ligand Docking)

The molecular docking simulation using the GOLD program was carried out using automatic genetic algorithm parameters settings for the population size, selection-pressure, number of islands, number of operations, niche size, and operator weights (migration, mutation, and crossover) (Jones et al., 1997). The search space was a 40 Å radius sphere from the 66.215, 105.567, and 81.040 (x, y, and z axes, respectively) coordinates. The scoring function used was ChemPLP, which is the default function for the GOLD program. Thus, the pose with the most positive score (the best interaction) was extracted for further analysis.

2.10.4 Docking Using AutoDock Vina 1.1.2

The PDBQT-formatted files for the AC1 model and ST034307 structure were generated using AutoDock Tools (ADT) scripts (Trott and Olson, 2010). Using the AutoDock Vina program, the grid size was set to 65.172 Å × 77.050 Å × 73.559 Å for x, y, and z axes, respectively, and the grid center was chosen using 66.215 (x), 105.567 (y), and 81.040 (z) as coordinates. Each docking run used an exhaustiveness setting of 16 and an energy range of 3 kcal/mol. Consequently,

the pose with the lowest energy was extracted for interaction analysis.

2.11 Data and Statistical Analyses

All statistical analyses were carried out using GraphPad Prism 9 software (GraphPad Software Inc.). Data normalization and nonlinear regressions were carried out similarly to previously described (Grim et al., 2020). For normalizations (representing a rescaling of the Y axis for enhanced clarity), the maximal possible effect was set as 100% (zero for formalin-induced paw licking and acid-induced writhing, and five for acid-depressed nesting) and the response to vehicle's average as 0%. For compound-inhibited nesting, the response from vehicle's average was defined as 100% and zero to 0%. Normalized data was fitted to three-parameter nonlinear regressions with the top constrained to 100% and the bottom to 0% (except for the cases where ST034307 did not reach a full response, where no top constrain was set—Figure 2C, Figure 3F). The constrains were done in order to reduce the number of animals used in the experiments and based on the assumption that lower compound doses would not cause an effect lower than the effect of vehicle and the fact that each experiment performed has a ceiling effect (e.g., the lowest amount of time a mouse can lick its paw is zero). All statistical analyses of mouse behavioral responses were performed using raw experimental data (without normalization). For the DRG studies, a matched vehicle control was included with each experiment and cAMP concentration was normalized to that control. Therefore, a one sample T test was carried out to compare the normalized values obtained from mice injected with ST034307 with 100%. T tests with Welch's correction were used for comparisons between genotypes, one-way ANOVAs for comparisons within groups, and two-way ANOVAs for time-course evaluations. All ANOVAs where F achieved a statistical level of significance ($p < 0.05$) were followed by Dunnett's corrections and significance was set at a $p < 0.05$.

3 RESULTS

3.1 ST034307 Relieves Inflammatory Pain, but Not Acute Nociception in Mice

We have previously shown that intrathecal administration of ST034307 relieves CFA-mediated allodynia in mice (Brust et al., 2017). Here, we used intraplantar formalin injections to the mice's right hind paws and compared the potency of ST034307 with that of morphine (both administered subcutaneously) for diminishing acute nociception and relieving inflammatory pain. The time spent tending to (licking) the injected paw was recorded (Figures 1A,B). As indicated by previous studies using AC1-KO mice (Wei et al., 2002), only morphine caused a significant reduction in acute nociception, with an ED₅₀ value equal to 5.87 mg/kg [95% CI 0.44 to 8.96] (Figure 1C—sum of measurements recorded between 0 and 10 min). No significant effect was observed with ST034307. In contrast, both compounds significantly reduced formalin-induced paw licking in the inflammatory pain phase of the model compared to vehicle and had ED₅₀ values equal to

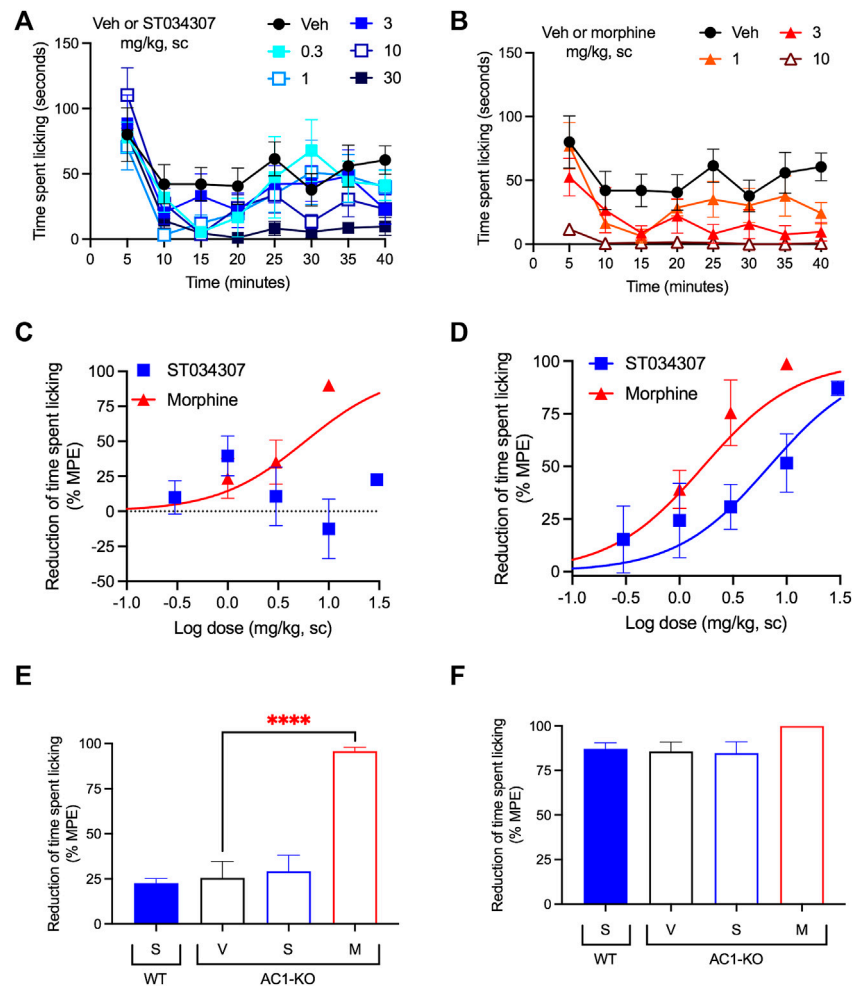


FIGURE 1 | ST034307 relieves inflammatory pain in mice. **(A)** Different doses of ST034307 reduce paw licking behavior caused by an intraplantar injection with 5% formalin. **(B)** Different doses of morphine reduce paw licking behavior caused by an intraplantar injection with 5% formalin. **(C)** Dose-response curves of the sum of time spent licking the paw during the first 10 min of the graphs in **(A)** and **(B)**. Vehicle's response was set as 0% and the maximal possible effect (0) to 100%. **(D)** Dose-response curves of the sum of time spent licking the paw during the period in between minute 16 and minute 40 of the graphs in **(A)** and **(B)**. Vehicle's response was set as 0% and the maximal possible effect (0) to 100%. **(E)** Reduction of time spent licking the injected paw in wild-type (WT) and in AC1-KO mice treated with vehicle (V), 30 mg/kg ST034307 (S), or 10 mg/kg morphine (M) during the first 10 min of the experiment. **(F)** Reduction of time spent licking the injected paw in wild-type (WT) and in AC1-KO mice treated with vehicle (V), 30 mg/kg ST034307 (S), or 10 mg/kg morphine (M) during the period in between minute 16 and minute 40 of the experiment. For E and F vehicle's response in wild-type mice was set to 0% and zero to 100%. Data in all graphs represent the average \pm S.E.M., $N = 6-8$. **** $p < 0.0001$ in one-way ANOVA with Dunnett's test.

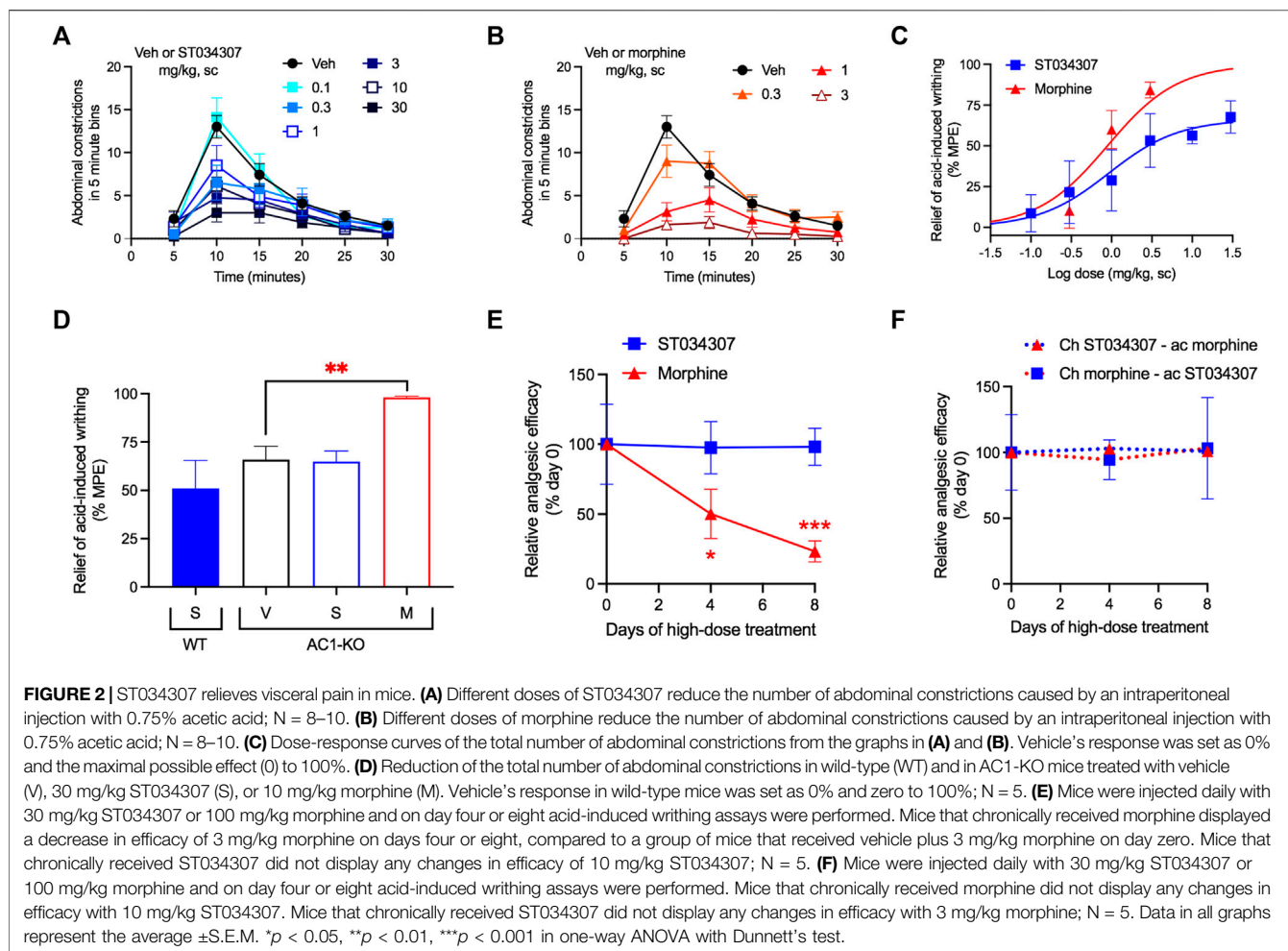
6.88 mg/kg [95% CI 0.85 to 14.05] and 1.67 mg/kg [95% CI 0.35 to 2.43] for ST034307 and morphine, respectively (**Figure 1D**—sum of measurements recorded between 16 and 40 min).

Consistent with the results from wild-type mice, AC1-KO mice did not present a reduction of licking during the acute nociception phase of the experiment compared to wild-type mice ($p = 0.2089$ in unpaired t test—**Figure 1E**). In addition, while morphine relieved acute nociception in AC1-KO mice ($p < 0.0001$ in one-way ANOVA), no effects were observed with ST034307 (**Figure 1E**). In contrast, AC1-KO mice displayed a significant reduction of licking in the inflammatory phase of the model, compared to wild-type mice ($p < 0.001$ in unpaired t test—**Figure 1F**). That reduction was similar to the effect 30 mg/kg ST034307 had in wild-type mice. No effects were

observed from a dose of 30 mg/kg ST034307 in AC1-KO mice. Morphine (10 mg/kg) had a small effect in the inflammatory phase, but it was not significantly different from vehicle ($p = 0.087$ in one-way ANOVA—**Figure 1F**).

3.2 ST034307 Relieves Visceral Pain and Does Not Induce Analgesic Tolerance in Mice

Visceral pain was induced by an intraperitoneal injection of 0.75% acetic acid. The number of abdominal stretches (writhing) the mice performed over a period of 30 min was recorded (**Figures 2A,B**). Both ST034307 and morphine significantly reduced acid-induced writhing in this model with



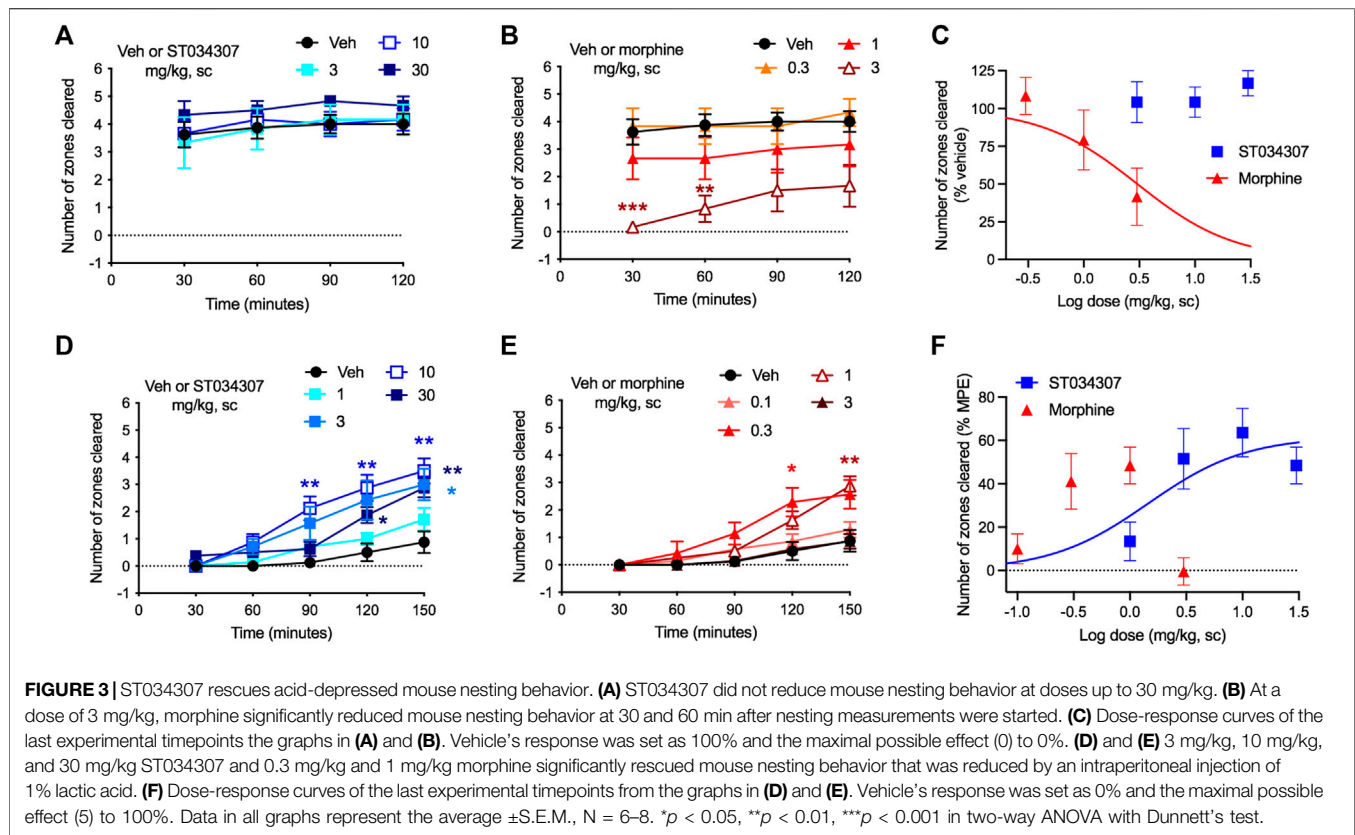
ED₅₀ values equal to 0.92 mg/kg [95% CI 0.15 to 4.41] and 0.89 mg/kg [95% CI 0.40 to 1.52], respectively (Figure 2C). However, ST034307 did not reach full efficacy at doses up to 30 mg/kg. Similarly, AC1-KO mice also only showed a partial reduction of acid-induced writhing in this model, compared to wild-type mice (p < 0.001 in unpaired t test, Figure 2D). This response was not enhanced by 10 mg/kg ST034307, but 3 mg/kg morphine caused a significant reduction of acid-induced writhing in AC1-KO mice (p < 0.01 in one-way ANOVA—Figure 2D).

Mice treated chronically with morphine display analgesic tolerance. Tolerance is expressed through the gradual loss in efficacy of a compound's dose over time (Raehal et al., 2011). After 4 days of daily subcutaneous injections with 100 mg/kg morphine, the efficacy of a 3 mg/kg dose of morphine decreased by nearly half (Figure 2E). At day eight, morphine's efficacy was nearly 20% of its initial response (Figure 2E). In contrast, daily subcutaneous injections with 30 mg/kg ST034307 (highest dose we were able to inject chronically due to solubility) caused no decrease in the analgesic efficacy of a 10 mg/kg ST034307 dose at day four or day eight (Figure 2E). Notably, no cross-tolerance was developed between the two compounds (Figure 2F). Mice treated daily with 100 mg/kg morphine were still fully responsive to 10 mg/kg ST034307 at days four and eight; and mice treated

daily with 30 mg/kg ST034307 were also fully responsive to 3 mg/kg morphine at days four and eight (Figure 2F).

3.3 ST034307 Promotes Analgesia in the Absence of Disruptions in the Mouse Nesting Model

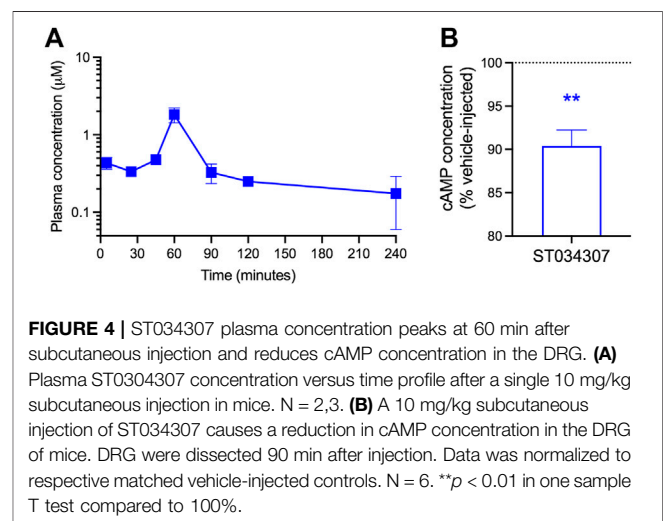
Nesting is an innate mouse behavior that can be disrupted by a number of different stimuli (Negus et al., 2015). Drugs, stress, and pain can all impede normal nesting behavior, making the model appropriate for detecting possible adverse reactions (Negus, 2019). In the experiment, nesting material (nestlets) was placed in six different zones of a mouse's cage. As the mouse makes its nest, it gathers all nestlets in a single zone (Negus et al., 2015). We measured the numbers of zones cleared over time. ST034307 did not disrupt nesting behaviors at doses up to 30 mg/kg compared to vehicle (Figure 3A). Morphine, on the other hand, caused a robust reduction of nesting behavior at 3 mg/kg (Figures 3B—two-way ANOVA, p < 0.001 and p < 0.01 at 30 and 60 min, respectively). Morphine's disruption of nesting behavior at the last time-point of the experiment resulted in an ED₅₀ equal to 3.04 mg/kg [95% CI 1.16 to 11.32] (Figure 3C).



As pain can also disrupt nesting behavior, we next tested whether ST034307 could recover nesting in mice that were treated with 1% lactic acid intraperitoneally. Lactic acid treatment caused a profound reduction in nesting behavior (Figures 3D,E). Mice that were treated with 3, 10, or 30 mg/kg ST034307 displayed a significant increase in nesting behavior compared to vehicle-treated animals (Figure 3D). For morphine, 0.3 and 1 mg/kg caused a significant recovery of nesting behavior during the assay, while 0.1 and 3 mg/kg did not (Figure 3E). ST034307's recovery of nesting behavior at the last time-point of the experiment resulted in an ED_{50} equal to 1.45 mg/kg [95% CI 0.22 to 4.93] (Figure 3F). As the 3 mg/kg dose of morphine depressed mouse nesting, an ED_{50} value was not calculated for the compound (Figure 3E). The ED_{50} value and partial response of ST034307 in this experiment are consistent with what was observed in the acid-induced writhing assay (Figure 2C).

3.4 ST034307 Reduces cAMP Concentration in Mouse DRG

Given the positive results from the nesting experiments, we decided to determine the concentrations of ST034307 in plasma and brain of mice at different timepoints following a subcutaneous injection with a dose of 10 mg/kg (Figure 4A). A plasma concentration of $0.44 (\pm 0.08) \mu\text{M}$ was observed immediately following the injection at 5 min. A sharp peak was present 60 min after the injection at $1.82 (\pm 0.39) \mu\text{M}$ and



after 90 min the plasma concentration dropped back to levels similar to the levels before the peak ($0.33 \mu\text{M} \pm 0.09$). The half-life of ST034307 was determined to be approximately 161 (± 88) minutes and the compound was rapidly cleared (CL/F) from the body at a rate of $305.04 (\pm 22.63) \text{ ml/min}$. ST034307 may be highly tissue bound as its volume of distribution (V/F) of 1619 (± 790) ml is much greater than the total body water volume (14.5 ml) of a 24 g (average weight) mouse (Davies and Morris, 1993). This type of distribution may also indicate extensive red

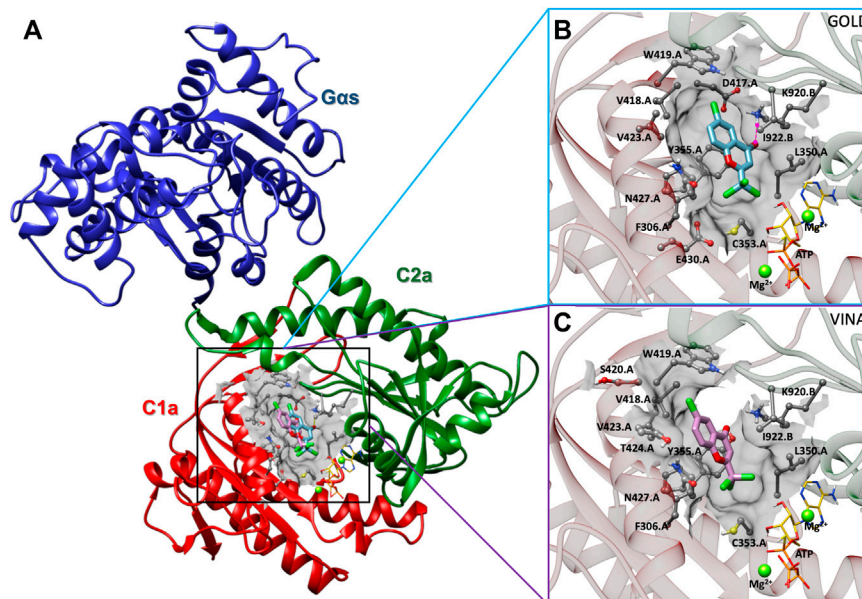


FIGURE 5 | Prediction of the interaction between AC1 and ST034307. **(A)** Cartoon representation of the AC1 model, showing its catalytic domain (C1a, in red, and C2a, in green) complexed to G_{α_s} (in blue), ST034307 (in cyan or purple), ATP (in yellow), and two magnesium ions (Mg^{2+} , in green). Predicted poses of ST034307, using Gold **(B)** and Autodock Vina **(C)** programs, presenting hydrogen-bond (interrupted purple line) and steric interactions. The AC1 residue structures are shown as ball and stick models, ST034307 and ATP as stick models, and Mg^{2+} ions as sphere models using UCSF Chimera program (Pettersen et al., 2004). All the structures are colored by atom: the nitrogen atoms are shown in blue, the oxygen atoms in red, the chlorine atoms in green, the hydrogen atoms in white, and the carbon chain in gray, cyan, or purple. Non-polar hydrogens have been omitted for clarity.

blood cell uptake. To our surprise, none of the timepoints measured resulted in detectable levels of ST034307 in the brains of those mice.

As we were unable to detect ST034307 in mouse brain and AC1 is expressed in the DRG, we decided to determine if a subcutaneous injection of 10 mg/kg ST034307 would cause a reduction in cAMP concentration in mouse DRG. A 10% reduction in cAMP concentration was observed in the DRG of ST034307-injected mice in comparison to vehicle-matched controls (**Figure 4B**).

3.5 ST034307 Interacts With the Interface of C1a and C2a Domains of AC1

In order to determine the binding interaction of ST034307 with AC1, we constructed a molecular model of AC1. The results of PROCHECK's Ramachandran regions (**Supplementary Figure S1**), main-chain (**Supplementary Figure S2**), and side-chain parameters (**Supplementary Figure S3**), as well as VERIFY 3D (**Supplementary Figure S4**), and QMEANDisCo (**Supplementary Figure S5**) analyses indicated that the AC1 model was structurally valid to further computational studies. Thus, to predict the binding mode of ST034307 to AC1, we carried out molecular docking simulations using two programs, GOLD 2020.3.0 and Autodock Vina 1.1.2 (Jones et al., 1997; Trott and Olson, 2010). Although these programs present differences concerning their search algorithm and scoring function, the best-predicted poses resulting from the different programs showed similar binding modes ($RMSD = 2.35\text{\AA}$) into the AC1 model

(**Figure 5A**). The binding site was located into a cavity adjacent to the ATP binding pocket and between domains C1a and C2a, at the catalytic site interface. The best predicted pose for ST034307 presents a chemPLP score of 49.36 a. u, using the GOLD software, showing a hydrogen bond with the amine group from the side chain of Lys920 (C2a), and steric interactions with Phe306, Leu350, Cys353, Tyr355, Asp417, Val418, Trp419, Val423, Asn427, and Glu430 from C1a and with Lys920 and Ile922 from C2a (**Figure 5B**; **Supplementary Figure S6A**). Using Autodock Vina, the best-predicted pose for ST034307 presents an interaction energy value of -6.9 kcal/mol, showing only steric interactions with Phe306, Leu350, Cys353, Tyr355, Asp417, Val418, Trp419, Ser420, Val423, Thr224, and Asn427 from C1a and with Lys920 and Ile922 from C2a (**Figures 5C**; **Supplementary Figure S6B**).

4 DISCUSSION AND CONCLUSION

Previous studies using AC1-KO mice have indicated that inhibition of AC1 could be a new strategy to treat pain and opioid dependence (Wei et al., 2002; Vadakkan et al., 2006; Xu et al., 2008; Zachariou et al., 2008; Luo et al., 2013). Inspired by those studies, we discovered and characterized ST034307 (Brust et al., 2017). The compound displayed remarkable selectivity for inhibition of AC1 vs. all other membrane-bound AC isoforms. And while our previous manuscript focused on the molecular characterization of ST034307, we also showed that the compound relieves pain in a mouse model of CFA-induced allodynia (Brust

et al., 2017). Here, those findings were expanded in multiple different ways.

First, we focused on the activity of the compound in two different models of pain-induced behaviors. In the first, intraplantar injections with formalin to the hind paws of the mice induce a paw licking behavior that is reflective of pain (Tjolsen et al., 1992). The experiment is divided into two distinct phases. The first phase, which includes the first 10 min, represents chemical nociception due to the action of formalin on primary afferent nerve fibers (Mcnamara et al., 2007). ST034307 had no effects on that phase of the experiment (**Figure 1C**). This is consistent with our results with AC1-KO mice (**Figure 1E**) and with a previous study that showed that AC1-KO mice do not have increased thresholds to thermal, mechanical, or chemical acute nociception compared to wild-type mice (Wei et al., 2002). Morphine, in contrast, reduced chemical nociception in both wild-type and AC1-KO mice in a manner that is consistent with the activation of the mu opioid receptor (MOR). Activation of the MOR induces inhibition of AC isoforms as well as modulation of ion channels through G $\beta\gamma$ subunits (Raehal et al., 2011). MOR-induced activation of G protein-coupled inwardly rectifying potassium channels (GIRK) and inhibition of voltage-gated calcium channels induces neuronal hyperpolarization and a reduction of neurotransmission that is consistent with morphine's effects on acute nociception assays (Raehal et al., 2011).

The formalin-induced paw licking behavior between minutes 16 and 40 is believed to be caused by the development of an inflammatory reaction that induces nerve sensitization (Woolf, 1983; Tjolsen et al., 1992; Negus, 2019). This process involves the strengthening of synaptic connections through LTP and requires cAMP (Ferguson and Storm, 2004; Latremoliere and Woolf, 2009; Sharif-Naeini and Basbaum, 2011; Zhuo, 2012). As expected, ST034307 caused a reduction in licking behavior during that phase. A reduction of formalin-induced paw licking during that phase was also observed in AC1-KO mice compared to wild-type animals. These data are consistent with previous work showing that AC1-KO mice have an increased threshold to inflammatory pain and indicate a possible use of selective AC1 inhibitors to treat this type of pain (Wei et al., 2002). As previously reported, morphine was also efficacious in this model (Pantouli et al., 2021). Morphine's higher potency in this phase of the experiment compared to its potency for reducing chemical nociception may be explained by the combination of the MOR's effects on G proteins, namely inhibition of ACs and activation of GIRK.

Next, we showed that ST034307 decreases the number of abdominal constrictions (writhing) in mice injected intraperitoneally with acetic acid. Intraperitoneal injections with irritant agents cause peritovisceral pain and previous studies suggest that all analgesics can reduce writhing in this model (Collier et al., 1968; Negus, 2019). In contrast to morphine, ST034307 did not result in the maximal possible effect in this experiment, an outcome that was mimicked by AC1-KO mice. This partial response allowed us to further confirm that the effect of ST034307 in this model was through AC1 inhibition, as morphine, but not ST034307, further reduced the number of

acid-induced abdominal constrictions in AC1-KO mice (**Figure 2D**).

The use of analgesic agents often requires chronic dosing, which may last days, months, or even years depending on the patient's condition. Unfortunately, chronic analgesic dosing may lead to analgesic tolerance (Stein, 2016). Opioid tolerance is well documented in humans and rodents, and results in a loss of analgesic efficacy over time (Raehal et al., 2011; Stein, 2016; Grim et al., 2020). At the molecular level, it has been proposed that opioid tolerance is caused by agonist-induced recruitment of β arrestins to the MOR. β arrestins induce receptor internalization (removal from the membrane) and, therefore, reduce the pool of available receptors for opioid action (Raehal et al., 2011). As ST034307 acts as an inhibitor of AC1, the mechanisms commonly linked to tolerance (receptor downregulation) should not be present. Consistently, we did not observe any tolerance to a high daily dose of ST034307 for up to 8 days in the mouse acid-induced writhing assay. This is in contrast to morphine, which displayed a marked reduction of analgesic efficacy, consistent with analgesic tolerance. As the two compounds act through different mechanisms (though the MOR inhibits AC1) (Brust et al., 2017), there was no observable development of cross-tolerance.

Paw licking and abdominal constrictions are examples of pain-stimulated behaviors. While useful in pain studies, a reduction of these behaviors may not necessarily indicate pain relief. Compounds that induce paralysis, sedation, or stimulate a competing behavior, for instance, can still cause a marked reduction of behavior in those experiments, but are not necessarily relieving pain (Negus et al., 2015; Negus, 2019). Therefore, we have employed the pain-depressed behavior of nesting as another method to determine the analgesic efficacy of ST034307. Different types of stimuli (such as pain, stress, and sedation) can cause disruptions of mouse innate behaviors. Therefore, in order for a compound to display pain relief in this model, it may not present disruptive properties, as if it does, nesting behavior will be further reduced (see the 3 mg/kg dose of morphine in **Figures 3C,E**) (Negus et al., 2015). ST034307 did not disrupt nesting behavior at doses up to 30 mg/kg, indicating good tolerability in this model. Furthermore, all doses that were effective at relieving pain in the previous models, also significantly recovered nesting behavior that was reduced by an intraperitoneal injection of lactic acid (**Figure 3D**). According to Negus (2019), the combination of the results from our nesting experiments and our pain-stimulated behavior experiments makes ST034307 (and possibly other AC1-selective inhibitors) a "high-priority" analgesic compound for "further testing" (Negus, 2019).

While the nesting experiments provide a measure of safety, studies describing the full spectrum of possible adverse reactions that result from AC1 inhibition are still needed. The high expression levels of AC1 in the hippocampus suggests that the initial focus of these studies should be on learning and memory. ST034307 is selective for AC1 vs. AC8. Nevertheless, AC1-KO mice still display impaired performance in certain learning and memory tasks (Shan et al., 2008; Zheng et al., 2016; Brust et al.,

2017). The use of a pharmacological agent will allow us to determine if those effects are a result of developmental issues (as AC1 expression is important for synaptic plasticity and development) (Haupt et al., 2010; Wang et al., 2011) or if there is an acute dose-dependent effect. If ST034307 is to be used for those experiments, intrathecal or intracerebroventricular injections will be required to ensure that the compound reaches the brain. The development of chronic adverse effects, other than analgesic tolerance, should also be investigated. It is not expected that AC1 inhibitors will be rewarding, but the current state of the opioid crisis indicates that this should be tested experimentally, and the effects of AC1 inhibitors on the release of dopamine in the nucleus accumbens should also be assessed.

It is noteworthy that the current experiments were performed with subcutaneous injections, instead of the intrathecal injections from Brust et al., 2017. This allowed us to determine the disposition of the compound in plasma and brain. The plasma concentration of ST034307 peaked 1 h after injection. Notably, we were unable to detect ST034307 in the brain. Nevertheless, the disposition of this compound in plasma indicates a wide distribution in the body and rapid clearance resulting in relatively low concentrations compared to the administered dose. These concentrations persist for at least 4 h to account for the effects that are seen in these experiments.

A recent study reported that the DRG is an important site for the role AC1 plays in pain and nociception (Johnson et al., 2020). This is related to the requirement of cAMP for central sensitization (Ferguson and Storm, 2004; Zhuo, 2012). Accordingly, we observed a reduction in cAMP concentrations in the DRG of mice injected with ST034307 compared to vehicle-matched controls. It should be noted that the DRG homogenates used in our experiments contain different cell types in addition to the peripheral sensory pain afferents, hence the relatively small reduction in cAMP observed. In addition, the decrease in cAMP concentration observed in the DRG does not prevent the involvement of other sites not examined in the present study in ST034307's effects. The fact that ST034307 appears not to reach the brain also precludes the compound's activity in the hippocampus and makes it unlikely that this particular compound, when administered subcutaneously, would cause adverse effects related to learning and memory.

In the last set of data presented in the manuscript, the interaction between ST034307 and AC1 was mapped using molecular docking. Those results, achieved using two different programs, suggest that ST034307 interacts at a site located between the ATP and forskolin binding sites. This binding site is located at the interface of the C1a and C2a domains and is indicative of a mixed or uncompetitive mechanism. The action of ST034307 is proposed to cause a disruption of the structure of AC1's catalytic domain and, consequently, enzymatic inhibition. As our modeling showed that ST034307 does not bind to the ATP binding site, it is consistent with our previous findings that indicate that the compound is not a P-site inhibitor (Brust et al., 2017; Dessauer et al., 2017).

As encouraging as the data presented in the manuscript appears, other compounds that looked promising in pre-clinical models of pain have failed to translate to clinic (Negus, 2019). While the nesting experiments account for some adverse effects and competing behaviors that may generate false positives, additional studies on ST034307 and the class of AC1 inhibitors are still needed. Particular attention should be devoted to possible impairments on learning and memory as well as other models of pain that reflect pain states that are different from the ones already examined. Experiments with AC1 inhibitors that can reach the brain are also desired. Nevertheless, the present work clearly demonstrates a correlation between selective inhibition of AC1 and behaviors that are consistent with analgesia in mice. More work is still needed to establish this class of compounds as novel pain therapeutics; however, the present study represents an important step that may signal that selective AC1 inhibitors should be prioritized for further testing and advancement for the treatment of pain.

DATA AVAILABILITY STATEMENT

The datasets presented in this study can be found in online repositories. The names of the repository/repositories and accession number(s) can be found in the article/ **Supplementary Material**.

ETHICS STATEMENT

The animal study was reviewed and approved by the Institutional Animal Care and Use Committee (IACUC) of Palm Beach Atlantic University, protocol number 2020-01AMOUSE approved on 10 January 2020.

AUTHOR CONTRIBUTIONS

Conceptualization: TB. Experimental design: TB, GG, AN, LH. Performed experiments: TB, GG, TP, LH, AS, SC, KV, TA, VS. Data analyses: TB, LH, AN. Provided needed equipment or materials: NB, HW. Writing: TB wrote the first draft of the manuscript and all authors contributed, reviewed, and edited.

FUNDING

This work is supported by the American Association of Colleges of Pharmacy's New Investigator Award (TB), the Lloyd L. Gregory School of Pharmacy's IntegraConnect grant (TB and AN), Palm Beach Atlantic University's Quality Initiative grant (TB), Fundação Carlos Chagas Filho de Amparo à Pesquisa do Estado do Rio de Janeiro (FAPERJ) (NB), Conselho Nacional de Desenvolvimento Científico e Tecnológico (CNPq), Fundação de Apoio à Fiocruz (FIOTEC) (NB), Coordenação de

Aperfeiçoamento de Pessoal de Nível Superior (CAPES)—Finance Code 001 (NB), and Programa Nacional de Apoio ao Desenvolvimento da Metrologia, Qualidade e Tecnologia (PRONAMETRO) from Instituto Nacional de Metrologia, Qualidade e Tecnologia (INMETRO) (TA).

REFERENCES

- Altschul, S. F., Gish, W., Miller, W., Myers, E. W., and Lipman, D. J. (1990). Basic Local Alignment Search Tool. *J. Mol. Biol.* 215, 403–410. doi:10.1016/S0022-2836(05)80360-2
- Berman, H. M., Battistuz, T., Bhat, T. N., Bluhm, W. F., Bourne, P. E., Burkhardt, K., et al. (2002). The Protein Data Bank. *Acta Crystallogr. D. Biol. Crystallogr.* 58, 899–907. doi:10.1107/S0907444902003451
- Brand, C. S., Hocker, H. J., Gorfe, A. A., Cavasotto, C. N., and Dessauer, C. W. (2013). Isoform Selectivity of Adenylyl Cyclase Inhibitors: Characterization of Known and Novel Compounds. *J. Pharmacol. Exp. Ther.* 347, 265–275. doi:10.1124/jpet.113.208157
- Brust, T. F., Alongkronrasmee, D., Soto-Velasquez, M., Baldwin, T. A., Ye, Z., Dai, M., et al. (2017). Identification of a Selective Small-Molecule Inhibitor of Type 1 Adenylyl Cyclase Activity with Analgesic Properties. *Sci. Signal* 10, 5381. doi:10.1126/scisignal.aah5381
- Brust, T. F., Conley, J. M., and Watts, V. J. (2015). Ga(i/o)-coupled Receptor-Mediated Sensitization of Adenylyl Cyclase: 40 Years Later. *Eur. J. Pharmacol.* 763, 223–232. doi:10.1016/j.ejphar.2015.05.014
- Brust, T. F., Morgenweck, J., Kim, S. A., Rose, J. H., Locke, J. L., Schmid, C. L., et al. (2016). Biased Agonists of the Kappa Opioid Receptor Suppress Pain and Itch without Causing Sedation or Dysphoria. *Sci. Signal* 9, ra117. doi:10.1126/scisignal.aai8441
- Collier, H. O., Dinneen, L. C., Johnson, C. A., and Schneider, C. (1968). The Abdominal Constriction Response and its Suppression by Analgesic Drugs in the Mouse. *Br. J. Pharmacol. Chemother.* 32, 295–310. doi:10.1111/j.1476-5381.1968.tb00973.x
- Colovos, C., and Yeates, T. O. (1993). Verification of Protein Structures: Patterns of Nonbonded Atomic Interactions. *Protein Sci.* 2, 1511–1519. doi:10.1002/pro.5560020916
- Cooper, D. M., and Crossthwaite, A. J. (2006). Higher-order Organization and Regulation of Adenylyl Cyclases. *Trends Pharmacol. Sci.* 27, 426–431. doi:10.1016/j.tips.2006.06.002
- Cumbay, M. G., and Watts, V. J. (2001). Heterologous Sensitization of Recombinant Adenylate Cyclases by Activation of D(2) Dopamine Receptors. *J. Pharmacol. Exp. Ther.* 297 (293), 1201
- Davies, B., and Morris, T. (1993). Physiological Parameters in Laboratory Animals and Humans. *Pharm. Res.* 10, 1093–1095. doi:10.1023/a:1018943613122
- Dessauer, C. W., Watts, V. J., Ostrom, R. S., Conti, M., Dove, S., and Seifert, R. (2017). International Union of Basic and Clinical Pharmacology. CI. Structures and Small Molecule Modulators of Mammalian Adenylyl Cyclases. *Pharmacol. Rev.* 69, 93–139. doi:10.1124/pr.116.013078
- Ferguson, G. D., and Storm, D. R. (2004). Why Calcium-Stimulated Adenylyl Cyclases? *Physiol. (Bethesda)* 19, 271–276. doi:10.1152/physiol.00010.2004
- Grim, T. W., Schmid, C. L., Stahl, E. L., Pantouli, F., Ho, J. H., Acevedo-Canabal, A., et al. (2020). A G Protein Signaling-Biased Agonist at the μ -opioid Receptor Reverses Morphine Tolerance while Preventing Morphine Withdrawal. *Neuropsychopharmacology* 45, 416–425. doi:10.1038/s41386-019-0491-8
- Haupt, C., Langhoff, J., and Huber, A. B. (2010). Adenylate Cyclase 1 Modulates Peripheral Nerve Branching Patterns. *Mol. Cell Neurosci.* 45, 439–448. doi:10.1016/j.mcn.2010.08.003
- Humphrey, W., Dalke, A., and Schulten, K. (1996). VMD: Visual Molecular Dynamics. *J. Mol. Graph* 14 (33–38), 33–38. doi:10.1016/0263-7855(96)00018-5
- Johnson, K., Doucette, A., Edwards, A., Watts, V. J., and Klein, A. H. (2020). Reduced Activity of Adenylyl Cyclase 1 Attenuates Morphine Induced Hyperalgesia and Inflammatory Pain in Mice. Cold Spring Harbor: Cold Spring Harbor Laboratory.
- Jones, G., Willett, P., Glen, R. C., Leach, A. R., and Taylor, R. (1997). Development and Validation of a Genetic Algorithm for Flexible Docking. *J. Mol. Biol.* 267, 727–748. doi:10.1006/jmbi.1996.0897
- Kaur, J., Soto-Velasquez, M., Ding, Z., Ghanbarpour, A., Lill, M. A., Van Rijn, R. M., et al. (2018). Optimization of a 1,3,4-oxadiazole Series for Inhibition of Ca2+/calmodulin-Stimulated Activity of Adenylyl Cyclases 1 and 8 for the Treatment of Chronic Pain. *Eur. J. Med. Chem.* 162, 568–585. doi:10.1016/j.ejmech.2018.11.036
- Laskowski, R. A., Macarthur, M. W., Moss, D. S., and Thornton, J. M. (1993). PROCHECK: a Program to Check the Stereochemical Quality of Protein Structures. *J. Appl. Cryst.* 26, 283–291. doi:10.1107/s0021889892009944
- Latremoliere, A., and Woolf, C. J. (2009). Central Sensitization: a Generator of Pain Hypersensitivity by Central Neural Plasticity. *J. Pain* 10, 895–926. doi:10.1016/j.jpain.2009.06.012
- Luo, J., Phan, T. X., Yang, Y., Garelick, M. G., and Storm, D. R. (2013). Increases in cAMP, MAPK Activity, and CREB Phosphorylation during REM Sleep: Implications for REM Sleep and Memory Consolidation. *J. Neurosci.* 33, 6460–6468. doi:10.1523/JNEUROSCI.5018-12.2013
- Masada, N., Schaks, S., Jackson, S. E., Sinz, A., and Cooper, D. M. (2012). Distinct Mechanisms of Calmodulin Binding and Regulation of Adenylyl Cyclases 1 and 8. *Biochemistry* 51, 7917–7929. doi:10.1021/bi300646y
- Mcnamara, C. R., Mandel-Brehm, J., Bautista, D. M., Siemens, J., Deranian, K. L., Zhao, M., et al. (2007). TRPA1 Mediates Formalin-Induced Pain. *Proc. Natl. Acad. Sci. U. S. A.* 104, 13525–13530. doi:10.1073/pnas.0705924104
- Mistry, J., Chuguransky, S., Williams, L., Qureshi, M., Salazar, G. A., Sonnhammer, E. L. L., et al. (2021). Pfam: The Protein Families Database in 2021. *Nucleic Acids Res.* 49, D412–D419. doi:10.1093/nar/gkaa913
- Negus, S. S. (2019). Core Outcome Measures in Preclinical Assessment of Candidate Analgesics. *Pharmacol. Rev.* 71, 225–266. doi:10.1124/pr.118.017210
- Negus, S. S., Neddenriep, B., Altarifi, A. A., Carroll, F. I., Leilt, M. D., and Miller, L. L. (2015). Effects of Ketoprofen, Morphine, and Kappa Opioids on Pain-Related Depression of Nesting in Mice. *Pain* 156, 1153–1160. doi:10.1097/j.pain.0000000000000171
- Ostrom, K. F., Lavigne, J. E., Brust, T. F., Seifert, R., Dessauer, C. W., Watts, V. J., et al. (2022). Physiological Roles of Mammalian Transmembrane Adenylyl Cyclase Isoforms. *Physiol. Rev.* 102, 815–857. doi:10.1152/physrev.00013.2021
- Pantouli, F., Grim, T. W., Schmid, C. L., Acevedo-Canabal, A., Kennedy, N. M., Cameron, M. D., et al. (2021). Comparison of Morphine, Oxycodone and the Biased MOR Agonist SR-17018 for Tolerance and Efficacy in Mouse Models of Pain. *Neuropharmacology* 185, 108439. doi:10.1016/j.neuropharm.2020.108439
- Pettersen, E. F., Goddard, T. D., Huang, C. C., Couch, G. S., Greenblatt, D. M., Meng, E. C., et al. (2004). UCSF Chimera-Aa Visualization System for Exploratory Research and Analysis. *J. Comput. Chem.* 25, 1605–1612. doi:10.1002/jcc.20084
- Raehal, K. M., Schmid, C. L., Groer, C. E., and Bohn, L. M. (2011). Functional Selectivity at the μ -opioid Receptor: Implications for Understanding Opioid Analgesia and Tolerance. *Pharmacol. Rev.* 63, 1001–1019. doi:10.1124/pr.111.004598
- Sali, A., and Blundell, T. L. (1993). Comparative Protein Modelling by Satisfaction of Spatial Restraints. *J. Mol. Biol.* 234, 779–815. doi:10.1006/jmbi.1993.1626
- Shan, Q., Chan, G. C., and Storm, D. R. (2008). Type 1 Adenylyl Cyclase Is Essential for Maintenance of Remote Contextual Fear Memory. *J. Neurosci.* 28, 12864–12867. doi:10.1523/JNEUROSCI.2413-08.2008
- Sharif-Naeini, R., and Basbaum, A. I. (2011). Targeting Pain where it Resides in the Brain. *Sci. Transl. Med.* 3, 65ps1. doi:10.1126/scitranslmed.3002077
- Sleigh, J. N., West, S. J., and Schiavo, G. (2020). A Video Protocol for Rapid Dissection of Mouse Dorsal Root Ganglia from Defined Spinal Levels. *BMC Res. Notes* 13, 302. doi:10.1186/s13104-020-05147-6
- Stein, C. (2016). Opioid Receptors. *Annu. Rev. Med.* 67, 433–451. doi:10.1146/annurev-med-062613-093100

SUPPLEMENTARY MATERIAL

The Supplementary Material for this article can be found online at: <https://www.frontiersin.org/articles/10.3389/fphar.2022.935588/full#supplementary-material>

- Studer, G., Rempfer, C., Waterhouse, A. M., Gumienny, R., Haas, J., and Schwede, T. (2020). Qmeandisco-Distance Constraints Applied on Model Quality Estimation. *Bioinformatics* 36, 1765–1771. doi:10.1093/bioinformatics/btz828
- Tarselli, M. A., Raehal, K. M., Brasher, A. K., Streicher, J. M., Groer, C. E., Cameron, M. D., et al. (2011). Synthesis of Conolidine, a Potent Non-Opioid Analgesic for Tonic and Persistent Pain. *Nat. Chem.* 3, 449–453. doi:10.1038/nchem.1050
- Tjølsen, A., Berge, O. G., Hunskaar, S., Rosland, J. H., and Hole, K. (1992). The Formalin Test: An Evaluation of the Method. *Pain* 51, 5–17. doi:10.1016/0304-3959(92)90003-t
- Trott, O., and Olson, A. J. (2010). Autodock Vina: Improving the Speed and Accuracy of Docking With a New Scoring Function, Efficient Optimization, and Multithreading. *J. Comput. Chem.* 31, 455–461. doi:10.1002/jcc.21334
- Uniprot, C. (2021). Uniprot: The Universal Protein Knowledgebase in 2021. *Nucleic Acids Res.* 49, D480–D489. doi:10.1093/nar/gkaa1100
- Vadakkan, K. I., Wang, H., Ko, S. W., Zastepa, E., Petrovic, M. J., Sluka, K. A., et al. (2006). Genetic Reduction of Chronic Muscle Pain in Mice Lacking Calcium/Calmodulin-Stimulated Adenylyl Cyclases. *Mol. Pain* 2, 7. doi:10.1186/1744-8069-2-7
- Wang, H., Liu, H., Storm, D. R., and Zhang, Z. W. (2011). Adenylate Cyclase 1 Promotes Strengthening and Experience-Dependent Plasticity of Whisker Relay Synapses in the Thalamus. *J. Physiol.* 589, 5649–5662. doi:10.1113/jphysiol.2011.213702
- Wang, H., Pineda, V. V., Chan, G. C., Wong, S. T., Muglia, L. J., and Storm, D. R. (2003). Type 8 Adenylyl Cyclase is Targeted to Excitatory Synapses and Required for Mossy Fiber Long-Term Potentiation. *J. Neurosci.* 23, 9710–9718. doi:10.1523/jneurosci.23-30-09710.2003
- Wei, F., Qiu, C. S., Kim, S. J., Muglia, L., Maas, J. W., Pineda, V. V., et al. (2002). Genetic Elimination of Behavioral Sensitization in Mice Lacking Calmodulin-Stimulated Adenylyl Cyclases. *Neuron* 36, 713–726. doi:10.1016/s0896-6273(02)01019-x
- Wei, F., Vadakkan, K. I., Toyoda, H., Wu, L. J., Zhao, M. G., Xu, H., et al. (2006). Calcium Calmodulin-Stimulated Adenylyl Cyclases Contribute to Activation of Extracellular Signal-Regulated Kinase in Spinal Dorsal Horn Neurons in Adult Rats and Mice. *J. Neurosci.* 26, 851–861. doi:10.1523/JNEUROSCI.3292-05.2006
- Wong, S. T., Athos, J., Figueroa, X. A., Pineda, V. V., Schaefer, M. L., Chavkin, C. C., et al. (1999). Calcium-Stimulated Adenylyl Cyclase Activity is Critical for Hippocampus-Dependent Long-Term Memory and Late Phase LTP. *Neuron* 23, 787–798. doi:10.1016/s0896-6273(01)80036-2
- Woolf, C. J. (1983). Evidence for a Central Component of Post-Injury Pain Hypersensitivity. *Nature* 306, 686–688. doi:10.1038/306686a0
- Xu, H., Wu, L. J., Wang, H., Zhang, X., Vadakkan, K. I., Kim, S. S., et al. (2008). Presynaptic and Postsynaptic Amplifications of Neuropathic Pain in the Anterior Cingulate Cortex. *J. Neurosci.* 28, 7445–7453. doi:10.1523/JNEUROSCI.1812-08.2008
- Yang, J., and Zhang, Y. (2015). I-TASSER Server: New Development for Protein Structure and Function Predictions. *Nucleic Acids Res.* 43, W174–W181. doi:10.1093/nar/gkv342
- Zachariou, V., Liu, R., Laplant, Q., Xiao, G., Renthal, W., Chan, G. C., et al. (2008). Distinct Roles of Adenylyl Cyclases 1 and 8 in Opiate Dependence: Behavioral, Electrophysiological, and Molecular Studies. *Biol. Psychiatry* 63, 1013–1021. doi:10.1016/j.biopsych.2007.11.021
- Zheng, F., Zhang, M., Ding, Q., Sethna, F., Yan, L., Moon, C., et al. (2016). Voluntary Running Depreciates the Requirement of Ca²⁺-Stimulated Camp Signaling in Synaptic Potentiation and Memory Formation. *Learn. Mem.* 23, 442–449. doi:10.1101/lm.040642.115
- Zhuo, M. (2012). Targeting Neuronal Adenylyl Cyclase for the Treatment of Chronic Pain. *Drug Discov. Today* 17, 573–582. doi:10.1016/j.drudis.2012.01.009

Conflict of Interest: The authors declare that the research was conducted in the absence of any commercial or financial relationships that could be construed as a potential conflict of interest.

Publisher's Note: All claims expressed in this article are solely those of the authors and do not necessarily represent those of their affiliated organizations, or those of the publisher, the editors and the reviewers. Any product that may be evaluated in this article, or claim that may be made by its manufacturer, is not guaranteed or endorsed by the publisher.

Copyright © 2022 Giacioletti, Price, Hoelz, Shremo Msdi, Cossin, Vazquez-Falto, Amorim Fernandes, Santos de Pontes, Wang, Boechat, Nornoo and Brust. This is an open-access article distributed under the terms of the Creative Commons Attribution License (CC BY). The use, distribution or reproduction in other forums is permitted, provided the original author(s) and the copyright owner(s) are credited and that the original publication in this journal is cited, in accordance with accepted academic practice. No use, distribution or reproduction is permitted which does not comply with these terms.



OPEN ACCESS

EDITED BY
Rennolds S. Ostrom,
Chapman University, United States

REVIEWED BY
Muhammad Aslam,
University of Giessen, Germany

*CORRESPONDENCE
Lonny R. Levin,
llevin@med.cornell.edu

SPECIALTY SECTION
This article was submitted to
Experimental Pharmacology and Drug
Discovery,
a section of the journal
Frontiers in Pharmacology

RECEIVED 26 May 2022
ACCEPTED 27 July 2022
PUBLISHED 25 August 2022

CITATION
Ferreira J, Levin LR and Buck J (2022),
Strategies to safely target widely
expressed soluble adenylyl cyclase
for contraception.
Front. Pharmacol. 13:953903.
doi: 10.3389/fphar.2022.953903

COPYRIGHT
© 2022 Ferreira, Levin and Buck. This is
an open-access article distributed
under the terms of the [Creative
Commons Attribution License \(CC BY\)](#).
The use, distribution or reproduction in
other forums is permitted, provided the
original author(s) and the copyright
owner(s) are credited and that the
original publication in this journal is
cited, in accordance with accepted
academic practice. No use, distribution
or reproduction is permitted which does
not comply with these terms.

Strategies to safely target widely expressed soluble adenylyl cyclase for contraception

Jacob Ferreira, Lonny R. Levin* and Jochen Buck

Department of Pharmacology, Weill Cornell Medicine, New York, NY, United States

In humans, the prototypical second messenger cyclic AMP is produced by 10 adenylyl cyclase isoforms, which are divided into two classes. Nine isoforms are G protein coupled transmembrane adenylyl cyclases (tmACs; ADCY1-9) and the 10th is the bicarbonate regulated soluble adenylyl cyclase (sAC; ADCY10). This review details why sAC is uniquely druggable and outlines ways to target sAC for novel forms of male and female contraception.

KEYWORDS

cAMP, sperm motility, capacitation, fertility, adcy10, birth control

Introduction

Cyclic adenosine monophosphate (cAMP), the prototypical second messenger, is a key player facilitating signal transduction throughout the bacterial and animal kingdoms. In mammalian cells, cAMP-dependent signaling is involved in various biological processes such as development, proliferation, and apoptosis via its various effectors, which include Protein Kinase A (PKA), exchange proteins activated by cAMP (EPACs), and cyclic nucleotide-gated channels (Bos, 2003; Kopperud et al., 2003; Kamenetsky et al., 2006; Biel, 2009). With the recognition that this second messenger has many divergent roles, oftentimes within a single cell type, it was appreciated that cAMP is compartmentalized into discreet signaling microdomains. Microdomains are defined by a specific adenylyl cyclase (AC) to produce cAMP and a phosphodiesterase (PDE) to degrade cAMP to prevent the signal from impacting neighboring microdomains and to limit its duration (Scott et al., 2013; Zaccolo et al., 2021). Thus, if one can selectively target the relevant microdomain, the cAMP cascade provides a plethora of targets for treating diseases, including receptors regulating AC activity, the ACs themselves, PDEs, and cAMP effector proteins. For example, increasing cAMP signaling in a microdomain can be pharmacologically manipulated by activating the appropriate AC or the receptor regulating it, or by inhibiting the relevant PDE. Similarly, decreasing cAMP signaling can be accomplished by inhibiting the AC or its receptor, activating the PDE, or blocking the action of the specific cAMP effector. Many therapeutics work via cAMP by modulating the hormone and neurotransmitter receptors regulating AC activity (Sriram and Insel, 2018), and recently, a number of therapeutics directly elevate cAMP within specific microdomains via isoform-selective PDE inhibitors (Baillie et al., 2019). In contrast, there are no approved therapeutics targeting individual AC isoforms.

In humans, there are 10 genes encoding AC isoforms, ADCY1-10, which can be divided into two classes (Figure 1): nine genes (ADCY1-9) encode transmembrane

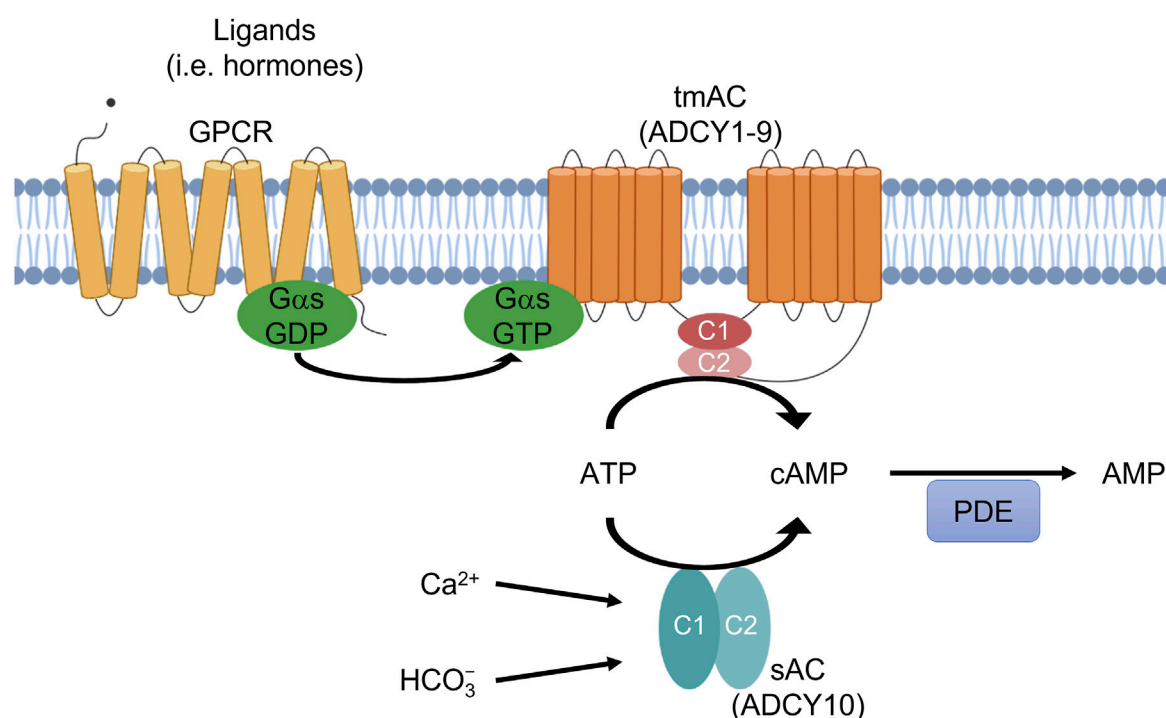


FIGURE 1

Two sources of cAMP in mammalian cells. ADCY1-9 are transmembrane adenylyl cyclases (tmACs) regulated by G-proteins. ADCY10 is soluble adenylyl cyclase (sAC) regulated by HCO₃⁻ and Ca²⁺ ions. Phosphodiesterases (PDEs) degrade cAMP. sAC and tmACs both produce cAMP which has distinct roles.

adenylyl cyclases (tmACs) while the most recently identified gene (ADCY10) encodes the soluble adenylyl cyclase (sAC) (Buck et al., 1999). The transmembrane adenylyl cyclases are regulated by heterotrimeric G proteins and are responsible for cAMP signaling downstream from hormones and neurotransmitters modulating G protein coupled receptors (GPCRs). In contrast, sAC has no predicted transmembrane domains, is not regulated by heterotrimeric G proteins, and is localized to different parts of the cell including the cytosol, mitochondria and nucleus (Zippin et al., 2003). Originally, biochemical studies identified a soluble AC activity, which was thought to be restricted to male germ cells in the testis (Braun and Dods, 1975; Neer, 1978). Its activity first appeared concurrently with the development of spermatids in rats (Braun and Dods, 1975; Braun et al., 1977) and humans (Gordeladze et al., 1982) and was present in testis fractions enriched for spermatids (Braun et al., 1977; Gordeladze et al., 1981). sAC activity is directly regulated by HCO₃⁻ and Ca²⁺ ions (Chen et al., 2000; Jaiswal and Conti, 2003; Litvin et al., 2003; Kleinboelting et al., 2014), and its activity is sensitive to physiologically relevant fluctuations in its substrate, ATP (Zippin et al., 2013). Because it is molecularly and biochemically distinct from other mammalian nucleotidyl cyclases, sAC defines cAMP signaling cascades in mammalian cells independent from the widely studied, hormone-responsive

tmACs (Kamenetsky et al., 2006; Tresguerres et al., 2011; Wiggins et al., 2018). Consistent with its biochemical activity profile, sAC is most abundantly expressed in male germ cells (Buck et al., 1999; Sinclair et al., 2000); however, sAC is also widely expressed at lower levels in somatic tissues (Buck et al., 1999; Geng et al., 2005). sAC-generated-cAMP has many functions that are distinct from tmAC-generated-cAMP (Wiggins et al., 2018; Ostrom et al., 2022); including motility and capacitation of sperm (Esposito et al., 2004; Hess et al., 2005; Akbari et al., 2019; Balbach et al., 2021), and regulation of liver inflammation and fibrosis (Wang et al., 2020), pH homeostasis (Tresguerres et al., 2010), oxidative phosphorylation (Acin-Perez et al., 2009; Di Benedetto et al., 2013; Lefkimmatis et al., 2013), lysosomal function (Rahman et al., 2016), ciliary beating frequency (Schmid et al., 2007; Chen et al., 2014), glucose homeostasis (Zippin et al., 2013; Holz et al., 2014), and intraocular pressure (Lee et al., 2011; Gandhi et al., 2017).

Soluble adenylyl cyclase can be selectively targeted by small molecule inhibitors

In contrast to the tmACs which generate isoform diversity via distinct genes (Ostrom et al., 2022), in humans and rodents, sAC

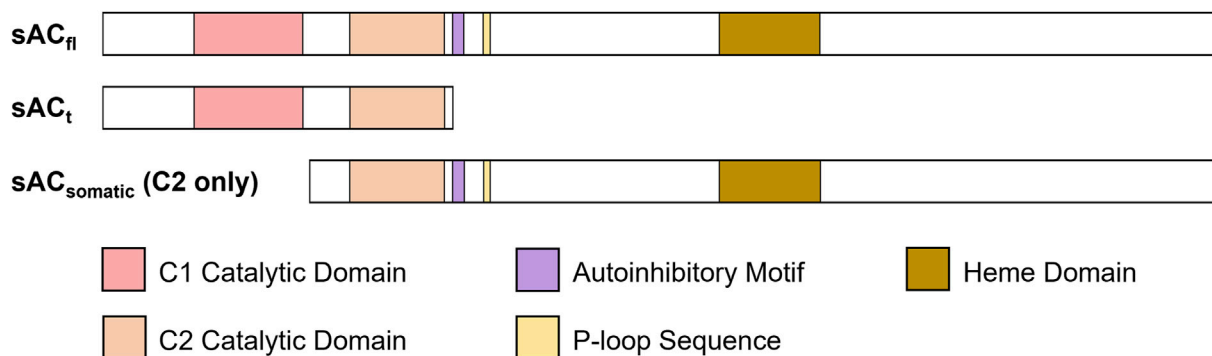


FIGURE 2

Different isoforms of sAC with catalytic and functional domains highlighted. sAC_t and sAC_{fl} are present in testis and sperm, while sAC_{somatic} appears to be ubiquitously expressed.

isoform diversity arises from splice variants of the single ADCY10 locus (Figure 2) (Jaiswal and Conti, 2001; Geng et al., 2005; Schmid et al., 2007; Farrell et al., 2008; Middelhaufe et al., 2012; Karczewski et al., 2020). When sAC was first purified, we isolated two independent cDNAs representing two alternatively spliced isoforms of sAC (Buck et al., 1999; Jaiswal and Conti, 2001). These two transcripts correspond to a full-length sAC (sAC_{fl}), encoding a 187 kDa protein, and a truncated sAC (sAC_t), encoding a 48 kDa protein, both of which are expressed in mouse testis (Hess et al., 2005). sAC_t is predominantly comprised of two homologous catalytic domains (C1 and C2) (Buck et al., 1999; Jaiswal and Conti, 2001), and because it is lacking an autoinhibitory domain present in longer isoforms, it exhibits 10-fold higher specific activity than sAC_{fl} (Chaloupka et al., 2006). Subsequent molecular cloning and 5' Rapid Amplification of cDNA Ends (RACE) experiments identified an alternate start site which generates sAC isoforms missing the first catalytic domain. Because these sAC-C2 only isoforms have not yet been biochemically characterized, all work describing sAC physiological regulators and pharmacological inhibitors refers to the sAC C1-C2 isoforms abundantly expressed in testis and sperm.

After cloning sAC, we appreciated the need for a selective sAC inhibitor to distinguish between sAC- and tmAC-specific physiologic processes. In a high throughput screen (Hess et al., 2005), we identified KH7, a modestly potent (IC₅₀ ~3 μM) sAC-selective inhibitor which has proven instrumental in many cellular studies (Bitterman et al., 2013; Steegborn, 2014; Wiggins et al., 2018). However, KH7 is not a very drug-like molecule and has off-target effects resulting in sAC-independent cytotoxicity (Tian et al., 2011; Di Benedetto et al., 2013). To identify a more suitable candidate for therapeutic development, we performed a new high throughput screen and identified LRE1, a non-toxic sAC inhibitor with a novel chemical structure (IC₅₀ ~3 μM) (Ramos-Espiritu et al., 2016). Crystal structures of sAC/

LRE1 complexes revealed that the 2-amino-6-chloropyrimidine moiety of the compound occupies the bicarbonate binding site (BBS) (Ramos-Espiritu et al., 2016). Consistently, LRE1 inhibition is competitive with bicarbonate but non-competitive with substrate ATP, rendering the compound the first truly allosteric BBS-targeting sAC inhibitor. In tmACs, the pseudo-symmetrical regulatory binding site analogous to the sAC BBS binds forskolin, a general activator of tmACs (Hurley, 1999). Forskolin is inert towards sAC (Buck et al., 1999) because it is too bulky to fit in the sAC BBS (Kleinboelting et al., 2014). Conversely, the forskolin binding site of individual tmAC isoforms appears to be able to accommodate LRE1, which is a weak activator of certain tmACs (Ramos-Espiritu et al., 2016). We took advantage of the drug design expertise of a unique public-private partnership (Meinke, 2022) to improve the potency, selectivity, and drug-like characteristics of LRE1. Ultimately, these efforts increased potency for sAC over 10,000-fold with corresponding increased efficacy in cell-based assays, diminished cross-reactivity with other mammalian nucleotidyl cyclases, and no significant cytotoxicity (Fushimi et al., 2021).

Soluble adenylyl cyclase can be safely targeted for contraception

A subset of the physiological functions ascribed to sAC have therapeutic implications (Wiggins et al., 2018). Chief among these is sAC's role in male fertility (Esposito et al., 2004; Hess et al., 2005; Akbari et al., 2019; Balbach et al., 2021). sAC, specifically isoforms containing both C1 and C2 domains (Hess et al., 2005), is most abundant in testis and sperm and is essential for sperm to fertilize an egg. After being produced in the testis, mammalian sperm are stored in the cauda region of the epididymis where they are morphologically mature but unable to

fertilize an egg. The cauda region is unique because it is characterized by low pH (i.e. 6.5–6.8 vs. 7.4 at physiological conditions) and low HCO_3^- concentration (i.e., 2–7 mM vs. 25 mM). These unique conditions maintain sperm in a dormant state (Levine and Kelly, 1978). Upon ejaculation, sperm encounter semen containing high concentrations of HCO_3^- and Ca^{2+} (Wennemuth et al., 2003; Carlson et al., 2005), which initiate motility and a post-ejaculation maturation process termed capacitation (Austin, 1951; Chang, 1951). The higher levels of HCO_3^- and Ca^{2+} in semen synergistically activate sAC in sperm which rapidly increases cAMP production and initiates sperm capacitation (Visconti et al., 1995; Visconti et al., 2002; Buffone et al., 2014; Balbach et al., 2018). Capacitation-induced changes include activation of motility, specifically, increased beat frequency and altered, asynchronous beating known as hyperactivation. These changes are essential for sperm to pass through the cervix to leave the inhospitable environment of the vagina and enter the permissive environment of the uterus (Visconti et al., 1995; Visconti et al., 2002; Suarez and Pacey, 2006; Buffone et al., 2014; Balbach et al., 2018).

sAC's essential role in male reproduction has been validated genetically (Esposito et al., 2004; Hess et al., 2005; Akbari et al., 2019; Balbach et al., 2021) and pharmacologically (Hess et al., 2005; Mannowetz et al., 2012; Ramos-Espiritu et al., 2016; Balbach et al., 2021; Ferreira et al., 2021) in both mice and men. Two different strains of sAC knockout (KO) mice show male-specific sterility; their sperm are immotile and unable to fertilize an oocyte *in vitro* (Esposito et al., 2004; Hess et al., 2005; Xie et al., 2006; Chen et al., 2013). sAC is also among the rare instances where a human mutation reveals a desired phenotype for a therapeutic approach. Two middle-aged infertile men were identified as homozygous for a frame shift mutation interrupting the catalytic domains of sAC (Akbari et al., 2019). Sperm from these men were immotile, similar to sperm from sAC KO mice (Esposito et al., 2004; Hess et al., 2005; Xie et al., 2006; Balbach et al., 2021), and their motility defect could be rescued by addition of membrane permeable cAMP (Akbari et al., 2019). sAC's essential role in fertility, and as a target for contraception, has also been validated pharmacologically in humans and mice. Multiple, structurally independent, sAC-specific inhibitors prevent the capacitation-induced changes in mouse and human sperm, including stimulation of cAMP production, protein kinase A (PKA) activation, alkalinization, increased beat frequency, hyperactivated motility, and ability to undergo a physiologically induced acrosome reaction (Hess et al., 2005; Mannowetz et al., 2012; Ramos-Espiritu et al., 2016; Balbach et al., 2021; Ferreira et al., 2021). sAC-specific inhibitors also prevent *in vitro* fertilization in mice (Ramos-Espiritu et al., 2016; Balbach et al., 2021). These data validate sAC inhibitors as potential contraceptives (Buffone et al., 2014; Balbach et al., 2020; Balbach et al., 2021); however, the question remains whether they can be administered safely and effectively to people.

Historically, the only targets in sperm pursued for contraceptive development were those that were exclusively expressed in testis (Amory, 2016; O'Rand et al., 2016); it had been assumed that expression of a target like sAC in somatic tissues would lead to unsurmountable mechanism-based side effects. However, three advances question this dogma:

- 1) sAC isoforms expressed in somatic tissues may differ from the C1-C2 containing isoforms abundantly expressed in testis and sperm.
- 2) Advances in vaginal delivery methods afford the opportunity to supply sAC inhibitors designed for topical use to selectively block sperm functions in the female reproductive tract with little systemic exposure.
- 3) The appreciation that besides male infertility, the phenotypes of sAC loss in humans and mice are due to chronic loss, which suggests acute acting inhibitors can safely provide “on-demand” contraception in men. Such contraceptives would be taken only as needed to temporarily render men infertile.

Targeting sperm specific soluble adenylyl cyclase isoforms

As described above, the biochemically characterized and pharmacologically targeted sAC isoforms, sACt and sACfl are expressed in testis and sperm (Jaiswal and Conti, 2001; Hess et al., 2005). According to a recent human gene expression profiling database (Karczewski et al., 2020), these C1-C2 containing isoforms are not found in somatic tissues; instead somatic tissues seem to use an alternate start site (Jaiswal and Conti, 2001; Geng et al., 2005; Schmid et al., 2007; Farrell et al., 2008; Middelhaufe et al., 2012; Karczewski et al., 2020) to express only C2-domain containing isoforms from the ADCY10 locus (Figure 2). cDNAs encoding sAC-C2 isoforms have been isolated from various organs, including the kidneys, small intestine (Geng et al., 2005) and lungs (Schmid et al., 2007) but more research needs to be done to fully elucidate their activity, expression, distribution, and localization. Like all mammalian nucleotidyl cyclases, sAC isoforms are Class III ACs, and their catalytic center is formed at the interface between two catalytic domains. In C1-C2 containing sACt and sACfl, the active site is formed from the intramolecular dimerization of two structurally similar but unique catalytic domains (i.e., C1 and C2) (Tang and Hurley, 1998; Wiggins et al., 2018). The interface of these domains contains a catalytic site which binds substrate ATP and a pseudo-symmetrical degenerate “active” site that is catalytically inactive and binds the sAC-specific activator HCO_3^- (BBS) (Kleinboelting et al., 2014; Steegborn, 2014). Like C1-C2 isoforms of sAC, tmACs' active sites are formed via intramolecular dimerization of two related catalytic domains, but guanylyl cyclases (GCs) employ different molecular architectures (Tesmer et al., 1997; Kamenetsky et al., 2006). The various genes encoding GCs all contain only a single catalytic domain; soluble GCs form active sites via

intermolecular dimerization of subunits containing structurally similar but unique catalytic domains while membrane GCs form intermolecular homodimers for activity. It remains unclear how sAC-C2 isoforms form an active cyclase. In C1-C2 sAC isoforms, the C1 domain contributes key catalytic residues that would be absent if sAC-C2 isoforms were to homodimerize, and no known C1-like binding partner has yet been identified for sAC-C2. The newest generation of potent and selective inhibitors were generated via structure-based drug design using a crystal structure of human C1-C2 containing sAC (Fushimi et al., 2021). These more potent inhibitors, which fill both the BBS and the active site formed at the interface of C1 and C2, making contacts in both domains, were used to validate sAC as a contraceptive target. Thus, it remains possible that these inhibitors are specific for the sAC isoform expressed predominantly, if not exclusively, in sperm; however, this strategy awaits further information about tissue distribution and characterization of other sAC isoforms, including the sAC-C2 isoforms which are hypothesized to be the isoforms expressed in somatic tissues.

Intravaginal drug delivery

Leveraging chemical modifications to tailor routes of administration or pharmacokinetic properties is a standard technique to target specific tissues (e.g., topical drugs which work locally with little systemic exposure) or organs (e.g., using first pass metabolism to concentrate drug in liver (Niemi, 2007; Tu et al., 2013; Zhou et al., 2015; Li et al., 2019) or increasing urinary excretion to target the kidneys). For contraception, because sAC is essential for hyperactivated motility of human sperm (Balbach et al., 2021), delivering a sAC inhibitor to the vagina would block ejaculated sperm from progressing beyond the cervix. Thus, inhibiting sAC in sperm inside the vagina would trap them in this inhospitable environment and prevent fertilization. This idea is already validated *in vitro* with post-ejaculated sperm (Balbach et al., 2021; Ferreira et al., 2021). Specifically, sAC inhibitors interrupt capacitation, inhibit progressive motility, and block acrosome reaction in human sperm when added post-ejaculation (i.e., after capacitation has begun), which is exactly when a vaginally delivered contraceptive would encounter activated sperm. sAC inhibitors suitable for intravaginal delivery would have to be tested for stability and efficacy in the acidic vagina, and they would be designed to include elements providing metabolic instabilities upon reaching systemic circulation. Metabolic instability in the bloodstream would limit distribution of compound absorbed through the vaginal mucosa and prevent inhibitors from affecting other organs. Such, topical sAC inhibitors, delivered *via* intravaginal devices (i.e., rings, films, gels, or suppositories), would provide non-hormonal female contraception with diminished concerns for systemic adverse effects.

Topical administration in the female reproductive tract is an area of active research in the contraception field. Many topical

formulations are well tolerated by women and each has their own advantages. Currently, there are multiple FDA-approved, hormone-based contraceptives in the form of vaginal rings (i.e. NuvaRing, Annovera). NuvaRing is a once monthly vaginal ring (FDA Insert, 2001), whereas Annovera is used for a full year (FDA Insert, 2018). Using a sAC inhibitor as the active drug for contraception provides the distinct advantage of being non-hormonal. Similar to existing intravaginal devices, sAC-based contraceptives could be formulated to be slow releasing rings providing long-term coverage for contraception, or as gels, films or suppositories, which would provide contraceptive protection acutely and used on-demand (i.e., only when necessary).

Vaginal delivery of a topical sAC inhibitor also offers an opportunity for developing multi-protection technology (MPTs) where contraception is provided along with protection from sexually transmitted infections (STIs) (Clark et al., 2014). Recent research has focused on developing vaginal topical delivery systems for the treatment of HIV-1 infections and other STIs (Woolfson et al., 2006; Robinson et al., 2018; Nel et al., 2021). A sAC inhibitor-based contraceptive would be ideal for incorporation into an MPT as it is non-hormonal and could be combined with other drugs in the topical formulation for multiple indications. Such a combination could be used long-term or acutely for short-term contraception and prevention of STIs.

Acute dosing

As mentioned above, sAC as a contraceptive target is genetically validated in both mice and men. KO mice (Esposito et al., 2004; Hess et al., 2005; Xie et al., 2006; Chen et al., 2013) and humans (Akbari et al., 2019) harboring sAC inactivating mutations are male specific sterile. In addition to being an uncommon example where a human mutation validates a therapeutic approach, the phenotypes of mice and men with sAC deletions reveal a strategy for an innovative paradigm for oral contraception. sAC KO humans and mice live relatively normal lives with modest adverse effects. Other than male-specific sterility, all known phenotypic consequences of sAC loss in mice and humans are “conditional” and dependent upon prolonged absence of sAC (Wiggins et al., 2018; Balbach et al., 2020). sAC KO men have increased propensity to form kidney stones (Akbari et al., 2019), which require years to form. Similarly, sAC KO mice have modestly increased intraocular pressure (Lee et al., 2011), which could eventually cause glaucoma but again, this would require years of sAC absence. These phenotypes indicate that intermittent dosing of an acutely acting sAC inhibitor would not elicit adverse effects, and suggest a paradigm of “on-demand” contraception, where a man would be rendered temporarily infertile minutes after a single dose of a fast-acting, short-lived inhibitor. With an on-demand birth control for men, the contraceptive effect as well as any other potential consequences would be gone after a few hours.

A similar on-demand strategy was successfully implemented with erectile dysfunction drugs. Like sAC, the cGMP-specific phosphodiesterase 5 (PDE5) is widely expressed (Bender and Beavo, 2006), yet acute PDE5 inhibitors (i.e., sildenafil, vardenafil) are sufficiently safe and used to treat erectile dysfunction (FDA Insert, 1998). In fact, the PDE5 inhibitor tadalafil lasts longer (~17 h) (FDA Insert, 2003) and is sufficiently safe for chronic use (Montorsi et al., 2004). Ideally, a sAC inhibitor for contraception would be taken 30–60 min before sexual activity and provide safe and effective contraception for 4–6 h. A sAC based on-demand contraceptive would change the contraception field, it would be a pharmacologic option that is non-hormonal while allowing for complete freedom for the individual to take the drug only when necessary.

On-demand oral contraception by sAC inhibitors may also be possible for females. For males, taking the drug before sexual activity, would inhibit sAC in epididymal sperm to block their ejaculation-induced activation. sAC inhibitors could also be formulated to achieve efficacious concentrations throughout the female reproductive tract. A female would take such a sAC inhibitor orally shortly before, or perhaps soon after, sex to interrupt capacitation and motility of post-ejaculated sperm. sAC inhibition would prevent sperm from progressing through the female reproductive tract to reach and fertilize the egg. Combining both ideas could lead to a “couples’ pill” where both partners take their respective drug at the same time to maximize contraceptive efficacy. A “couples’ pill” would enhance compliance by engaging both partners, and it could increase adoption by making the choice for contraception a joint decision.

Discussion

There is large unmet need in contraception and new methods must be developed, especially contraceptive methods which are non-hormonal and which provide additional choices for men. Currently, contraception is largely the responsibility of women; of all modern forms of contraception available, all but two are for women. The most widely used options for women are hormone-based pharmacologic methods (pills, patches, injectables, or rings), which have significant drawbacks including adverse effects and compliance issues (La Vecchia et al., 2001; Cushman et al., 2004; Kulier et al., 2004; Huber et al., 2006; Peachman, 2018; Cooper and Mahdy, 2021). Similarly, the only two options for men, surgical vasectomy or condoms, also suffer from compliance and inconvenience issues (Amory, 2016). Here we describe three innovative strategies for inhibiting the

bicarbonate-regulated sAC for contraceptive effect to fulfill this need: (1) targeting organ specific sAC isoforms; (2) leveraging chemical modification to alter route of administration and pharmacokinetic properties to have sAC-based drugs exert their effect only on the organ of interest; (3) using acute dosing instead of chronic dosing.

Data availability statement

The original contributions presented in the study are included in the article/supplementary material, further inquiries can be directed to the corresponding author.

Author contributions

All authors listed have made a substantial, direct, and intellectual contribution to the work and approved it for publication.

Funding

JF was supported by a fellowship from NIH (F31 HD105363). Work in the LL/JB laboratory is supported by grants from NIH (P50 HD100549, R01 HD088571, and R01 AG061290), Male Contraceptive Initiative, and USAID.

Conflict of interest

JB and LL licensed a panel of monoclonal antibodies directed against mammalian sAC to Millipore.

The remaining author declares that the research was conducted in the absence of any commercial or financial relationships that could be construed as a potential conflict of interest.

Publisher’s note

All claims expressed in this article are solely those of the authors and do not necessarily represent those of their affiliated organizations, or those of the publisher, the editors and the reviewers. Any product that may be evaluated in this article, or claim that may be made by its manufacturer, is not guaranteed or endorsed by the publisher.

Reference

- Acin-Perez, R., Salazar, E., Kamenetsky, M., Buck, J., Levin, L. R., and Manfredi, G. (2009). Cyclic AMP produced inside mitochondria regulates oxidative phosphorylation. *Cell Metab.* 9, 265–276. doi:10.1016/j.cmet.2009.01.012
- Akbari, A., Pipitone, G. B., Anvar, Z., Jaafarinia, M., Ferrari, M., Carrera, P., et al. (2019). ADCY10 frameshift variant leading to severe recessive asthenozoospermia and segregating with absorptive hypercalciuria. *Hum. Reprod.* 34, 1155–1164. doi:10.1093/humrep/dez048
- Amory, J. K. (2016). Male contraception. *Fertil. Steril.* 106, 1303–1309. doi:10.1016/j.fertnstert.2016.08.036
- Austin, C. R. (1951). Activation and the correlation between male and female elements in fertilization. *Nature* 168, 558–559. doi:10.1038/168558c0
- Baillie, G. S., Tejeda, G. S., and Kelly, M. P. (2019). Therapeutic targeting of 3', 5'-cyclic nucleotide phosphodiesterases: Inhibition and beyond. *Nat. Rev. Drug Discov.* 18, 770–796. doi:10.1038/s41573-019-0033-4
- Balbach, M., Beckert, V., Hansen, J. N., and Wachten, D. (2018). Shedding light on the role of cAMP in mammalian sperm physiology. *Mol. Cell. Endocrinol.* 468, 111–120. doi:10.1016/j.mce.2017.11.008
- Balbach, M., Fushimi, M., Huggins, D. J., Steegborn, C., Meinke, P. T., Levin, L. R., et al. (2020). Optimization of lead compounds into on-demand, nonhormonal contraceptives: Leveraging a public-private drug discovery institute collaboration. *Biol. Reprod.* 103, 176–182. doi:10.1093/biolre/iaaa052
- Balbach, M., Ghanem, L., Rossetti, T., Kaur, N., Ritagliati, C., Ferreira, J., et al. (2021). Soluble adenylyl cyclase inhibition prevents human sperm functions essential for fertilization. *Mol. Hum. Reprod.* 27, gaab054. doi:10.1093/molehr/gaab054
- Bender, A. T., and Beavo, J. A. (2006). Cyclic nucleotide phosphodiesterases: Molecular regulation to clinical use. *Pharmacol. Rev.* 58, 488–520. doi:10.1124/pr.58.3.5
- Biel, M. (2009). Cyclic nucleotide-regulated cation channels. *J. Biol. Chem.* 284, 9017–9021. doi:10.1074/jbc.R800075200
- Bitterman, J. L., Ramos-Espiritu, L., Diaz, A., Levin, L. R., and Buck, J. (2013). Pharmacological distinction between soluble and transmembrane adenylyl cyclases. *J. Pharmacol. Exp. Ther.* 347, 589–598. doi:10.1124/jpet.113.208496
- Bos, J. L. (2003). Epac: A new cAMP target and new avenues in cAMP research. *Nat. Rev. Mol. Cell Biol.* 4, 733–738. doi:10.1038/nrm1197
- Braun, T., and Dods, R. F. (1975). Development of a Mn²⁺-sensitive, "soluble" adenylate cyclase in rat testis. *Proc. Natl. Acad. Sci. U. S. A.* 72, 1097–1101. doi:10.1073/pnas.72.3.1097
- Braun, T., Frank, H., Dods, R., and Sepsenwol, S. (1977). Mn²⁺-sensitive, soluble adenylate cyclase in rat testis. Differentiation from other testicular nucleotide cyclases. *Biochim. Biophys. Acta* 481, 227–235. doi:10.1016/0005-2744(77)90155-3
- Buck, J., Sinclair, M. L., Schapal, L., Cann, M. J., and Levin, L. R. (1999). Cytosolic adenylyl cyclase defines a unique signaling molecule in mammals. *Proc. Natl. Acad. Sci. U. S. A.* 96, 79–84. doi:10.1073/pnas.96.1.79
- Buffone, M. G., Wertheimer, E. V., Visconti, P. E., and Krapf, D. (2014). Central role of soluble adenylyl cyclase and cAMP in sperm physiology. *Biochim. Biophys. Acta* 1842, 2610–2620. doi:10.1016/j.bbdis.2014.07.013
- Carlson, A. E., Quill, T. A., Westenbroek, R. E., Schuh, S. M., Hille, B., and Babcock, D. F. (2005). Identical phenotypes of CatSper1 and CatSper2 null sperm. *J. Biol. Chem.* 280, 32238–32244. doi:10.1074/jbc.M501430200
- Chaloupka, J. A., Bullock, S. A., Iourgenko, V., Levin, L. R., and Buck, J. (2006). Autoinhibitory regulation of soluble adenylyl cyclase. *Mol. Reprod. Dev.* 73, 361–368. doi:10.1002/mrd.20409
- Chang, M. C. (1951). Fertilizing capacity of spermatozoa deposited into the fallopian tubes. *Nature* 168, 697–698. doi:10.1038/168697b0
- Chen, J., Martinez, J., Milner, T. A., Buck, J., and Levin, L. R. (2013). Neuronal expression of soluble adenylyl cyclase in the mammalian brain. *Brain Res.* 1518, 1–8. doi:10.1016/j.brainres.2013.04.027
- Chen, X., Baumlín, N., Buck, J., Levin, L. R., Fregien, N., and Salathe, M. (2014). A soluble adenylyl cyclase form targets to axonemes and rescues beat regulation in soluble adenylyl cyclase knockout mice. *Am. J. Respir. Cell Mol. Biol.* 51, 750–760. doi:10.1165/rcmb.2013-0542OC
- Chen, Y., Cann, M. J., Litvin, T. N., Iourgenko, V., Sinclair, M. L., Levin, L. R., et al. (2000). Soluble adenylyl cyclase as an evolutionarily conserved bicarbonate sensor. *Science* 289, 625–628. doi:10.1126/science.289.5479.625
- Clark, J. T., Clark, M. R., Shelke, N. B., Johnson, T. J., Smith, E. M., Andreassen, A. K., et al. (2014). Engineering a segmented dual-reservoir polyurethane intravaginal ring for simultaneous prevention of HIV transmission and unwanted pregnancy. *PLoS One* 9, e88509. doi:10.1371/journal.pone.0088509
- Cooper, D. B., and Mahdy, H. (2021). *Oral contraceptive pills*. Treasure Island (FL): StatPearls.
- Cushman, M., Kuller, L. H., Prentice, R., Rodabough, R. J., Psaty, B. M., Stafford, R. S., et al. (2004). Estrogen plus progestin and risk of venous thrombosis. *JAMA* 292, 1573–1580. doi:10.1001/jama.292.13.1573
- Di Benedetto, G., Scalzotto, E., Mongillo, M., and Pozzan, T. (2013). Mitochondrial Ca²⁺ uptake induces cyclic AMP generation in the matrix and modulates organelle ATP levels. *Cell Metab.* 17, 965–975. doi:10.1016/j.cmet.2013.05.003
- Esposito, G., Jaiswal, B. S., Xie, F., Krajnc-Franken, M. A., Robben, T. J., Strik, A. M., et al. (2004). Mice deficient for soluble adenylyl cyclase are infertile because of a severe sperm-motility defect. *Proc. Natl. Acad. Sci. U. S. A.* 101, 2993–2998. doi:10.1073/pnas.0400050101
- Farrell, J., Ramos, L., Tresguerres, M., Kamenetsky, M., Levin, L. R., and Buck, J. (2008). Somatic 'soluble' adenylyl cyclase isoforms are unaffected in Sacy tm1Lex/Sacy tm1Lex 'knockout' mice. *PLoS One* 3, e3251. doi:10.1371/journal.pone.0003251
- FDA Insert (2018). ANNOVERA™ (segestrone acetate and ethinyl estradiol vaginal system). New York, NY: Food and Drug Administration.
- FDA Insert (2003). CIALIS (tadalafil) tablets, for oral use. Indianapolis, IN: Food and Drug Administration.
- FDA Insert (2001). NuvaRing® (etonogestrel/ethinyl estradiol vaginal ring). Whitehouse, NJ: Food and Drug Administration.
- FDA Insert (1998). VIAGRA (Sildenafil citrate) tablets, for oral use. New York, NY: Food and Drug Administration.
- Ferreira, J. J., Lybaert, P., Puga-Molina, L. C., and Santi, C. M. (2021). Conserved mechanism of bicarbonate-induced sensitization of CatSper channels in human and mouse sperm. *Front. Cell Dev. Biol.* 9, 733653. doi:10.3389/fcell.2021.733653
- Fushimi, M., Buck, H., Balbach, M., Gorovoy, A., Ferreira, J., Rossetti, T., et al. (2021). Discovery of TDI-10229: A potent and orally bioavailable inhibitor of soluble adenylyl cyclase (sAC, ADCY10). *ACS Med. Chem. Lett.* 12, 1283–1287. doi:10.1021/acsmchemlett.1c00273
- Gandhi, J. K., Roy Chowdhury, U., Manzar, Z., Buck, J., Levin, L. R., Fautsch, M. P., et al. (2017). Differential intraocular pressure measurements by tonometry and direct cannulation after treatment with soluble adenylyl cyclase inhibitors. *J. Ocul. Pharmacol. Ther.* 33, 574–581. doi:10.1089/jop.2017.0027
- Geng, W., Wang, Z., Zhang, J., Reed, B. Y., Pak, C. Y., and Moe, O. W. (2005). Cloning and characterization of the human soluble adenylyl cyclase. *Am. J. Physiol. Cell Physiol.* 288, C1305–C1316. doi:10.1152/ajpcell.00584.2004
- Gordeladze, J. O., Abyholm, T., Cusan, L., Clausen, O. P., and Hansson, V. (1982). Cellular localization of the Mn²⁺-dependent adenylyl cyclase in the human testis. *Arch. Androl.* 8, 199–204. doi:10.3109/01485018208987040
- Gordeladze, J. O., Purvis, K., Clausen, O. P., Rommerts, F. F., and Hansson, V. (1981). Cellular localization of the Mn²⁺-dependent adenylyl cyclase (AC) in rat testis. *Int. J. Androl.* 4, 172–182. doi:10.1111/j.1365-2605.1981.tb00701.x
- Hess, K. C., Jones, B. H., Marquez, B., Chen, Y., Ord, T. S., Kamenetsky, M., et al. (2005). The "soluble" adenylyl cyclase in sperm mediates multiple signaling events required for fertilization. *Dev. Cell* 9, 249–259. doi:10.1016/j.devcel.2005.06.007
- Holz, G. G., Leech, C. A., and Chepurny, O. G. (2014). New insights concerning the molecular basis for defective glucoregulation in soluble adenylyl cyclase knockout mice. *Biochim. Biophys. Acta* 1842, 2593–2600. doi:10.1016/j.bbdis.2014.06.023
- Huber, L. R., Hogue, C. J., Stein, A. D., Drews, C., Ziemann, M., King, J., et al. (2006). Contraceptive use and discontinuation: Findings from the contraceptive history, initiation, and choice study. *Am. J. Obstet. Gynecol.* 194, 1290–1295. doi:10.1016/j.ajog.2005.11.039
- Hurley, J. H. (1999). Structure, mechanism, and regulation of mammalian adenylyl cyclase. *J. Biol. Chem.* 274, 7599–7602. doi:10.1074/jbc.274.12.7599
- Jaiswal, B., and Conti, M. (2001). Identification and functional analysis of splice variants of the germ cell soluble adenylyl cyclase. *J. Biol. Chem.* 276, 31698–31708. doi:10.1074/jbc.M011698200
- Jaiswal, B. S., and Conti, M. (2003). Calcium regulation of the soluble adenylyl cyclase expressed in mammalian spermatozoa. *Proc. Natl. Acad. Sci. U. S. A.* 100, 10676–10681. doi:10.1073/pnas.1831008100
- Kamenetsky, M., Middelhaufe, S., Bank, E. M., Levin, L. R., Buck, J., and Steegborn, C. (2006). Molecular details of cAMP generation in mammalian cells: A tale of two systems. *J. Mol. Biol.* 362, 623–639. doi:10.1016/j.jmb.2006.07.045
- Karczewski, K. J., Francioli, L. C., Tiao, G., Cummings, B. B., Alfoldi, J., Wang, Q., et al. (2020). The mutational constraint spectrum quantified from variation in 141,456 humans. *Nature* 581, 434–443. doi:10.1038/s41586-020-2308-7

- Kleinboelting, S., Diaz, A., Moniot, S., Van Den Heuvel, J., Weyand, M., Levin, L. R., et al. (2014). Crystal structures of human soluble adenylyl cyclase reveal mechanisms of catalysis and of its activation through bicarbonate. *Proc. Natl. Acad. Sci. U. S. A.* 111, 3727–3732. doi:10.1073/pnas.1322778111
- Kopperud, R., Krakstad, C., Selheim, F., and Døskeland, S. O. (2003). cAMP effector mechanisms. Novel twists for an 'old' signaling system. *FEBS Lett.* 546, 121–126. doi:10.1016/s0014-5793(03)00563-5
- Kulier, R., Helmerhorst, F. M., Maitra, N., and Gulmezoglu, A. M. (2004). Effectiveness and acceptability of progestogens in combined oral contraceptives - a systematic review. *Reprod. Health* 1, 1. doi:10.1186/1742-4755-1-1
- La Vecchia, C., Altieri, A., Franceschi, S., and Tavani, A. (2001). Oral contraceptives and cancer: An update. *Drug Saf.* 24, 741–754. doi:10.2165/0002018-200124100-00003
- Lee, Y. S., Tresguerres, M., Hess, K., Marmorstein, L. Y., Levin, L. R., Buck, J., et al. (2011). Regulation of anterior chamber drainage by bicarbonate-sensitive soluble adenylyl cyclase in the ciliary body. *J. Biol. Chem.* 286, 41353–41358. doi:10.1074/jbc.M111.284679
- Lefkimmiatis, K., Leronni, D., and Hofer, A. M. (2013). The inner and outer compartments of mitochondria are sites of distinct cAMP/PKA signaling dynamics. *J. Cell Biol.* 202, 453–462. doi:10.1083/jcb.201303159
- Levine, N., and Kelly, H. (1978). Measurement of pH in the rat epididymis *in vivo*. *J. Reprod. Fertil.* 52, 333–335. doi:10.1530/jrf.0.0520333
- Li, T. T., An, J. X., Xu, J. Y., and Tuo, B. G. (2019). Overview of organic anion transporters and organic anion transporter polypeptides and their roles in the liver. *World J. Clin. Cases* 7, 3915–3933. doi:10.12998/wjcc.v7.i23.3915
- Litvin, T. N., Kamenetsky, M., Zarifyan, A., Buck, J., and Levin, L. R. (2003). Kinetic properties of "soluble" adenylyl cyclase. Synergism between calcium and bicarbonate. *J. Biol. Chem.* 278, 15922–15926. doi:10.1074/jbc.M212475200
- Mannowetz, N., Wandernoth, P. M., and Wennemuth, G. (2012). Glucose is a pH-dependent motor for sperm beat frequency during early activation. *PLoS ONE* 7, e41030. doi:10.1371/journal.pone.0041030
- Meinke, P. T. (2022). Transforming academic drug discovery. *Chembiochem* 23, e202100671. doi:10.1002/cbic.202100671
- Middelhaufe, S., Leipelt, M., Levin, L. R., Buck, J., and Steegborn, C. (2012). Identification of a haem domain in human soluble adenylate cyclase. *Biosci. Rep.* 32, 491–499. doi:10.1042/BSR20120051
- Montorsi, F., Verheyden, B., Meuleman, E., Junemann, K. P., Moncada, I., Valiquette, L., et al. (2004). Long-term safety and tolerability of tadalafil in the treatment of erectile dysfunction. *Eur. Urol.* 45, 339–344; discussion 344–345. doi:10.1016/j.eururo.2003.11.010
- Neer, E. J. (1978). Multiple forms of adenylyl cyclase. *Adv. Cycl. Nucleotide Res.* 9, 69–83. doi:10.1016/S0021-9258(17)30340-X
- Nel, A., Van Niekerk, N., Van Baelen, B., Malherbe, M., Mans, W., Carter, A., et al. (2021). Safety, adherence, and HIV-1 seroconversion among women using the dapivirine vaginal ring (DREAM): An open-label, extension study. *Lancet. HIV* 8, e77–e86. doi:10.1016/S2352-3018(20)30300-3
- Niemi, M. (2007). Role of OATP transporters in the disposition of drugs. *Pharmacogenomics* 8, 787–802. doi:10.2217/14622416.8.7.787
- O'Rand, M. G., Silva, E. J., and Hamil, K. G. (2016). Non-hormonal male contraception: A review and development of an eppin based contraceptive. *Pharmacol. Ther.* 157, 105–111. doi:10.1016/j.pharmthera.2015.11.004
- Ostrom, K. F., Lavigne, J. E., Brust, T. F., Seifert, R., Dessauer, C. W., Watts, V. J., et al. (2022). Physiological roles of mammalian transmembrane adenylyl cyclase isoforms. *Physiol. Rev.* 102, 815–857. doi:10.1152/physrev.00013.2021
- Peachman, R. R. (2018). Weighing the risks and benefits of hormonal contraception. *JAMA* 319, 1083–1084. doi:10.1001/jama.2018.0448
- Rahman, N., Ramos-Espiritu, L., Milner, T. A., Buck, J., and Levin, L. R. (2016). Soluble adenylyl cyclase is essential for proper lysosomal acidification. *J. Gen. Physiol.* 148, 325–339. doi:10.1085/jgp.201611606
- Ramos-Espiritu, L., Kleinboelting, S., Navarrete, F. A., Alvau, A., Visconti, P. E., Valsecchi, F., et al. (2016). Discovery of LRE1 as a specific and allosteric inhibitor of soluble adenylyl cyclase. *Nat. Chem. Biol.* 12, 838–844. doi:10.1038/nchembio.2151
- Robinson, J. A., Marzinke, M. A., Fuchs, E. J., Bakshi, R. P., Spiegel, H. M. L., Coleman, J. S., et al. (2018). Comparison of the pharmacokinetics and pharmacodynamics of single-dose tenofovir vaginal film and gel formulation (FAME 05). *J. Acquir. Immune Defic. Syndr.* 77, 175–182. doi:10.1097/QAI.0000000000001587
- Schmid, A., Sutto, Z., Nlend, M. C., Horvath, G., Schmid, N., Buck, J., et al. (2007). Soluble adenylyl cyclase is localized to cilia and contributes to ciliary beat frequency regulation via production of cAMP. *J. Gen. Physiol.* 130, 99–109. doi:10.1085/jgp.200709784
- Scott, J. D., Dessauer, C. W., and Taskén, K. (2013). Creating order from chaos: Cellular regulation by kinase anchoring. *Annu. Rev. Pharmacol. Toxicol.* 53, 187–210. doi:10.1146/annurev-pharmtox-011112-140204
- Sinclair, M. L., Wang, X. Y., Mattia, M., Conti, M., Buck, J., Wolgemuth, D. J., et al. (2000). Specific expression of soluble adenylyl cyclase in male germ cells. *Mol. Reprod. Dev.* 56, 6–11. doi:10.1002/(SICI)1098-2795(200005)56:1<6::AID-MRD2>3.0.CO;2-M
- Sriram, K., and Insel, P. A. (2018). G protein-coupled receptors as targets for approved drugs: How many targets and how many drugs? *Mol. Pharmacol.* 93, 251–258. doi:10.1124/mol.117.111062
- Steegborn, C. (2014). Structure, mechanism, and regulation of soluble adenylyl cyclases - similarities and differences to transmembrane adenylyl cyclases. *Biochim. Biophys. Acta* 1842, 2535–2547. doi:10.1016/j.bbdis.2014.08.012
- Suarez, S. S., and Pacey, A. A. (2006). Sperm transport in the female reproductive tract. *Hum. Reprod. Update* 12, 23–37. doi:10.1093/humupd/dmi047
- Tang, W. J., and Hurley, J. H. (1998). Catalytic mechanism and regulation of mammalian adenylyl cyclases. *Mol. Pharmacol.* 54, 231–240. doi:10.1124/mol.54.2.231
- Tesmer, J. J. G., Sunahara, R. K., Gilman, A. G., and Sprang, S. R. (1997). Crystal structure of the catalytic domains of adenylyl cyclase in a complex with G_{sa}-GTPγS. *Science* 278, 1907–1916. doi:10.1126/science.278.5345.1907
- Tian, G., Sandler, S., Gylfe, E., and Tengholm, A. (2011). Glucose- and hormone-induced cAMP oscillations in α- and β-cells within intact pancreatic islets. *Diabetes* 60, 1535–1543. doi:10.2337/db10-1087
- Tresguerres, M., Levin, L. R., and Buck, J. (2011). Intracellular cAMP signaling by soluble adenylyl cyclase. *Kidney Int.* 79, 1277–1288. doi:10.1038/ki.2011.95
- Tresguerres, M., Parks, S. K., Salazar, E., Levin, L. R., Goss, G. G., and Buck, J. (2010). Bicarbonate-sensing soluble adenylyl cyclase is an essential sensor for acid/base homeostasis. *Proc. Natl. Acad. Sci. U. S. A.* 107, 442–447. doi:10.1073/pnas.0911790107
- Tu, M., Mathiowetz, A. M., Pfefferkorn, J. A., Cameron, K. O., Dow, R. L., Litchfield, J., et al. (2013). Medicinal chemistry design principles for liver targeting through OATP transporters. *Curr. Top. Med. Chem.* 13, 857–866. doi:10.2174/1568026611313070008
- Visconti, P. E., Moore, G. D., Bailey, J. L., Leclerc, P., Connors, S. A., Pan, D., et al. (1995). Capacitation of mouse spermatozoa. II. Protein tyrosine phosphorylation and capacitation are regulated by a cAMP-dependent pathway. *Development* 121, 1139–1150. doi:10.1242/dev.121.4.1139
- Visconti, P. E., Westbrook, V. A., Chertihin, O., Demarco, I., Sleight, S., and Diekmann, A. B. (2002). Novel signaling pathways involved in sperm acquisition of fertilizing capacity. *J. Reprod. Immunol.* 53, 133–150. doi:10.1016/s0165-0378(01)00103-6
- Wang, X., Cai, B., Yang, X., Sonubi, O. O., Zheng, Z., Ramakrishnan, R., et al. (2020). Cholesterol stabilizes TAZ in hepatocytes to promote experimental non-alcoholic steatohepatitis. *Cell Metab.* 31, 969–986.e7. doi:10.1016/j.cmet.2020.03.010
- Wennemuth, G., Carlson, A. E., Harper, A. J., and Babcock, D. F. (2003). Bicarbonate actions on flagellar and Ca²⁺-channel responses: Initial events in sperm activation. *Development* 130, 1317–1326. doi:10.1242/dev.00353
- Wiggins, S. V., Steegborn, C., Levin, L. R., and Buck, J. (2018). Pharmacological modulation of the CO₂/HCO₃⁻/pH-calcium-and ATP-sensing soluble adenylyl cyclase. *Pharmacol. Ther.* 190, 173–186. doi:10.1016/j.pharmthera.2018.05.008
- Woolfson, A. D., Malcolm, R. K., Morrow, R. J., Toner, C. F., and McCullagh, S. D. (2006). Intravaginal ring delivery of the reverse transcriptase inhibitor TMC 120 as an HIV microbicide. *Int. J. Pharm.* 325, 82–89. doi:10.1016/j.ijpharm.2006.06.026
- Xie, F., Garcia, M. A., Carlson, A. E., Schuh, S. M., Babcock, D. F., Jaiswal, B. S., et al. (2006). Soluble adenylyl cyclase (sAC) is indispensable for sperm function and fertilization. *Dev. Biol.* 296, 353–362. doi:10.1016/j.ydbio.2006.05.038
- Zaccolo, M., Zerio, A., and Lobo, M. J. (2021). Subcellular organization of the cAMP signaling pathway. *Pharmacol. Rev.* 73, 278–309. doi:10.1124/pharmrev.120.000086
- Zhou, J., Xu, J., Huang, Z., and Wang, M. (2015). Transporter-mediated tissue targeting of therapeutic molecules in drug discovery. *Bioorg. Med. Chem. Lett.* 25, 993–997. doi:10.1016/j.bmcl.2015.01.016
- Zippin, J. H., Chen, Y., Nahirney, P., Kamenetsky, M., Wuttke, M. S., Fischman, D. A., et al. (2003). Compartmentalization of bicarbonate-sensitive adenylyl cyclase in distinct signaling microdomains. *FASEB J.* 17, 82–84. doi:10.1096/fj.02-0598fj
- Zippin, J. H., Chen, Y., Straub, S. G., Hess, K. C., Diaz, A., Lee, D., et al. (2013). CO₂/HCO₃⁻ and calcium-regulated soluble adenylyl cyclase as a physiological ATP sensor. *J. Biol. Chem.* 288, 33283–33291. doi:10.1074/jbc.M113.510073



OPEN ACCESS

EDITED BY

Val Watts,
Purdue University, United States

REVIEWED BY

Angelo Giovanni Torrente,
Université de Montpellier, France
Jules Hancox,
University of Bristol, United Kingdom

*CORRESPONDENCE

Rebecca A. B. Burton,
rebecca.burton@pharm.ox.ac.uk

SPECIALTY SECTION

This article was submitted to
Experimental Pharmacology and Drug
Discovery,
a section of the journal
Frontiers in Pharmacology

RECEIVED 24 May 2022

ACCEPTED 01 August 2022

PUBLISHED 29 August 2022

CITATION

Bose SJ, Read MJ, Akerman E, Capel RA,
Ayagama T, Russell A, Terrar DA,
Zaccolo M and Burton RAB (2022),
Inhibition of adenylyl cyclase 1 by
ST034307 inhibits IP₃-evoked changes
in sino-atrial node beat rate.
Front. Pharmacol. 13:951897.
doi: 10.3389/fphar.2022.951897

COPYRIGHT

© 2022 Bose, Read, Akerman, Capel,
Ayagama, Russell, Terrar, Zaccolo and
Burton. This is an open-access article
distributed under the terms of the
[Creative Commons Attribution License](https://creativecommons.org/licenses/by/4.0/)
(CC BY). The use, distribution or
reproduction in other forums is
permitted, provided the original
author(s) and the copyright owner(s) are
credited and that the original
publication in this journal is cited, in
accordance with accepted academic
practice. No use, distribution or
reproduction is permitted which does
not comply with these terms.

Inhibition of adenylyl cyclase 1 by ST034307 inhibits IP₃-evoked changes in sino-atrial node beat rate

Samuel J. Bose¹, Matthew J. Read¹, Emily Akerman¹,
Rebecca A. Capel¹, Thamali Ayagama¹, Angela Russell^{1,2},
Derek A. Terrar¹, Manuela Zaccolo³ and Rebecca A. B. Burton^{1*}

¹Department of Pharmacology, University of Oxford, Oxford, United Kingdom, ²Department of Chemistry, Chemistry Research Laboratory, University of Oxford, Oxford, United Kingdom,

³Department of Physiology, Anatomy and Genetics, University of Oxford, Oxford, United Kingdom

Atrial arrhythmias, such as atrial fibrillation (AF), are a major mortality risk and a leading cause of stroke. The IP₃ signalling pathway has been proposed as an atrial-specific target for AF therapy, and atrial IP₃ signalling has been linked to the activation of calcium sensitive adenylyl cyclases AC1 and AC8. We investigated the involvement of AC1 in the response of intact mouse atrial tissue and isolated guinea pig atrial and sino-atrial node (SAN) cells to the α -adrenoceptor agonist phenylephrine (PE) using the selective AC1 inhibitor ST034307. The maximum rate change of spontaneously beating mouse right atrial tissue exposed to PE was reduced from 14.5% to 8.2% ($p = 0.005$) in the presence of 1 μ M ST034307, whereas the increase in tension generated in paced left atrial tissue in the presence of PE was not inhibited by ST034307 (Control = 14.2%, ST034307 = 16.3%; $p > 0.05$). Experiments were performed using isolated guinea pig atrial and SAN cells loaded with Fluo-5F-AM to record changes in calcium transients (CaT) generated by 10 μ M PE in the presence and absence of 1 μ M ST034307. ST034307 significantly reduced the beating rate of SAN cells (0.34-fold decrease; $p = 0.003$) but did not inhibit changes in CaT amplitude in response to PE in atrial cells. The results presented here demonstrate pharmacologically the involvement of AC1 in the downstream response of atrial pacemaker activity to α -adrenoceptor stimulation and IP₃R calcium release.

KEYWORDS

inositol trisphosphate, adenylyl cyclase, cyclic AMP, cardiac atria, calcium signalling, pacemaking, sinoatrial node

Introduction

Cardiac activity is closely regulated by the action of Ca^{2+} dependent enzymes including calcineurin and Ca^{2+} /calmodulin-dependent kinase II (CaMKII), as well as Ca^{2+} mobilising agents such as inositol-1,4,5-trisphosphate (IP_3), cyclic ADP-ribose (cADPR) and nicotinic acid adenine-dinucleotide phosphate (NAADP) (Bers, 2002; Terrar, 2020). In ventricular and atrial cardiomyocytes, calcium handling is key to the process of excitation contraction coupling (ECC), which is primarily regulated via the action of β -adrenergic signalling (Bers, 2002). Although a more modest component, ECC in the atria and sino-atrial node (SAN) is also regulated by α -adrenergic signalling (Lipp et al., 2000; Mackenzie et al., 2002; Capel et al., 2021). In addition to the regulation of ECC, currents that contribute to the pacemaker potential in the SAN and atrioventricular node (AVN) are also highly dependent on the regulation of intracellular Ca^{2+} signalling (Hancox and Mitcheson, 1997; Lakatta et al., 2010; Capel and Terrar, 2015; Burton and Terrar, 2021). In nodal cells, the pacemaker potential is dependent upon diastolic depolarisation, in part due to the influence of the hyperpolarisation activated “funny” current I_f and local calcium release events from the sarcoplasmic reticulum (SR). Depolarisation leads to Ca^{2+} influx through L-type Ca^{2+} channels (LTCC, principally $\text{Ca}_v1.3$ in the SAN) subsequent Ca^{2+} release from the sarcoplasmic reticulum (SR) via ryanodine receptors (RyR), and activation of $\text{Na}^+/\text{Ca}^{2+}$ exchanger (NCX) (Lakatta et al., 2010; Tsutsui et al., 2018). In the atria and SAN, activation of the IP_3 signalling pathway and subsequent release of Ca^{2+} from the SR may also lead to downstream activation of calcium sensitive adenylyl cyclase (AC), including isoforms AC1 and AC8 (Georget et al., 2002; Mattick et al., 2007; Burton and Terrar, 2021; Capel et al., 2021).

Under normal physiological conditions, both cardiac ECC and pacemaker activity are primarily regulated via β -adrenergic and muscarinic signalling, leading to downstream activation of adenylyl cyclase, predominantly AC5 and AC6 (Katsushika et al., 1992; Premont et al., 1992), and subsequent generation of cyclic-adenosine monophosphate (cAMP) (Bers, 2002; Burton and Terrar, 2021). In ventricular cardiomyocytes, IP_3 receptors (IP_3R) are largely confined to the nuclear envelope and IP_3 signalling is not thought to play a major role in cellular Ca^{2+} handling (Nakayama et al., 2010; Tinker et al., 2016). However, IP_3 is thought to play a greater role in Ca^{2+} handling downstream of α -adrenergic signalling within the atria, and atrial cardiomyocytes show a higher overall expression of IP_3R with expression in the subsarcolemmal space (Lipp et al., 2000; Mackenzie et al., 2002; Tinker et al., 2016). Whilst the role of β -adrenergic signalling in the regulation of ECC and pacemaker activity is relatively well studied, less is known about the potential involvement of α -adrenergic activation, leading to the generation of IP_3 and diacylglycerol (DAG) *via* activation of protein kinase

C (PKC) in the regulation of these processes in the atria and SAN. Increasing evidence indicates that activation of IP_3R and subsequent Ca^{2+} release from SR, leads to downstream activation of adenylyl cyclase, potentially via the activation of calcium-sensitive isoforms AC1 and AC8 (Domeier et al., 2008; Terrar, 2020; Burton and Terrar, 2021; Capel et al., 2021). In the present study, we therefore chose to focus on investigating the downstream effects of α -adrenergic stimulation in these processes.

The role of AC1 in cardiac pacemaker cells

AC1 is preferentially expressed in the SAN compared to other regions of the heart, and is thought to play a role in the regulation of pacemaker activity via modulation of the hyperpolarisation activated “funny” current (I_f) (Mattick et al., 2007; Younes et al., 2008). In the SAN, spontaneous pacemaker activity is the result of the “coupled-clock” mechanism, involving tight coupling between rhythmic Ca^{2+} release from the SR (i.e., “ Ca^{2+} clock”), and rhythmic oscillations in the membrane potential (i.e., “membrane clock”) (Lakatta et al., 2010; Tsutsui et al., 2018). Indeed, it appears this coupling is essential for pacemaker function in human SAN cells (Tsutsui et al., 2018). Membrane clock activity results from the alternation and balance between depolarising currents (e.g., I_f , I_{CaL} , I_{sust}) and repolarising currents (e.g., I_{Ks} and I_{Kr}) (Difrancesco and Tromba, 1988; Difrancesco et al., 1991; Burton and Terrar, 2021). I_f is carried by the HCN channels and modulated by changes in cytosolic Ca^{2+} (Rigg et al., 2003), as well as sub-sarcolemmal cAMP (Difrancesco and Tortora, 1991; Burton and Terrar, 2021). I_f , and therefore SAN pacemaking, can thereby be influenced by phosphodiesterase (PDE) and AC activity (Difrancesco and Tortora, 1991; Mattick et al., 2007; Vinogradova et al., 2008).

AC1 activity modulates the I_f current in the SAN in the absence of β -adrenergic stimulation and contributes to the higher resting cAMP level in SAN cells compared to ventricular cells (Mattick et al., 2007; Younes et al., 2008). In addition, cAMP generated by AC1 may modulate RyR, SR Ca^{2+} -ATPase, NCX and LTCC, all of which are involved in determining spontaneous beating in the SAN (Younes et al., 2008). These observations suggest cAMP signalling, downstream of AC1 activation, is a crucial mechanism by which the Ca^{2+} clock and membrane clock are coupled in the SAN. Furthermore, the modulation of I_f by cytosolic Ca^{2+} appears to be independent of CaMKII as chelation of SAN Ca^{2+} using BAPTA reduces I_f , whereas inhibition of CaMKII is without effect (Rigg et al., 2003). Although CaMKII is essential for SAN pacemaker activity (Yaniv et al., 2013), the actions of CaMKII on pacemaker function are linked to effects on I_{CaL} rather than I_f (Vinogradova et al., 2000; Rigg et al., 2003). Conversely, inhibition of SAN ACs using the non-specific AC inhibitor MDL-12,330A reduces I_f , whilst inhibition of phosphodiesterase using IBMX to inhibit the breakdown of

basal cAMP increases I_f , suggesting a role for Ca^{2+} -activated ACs in regulating the I_f current in SAN cells (Mattick et al., 2007).

AC1 expression in atrial cardiomyocytes

In guinea pig atrial cardiomyocytes, AC1 and AC8 are localised in the plasma membrane in close proximity to type 2 IP_3 receptors ($\text{IP}_3\text{R2}$) on the SR (Capel et al., 2021). Non-specific inhibition of ACs using MDL-12,330A, or inhibition of PKA using H89, inhibits the increase in Ca^{2+} transient amplitude observed in isolated guinea pig atrial cardiomyocytes in response to either intracellular photorelease of caged IP_3 (IP_3/PM) or external stimulation of α -adrenergic signalling using phenylephrine (PE), thereby demonstrating that ACs can be activated downstream of IP_3R . The increase in spontaneous beating rate observed in intact murine right atria in response to PE is similarly inhibited using either MDL-12,330A or H89 (Capel et al., 2021), suggesting a role for Ca^{2+} -activated AC1 and/or AC8 in the positive inotropic response to IP_3 signalling in cardiac atria.

Given the potential role of AC1 in regulating the downstream effects of α -adrenergic signalling in both atrial cardiomyocytes and the SAN, we were interested in investigating the pharmacological modulation of AC1 in cardiac tissue. The development of small molecule AC1 inhibitors that are highly selective for AC1 over AC8 has been of interest for treatment of neuropathic and inflammatory pain, leading to the development of the compounds such as NB001 (Wang et al., 2011) and the chromone derivative ST034307 (Brust et al., 2017). In this study, we chose to investigate whether pharmacological inhibition of cardiac AC1 by ST034307 could affect the response to α -adrenergic signalling in both intact atrial tissue as well as isolated SAN cells.

Materials and methods

Animals

All animal experiments were performed in accordance with the United Kingdom Home Office Guide on the Operation of Animal (Scientific Procedures) Act of 1986. All experimental protocols (Schedule 1) were approved by the University of Oxford, Procedures Establishment License (PEL) Number XEC303F12.

Drugs and reagents

AC1 was inhibited using the AC1 selective inhibitor ST034307 (Tocris, United Kingdom), which has been shown to demonstrate selectivity for AC1 over other AC isoforms at concentrations below 30 μM (Brust et al., 2017). In all experiments, ST034307 was dissolved in DMSO to make 3 mM stock prior to addition to experimental solutions at a

final concentration of 1 μM and applied for at least 5 min for isolated cells, or 30 min for whole-tissue experiments in order to ensure sufficient tissue penetration.

Atrial myocyte isolation

Male Dunkin Hartley guinea pigs (300–550 g, Envigo, United Kingdom) were housed and maintained in a 12 h light-dark cycle with *ad libitum* access to standard diet and sterilized water. Guinea pigs were culled by concussion followed by cervical dislocation in accordance with Home Office Guidance on the Animals (Scientific Procedures) Act (1986). Atrial myocytes were isolated following the method of Collins et al. (2011). Hearts were rapidly excised and washed in physiological salt solution (PSS, in mM): NaCl 125, NaHCO_3 25, KCl 5.4, NaH_2PO_4 1.2, MgCl_2 1, glucose 5.5, CaCl_2 1.8, oxygenated with 95% O_2 /5% CO_2 (solution pH 7.4 after oxygenation and heating) to which heparin was added (final concentration = 20 $\text{IU}\cdot\text{mL}^{-1}$) to prevent clot formation in the coronary vessels. Hearts were then mounted on a Langendorff apparatus for retrograde perfusion via the aorta. Perfusion was initially carried out in a modified Tyrode solution containing (mM): NaCl 136, KCl 5.4, NaHCO_3 12, Na^+ pyruvate 1, NaH_2PO_4 1, MgCl_2 1, EGTA 0.04, glucose 5; gassed with 95% O_2 /5% CO_2 to maintain a pH of 7.4 at $35 \pm 1^\circ\text{C}$. After 2 min this was replaced with a digestion solution: the modified Tyrode above containing 100 μM CaCl_2 and either 0.6 mg/ml of collagenase (type II, Worthington Biochemical Corp., Lakewood, NJ, United States) or 0.02–0.04 mg/ml LiberaseTM TH (Roche, Penzberg, Germany), but no EGTA.

After this enzymatic digestion, the heart was removed from the cannula and the atria were separated from the ventricles. For the isolation of atrial myocytes, slices of the atria were triturated using a glass pipette and stored at 4°C in a high potassium medium containing (in mM): KCl 70, MgCl_2 5, K^+ glutamine 5, taurine 20, EGTA 0.1, succinic acid 5, KH_2PO_4 20, HEPES 5, glucose 10; pH to 7.2 with KOH. For the isolation of SAN cells, the translucent SAN region, located on the upper surface of the right atrium, in between the inferior and superior vena cava (Rigg et al., 2003), immediately medial to the crista terminalis was identified under a dissection microscope. Thin tissue strips encompassing the nodal region were dissected, triturated using a glass pipette and stored at 4°C in high potassium medium. For experiments, healthy atrial myocytes were identified based on morphology, and healthy SAN myocytes by morphology and the presence of spontaneous, rhythmic beating in the absence of electrical stimulation.

Murine atrial studies

Adult male CD1 mice (30–35 g, Charles River, United Kingdom) were housed in a 12 h light-dark cycle with

ad libitum access to standard diet and sterilized water. Mice were culled by concussion followed by cervical dislocation in accordance with Home Office Guidance on the Animals (Scientific Procedures) Act (1986). The heart was rapidly excised and washed in heparin-containing PSS. The ventricles were dissected away under a microscope and the atria were cleared of connective tissue before being separated. Right and left atrial preparations were mounted separately in a 37°C organ bath containing oxygenated PSS and connected to a force transducer (MLT0201 series, ADInstruments, United Kingdom) in order to visualize contractions. Resting tension was set between 0.2 and 0.3 g, and the tension signals were low-pass filtered (20 Hz for right atria and 25 Hz for left atria). Right atrial beating rate was calculated from the time interval between contractions. Left atria were electrically field stimulated at a constant rate of 5 Hz using a custom-built stimulator connected to coil electrodes positioned both sides lateral to the left atrial tissue. Voltage was set at the threshold for stimulating contraction plus 5 V, and was within the range 10–20 V for all experiments. In all experiments, preparations were allowed to stabilise at a resting beating rate (>300 bpm) in PSS for at least 30 min. After stabilisation (variation in average rate of a 10 s sample of no more than 2 bpm over a 10-min period or 0.01 g change in tension), metoprolol (1 µM) was added to the bath to ensure specificity to α -adrenergic effects, plus or minus ST034307 (1 µM). Each addition was allowed to stabilise for a further 30 min or until stability was achieved as described above. Cumulative concentrations of PE were added to the bath at intervals of 5 min (range 0.1–30 µM) in the presence of metoprolol. Preparations were excluded if stabilized beating rate under control conditions (PSS only) was less than 300 bpm, in the case of the right atrium, or if preparations were not rhythmic. Data were fitted using Log(agonist) versus response curves (three parameter model) by nonlinear regression using a least squares method (Prism v9). AC1 was inhibited using the AC1 selective inhibitor ST034307 (Tocris, United Kingdom) (Brust et al., 2017). ST034307 (1 µM) was added after stabilization of the preparations in the presence of metoprolol and applied for at least 30 min prior to PE additions. PE dose-response curves were started only after tissue had reached a stable response.

Immunocytochemistry

Immunocytochemical labelling and analysis was carried out using the method of Collins and Terrar (2012). Rabbit anti-AC1 (55067-1-AP) primary antibody was purchased commercially (ProteinTech, Manchester, United Kingdom) and used at a dilution of 1:200. Mouse anti-IP₃R monoclonal primary antibody IP₃R2 (sc-398434) was purchased commercially (Santa Cruz Biotechnology, Santa Cruz, CA, United States) and used at a dilution of 1:50. The specificity of antibody sc-398434 has been previously verified using Western blot by Lou et al. (2021). IP₃R

antibodies have been extensively covered in previous studies (Hattori et al., 2004; Ando et al., 2006; Uchida et al., 2010; Salvador and Egger, 2018). Isolated cardiac cells were plated onto flamed coverslips and left to adhere for 30 min at 4°C. Cells were first fixed in 4% paraformaldehyde-phosphate buffered saline (PBS) for 15 min. Once the cells were fixed, they were washed in PBS (3 changes, 5 min each). Cells were then permeabilised and blocked using the detergent Triton X-100 (0.1%), 10% horse serum and 10% BSA in PBS (Sigma-Aldrich) for 60 min at room temperature to reduce non-specific binding. After blocking, the cells were incubated with primary antibodies at 4°C overnight dissolved in blocking solution. The next day, cells were first washed with PBS (3 changes, 5 min each) before being incubated with secondary antibodies; AlexaFluor -488 or -546 conjugated secondary antibodies (Invitrogen, United Kingdom), raised against the appropriate species, at room temperature for 120 min in PBS then washed with PBS (3 changes, 5 min each). Finally, the cells were mounted using Vectashield with DAPI and permanently sealed with nail polish. Control cells where the primary or secondary was to be excluded were incubated with 10% horse serum and 10% BSA in PBS without addition of the relevant antibody.

Cells were stored in the dark at 4°C before imaging. Observations were carried out using a Nikon eclipse Ti inverted confocal microscope (Nikon) with a 63x/1.2 water objective Plan Apo VC 60x/1.2 WI DIC N2 lens. NIS-Element viewer (Nikon) was used to acquire multichannel fluorescence images. For detection of DAPI, fluorescence excitation was at 405 nm with emission collected at 450 nm. For detection of AlexaFluor 488, fluorescence excitation was at 488 nm with emission collected at 525 nm. Excitation at 561 nm was collected at 595 nm for detection of AlexaFluor 568. The two channels were imaged sequentially at 2048 × 2048 (12 bits). Z-stack images were collected at 2.112 µm sections.

Ca²⁺ transient imaging

For whole-cell fluorescence experiments, isolated atrial myocytes were incubated with membrane permeant Fluo-5F-AM (3 µM) for 10 min then plated to a glass cover slip for imaging. Cells were incubated for a further 10 min *in-situ* in the organ bath to allow time for cells to adhere to the cover slip before perfusion with PSS. Carbon fibre electrodes were used to field-stimulate Ca²⁺ transients at a rate of 1 Hz. All experiments were carried out at 35 ± 2°C (fluctuation within a single experiment was <0.5°C) under gravity-fed superfusion with PSS, oxygenated with 95% O₂/5% CO₂ (solution pH 7.4 after oxygenation and heating). Solution flow rate was 3 ml min⁻¹. Cells were visualized using a Zeiss Axiovert 200 with attached Nipkow spinning disc confocal unit (CSU-10, Yokogawa Electric Corporation, Japan). Excitation light, transmitted through the CSU-10, was provided by a 488 nm diode laser (Vortran Laser Technology Inc., Sacramento, CA, United States). Emitted light was passed through the CSU-10 and collected by an Andor

iXON897 EM-CCD camera (Oxford Instruments, United Kingdom) recorded at a minimum acquisition frame rate of 60 frames per second using μ Manager software (v2.0) and ImageJ (Exposure time = 3–10 ms; binning = 4×4). In order to avoid dye bleaching the cells were not continually exposed to 488 nm light. Instead, a video of 8–10 s of Ca^{2+} transients was recorded at discrete timepoints. Ca^{2+} transient time courses were analysed in ImageJ and ClampFit (version 10.4). For analysis of Ca^{2+} transient rise and decay times Ca^{2+} data were analysed using pClamp v10 (Molecular Devices, CA, United States) to generate times corresponding to 10%–90% and 10%–50% rise time, and 90%–10%, 90%–75%, 90%–50% and half width decay time. Decay phases of transients were also fitted using one phase decay least squares regression (Prism v9).

Statistics

Data were tested for normality by using a Shapiro-Wilk test in Prism v9 software (GraphPad, CA, United States). For all single cell data, two-way t-tests, repeated measures 2-way ANOVA or mixed effects analysis were used as appropriate, with Dunnett's or Tukey's post hoc test to compare groups to a single control or to all other groups as required ($\alpha = 0.05$). For SAN data, Sidak's multiple comparison was used to compare control and ST034307 data at all time points. Log[concentration]-response curves, used to estimate EC50s and maximum responses, were calculated using Prism v9 software (GraphPad, CA, United States), by fitting an agonist-response curve with a fixed slope to normalized response data. Normalized data was used to compare responses. Fitted values were compared using 2-way repeated measures ANOVA followed by Šidák's multiple comparisons or Fisher's LSD test. Data are presented as mean \pm SEM of recorded values, other than dose-response curve maximums and EC50 which are given as mean \pm 95% confidence interval of best-fit value.

Results

Inhibition of AC1 by ST034307 reduces the positive chronotropic effect of PE in the intact sino-atrial node

Spontaneously beating right atrial tissue preparations, which contain the intact SAN, can be used to indirectly record activity of the SAN through the measurement of beating rate using a force transducer (Capel et al., 2015; Macdonald, 2020; Capel et al., 2021), whilst intact left atria can be used to record changes in contractile force generated when stimulated at a constant rate and voltage (Capel et al., 2015; Capel et al., 2021). Inhibition of ACs has previously been shown to reduce the response of intact mouse right atria to α -adrenergic stimulation (Capel et al., 2021). We were therefore interested to see if the effect of ST034307 was specific to the right atria, or whether the inotropic effects of PE would be inhibited

by ST034307 in left atrial preparations. Isolated murine right and left atria were mounted separately in organ baths and perfused with PSS at 37°C in the presence of 1.0 μM metoprolol to inhibit β -adrenergic signalling. Dose response curves for either spontaneous beating rate (right atria, Figure 1A) or tension generated (left atria, Figure 1B) were generated in response to 0.1–30 μM PE.

In the absence of ST034307 but in the presence of metoprolol, the spontaneous beating rate of right atria increased by a maximum of 14.5% (95% confidence interval (CI) = 12.2–17.1%; $n = 15$) at 30 μM PE, with an EC50 of 0.9 μM (95% CI = 0.4–2.2 μM) (Figure 1A, round symbols). 1 μM ST034307 reduced the response of beating rate to PE at all concentrations tested (Figure 1A, square symbols), with a maximum increase of 8.2% (95% CI = 6.1–12.6%; $n = 12$) at 30 μM PE (EC50 = 3.9 μM ; 95% CI = 1.1–17.6 μM). This represented a significant overall reduction in the response to PE in the presence of ST034307 ($p = 0.005$, 2-way repeated measures ANOVA, PE vs. ST034307). For left atrial preparations (Figure 1B), PE increased the tension generated in response to electrical stimulation at 5 Hz. The maximum increase was 14.2% (95% CI = 11.2–18.5%; $n = 5$) at 30 μM PE, with an EC50 of 4.4 μM (95% CI = 1.92–18.5 μM). In the presence of ST034307, no difference was observed in the response to PE compared with control ($p > 0.05$, 2-way repeated measures ANOVA, PE vs ST034307). The maximum change in tension generated in the presence of ST034307 was 16.3% (95% CI = 11.7–23.3; $n = 7$) at 30 μM PE, with an EC50 of 0.9 μM (95% CI = 0.8–10.8 μM). The basal heart rate of right atria after stabilisation and before addition of metoprolol was 364 ± 15.5 bpm ($n = 12$). No change in the right atrial basal heart rate was observed on addition of either metoprolol (362 ± 16.3 bpm) or metoprolol plus ST034307 (359 ± 16.8 bpm) before addition of PE (Supplementary Figure S1).

Immunohistochemistry suggests IP₃R2 and AC1 are colocalised in isolated Guinea pig atrial and sino-atrial node myocytes

ST034307 inhibited the beating rate response of the intact SAN (right atrial preparations) but did not alter tension generation in the left atria in response to PE. This suggested that the effects of AC1 inhibition were limited to affecting chronotropy in the SAN but not inotropy in atrial tissue (Figure 1). We were interested in testing whether the pattern of AC1 and IP₃R2 in the SAN matched that observed in atrial cardiomyocytes reported previously (Capel et al., 2021). To determine structural and anatomical characterisation of AC1 and IP₃R2 in SAN myocytes from healthy guinea pig adult hearts, isolated SAN myocytes were fixed and immunolabelled for AC1 and IP₃R2. Figure 2 shows representative confocal images of SAN myocytes stained with primary antibodies raised against the AC1 (cyan) and IP₃R

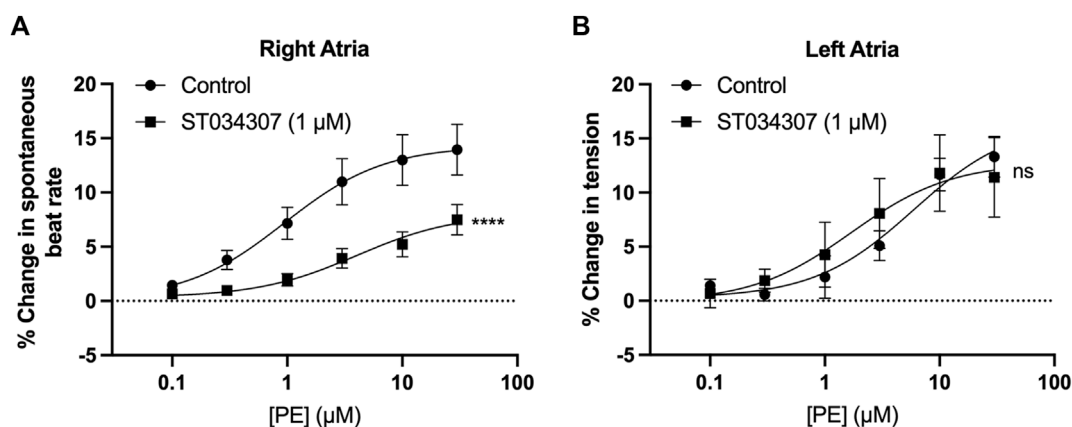


FIGURE 1

1 μ M ST034307 inhibits changes in chronotropy in intact mouse right atria with intact SAN but not inotropy in left atria. (A) Dose response curves to show the change in beating rate on cumulative addition of PE to spontaneously beating mouse right atria preparations under control conditions (circles, $n = 15$) and in the presence of 1 μ M ST034307 (squares, $n = 12$). (B) Dose response curves to show the change in tension generated on cumulative addition of PE to mouse left atria preparations under control conditions (circles, $n = 5$) and in the presence of 1 μ M ST034307 (squares, $n = 7$). Dose-response curves in (A,B) (solid lines) were fitted using log(agonist) vs. response (three-parameter model) using Graphpad Prism v9. Asterisks indicate significance level for effect of ST034307 compared to control at individual concentrations as determined using 2-way repeated measures ANOVA followed by Šidák's multiple comparisons test. Data are represented as mean \pm SEM; ns = not significant; *, $p < 0.05$; **, $p < 0.01$; ***, $p < 0.001$.

(magenta) proteins. IP₃R2 showed the expected staining on the sarcoplasmic reticulum membrane in SAN myocytes (Figure 2Ai) and AC1 puncta are located in close proximity to IP₃R2 (Figure 2Aiii, pixel size = $0.05 \times 0.05 \mu\text{m}$). ImageJ intensity analysis revealed, pixel by pixel by line intensity plots (Figures 2A,B) and in whole image intensity plots (Figures 2C–E), levels of colocalization between AC1 and IP₃R2 in SAN cells were higher ($R = 0.82 \pm 0.02$, $n = 7$) compared to atrial myocytes (Supplementary Figure S2, $R = 0.69 \pm 0.02$, $n = 11$, $p < 0.001$) and reported by Capel et al (2021) ($R = 0.5 \pm 0.05$, $n = 5$). These results together with recently published data (Capel et al., 2021), suggest that IP₃R-dependent signalling may be capable of stimulating Ca²⁺-dependent ACs and the close positioning of AC1 to IP₃R2 suggests that AC1 may be an effector of this interaction. To determine any non-specific labelling of secondary antibodies, control cells with no primary antibody, incubated with AlexaFluor -488 or -546 conjugated secondary antibodies alone, were imaged and found to give no detectable signal (data not shown).

Inhibition of AC1 by ST034307 does not alter Ca²⁺ transient amplitude in isolated Guinea pig atrial myocytes, but does inhibit pacemaker activity in isolated sino-atrial node myocytes

To further investigate the differences observed between SAN and left atria in Figure 1, and to determine if the effect

of AC1 inhibition by ST034307 is specific to the SAN, we investigated the effect of ST034307 on calcium transients generated in isolated guinea pig right atrial and SAN cells. We chose to investigate calcium transients in guinea pig cells, rather than mouse as guinea pig cardiac electrophysiology more closely resembles that of human. Whilst mouse heart physiology is comparable to human at the level of the whole heart, at the cellular level, guinea pig hearts share a more comparable action potential profile and heart rate to human and so is more appropriate for the study of isolated cells (O'Hara and Rudy, 2012).

Effect of ST034307 on calcium transients stimulated Guinea pig atrial cells

To measure changes in cytosolic Ca²⁺ in response to PE, isolated guinea pig right atrial myocytes were loaded with the cell-permeant Ca²⁺ sensitive dye Fluo-5F-AM. When stimulated at 1 Hz in PSS at 37°C, atrial myocytes exhibited the classical pattern of Ca²⁺ transient observed previously (Huser et al., 1996; Capel et al., 2021). We expressed calcium transient amplitude as change in mean cell fluorescence (F-F₀)/F₀ (Figures 3A–E). Addition of PE (10 μ M) to the perfusion solution resulted in a 0.4-fold increase in Ca²⁺ transient amplitude from 3.6 ± 0.8 to 4.8 ± 1.0 ($p = 0.009$; $n = 6$; paired t-test) (Figures 3A,C). As shown in Figure 3D, addition of 1 μ M ST034307 did not alter the basal Ca²⁺ transient amplitude compared to perfusion with PSS alone (PSS = 2.5 ± 0.3 , $n = 18$; 1 μ M ST = 1.9 ± 0.3 , $n = 15$; $p > 0.05$, unpaired t-test). In the

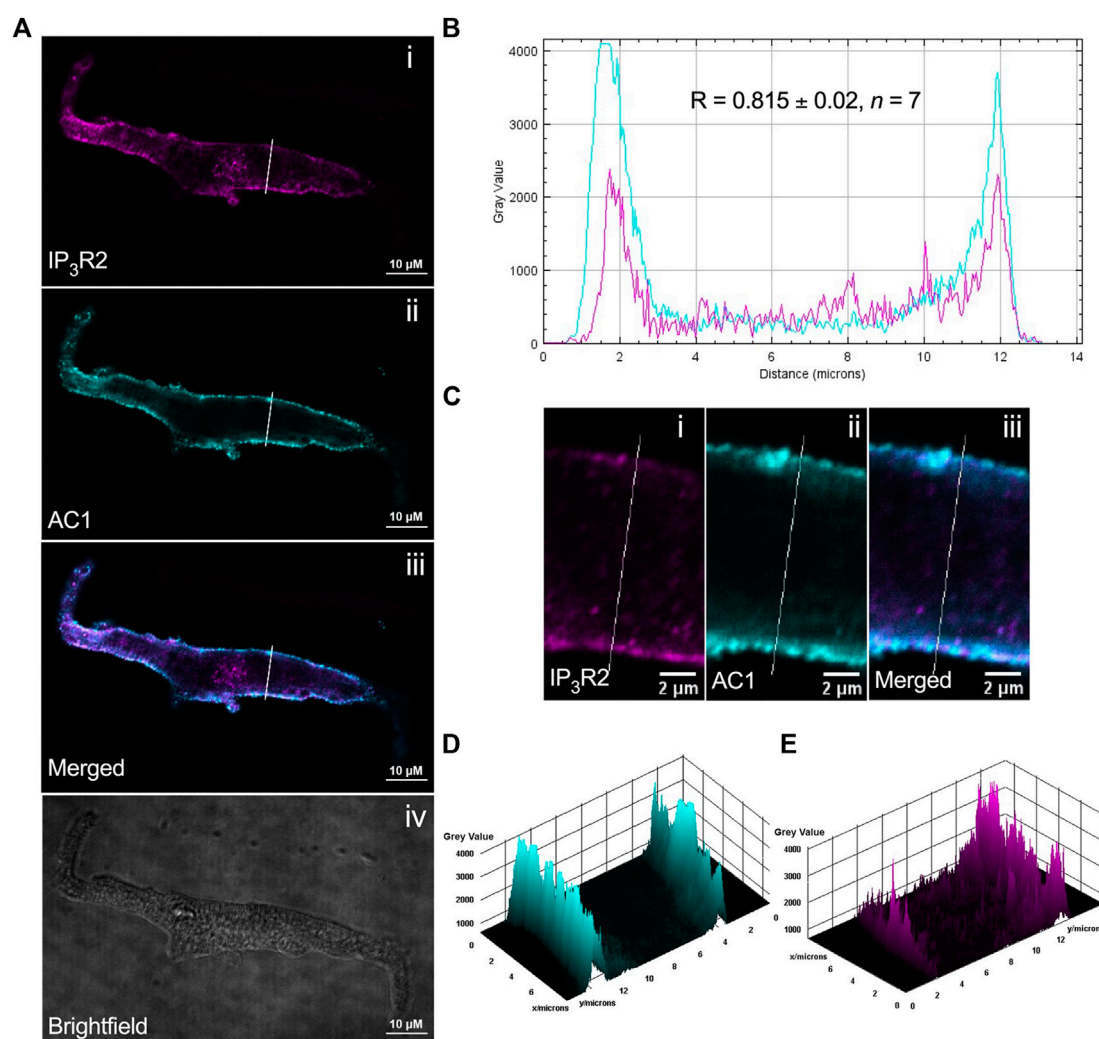


FIGURE 2

IP₃R2 is expressed in close proximity with AC1 in guinea pig SAN myocytes. **(A)** Representative example of a fixed, isolated guinea pig SAN myocyte immunolabelled for (i) IP₃R2 (magenta), (ii) AC1 (cyan), (iii) co-immunolabelled for IP₃R2 (magenta) and AC1 (cyan). Example brightfield image shown in (iv). **(B)** Intensity plot to show staining intensity along the white line shown in **(A)**. R-value calculated from $n = 7$ cells. **(C–E)** Intensity surface plots showing the distribution of staining of IP₃R2 [magenta, **(D)**] and AC1 [cyan, **(E)**] for the regions of cell shown in **(C)**. Scale bars representing 10 μm are indicated in **(A)** and 2 μm in **(C)**. For the purposes of presentation only, red and green channels have been represented as magenta and cyan, respectively.

presence of 1 μM ST034307, a 0.4-fold increase in the Ca^{2+} transient amplitude was observed in response to 10 μM PE added to the perfusion solution, resulting in a Ca^{2+} transient amplitude of 2.7 ± 0.4 ($p = 6.0 \times 10^{-4}$; $n = 15$) (Figures 3B,E). Comparison of the percentage change in response to PE between control and 1 μM ST034307 confirmed that there was no significant difference between the amplitude of change in the presence of ST ($p > 0.05$, unpaired t-test).

Further analysis of Ca^{2+} transient rise time and decay times confirmed that PE resulted in a significant decrease in the 90%–

10% decay time in control experiments from 369.5 ± 33.5 ms to 281.3 ± 24.8 ms ($p = 0.02$, 2-way ANOVA, $n = 8$) (Figure 3F, black bars) without changing the 10–90% rise time (Figure 3G, black bars). In the presence of 1 μM ST034307, the same pattern was also observed with a decrease in 90%–10% decay time from 355.0 ± 26.8 ms to 287.4 ± 22.5 ms ($p = 0.01$, 2-way ANOVA, $n = 17$) and no change in 10–90% rise time (Figures 3F,G, grey bars). These effects on decay and rise times were found not to differ between ST034307 and control experiments ($p > 0.05$, 2-way ANOVA).

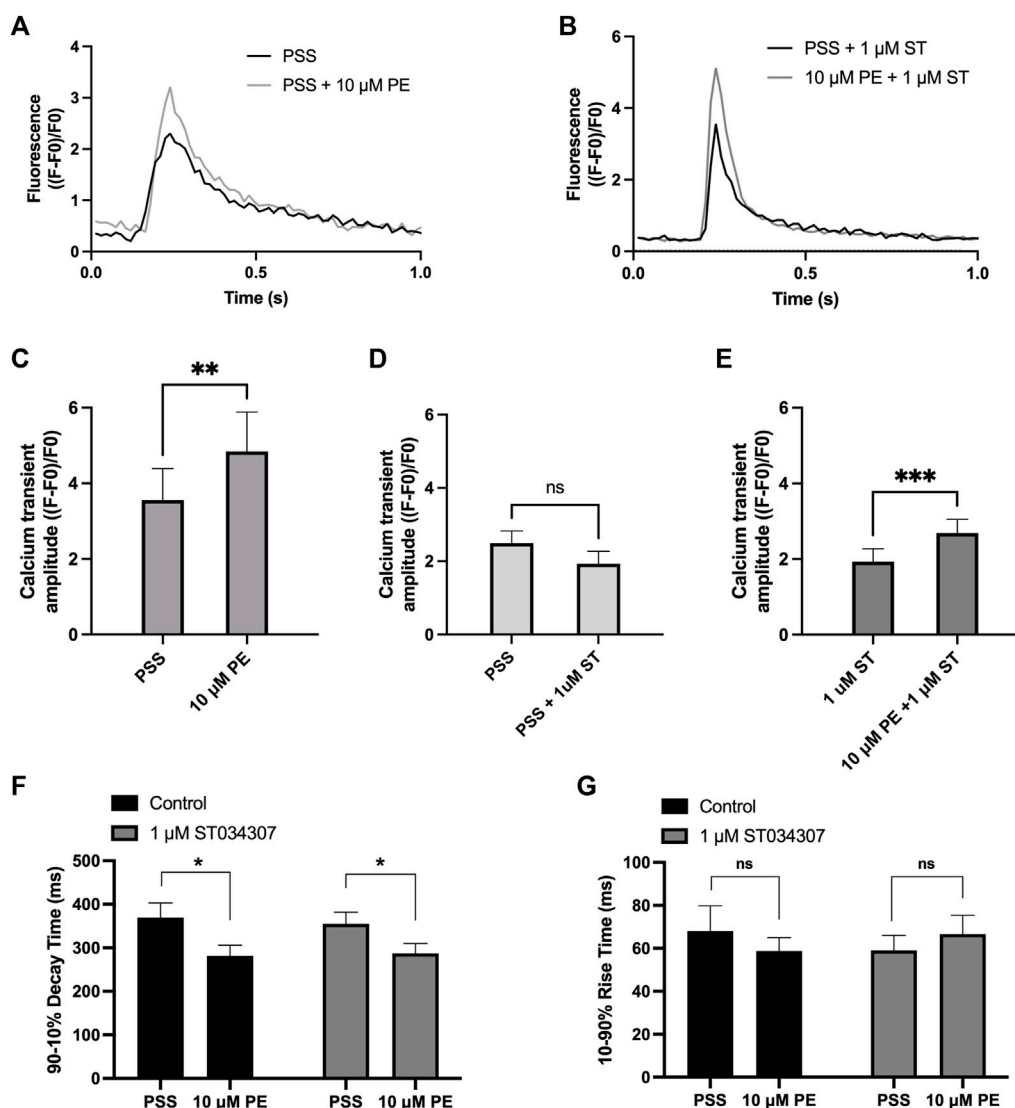


FIGURE 3

1 μM ST034307 does not alter the effect of PE on Ca^{2+} transients in isolated guinea pig atrial myocytes. (A,B): Representative average Ca^{2+} transients recorded from atrial myocytes during baseline recording (black trace) and following addition of PE (grey trace) in the absence (B) or presence (C) of 1 μM ST034307. (C): Effect of 10 μM PE on the Ca^{2+} transient amplitude recorded from isolated guinea pig atrial cells ($n = 6$; $N = 3$). (D): Effect of 1 μM ST034307 on the basal Ca^{2+} transient amplitude before addition of PE (PE, $n = 18$; ST, $n = 15$; $N = 3$). (E): Effect of 10 μM PE on the Ca^{2+} transient amplitude of cells in the presence of 1 μM ST034307 ($n = 15$; $N = 3$). (F,G): Effect of 10 μM PE on the 90–10% decay time (F) and 10–90% rise time (G) of Ca^{2+} transients recorded from cells perfused with PSS in the absence (black bars) or presence (grey bars) of 1 μM ST034307 before and after addition of 10 μM PE. All experiments were carried out at $35 \pm 2^\circ\text{C}$ and recordings were made 5 min following the start of each solution perfusion. Data are represented as mean \pm SEM. Data in C and E were analysed using paired t-test. Data in D were analysed using unpaired t-test. Data in F and G were analysed using two-way, repeated measures ANOVA followed by Šidák's multiple comparisons test; ns = not significant; *, $p < 0.05$; **, $p < 0.01$; ***, $p < 0.001$; n = cells; N = animals.

Effect of ST034307 on pacemaker activity in isolated sino-atrial node myocytes

To assess the contribution of AC1 to rate and calcium signalling in SAN cells, the response to PE under control conditions and during AC1 inhibition with ST034307 was measured in isolated, spontaneously firing guinea pig SAN

myocytes loaded with Fluo-5F-AM. Active, spontaneously beating SAN cells were identified based on morphology as indicated by the black arrow in Figure 4A. Under control conditions, fluorophore-loaded SAN myocytes superfused with PSS at 35°C spontaneously contracted at a rate of 104.9 ± 6.2 bpm ($n = 6$, Figure 4B, black bar). Although this rate is below the normal physiological rate for guinea pig SAN, lower rates are

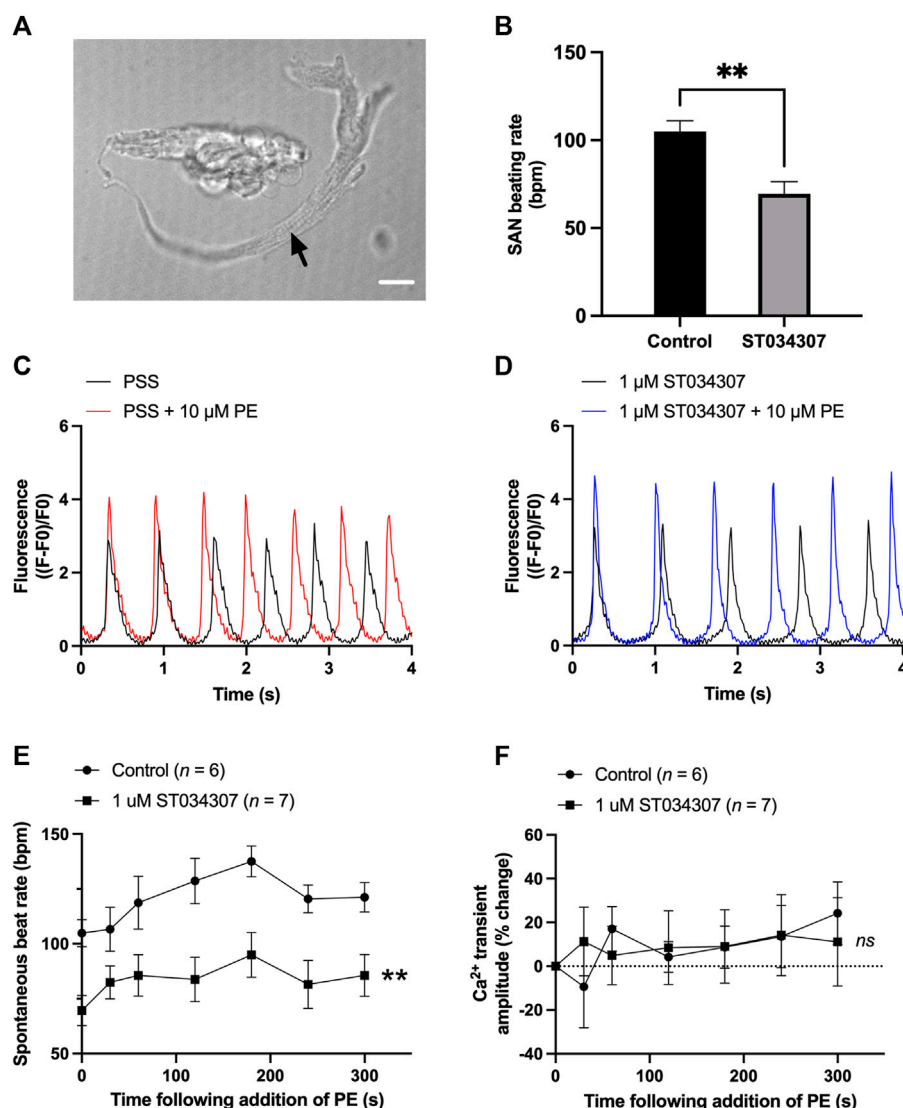


FIGURE 4

1 μM ST034307 inhibits the basal spontaneous beating rate and response to PE of isolated guinea pig SAN cells. (A) Brightfield image to show example of an isolated guinea pig SAN cell as indicated by black arrow. Scale bar represents 10 μm . (B) Effect of 1 μM ST034307 on the basal SAN cell Ca^{2+} transient amplitude before addition of PE. (C,D) Representative 4 s recordings of changes in fluorescence (expressed as $(F-F_0)/F_0$) from spontaneously beating guinea pig SAN cells loaded with Fluo-5F-AM in PSS (C) or in PSS + 1 μM ST034307 (D). Black and red/blue traces represent recordings before and 5 min after addition of 10 μM PE, respectively. Traces have been aligned according to the peak of the first transient. (E) Effect of 10 μM PE on the spontaneous beating rate of isolated SAN cells in the presence (squares) and absence (circles) of 1 μM ST034307. (F) Effect of 10 μM PE on the Ca^{2+} transient amplitude recorded from isolated SAN cells in the presence (squares) and absence (circles) of 1 μM ST034307. Time in E and F represents time following addition of PE to the perfusion solution with 0s representing levels in absence of PE. All experiments were carried out at $35 \pm 2^\circ\text{C}$. Data are represented as mean \pm SEM. Data in (B) were analysed using unpaired t-test. Data in (E) were analysed using two-way, repeated measures ANOVA followed by Šidák's multiple comparisons test. Data in (F) were analysed using mixed effects analysis followed by Šidák's multiple comparisons test; ns = not significant; ** = $p < 0.01$; n (control) = 6; n (ST034307) = 7; N = 5 animals.

expected following the loading of cells with a calcium fluorophore (Rigg and Terrar, 1996). Inclusion of 1 μM ST034307 in the perfusion solution resulted in a mean beating rate of 69.6 ± 6.8 bpm ($n = 7$, Figure 4B, grey bar) representing a significantly lower (0.34-fold) beat rate compared to control ($p =$

0.003, unpaired t-test). Superfusion of 10 μM PE led to a gradual increase in both calcium transient amplitude as well as the peak-to-peak firing rate over the course of 5 min as shown by the example traces in Figures 4C,D. On addition of 10 μM PE, the beating rate of SAN cells in the absence of ST034307 rose from

104.9 ± 6.2 bpm to a peak of 137.5 ± 7.0 bpm after 3 min ($p < 0.05$), before decreasing to a plateau, corresponding to 121.2 ± 6.7 at 5 min (Figure 4E, $n = 6$), potentially caused by desensitisation of α -adrenoceptors (Hiremath et al., 1991; Arce et al., 2017). In the presence of ST034307, beating rate increased to 94.9 ± 10.2 after 60s (Figure 4E, $n = 7$, $p < 0.05$). Overall, 1 μ M ST034307 was found to significantly inhibit the rise in SAN cell spontaneous beating rate in response to superfusion with 10 μ M PE ($p = 0.008$, mixed-effects analysis) (Figure 4E). Qualitatively, this increase was no longer gradual but plateaued rapidly, being complete by the time of the 30 s recordings (Figure 4E). Although qualitatively an increase in Ca^{2+} transient amplitude was observed in response to 10 μ M PE, as shown by the representative traces in Figures 4C,D, this increase was not found to be significant, as shown in Figure 4F ($p = 0.10$, mixed-effects analysis). This may be a consequence of the increased firing rate in response to PE, which would be expected to limit increases in calcium transient. However, in the presence of ST034307, mean Ca^{2+} transient amplitude was found to be consistently lower in the presence of ST034307 after 60 s perfusion with PE (Figure 4F).

Discussion

There is increasing evidence that activation of the IP_3 signalling pathway in atrial cells leads to the downstream activation of membrane bound Ca^{2+} -sensitive adenylyl cyclases, principally AC1 and AC8 (Mattick et al., 2007; Burton and Terrar, 2021; Capel et al., 2021). Recently published work has demonstrated that inhibition of IP_3 R using 2-APB, and non-specific inhibition of ACs using MDL-12,330A, prevents the rise in spontaneous beating rate observed in response to the α -adrenergic agonist PE in intact mouse right atria, as well as the rise in Ca^{2+} transient amplitude resulting from the intracellular release of caged- IP_3 in isolated guinea pig atrial myocytes (Capel et al., 2021). The purpose of the current study was therefore to investigate the effect of pharmacological modulation of AC1, using the drug ST034307, to determine if AC1 may play a role in the downstream effects of IP_3 signalling in cardiac tissue. Taken together, the data presented here suggest that AC1 plays a role in rate regulation at the SAN but is less important in determining inotropic responses.

The role of AC1 and IP_3 signalling in the heart

As shown in Figure 1A, 1 μ M ST034307 was found to significantly inhibit the increase in spontaneous beating rate of intact right atrial preparations. In contrast, ST034307 did not have a significant effect on the positive inotropic response to PE in paced murine left atria (Figure 1B) or potentiation of the

Ca^{2+} transient in isolated guinea-pig atrial myocytes (Figure 3). The simplest explanation for this observation is that AC1 is not involved or minimally contributes to the downstream effect of IP_3 signalling in non-SAN atrial myocytes but plays a more dominant role in the regulation of SAN pacemaker cells. Such an observation would be consistent with the observation that AC1 is preferentially expressed in the SAN and able to regulate I_f (Mattick et al., 2007).

Our immunohistochemistry work suggests that AC1 and IP_3 R2 are located within close proximity in guinea-pig atrial and SAN myocytes (Figure 2). Colocalization in SAN was higher than that observed in right atrial cells (Supplementary Figure S2). Although higher resolution studies would be required to establish colocalization within the level required to form a localised signalling domain, the proximity of IP_3 R2 and AC1 in both SAN and atrial cells demonstrated in Figure 2 and Supplementary Figure S2 raises the possibility that Ca^{2+} released *via* IP_3 R2 may influence the activity of AC1 in the SAN. Due to the relatively low resolution of fluorescent immunocytochemistry, the exact localisation of AC1 in cardiac cells, which may be dynamic, remains unclear. In both SAN (Figure 2A) and atrial cells (Supplementary Figure S2), expression of both AC1 and IP_3 R2 was concentrated most strongly within the periphery of the cells, however it was also seen along the striations, corresponding to t-tubules. AC1 has previously been found to be preferentially found in caveolae in rabbit SAN cells (Younes et al., 2008), while in mouse SAN cells, IP_3 R have been found to be in terminal SR in close proximity to the plasma membrane (Ju et al., 2011). These patterns of expression appear to coincide with our own observations for expression in guinea pig atrial and SAN cells (Figure 2). Previous work has suggested that AC1 might be located close to but not at the surface membrane, though still within reach of Ca^{2+} released *via* IP_3 R (Collins and Terrar, 2012; and see Burton and Terrar, 2021). Higher resolution EM work will be required in the future to provide more information on the precise location of AC1.

Ca^{2+} -sensitive ACs are implicated in atrial IP_3 signalling since BAPTA, MDL-12,330A and W-7 (calmodulin inhibitor) all abolish the effects of PE on I_{CaL} (Wang et al., 2005). It is possible that IP_3 mediated Ca^{2+} release can lead indirectly to AC1 activation via triggering other Ca^{2+} signals in different regions of the cells. One hypothesis that has been proposed is that local SR Ca^{2+} release from IP_3 R leads to a localized elevation in $[\text{Ca}^{2+}]$ at the ryanodine receptor, leading to amplification of RyR Ca^{2+} release and activation of LTCC (Lipp et al., 2000; Liang et al., 2009). However, the abolition of response to exogenously applied IP_3 in the presence of MDL appears to rule out this possibility, as this pathway would be expected to remain following inhibition of ACs (Capel et al., 2021). Another possibility however is that IP_3 R Ca^{2+} release triggers activation of AC1 indirectly, for example *via* amplification of store operated Ca^{2+} entry (SOCE). In HEK293 cells, AC1 and AC8 are significantly activated by SOCE (Fagan et al., 1996) and SOCE

is known to occur in close proximity to IP₃Rs (Sampieri et al., 2018). Furthermore, it has been shown that AC8 interacts directly with Orai1, the pore forming subunit of SOCE channels (Willoughby et al., 2012), and in HeLa cells, activation of IP₃R clusters tethered below the plasma membrane by the KRas-induced actin-interacting protein (KRAP) leads to localised depletion of ER Ca²⁺, which in turn leads to SOCE via the activation of stromal interaction molecule 1 (STIM1) (Thillaiappan et al., 2021). Interestingly, in isolated mouse SAN cells, the SOCE inhibitor SKF-9665 inhibited Ca²⁺ influx in SAN in response to pharmacological SR unloading and reduced the spontaneous rate by 27% in these conditions (Ju et al., 2007). It remains to be explored whether this finding involves Ca²⁺-activated adenylyl cyclases. The roles of IP₃ and activation of SOCE in cardiac cells, and the potential for downstream regulation of AC activity, therefore warrants future investigation.

The role of AC1 and IP₃ signalling in cardiac pacemaker activity

Pacemaker activity in mouse SAN cells can undergo modulation by both IP₃ agonists and antagonists, and this modulation can be abolished following IP₃R2 knock-out, demonstrating that IP₃ signalling can play a role in regulating pacemaker activity (Ju et al., 2011). In addition, IP₃ has been shown to induce Ca²⁺ sparks in close proximity to the surface membrane in pacemaker cells, and it has been suggested that this may lead to modulation of inward Na⁺/Ca²⁺ exchange current or activation of alternative Ca²⁺ dependent currents (Ju et al., 2012). Both IP₃R2 (Ju et al., 2011) and AC1 (Mattick et al., 2007; Younes et al., 2008) are expressed in the SAN (Figure 2), and previous studies have shown potential for activation of Ca²⁺-sensitive adenylyl cyclases downstream of IP₃R Ca²⁺ release in SAN cells as well as in non-pacemaker cells (Mattick et al., 2007; Ju et al., 2012). These previous observations support a role for the Ca²⁺-activated adenylyl cyclases AC1 and AC8 in atrial and SAN IP₃ signalling, however the involvement of other adenylyl cyclases cannot be ruled out based on these data alone.

In our experiments, ST034307 was found to significantly reduce the positive chronotropic effect of PE in mouse right atria, reducing the maximal response to PE without changing EC₅₀ (Figure 1A), suggesting that the effects of ST034307 are via inhibition of a target within the IP₃ signalling pathway. However, the effects of PE on inotropy in the left atria were unaffected by ST034307 (Figure 1B). Similarly, ST034307 reduced the spontaneous Ca²⁺ transient firing rate in isolated guinea-pig SAN cells (Figure 4B), as well as the response to PE in SAN cells (Figure 4E) but did not inhibit increases in Ca²⁺ transient amplitude in response to PE in either atrial (Figure 3) or SAN cells (Figure 4). AC1 is implicated as being directly involved in the positive chronotropic effect of the

IP₃ signalling pathway since application of the non-specific AC inhibitor MDL-12,330A abolishes the positive chronotropic response to PE in the absence of β-adrenergic signalling (Capel et al., 2021), thus supporting that cAMP production by ACs is involved in the chronotropic response to IP₃R activation. Consistent with this hypothesis, AC1 and AC8 are present in the SAN plasma membrane and either or both isoforms potentiate the pacemaker current (Mattick et al., 2007). Furthermore, both AC1 (Younes et al., 2008) and IP₃R2 localise in close proximity to caveolae in SAN cells (Barbuti et al., 2004; Ju et al., 2011).

Interestingly, in intact, spontaneously beating right atria, we did not observe a decrease in beating rate on addition of ST034307 before addition of phenylephrine (Supplementary Figure S1). Based on the observation that basal rate was decreased in isolated guinea pig SAN cells (Figure 4B), it would be expected that a decrease would also be observed in the intact SAN on addition of ST034307. In previous work, non-selective inhibition of adenylyl cyclase using MDL-12330 has been shown to decrease basal activity in mouse right atria in the presence of β-adrenergic inhibition (Capel et al., 2021). In the present study, the lack of inhibition in basal activity in the intact mouse right atria following inhibition of AC1 may reflect compensation by the calcium sensitive adenylyl cyclase AC8.

The specificity of cAMP signalling is known to rely on localisation within micro- (Zaccolo and Pozzan, 2002) and nano-domains (Surdo et al., 2017). Traditionally, cAMP has been thought to act primarily *via* protein kinase A (PKA) (Walsh et al., 1968; Krebs and Beavo, 1979), and cyclic nucleotide-gated ion channels (Fesenko et al., 1985) to influence cardiomyocyte contractile sensitivity as well as regulating L-type Ca²⁺ channel (LTCC) activity (Chen-Izu et al., 2000; Harvey and Clancy, 2021). However more recent work has demonstrated that cAMP may also act via exchange proteins directly activated by cAMP (EPACs) (de Rooij et al., 1998), as well as “Popeye domain” containing proteins (Brand, 2005; Zaccolo et al., 2021). The downstream effects of cAMP signalling in cardiomyocytes can therefore influence a wide range of cellular processes, including gene expression and cell morphology, in addition to electrical and contractile activity (Harvey and Clancy, 2021). This heterogeneity in function is the result of spatial confinement and localised compartmentalisation of cAMP signalling (Zaccolo and Pozzan, 2002; Zaccolo et al., 2021). The existence of a compartmentalised signalling domain involving both AC1 and IP₃R2 in SAN cells could explain the results demonstrated in the current study as well as previous observations (Capel et al., 2021). Such localisation would explain why the specificity of this Ca²⁺ signal is not lost despite constant global Ca²⁺ transients within SAN cells and may also explain why inhibition of AC1 by ST034307 inhibits beating rate in the SAN without causing an inhibition of calcium transients, which result from downstream release of calcium via RyR, in atrial and SAN cells (Figures 3, 4). Moreover, since AC1 regulation by Ca²⁺ is biphasic (Fagan et al.,

1996), it is possible that IP₃ induced stimulation of AC1 only occurs after cytosolic Ca²⁺ and the membrane potential have decreased, meaning this additional cAMP is likely only produced during the early and late phase of diastole allowing stimulation of I_f by AC1 at the correct time point. Our findings suggest that within SAN cells, Ca²⁺ released from IP₃R can activate either directly or indirectly AC1 and that this can modulate both basal and stimulated pacemaker mechanisms. Such a mechanism would be comparable but independent of that by which the release of Ca²⁺ from RyR (Rigg and Terrar, 1996; Bogdanov et al., 2001), or Ca²⁺ influx via the L-type (Mangoni et al., 2003; Jones et al., 2007) or T-type Ca²⁺ channels (Huser et al., 1996) regulates basal pacemaker activity.

In the present study, β -adrenergic stimulation was excluded by the inhibition of β -adrenergic receptors using metoprolol, however calcium release following β -adrenergic stimulation could also be expected to result in activation of AC1, which has been shown to respond to Ca²⁺ at concentrations corresponding to the full physiological range (Younes et al., 2008). It has been previously shown however that basal cAMP in the SAN is maintained by Ca²⁺-sensitive ACs and that this process is sensitive to cytosolic Ca²⁺ buffering using BAPTA, whereas changes in cAMP in response to β -adrenergic stimulation are not (Younes et al., 2008). These previous observations, together with our current observations in the absence of β -adrenergic stimulation provide further indirect evidence that the regulation of calcium sensitive ACs in the SAN occurs independently of β -adrenergic stimulation, likely due to the compartmentalisation of calcium signalling with these cells, which would result from the combination of close proximity of IP₃R2 and AC1, coupled with the limitation of cAMP diffusion by PDEs (Zaccolo and Pozzan, 2002; Surdo et al., 2017).

Of note, 1 μ M ST034307 did not abolish the response to PE in right atrial tissue (Figure 2A), although based on the reported IC₅₀ of 2.3 μ M (Brust et al., 2017), this dose of ST may have been insufficient to cause maximal AC1 inhibition. Whilst our findings suggest a role for AC1 downstream of IP₃ mediated Ca²⁺ release, in the absence of a specific AC8 inhibitor, our results cannot rule out the possibility that AC8 is also involved. At the time of writing no such specific AC8 inhibitor is commercially available.

Clinical relevance

Abnormal Ca²⁺ signalling underlies the pathology of many forms of cardiac disorders and arrhythmias, including AF (Landstrom et al., 2017). Current rate control medication for diseases such as heart failure and AF target either β -adrenergic signalling, Na⁺/K⁺-ATPase, or I_f, while few selective pharmacological treatments exist for sinus node dysfunction. Expression of IP₃R2 in atrial cardiomyocytes is known to be six

times greater in atrial myocytes compared to ventricular myocytes (Lipp et al., 2000), and IP₃R2 is the predominant isoform in the SAN, showing similar expression levels to right atrial tissue (Ju et al., 2011). Expression of IP₃R is known to be upregulated in human patients with chronic AF (Yamda et al., 2001) as well as the canine AF model (Zhao et al., 2007). The IP₃ signalling pathway has therefore been identified as a potential atrial-specific target for the treatment of AF (Tinker et al., 2016), and the existence of a downstream AC1 dependent pathway in atrial and SAN tissue could therefore hold promise for the development of pharmacological interactions that selectively target cardiac AC1. Despite this, a definitive link between IP₃R Ca²⁺ release, AC1 and pathogenesis of AF is yet to be shown and further research investigating this link is required. Additionally, sinus node dysfunction (or sick sinus syndrome) comprises a group of progressive non-curable diseases where the heart rate is inappropriately bradycardic or tachycardic, resulting in increased morbidity rates (Alonso et al., 2014). In familial sinus node dysfunction, multiple different mutated proteins have been implicated including key Ca²⁺ handling proteins such as RyR2, calsequestrin and Cav1.3, alongside HCN4 (Wallace et al., 2021). The crucial importance of Ca²⁺ handling and signalling to pacemaker function and apparent importance in sinus node dysfunction makes this an important potential target for the modulation of pacemaker activity in patients with sinus node dysfunction as well as patients with heart failure and AF. However, a directed approach to finely modulate SAN Ca²⁺ signalling directly is as yet to be described.

Limitations of this study

ST034307 is reported to be highly selective for AC1 at lower concentrations and does not inhibit other AC isoforms at concentrations below 30 μ M (Brust et al., 2017). Despite this, we found that in the presence of 10 μ M ST034307 heart rate was dramatically reduced compared to baseline on addition of PE at concentrations over 10 μ M, and as such we used a lower concentration of 1 μ M ST034307. Although this concentration is below the reported IC₅₀ of 2.3 μ M reported by Brust et al. (2017) 1 μ M ST034307 would still be expected to result in around 40% occupancy based on the inhibition of the effect of A-23187 in HEK cells reported previously (Brust et al., 2017). Despite the use of this lower concentration, chromones have a widely documented biological activity in a range of biological settings (Gaspar et al., 2014), and the possibility of off target effects of ST034307 cannot be eliminated. At higher concentrations (≥ 30 μ M), ST034307 shows potentiation of AC2, and moderate potentiation of AC5/6, however these observations have not been reported at the lower concentration (1 μ M) used in the present study (Brust et al., 2017). Furthermore, the net effect of ST034307 in the SAN is

expected to favour AC1 inhibition due to the higher expression (Mattick et al., 2007; Younes et al., 2008) and activity of AC1 (Younes et al., 2008) compared to AC2, AC5 and AC6 within SAN cells. Of note, entry of the structure of ST034307 into the SwissTargetPrediction tool (Gfeller et al., 2014) did not identify a high probability of interactions in either mouse or human and failed to identify any potential interactions with ion channels. For mouse, the SwissTargetPrediction tool identified, as the highest likelihood, only a 0.06% probability of interaction with histone deacetylase 6 and 8, and D-amino-acid oxidase with no other predicted interactions. In human, in addition to those interactions also identified for mouse, a 0.06% probability of interaction was also identified for quinone reductase 2 and histone deacetylase 2. To validate this low prediction of off-target interactions, future investigations using the genetic knockdown or knockout of AC1 in cardiac tissue, including the SAN, would provide a more comprehensive understanding of the role played by AC1 downstream of IP₃ signalling in the heart.

By using intact tissue and cells, the data presented here provide indirect evidence that modulation of AC1 regulates SAN pacemaker activity downstream of α -adrenergic stimulation. However, additional electrophysiological data would be required to demonstrate this influence directly, and further experiments are required to determine the mechanism by which AC1 activity regulates pacemaker function. Despite this however, by using intact cells, the pharmacological approach used in the present study avoids the disruption of intracellular signalling that would be expected using more cellular invasive techniques such as whole-cell patch clamp.

Conclusion

The present study highlights a role for the Ca²⁺-dependent AC isoform AC1 in influencing cardiac pacemaker activity, both at the level of the isolated SAN cell as well as at the level of the intact beating right atria. The most likely explanation for the blunting of the positive chronotropic response of the SAN to PE is inhibition of AC1 by ST034307. Moreover, the cause of the divergent effects of 1 μ M ST034307 between the SAN and atrial myocytes merits further investigation of the mechanisms regulating both atrial and SAN IP₃ signalling.

Overall, this study provides additional support for the existence of an IP₃ \rightarrow AC1 \rightarrow cAMP signalling pathway, and a role for this pathway in the regulation of SAN pacemaker activity in response to α -adrenergic signalling. The findings presented support a role for AC1 downstream of IP₃-mediated Ca²⁺ release, providing a new example of how crosstalk between Ca²⁺ and cAMP signalling is involved in regulating SAN pacemaker activity. These data add to the already published mechanism of crosstalk between Ca²⁺ and cAMP signalling

within the SAN, with Ca²⁺ already having been shown to control basal cAMP levels and pacemaker activity (Mattick et al., 2007; Younes et al., 2008), and provide further support for previous work identifying a link between IP₃ signalling and the downstream activation of Ca²⁺-dependent ACs (Capel et al., 2021). Furthermore, the concept that SAN IP₃ signalling, and automaticity can be targeted through cyclic nucleotide signalling suggests further investigation of putative IP₃-cAMP signalling pathways in cardiac atria may identify novel targets, for example phosphodiesterases, to modulate pacemaker activity and also prevent the triggering of atrial arrhythmias such as AF.

Data availability statement

The raw data supporting the conclusion of this article will be made available by the authors, without undue reservation.

Ethics statement

The animal study was reviewed and approved by the University of Oxford, Procedures Establishment License (PEL) Number XEC303F12.

Author contributions

RABB conceived the research. DAT, MZ, and AR contributed intellectually to the study. SJB and RABB designed the study. SJB and MJR carried out intact atrial preparations. SJB, MJR, and RAC carried out SAN isolated cell work. EA and TA carried out immunofluorescence work and produced Figure 2. SJB and MJR wrote the manuscript. SJB, RAC, and EA carried out animal dissections and cell isolations. All authors have contributed to refinement of the manuscript.

Funding

SJB is a post-doctoral scientist funded by the British Heart Foundation (PG/18/4/33521). RABB is funded by a Sir Henry Dale Wellcome Trust and Royal Society Fellowship (109371/Z/15/Z) and holds a Senior Research Fellowship at Linacre College, Oxford. RAC is a post-doctoral scientist funded by the Wellcome Trust and Royal Society (109371/Z/15/Z). MZ is supported by the British Heart Foundation (RG/17/6/32944). TA received funding from the Returners Carers Fund (PI RABB), Medical Science Division, University of Oxford, the Nuffield Benefaction for Medicine and the Wellcome Institutional Strategic Support Fund (ISSF), University of Oxford. EA received funding from the Returners Carers Fund (PI RAC), University of Oxford.

Acknowledgments

We acknowledge the support of Dr Tim Viney and Dr Thomas P. Collins, Department of Pharmacology, University of Oxford for their assistance with this manuscript. RABB and MZ acknowledge support from the BHF Centre of Research Excellence, Oxford. RABB acknowledges support from the Covid-19 Rebuilding Research Momentum Fund (CRRMF) Oxford Funds.

Conflict of interest

The authors declare that the research was conducted in the absence of any commercial or financial relationships that could be construed as a potential conflict of interest.

Publisher's note

All claims expressed in this article are solely those of the authors and do not necessarily represent those of their affiliated organizations, or those of the publisher, the editors and the reviewers. Any product that may be evaluated in this article, or

claim that may be made by its manufacturer, is not guaranteed or endorsed by the publisher.

Supplementary material

The Supplementary Material for this article can be found online at: <https://www.frontiersin.org/articles/10.3389/fphar.2022.951897/full#supplementary-material>

SUPPLEMENTARY FIGURE S1

Effect of different combinations of metoprolol (1 μ M), ST034307 (1 μ M) and PE (10 μ M) on mouse right atrial beating rate. Bars represent mean heart rate (bpm) under different conditions as indicated below the x-axis. Significance bars represent comparison of the data using ANOVA followed by Fisher's LSD test to compare all conditions (non-significant comparisons are not shown) ($n = 11$ –14). Data are represented as mean \pm SEM.

SUPPLEMENTARY FIGURE S2

(A) Representative example of a fixed, isolated guinea pig atrial myocyte (i) immunolabelled for IP₃R2 (magenta), (ii) AC1 (cyan), (iii) co-immunolabelled for IP₃R2 (magenta) and AC1 (cyan) and (iv) bright field. (B) Intensity plot to show staining intensity along the line shown in (A). (C,D) Intensity surface plot showing the distribution of staining of IP₃R2 [magenta, (C)] and AC1 [cyan, (D)] for the whole cell, as shown in (A) (iii). Scale bars representing 10 μ m are indicated in (A). For the purposes of presentation only, red and green channels have been represented as magenta and cyan, respectively.

References

- Alonso, A., Jensen, P. N., Lopez, F. L., Chen, L. Y., Psaty, B. M., Folsom, A. R., et al. (2014). Association of sick sinus syndrome with incident cardiovascular disease and mortality: the atherosclerosis risk in communities study and cardiovascular health study. *Plos One* 9, e109662. doi:10.1371/journal.pone.0109662
- Ando, H., Mizutani, A., Kiefer, H., Tsuzurugi, D., Michikawa, T., and Mikoshiba, K. (2006). IRBIT suppresses IP₃ receptor activity by competing with IP₃ for the common binding site on the IP₃ receptor. *Mol. Cell* 22, 795–806. doi:10.1016/j.molcel.2006.05.017
- Arce, C., Vicente, D., Segura, V., Flacco, N., Monto, F., Almenar, L., et al. (2017). Activation of α 1A -adrenoceptors desensitizes the rat aorta response to phenylephrine through a neuronal NOS pathway, a mechanism lost with ageing. *Br. J. Pharmacol.* 174 (13), 2015–2030. doi:10.1111/bph.13800
- Barbuti, A., Gravante, B., Riolfo, M., Milanesi, R., Terragni, B., and DiFrancesco, D. (2004). Localization of pacemaker channels in lipid rafts regulates channel kinetics. *Circ. Res.* 94, 1325–1331. doi:10.1161/01.RES.0000127621.54132.AE
- Bers, D. M. (2002). Cardiac excitation-contraction coupling. *Nature* 415, 198–205. doi:10.1038/415198a
- Bogdanov, K. Y., Vinogradova, T. M., and Lakatta, E. G. (2001). Sinoatrial nodal cell ryanodine receptor and Na⁺-Ca²⁺ exchanger - molecular partners in pacemaker regulation. *Circ. Res.* 88, 1254–1258. doi:10.1161/hh1201.092095
- Brand, T. (2005). The Popeye domain-containing gene family. *Cell biochem. Biophys.* 43, 95–103. doi:10.1385/CBB:43:1:095
- Brust, T. F., Alongkronrusmee, D., Soto-Velasquez, M., Baldwin, T. A., Ye, Z. S., Dai, M. J., et al. (2017). Identification of a selective small-molecule inhibitor of type 1 adenylyl cyclase activity with analgesic properties. *Sci. Signal.* 10, eaah5381. doi:10.1126/scisignal.aah5381
- Burton, R. A. B., and Terrar, D. A. (2021). Emerging evidence for cAMP-calcium cross talk in heart atrial nanodomains where IP₃-evoked calcium release stimulates adenylyl cyclases. *Contact* 4, 251525642110083–13. doi:10.1177/25152564211008341
- Capel, R. A., and Terrar, D. A. (2015). The importance of Ca(2+)-dependent mechanisms for the initiation of the heartbeat. *Front. Physiol.* 25 (6), 80. doi:10.3389/fphys.2015.00080
- Capel, R. A., Bolton, E. L., Lin, W. K., Aston, D., Wang, Y., Liu, W., et al. (2015). Two-pore channels (TPC2s) and Nicotinic Acid Adenine Dinucleotide Phosphate (NAADP) at lysosomal-sarcoplasmic reticular junctions contribute to acute and chronotropic β -adrenoceptor signalling in the heart. *J. Biol. Chem.* 290 (50), 30087–30098.
- Capel, R. A., Bose, S. J., Collins, T. P., Rajasundaram, S., Ayagama, T., Zaccolo, M., et al. (2021). IP₃-mediated Ca²⁺ release regulates atrial Ca²⁺ transients and pacemaker function by stimulation of adenylyl cyclases. *Am. J. Physiol. Heart Circ. Physiol.* 320, H95–H107. doi:10.1152/ajpheart.00380.2020
- Chen-Izu, Y., Xiao, R. P., Izu, L. T., Cheng, H., Kuschel, M., Spurgeon, H., et al. (2000). G_i-dependent localization of beta2-adrenergic receptor signaling to L-type Ca²⁺ channels. *Biophys. J.* 79, 2547–2556. doi:10.1016/S0006-3495(00)76495-2
- Collins, T. P., and Terrar, D. A. (2012). Ca(2+)-stimulated adenylyl cyclases regulate the L-type Ca(2+) current in Guinea-pig atrial myocytes. *J. Physiol.* 590, 1881–1893. doi:10.1113/jphysiol.2011.227066
- Collins, T. P., Bayliss, R., Churchill, G. C., Galione, A., and Terrar, D. A. (2011). NAADP influences excitation-contraction coupling by releasing calcium from lysosomes in atrial myocytes. *Cell calcium* 50, 449–458. doi:10.1016/j.ceca.2011.07.007
- de Rooij, J., Zwartkruis, F. J., Verheijen, M. H., Cool, R. H., Nijman, S. M., Wittinghofer, A., et al. (1998). Epac is a Rap1 guanine-nucleotide-exchange factor directly activated by cyclic AMP. *Nature* 396, 474–477. doi:10.1038/24884
- Difrancesco, D., and Tortora, P. (1991). Direct activation of cardiac pacemaker channels by intracellular cyclic-AMP. *Nature* 351, 145–147. doi:10.1038/351145a0
- Difrancesco, D., and Tromba, C. (1988). Muscarinic control of the hyperpolarization-activated current (I_h) in rabbit sino-atrial node myocytes. *J. Physiol.* 405, 493–510. doi:10.1113/jphysiol.1988.sp017344
- Difrancesco, D., Noble, D., and Denyer, J. C. (1991). The contribution of the pacemaker current (I_h) to generation of spontaneous activity in rabbit sinoatrial node myocytes. *J. Physiol.* 434, 23–40. doi:10.1113/jphysiol.1991.sp018457
- Domeier, T. L., Zima, A. V., Maxwell, J. T., Huke, S., Mignery, G. A., and Blatter, L. A. (2008). IP₃ receptor-dependent Ca²⁺ release modulates excitation-contraction coupling in rabbit ventricular myocytes. *Am. J. Physiol. Heart Circ. Physiol.* 294, H596–604. doi:10.1152/ajpheart.01155.2007

- Fagan, K. A., Mahey, R., and Cooper, D. M. F. (1996). Functional co-localization of transfected Ca^{2+} -stimulable adenyl cyclases with capacitative Ca^{2+} entry sites. *J. Biol. Chem.* 271, 12438–12444. doi:10.1074/jbc.271.21.12438
- Fesenko, E. E., Kolesnikov, S. S., and Lyubarsky, A. L. (1985). Induction by cyclic GMP of cationic conductance in plasma membrane of retinal rod outer segment. *Nature* 313, 310–313. doi:10.1038/313310a0
- Gaspar, A., Matos, M. J., Garrido, J., Uriarte, E., and Borges, F. (2014). Chromone: A valid scaffold in medicinal chemistry. *Chem. Rev.* 114, 4960–4992. doi:10.1021/cr400265z
- Georget, M., Mateo, P., Vandecasteele, G., Jurevicius, J., Lipskaia, L., Defer, N., et al. (2002). Augmentation of cardiac contractility with no change in L-type Ca^{2+} current in transgenic mice with a cardiac-directed expression of the human adenyl cyclase type 8 (AC8). *FASEB J.* 16 (12), 1636–1638. doi:10.1096/fj.02-0292je
- Gfeller, D., Grosdidier, A., Wirth, M., Dains, A., Michielin, O., and Zoete, V. (2014). SwissTargetPrediction: A web server for target prediction of bioactive small molecules. *Nucleic Acids Res.* 42, W32–W38. doi:10.1093/nar/gku293
- Hancox, J. C., and Mitcheson, J. S. (1997). Ion channel and exchange currents in single myocytes isolated from the rabbit atrioventricular node. *Can. J. Cardiol.* 13, 1175–1182.
- Harvey, R. D., and Clancy, C. E. (2021). Mechanisms of cAMP compartmentation in cardiac myocytes: experimental and computational approaches to understanding. *J. Physiol.* 599, 4527–4544. doi:10.1113/jp280801
- Hattori, M., Suzuki, A. Z., Higo, T., Miyauchi, H., Michikawa, T., Nakamura, T., et al. (2004). Distinct roles of inositol 1, 4, 5-trisphosphate receptor types 1 and 3 in Ca^{2+} signaling. *J. Biol. Chem.* 279, 11967–11975. doi:10.1074/jbc.M311456200
- Hiremath, A. N., Hu, Z. W., and Hoffman, B. B. (1991). Desensitization of alpha-adrenergic receptor-mediated smooth muscle contraction: role of the endothelium. *J. Cardiovasc. Pharmacol.* 18 (1), 151–157. doi:10.1097/00005344-199107000-00020
- Huser, J., Lipsius, S. L., and Blatter, L. A. (1996). Calcium gradients during excitation-contraction coupling in cat atrial myocytes. *J. Physiol.* 494, 641–651. doi:10.1113/jphysiol.1996.sp021521
- Jones, S. A., Boyett, M. R., and Lancaster, M. K. (2007). Declining into failure - the age-dependent loss of the L-type calcium channel within the sinoatrial node. *Circulation* 115, 1183–1190. doi:10.1161/CIRCULATIONAHA.106.663070
- Ju, Y. K., Chu, Y., Chaulet, H., Lai, D., Gervasio, O. L., Graham, R. M., et al. (2007). Store-operated Ca^{2+} influx and expression of TRPC genes in mouse sinoatrial node. *Circ. Res.* 100, 1605–1614. doi:10.1161/CIRCRESAHA.107.152181
- Ju, Y. K., Liu, J., Lee, B. H., Lai, D., Woodcock, E. A., Lei, M., et al. (2011). Distribution and functional role of inositol 1, 4, 5-trisphosphate receptors in mouse sinoatrial node. *Circ. Res.* 109, 848–857. doi:10.1161/CIRCRESAHA.111.243824
- Ju, Y. K., Woodcock, E. A., Allen, D. G., and Cannell, M. B. (2012). Inositol 1, 4, 5-trisphosphate receptors and pacemaker rhythms. *J. Mol. Cell. Cardiol.* 53, 375–381. doi:10.1016/j.yjmcc.2012.06.004
- Katsushika, S., Chen, L., Kawabe, J. I., Nilakantan, R., Halnon, N. J., Homcy, C. J., et al. (1992). Cloning and characterization of a sixth adenyl cyclase isoform: types V and VI constitute a subgroup within the mammalian adenyl cyclase family. *Proc. Natl. Acad. Sci. U. S. A.* 89, 8774–8778. doi:10.1073/pnas.89.18.8774
- Krebs, E. G., and Beavo, J. A. (1979). Phosphorylation-dephosphorylation of enzymes. *Annu. Rev. Biochem.* 48, 923–959. doi:10.1146/annurev.bi.48.070179.004423
- Lakatta, E. G., Maltsev, V. A., and Vinogradova, T. M. (2010). A coupled SYSTEM of intracellular Ca^{2+} clocks and surface membrane voltage clocks controls the timekeeping mechanism of the heart's pacemaker. *Circ. Res.* 106, 659–673. doi:10.1161/CIRCRESAHA.109.206078
- Landstrom, A. P., Dobrev, D., and Wehrens, X. H. T. (2017). Calcium signaling and cardiac arrhythmias. *Circ. Res.* 120, 1969–1993. doi:10.1161/CIRCRESAHA.117.310083
- Liang, X., Xie, H., Zhu, P. H., Hu, J., Zhao, Q., Wang, C. S., et al. (2009). Enhanced activity of inositol-1, 4, 5-trisphosphate receptors in atrial myocytes of atrial fibrillation patients. *Cardiology* 114, 180–191. doi:10.1159/000228584
- Lipp, P., Laine, M., Tovey, S. C., Burrell, K. M., Berridge, M. J., Li, W. H., et al. (2000). Functional $\text{InsP}(3)$ receptors that may modulate excitation-contraction coupling in the heart. *Curr. Biol.* 10, 939–942. doi:10.1016/s0960-9822(00)00624-2
- Lou, L. X., Li, C. H., Wang, J., Wu, A. M., Zhang, T., Ma, Z., et al. (2021). Yiqi Huoxue preserves heart function by upregulating the Sigma-1 receptor in rats with myocardial infarction. *Exp. Ther. Med.* 22, 1308. doi:10.3892/etm.2021.10743
- Macdonald, E. A., Madl, J., Greiner, J., Ramadan, A. F., Wells, S. M., Torrente, A. G., et al. (2020). Sinoatrial node structure, mechanisms, electrophysiology and the chronotropic response to stretch in rabbit and mouse. *Front. Physiol.* 11, 809. doi:10.3389/fphys.2020.00809
- Mackenzie, L., Bootman, M. D., Laine, M., Berridge, M. J., Thuring, J., Holmes, A., et al. (2002). The role of inositol 1, 4, 5, -trisphosphate receptors in Ca^{2+} signalling and the generation of arrhythmias in rat atrial myocytes. *J. Physiol.* 541, 395–409. doi:10.1113/jphysiol.2001.013411
- Mangoni, M. E., Couette, B., Bourinet, E., Platzer, J., Reimer, D., Striessnig, J., et al. (2003). Functional role of L-type $\text{Ca}(\text{v})13\text{Ca}(2+)$ channels in cardiac pacemaker activity. *Proc. Natl. Acad. Sci. U. S. A.* 100, 5543–5548. doi:10.1073/pnas.0935295100
- Mattick, P., Parrington, J., Oda, E., Simpson, A., Collins, T., and Terrar, D. (2007). Ca^{2+} -stimulated adenyl cyclase isoform AC1 is preferentially expressed in Guinea-pig sino-atrial node cells and modulates the I(f) pacemaker current. *J. Physiol.* 582, 1195–1203. doi:10.1113/jphysiol.2007.133439
- Nakayama, H., Bodi, I., Maillet, M., Desantiago, J., Domeier, T. L., Mikoshiba, K., et al. (2010). The IP_3 receptor regulates cardiac hypertrophy in response to select stimuli. *Circ. Res.* 105, 659–666. doi:10.1161/CIRCRESAHA.110.220038
- O'Hara, T., and Rudy, Y. (2012). Quantitative comparison of cardiac ventricular myocyte electrophysiology and response to drugs in human and nonhuman species. *Am. J. Physiol. Heart Circ. Physiol.* 302 (5), H1023–H1030. doi:10.1152/ajpheart.00785.2011
- Premont, R. T., Chen, J. Q., Ma, H. W., Ponnappalli, M., and Iyengar, R. (1992). Two members of a widely expressed subfamily of hormone-stimulated adenyl cyclases. *Proc. Natl. Acad. Sci. U. S. A.* 89, 9809–9813. doi:10.1073/pnas.89.20.9809
- Rigg, L., and Terrar, D. A. (1996). Possible role of calcium release from the sarcoplasmic reticulum in pacemaking in Guinea-pig sino-atrial node. *Exp. Physiol.* 81, 877–880. doi:10.1113/expphysiol.1996.sp003983
- Rigg, L., Mattick, P. A. D., Heath, B. M., and Terrar, D. A. (2003). Modulation of the hyperpolarization-activated current (I-f) by calcium and calmodulin in the Guinea-pig sino-atrial node. *Cardiovasc. Res.* 57, 497–504. doi:10.1016/s0008-6363(02)00668-5
- Salvador, J. B. I., and Egger, M. (2018). Obstruction of ventricular Ca^{2+} -dependent arrhythmogenicity by inositol 1, 4, 5-trisphosphate-triggered sarcoplasmic reticulum Ca^{2+} release. *J. Physiol.* 596, 4323–4340. doi:10.1113/jp276319
- Sampieri, A., Santoyo, K., Asanov, A., and Vaca, L. (2018). Association of the IP_3R to STIM1 provides a reduced intraluminal calcium microenvironment, resulting in enhanced store-operated calcium entry. *Sci. Rep.* 8, 13252. doi:10.1038/s41598-018-31621-0
- Surdo, N. C., Berrera, M., Koschinski, A., Brescia, M., Machado, M. R., Carr, C., et al. (2017). FRET biosensor uncovers cAMP nano-domains at beta-adrenergic targets that dictate precise tuning of cardiac contractility. *Nat. Commun.* 8, 15031. doi:10.1038/ncomms15031
- Terrar, D. A. (2020). Calcium signaling in the heart. *Adv. Exp. Med. Biol.* 1131, 395–443. doi:10.1007/978-3-030-12457-1_16
- Thillaipappan, N. B., Smith, H. A., Atakpa-Adaji, P., and Taylor, C. W. (2021). KRAP tethers IP_3 receptors to actin and licenses them to evoke cytosolic Ca^{2+} signals. *Nat. Commun.* 12, 4514. doi:10.1038/s41467-021-24739-9
- Tinker, A., Finlay, M., Nobles, M., and Opel, A. (2016). The contribution of pathways initiated via the G(q/11) G-protein family to atrial fibrillation. *Pharmacol. Res.* 105, 54–61. doi:10.1016/j.phrs.2015.11.008
- Tsutsui, K., Monfredi, O. J., Sirenko-Tagirova, S. G., Maltseva, L. A., Bychkov, R., Kim, M. S., et al. (2018). A coupled-clock system drives the automaticity of human sinoatrial nodal pacemaker cells. *Sci. Signal.* 11, eaap7608. doi:10.1126/scisignal.aap7608
- Uchida, K., Aramaki, M., Nakazawa, M., Yamagishi, C., Makino, S., Fukuda, K., et al. (2010). Gene knock-outs of inositol 1, 4, 5-trisphosphate receptors types 1 and 2 result in perturbation of cardiogenesis. *Plos One* 5, e12500. doi:10.1371/journal.pone.0012500
- Vinogradova, T. M., Zhou, Y., Bogdanov, K. Y., Yang, D., Kuschel, M., Cheng, H., et al. (2000). Sinoatrial node pacemaker activity requires Ca^{2+} /Calmodulin-dependent kinase II activation. *Circ. Res.* 87, 760–767. doi:10.1161/01.res.87.9.760
- Vinogradova, T. M., Sirenko, S., Lyashkov, A. E., Younes, A., Li, Y., Zhu, W., et al. (2008). Constitutive phosphodiesterase activity restricts spontaneous beating rate of cardiac pacemaker cells by suppressing local Ca^{2+} releases. *Circ. Res.* 102, 761–769. doi:10.1161/CIRCRESAHA.107.161679
- Wallace, M. J., El Refaey, M., Mesirca, P., Hund, T. J., Mangoni, M. E., and Mohler, P. J. (2021). Genetic complexity of sinoatrial node dysfunction. *Front. Genet.* 12, 654925. doi:10.3389/fgene.2021.654925
- Walsh, D. A., Perkins, J. P., and Krebs, E. G. (1968). An adenosine 3', 5'-monophosphate dependent protein kinase from rabbit skeletal muscle. *J. Biol. Chem.* 243, 3763–3765. doi:10.1016/s0021-9258(19)34204-8
- Wang, Y. G., Dedkova, E. N., Ji, X., Blatter, L. A., and Lipsius, S. L. (2005). Phenylephrine acts via IP_3 -dependent intracellular NO release to stimulate L-type Ca^{2+} current in cat atrial myocytes. *J. Physiol.* 143, 157.

Wang, H., Xu, H., Wu, L. J., Kim, S. S., Chen, T., Koga, K., et al. (2011). Identification of an adenylyl cyclase inhibitor for treating neuropathic and inflammatory pain. *Sci. Transl. Med.* 3 (65), 65ra3. doi:10.1126/scitranslmed.3001269

Willoughby, D., Everett, K. L., Halls, M. L., Pacheco, J., Skroblin, P., Vaca, L., et al. (2012). Direct binding between Orai1 and AC8 mediates dynamic interplay between Ca^{2+} and cAMP signaling. *Sci. Signal.* 5 (219), ra29. doi:10.1126/scisignal.2002299

Yamada, J., Ohkusa, T., Nao, T., Ueyama, T., Yano, M., Kobayashi, S., et al. (2001). Up-regulation of inositol 1, 4, 5 trisphosphate receptor expression in atrial tissue in patients with chronic atrial fibrillation. *J. Am. Coll. Cardiol.* 37, 1111–1119. doi:10.1016/s0735-1097(01)01144-5

Yaniv, Y., Spurgeon, H. A., Ziman, B. D., and Lakatta, E. G. (2013). Ca^{2+} /Calmodulin-Dependent protein kinase II (CaMKII) activity and sinoatrial nodal pacemaker cell energetics. *PLoS One* 8, e57079. doi:10.1371/journal.pone.0057079

Younes, A., Lyashkov, A. E., Graham, D., Sheydina, A., Volkova, M. V., Mitsak, M., et al. (2008). Ca^{2+} -stimulated basal adenylyl cyclase activity localization in membrane lipid microdomains of cardiac sinoatrial nodal pacemaker cells. *J. Biol. Chem.* 283, 14461–14468. doi:10.1074/jbc.M707540200

Zaccolo, M., and Pozzan, T. (2002). Discrete microdomains with high concentration of cAMP in stimulated rat neonatal cardiac myocytes. *Science* 295, 1711–1715. doi:10.1126/science.1069982

Zaccolo, M., Zerio, A., and Lobo, M. J. (2021). Subcellular organization of the cAMP signaling pathway. *Pharmacol. Rev.* 73, 278–309. doi:10.1124/pharmrev.120.000086

Zhao, Z. H., Zhang, H. C., Xu, Y., Zhang, P., Li, X. B., Liu, Y. S., et al. (2007). Inositol-1, 4, 5-trisphosphate and ryanodine-dependent Ca^{2+} signaling in a chronic dog model of atrial fibrillation. *Cardiology* 107, 269–276. doi:10.1159/000095517



OPEN ACCESS

EDITED BY

Muhammad Afzal,
Jouf University, Saudi Arabia

REVIEWED BY

Victor Ruiz-Velasco,
The Pennsylvania State University,
United States
Guanxing Chen,
University of Texas MD Anderson
Cancer Center, United States
Homa Manaheji,
Shahid Beheshti University of Medical
Sciences, Iran

*CORRESPONDENCE

Amanda H. Klein,
ahklein@d.umn.edu

SPECIALTY SECTION

This article was submitted to
Experimental Pharmacology and Drug
Discovery,
a section of the journal
Frontiers in Pharmacology

RECEIVED 06 May 2022

ACCEPTED 02 August 2022

PUBLISHED 02 September 2022

CITATION

Johnson K, Doucette A, Edwards A,
Verdi A, McFarland R, Hulke S, Fowler A,
Watts VJ and Klein AH (2022), Reduced
activity of adenylyl cyclase 1 attenuates
morphine induced hyperalgesia and
inflammatory pain in mice.
Front. Pharmacol. 13:937741.
doi: 10.3389/fphar.2022.937741

COPYRIGHT

© 2022 Johnson, Doucette, Edwards,
Verdi, McFarland, Hulke, Fowler, Watts
and Klein. This is an open-access article
distributed under the terms of the
[Creative Commons Attribution License](https://creativecommons.org/licenses/by/4.0/)
(CC BY). The use, distribution or
reproduction in other forums is
permitted, provided the original
author(s) and the copyright owner(s) are
credited and that the original
publication in this journal is cited, in
accordance with accepted academic
practice. No use, distribution or
reproduction is permitted which does
not comply with these terms.

Reduced activity of adenylyl cyclase 1 attenuates morphine induced hyperalgesia and inflammatory pain in mice

Kayla Johnson¹, Alexis Doucette¹, Alexis Edwards¹,
Aleeya Verdi¹, Ryan McFarland¹, Shelby Hulke¹,
Amanda Fowler¹, Val J. Watts² and Amanda H. Klein^{1*}

¹Department of Pharmacy Practice and Pharmaceutical Sciences, University of Minnesota, Duluth, MN, United States, ²Department of Medicinal Chemistry and Molecular Pharmacology, Purdue University, West Lafayette, IN, United States

Opioid tolerance, opioid-induced hyperalgesia during repeated opioid administration, and chronic pain are associated with upregulation of adenylyl cyclase activity. The objective of this study was to test the hypothesis that a reduction in adenylyl cyclase 1 (AC1) activity or expression would attenuate morphine tolerance and hypersensitivity, and inflammatory pain using murine models. To investigate opioid tolerance and opioid-induced hyperalgesia, mice were subjected to twice daily treatments of saline or morphine using either a static (15 mg/kg, 5 days) or an escalating tolerance paradigm (10–40 mg/kg, 4 days). Systemic treatment with an AC1 inhibitor, ST03437 (2.5–10 mg/kg, IP), reduced morphine-induced hyperalgesia in mice. Lumbar intrathecal administration of a viral vector incorporating a short-hairpin RNA targeting *Adcy1* reduced morphine-induced hypersensitivity compared to control mice. In contrast, acute morphine antinociception, along with thermal paw withdrawal latencies, motor performance, exploration in an open field test, and burrowing behaviors were not affected by intrathecal *Adcy1* knockdown. Knockdown of *Adcy1* by intrathecal injection also decreased inflammatory mechanical hyperalgesia and increased burrowing and nesting activity after intraplantar administration of Complete Freund's Adjuvant (CFA) one-week post-injection.

KEYWORDS

pain, adenylyl cyclase, tolerance, hypersensitivity, inflammation

Introduction

Of the principal intracellular mechanisms thought to produce tolerance and opioid-induced hyperalgesia in the nervous system, increased adenylyl cyclase (AC) expression and activity is a promising lead candidate (Corder et al., 2013). On a cellular level, upon agonist binding to the mu-opioid receptor (MOR), AC is inhibited and the formation of cyclic adenosine monophosphate (cAMP) is decreased. Paradoxically, prolonged agonist

stimulation of the MOR can lead to loss of AC suppression, causing increased intracellular activity of AC, thereby increasing intracellular levels of cAMP (Williams et al., 2001). Enhancement of cAMP levels due to prolonged opioid exposure has long been connected to opioid tolerance and opioid dependence in both *in vitro* (Collier and Francis, 1975; Sharma et al., 1975) and *in vivo* studies, particularly in the spinal cord and dorsal root ganglia (DRG) (Crain and Makman, 1987; Makman et al., 1988).

To date, nine membrane-bound AC isoforms (AC1-9) and one soluble isoform (AC 10) have been confirmed in mammalian nervous systems (Sunahara et al., 1996). AC1 is present in the brain, particularly in the cortex, hippocampus, and cerebellum, and historically has been thought to play a large role in learning and memory (Wu et al., 1995; Defer et al., 2000). AC1 is also present in the spinal cord (Wei et al., 2002) and TrkA positive neurons in the DRG of mice (Haupt et al., 2010). A global loss in AC1 activity results in attenuated nociceptive behaviors after formalin hind paw injection and reduces pCREB activation in the superficial dorsal horn of the spinal cord (Wei et al., 2002).

Although all of the underlying mechanisms behind tolerance and opioid-induced hyperalgesia are not currently known, increased AC expression and activity have been suggested to be one of the major causative agents. To date, it is unknown if selectively inhibiting AC1 activity or reducing AC1 expression after chronic MOR stimulation alters the development of opioid tolerance and opioid-induced hypersensitivity. The purpose of this study was to better understand how the activity of AC1 in the spinal cord and dorsal root ganglia contributes to hypersensitivity seen during morphine tolerance, opioid-induced hypersensitivity, and chronic inflammatory pain. To accomplish this, systemic pharmacological inhibition of AC1 or intrathecal delivery of a short hairpin RNA (shRNA) through a viral vector was used to decrease *Adcy1* expression in mice. Mechanical withdrawal thresholds were measured in morphine tolerant and morphine withdrawn mice. Similarly, several evoked and spontaneous behavioral measures were used to determine if *Adcy1* knockdown would also decrease hypersensitivity or improve mobility in a mouse model of inflammatory pain.

Materials and methods

Animals

All experimental procedures involving animals were approved and performed under the University of Minnesota Institutional Animal Care and Use Committee guidelines. Adult male and female C57Bl6 mice were obtained via Charles River (5–6 weeks old, Raleigh, NC) having an average weight of ~25 g (23–31 g). Mice were housed in a facility ranging from 20 to 26°C on a 14 h light/10 h dark cycle with water and rodent chow (Purina 5015) *ad libitum*. Mice were kept in conventional microisolator cages with no more than five animals per cage.

The cages contained irradiated corn cob bedding enriched with aspen and cotton nesting materials. After drug administration and CFA injections, mice were monitored for overall wellbeing and any adverse reactions. Mice were acclimated to individual testing apparatuses before behavioral testing. All experiments were conducted during the 14 h day cycle except for nesting behaviors. Mice were euthanized by isoflurane anesthesia (5%) followed by decapitation at the end of the study. A Table of experimental studies is provided in Table 1.

In behavioral studies, 5–10 male and female mice were randomly assigned to either a control or ST034307 treatment group. Viral vector studies consisted of two treatment groups, each containing 10 randomly assigned male and female mice. Use of male and female animals is consistent with the National Institute of Health's Sex as a Biological Variable policy. For all experiments, male mice were tested before female mice and equipment cleaned in between testing of sexes.

Drugs and delivery

Morphine (Sigma Chemical, St. Louis, MO, United States) was administered through a 100 µl subcutaneous injection in saline. For morphine tolerance experiments, baseline mechanical paw withdrawal testing was performed before and after administration of 15 mg/kg of morphine for 5 days (Liang et al., 2011). Baseline measurements were measured every morning before morphine injection (Pre) to assess opioid-induced hyperalgesia, and 30 min post injection (Post) to assess tolerance. Escalating morphine tolerance was performed similarly, except increasing doses of morphine, starting at 10 mg/kg and increasing 10 mg/kg/day, were administered over 4 days. Day 5 and day 6 thresholds measured ~18 and ~42 h, respectfully, after last morphine injection. In each model, morphine was delivered twice per day (~0800 and ~1800 h).

ST034307 (6271, Tocris Bioscience, Minneapolis, MN, United States) was dissolved in 10% β-cyclodextrin with 5% DMSO in saline and administered in a 100 µl intraperitoneal injection. ST034307 or vehicle was administered 15 min after morphine in tolerance experiments.

In separate experiments, Complete Freund's Adjuvant (CFA, F5881, Sigma Chemical, St. Louis, MO, United States) was administered through an intraplantar injection (20 µl, undiluted) into the left hind paw.

Mechanical paw withdrawal

Mice were acclimated to the testing environment on at least two separate occasions for 30–60 min before formal testing. The testing environment consisted of a mesh floor, allowing access to animal hind paws, and individual clear acrylic chambers. Mechanical paw withdrawal thresholds, in grams, were determined by electronic von Frey testing equipment (Electric von Frey Anesthesiometer, 2390,

TABLE 1 List of behavioral experiments.

Experiment	Experiment description	Treatment conditions	Behavioral tests administered
1	mRNA of adenylyl cyclases in DRG and spinal cord	Systemic morphine or saline twice daily for 5 days (15 mg/kg, sc)	N/A
2	ST034307 Mechanical and thermal antinociception	Vehicle or ST034307 (2.5–10 mg/kg, ip, 100 µl) 15 min post-morphine	Von frey and thermal paw withdrawal
3	ST034307 Escalating morphine tolerance	Systemic morphine twice daily for 5 days (10 mg/kg on day 1 increasing to 40 mg/kg by day 4, sc, 100µl) + vehicle or ST034307 (2.5–10 mg/kg, ip, 100 µl) 15 min post-morphine, vehicle or ST034307 (2.5–10 mg/kg, ip, 100 µl) on Day 5	Von frey paw withdrawal
4	AC1 knockdown <i>via</i> intrathecal delivery: morphine antinociception	AAV9-Adcy1-shRNA or AAV9-Scrambl-shRNA delivered intrathecally, morphine doses 5–20 mg/kg, sc, measurements taken 30 min after morphine injection	Von frey paw withdrawal
5	AC1 knockdown <i>via</i> intrathecal delivery: escalating morphine tolerance	AAV9-Adcy1-shRNA or AAV9-Scrambl-shRNA delivered intrathecally, Twice daily escalating injections of morphine (10 mg/kg on day 1 increasing to 40 mg/kg by day 4, sc, 100 µl)	Von frey paw withdrawal
6	AC1 knockdown <i>via</i> intrathecal delivery: morphine tolerance	AAV9-Adcy1-shRNA or AAV9-Scrambl-shRNA delivered intrathecally, twice daily injections of morphine for 5 days (15 mg/kg, sc)	Von frey paw withdrawal
7	AC1 knockdown <i>via</i> intrathecal delivery: CFA model of inflammatory pain	AAV9-Adcy1-shRNA or AAV9-Scrambl-shRNA delivered intrathecally, CFA delivered intraplantar (one hindpaw)	Before CFA: Rotarod performance test, open field testing, thermal paw withdrawal testing, Von frey paw withdrawal (baseline) after CFA: Von frey paw withdrawal, burrowing testing, nesting

Almemo® 2450, IITC Life Science, Woodland Hills, CA, United States). The plantar surface of the hind paws was gently pressed with the probe until a nocifensive response (i.e., paw lifting, jumping, and licking) was elicited. Baseline measurements were collected five times from both the right and left hind paw and averaged, with an interstimulus interval of at least 1 minute.

Adeno-associated virus-mediated Adcy1 knockdown.

Gene knockdown of Adcy1 using shRNA was achieved using AAV9-GFP-U6-m-Adcy1-shRNA. A scrambled vector, AAV9-GFP-U6-scramble-shRNA, was used in a different group of mice as a control (shAAV-251792 and 7045, titer: 1.4×10^{13} GC/mL, in PBS with 5% glycerol, Vector Biolabs, Malvern, PA, United States). Viruses were delivered by direct lumbar puncture (10 µL) in awake mice and behavioral assessments were performed 3–8 weeks post-injection (Fairbanks, 2003; Vulchanova et al., 2010). Intrathecal delivery of AAV9 serotypes in live mice yield high efficacy of transduction efficiency in DRG and lumbar spinal cord while yielding sporadic labeling in the cortex and other peripheral tissues (Schuster et al., 2013).

Four weeks post-virus injections morphine efficacy was determined using an escalating dose-response curve (5–20 mg/kg) waiting 30 min after each injection (Klein

et al., 2018). Morphine tolerance or escalating morphine tolerance tests were initiated 5 weeks post-virus injections (see *Drugs and Delivery*). CFA was injected into a cohort of mice 7-weeks post inoculation. CFA treated mice underwent a series of behavioral tests 3–4 weeks after virus injections but before CFA administration (see—*Rotarod Performance Test*, *Open Field Testing*, *Thermal Paw Withdrawal Testing*) and after CFA administration (see – *Burrowing Testing*, *Nesting*).

Rotarod performance test

Agility assessment was conducted using Rotamex-5 automated rotarod system (0254–2002L, 3 cm rod, Columbus Instruments, Columbus, OH, United States). Mice were placed onto a stationary knurled PCV rod suspended in the air. The initial rotation speed of 4 rpm was gradually increased by 1 rpm in 30-s intervals until animals fell off the rod or reached a speed of 14 rpm (300 s). Two tests were administered per animal and averaged.

Thermal paw withdrawal test

Latencies to a radiant light beam focused on the plantar surface of each mouse hind paw were obtained using a modified Hargreaves Method (Plantar Test Analgesia Meter, 400, IITC,

Woodland Hills, CA, United States) (Hargreaves et al., 1988). The average time required to elicit a nocifensive response of at least three measurements per hind paw were recorded. Mice were acclimated on multiple separate occasions to individual acrylic containers on a shared glass floor heated to 30°C 1 week prior to the start of each experiment.

Open field testing

The open-field testing arena consisted of a 40 × 40 cm box with a white floor and black walls. Animals were placed in the open-field arena, in a room with controlled adjustable lighting, and baseline activity was recorded for 30 min (Sony Handycam, HDR-CX405, Sony Corp., Tokyo, Japan). The distance traveled (cm), time spent immobile (sec), average velocity (cm/s), and the change in orientation angle (degrees) were computed by using data output from the Ethowatcher computational tool software (Laboratory of Bioengineering of the Institute of Biomedical Engineering and the Laboratory of Comparative Neurophysiology of the Federal University of Santa Catarina, UFSC, available: <http://ethowatcher.paginas.ufsc.br/>) (Crispim Junior et al., 2012).

Burrowing testing

Two days after the completion of the mechanical testing (one-week after CFA inoculation), AAV9-*Adcy1* and AAV9-scramble mice were subjected to burrowing testing. Mice were acclimated to empty burrowing tubes for ~2 h on at least two separate occasions before formal testing. The burrows were made from a 6 cm diameter plastic pipe and 5 cm machine screws were used to elevate the open end by 3 cm (Deacon, 2012). During testing, each mouse was placed in an individual cage with a burrowing tube containing 500 g of pea gravel. The amount of gravel remaining in the tube after 2 h was used to calculate the total percent of gravel displaced from the burrow.

Nesting

Mice were individually housed in plastic cages containing cob bedding with food and water *ad libitum* overnight. A single 2" Nestlets™ (Ancare Corp., Bellmore, NY, United States) square was weighed and added to each cage. The next morning (~14 h) untorn pieces of each nesting square were weighed and the resulting nests were photographed and scored on a 5-point scale as described previously (Deacon, 2012). Briefly the scoring system was: 1 = >90% intact, 2 = partially torn, 3 = mostly shredded but no identifiable nest, 4 = >90% torn but flat nest site, 5 = >90% torn with resulting crater nest. Scores with 0.5 units were used for nests with scores in between the aforementioned intervals. Nesting scores were tabulated 3 days after CFA injections.

Tissue collection and mRNA isolation

Lumbar spinal cord and L3-L6 DRG tissues harvested from animals were flash frozen in liquid nitrogen and stored at -80°C 8 weeks after virus inoculation. Total mRNA was isolated from tissues using Tri Reagent (T9424, Sigma Aldrich, St. Louis, MO, United States) and RNeasy Mini Kit (Qiagen, Germantown, MD, United States) according to the manufacturer's protocol with 30 min DNase 1 digestion. Complementary DNA synthesis was performed with 50 ng total mRNA using Omniscript RT Kit (Qiagen, Germantown, MD) and random nonamers (Integrated DNA Technologies, Coralville, Iowa) according to the manufacturer's protocol.

Quantitative PCR

Quantitative PCR was performed using SYBR Green I dye with a LightCycler 480 machine (Roche, Branchburg, NJ, United States). The cDNA copy number was typically quantified against a ≥5 point, 10-fold serial dilution of a gene-specific cDNA standard (~5e1 to 5e6 copies/μL) cDNA standards were created using block PCR for one gene (Amplitaq Gold, Applied Biosystems) and purified using Qiaquick (Qiagen). Standards were quantified using a UV-Vis spectrophotometer and DNA copies/μL calculated using the equation: (DNA μg/μL) (μmoles/DNA m. w. μg) (1 mol/1 × 10⁶ μmoles) (6.022 × 10²³copies/mole). Internal controls included negative RT-PCR samples and comparative expression versus housekeeping genes, 18S and Gapdh. Amplification efficiencies were >1.8 and the targeted ΔCt between two dilutions was around -3.3. Fold expression of each gene of interest was determined by: (mean gene concentration/mean 18s concentration)/(mean gene concentration in saline/mean 18s concentration in saline). See Table 2 for gene-specific primers used.

AC1 enzyme-linked immunosorbent assay

Quantitative measurement of AC1 in spinal cord tissue was performed using the Mouse Adenylate cyclase type 1 (*Adcy1*) ELISA Kit (RK08031, ABclonal, Woburn, MA, United States) kit according to manufacturer instructions. Briefly, spinal cords were homogenized in RIPA lysis buffer (100 mM Tris, 150 mM NaCl, 1 mM EGTA, 1 mM EDTA, 1% Triton X-100, 0.5% sodium deoxycholate) with added protease (P8340 and phenylmethylsulfonyl fluoride, Sigma) and phosphatase (P0044 and P5726, Sigma) inhibitors. Spinal cord homogenates were centrifuged and further diluted in Sample Diluent provided by ABclonal. After incubation in Biotin Conjugate Antibody, Streptavidin-HRP, and TMB substrate, each well was read in microplate reader (Biotek Instruments, Santa Clara, CA, United States) at 450 nm with a

TABLE 2 Gene specific primers used for qRT-PCR. The NCBI gene accession number, resulting base pair length, and both the forward and reverse primers for each gene for qRT-PCR analysis.

Gene	NCBI number	Length	Forward	Reverse
<i>18s</i>	NR_003278.3	149bp	5'-CGCCGCTAGAAAGTGAATTCCTT-3'	5'-CAGTCGGCATCGTTTATGGTC-3'
<i>Adcy1</i>	NM_009622.1	115bp	5'-TGCAGACATCGTGGGTTTCA-3'	5'-ACAGTGGTTTTTCGGCTA-3'
<i>Adcy2</i>	NM_153534.2	140bp	5'-CTAAACCGAGTGCTGCTGGA-3'	5'-TTGAAGTCCGGAATGGAGGC-3'
<i>Adcy3</i>	NM_138305.3	199bp	5'-TCTGGGGTCCAAGAAGAGAGA-3'	5'-GACCCGGAATTTGGGATTGTC-3'
<i>Adcy5</i>	NM_001012765.4	151bp	5'-TGATCGAGGCCATCTCGTTG-3'	5'-TGGTTGGCCAGAGTGACATC-3'
<i>Adcy6</i>	NM_007405.2	162bp	5'-TGCGGTGAGGGAGAATCACT-3'	5'-ACACCTGTTACCTCACGCAC-3'
<i>Adcy8</i>	NM_001291903.1	191bp	5'-CCGCATCTACATCCATCGCT-3'	5'-AGTAGTAGCAGTCCCCCAGG-3'
<i>Prkaca</i>	NM_008854.5	96bp	5'-TTTGCCAAGCGTGTGAAAGG-3'	5'-AGCCTTGTTGTAGCCTTTGCT-3'
<i>Prkacb</i>	NM_011100.4	122bp	5'-TGCAGCCCAGATTGTGCTAA-3'	5'-ACCCGAAATCTGTGACCTGG-3'
<i>Rapgef3</i>	NM_001177810.1	145bp	5'-GGAAGTGCATGAGCTGACCC-3'	5'-CACCTGGTGGATCCTGTTGAAG-3'
<i>Rapgef4</i>	NM_001204165.1	96bp	5'-TCCAAGAGCTGCCTCCATTG-3'	5'-GAATCAACGTCCCTCAGAAT-3'
<i>Gapdh</i>	NM_001289726.1	85bp	5'-TGACCTCAACTACATGGTCTACA-3'	5'-CTTCCCATTTCTCGGCCTTG-3'

wavelength correction at 570 nm. Samples were compared against an 8-point standard calibration provided by ABclonal.

Microscopy

Histological sections were taken from spinal cord, DRG, and sciatic nerves to verify the delivery of the AAV9 virus within the lumbar intrathecal space 8-weeks post inoculation. Verification of virus inoculation was visible by the presence of green fluorescent protein (GFP). Sections (10 μ M, Leica CM3050) were mounted onto electrostatically charged slides and images were collected using a Nikon TiS Microscope and associated software.

C-fiber compound action potentials

Compound action potentials (CAPs) were measured from both left and right desheathed sciatic nerves from AAV9-GFP-U6-m-Adcy1-shRNA and AAV9-GFP-U6-scramble-shRNA8 weeks after intrathecal injection. Sciatic nerves were dissected from the hind limbs of mice and recordings were performed the same day. Each nerve was mounted in a chamber filled with superficial interstitial fluid composed of 107.7 mM NaCl, 3.5 mM KCl, 0.69 mM MgSO₄, 26.2 mM NaCO₃, 1.67 mM NaH₂PO₄, 1.5 mM CaCl₂, 9.64 mM Na⁺ gluconate, 5.5 mM d-glucose, and 7.6 mM sucrose, pH 7.4 (bubbled with 95% O₂, 5% CO₂). Electrical stimulation was performed at a frequency of 0.3 Hz with electric pulses of 100- μ s duration at 100–10,000 μ A delivered by a pulse stimulator (2100, AM Systems, Carlsborg, WA, United States). Evoked CAPs were recorded with electrodes placed ~5 mm from the stimulating electrodes. Dapsys software was used for data capture and analysis (Brian Turnquist, Bethel University, St. Paul, MN, United States, www.dapsys.net). The lowest stimulus producing a detectable response in

the nerve was determined as the threshold stimulus and the peak amplitude determined when the response no longer increased in amplitude. The conduction velocity was calculated by dividing the latency period, the time from stimulus application to neuronal initial response, by the stimulus-to-recording electrode distance. The sciatic nerves were collected in mice previously used in the morphine escalating dose-response curve studies.

Data analysis

Data were collected by personnel blinded to the animal's condition and treatment. The appropriate *t*-test, one-way,

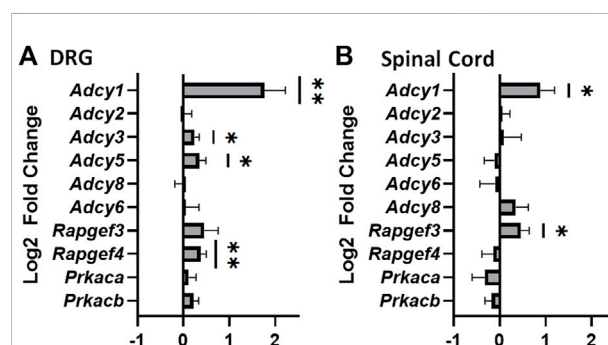


FIGURE 1

Significant increase in mRNA of adenylyl cyclase 1 in the dorsal root ganglia and spinal cords of mice that have undergone chronic morphine administration. Mice were given systemic morphine or saline twice daily for 5 days (15 mg/kg, sc). (A) Dorsal root ganglia (DRG) from morphine treated mice have elevated levels of *Adcy1*, *Adcy3*, *Adcy5*, and *Rapgef4* mRNA compared to saline treated mice (one-sample *t*-test, *n* = 11–12/group). (B) Spinal cords from morphine treated mice have elevated levels of *Adcy1* and *Rapgef3* mRNA compared to saline treated mice (one-sample *t*-test, *n* = 14/group). Data are displayed as the Log2 fold change of morphine treated mice over the average of the saline treatment group, \pm SEM, **p* < 0.05, ***p* < 0.01.

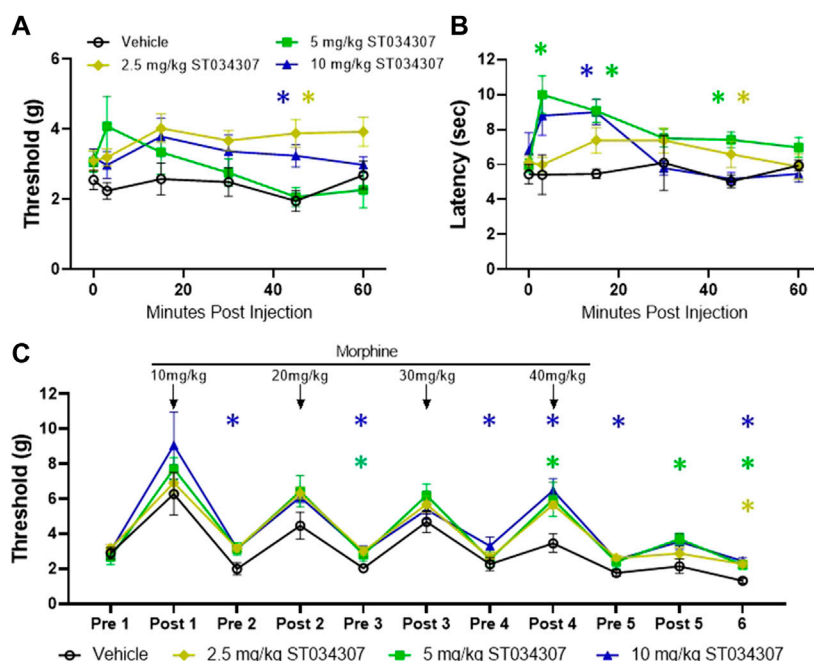


FIGURE 2

ST034307 produces mechanical and thermal antinociception and attenuates morphine induced hyperalgesia (A) Mechanical paw withdrawal thresholds and thermal latencies (B) between vehicle and ST034307 treated mice. Significant increases in paw thresholds and latencies were seen between vehicle and ST034307 treated mice (repeated measures ANOVA with Dunnett's post hoc test vs. vehicle, $F(3, 31) = 3.691$, $p = 0.0221$ and $F(3, 29) = 5.460$, $p = 0.0042$, respectively). (C) To induce escalating morphine tolerance, mice received twice daily injections of morphine (10 mg/kg on day 1 increasing to 40 mg/kg by day 4, sc, 100 μ L) along with an injection of either vehicle or ST034307 (2.5–10 mg/kg, ip, 100 μ L) 15 min post-morphine. Baseline measurements were measured every morning before morphine injection (Pre) and 30 min post injection (Post) with day 5 and day 6 thresholds measured ~18 and ~42 h, respectively, after last morphine injection (repeated measures ANOVA with Dunnett's post hoc test vs. vehicle, $F(3, 32) = 8.424$, $p = 0.0003$). Asterisk indicates statistical significance at each individual time point ($p < 0.05$). Data presented as mean \pm SEM. Data presented as mean \pm SEM with an $n = 5$ (vehicle) or 10 (2.5–10 mg/kg ST034307)/group.

two-way, or repeated-measures ANOVA followed by either Dunnett's or Bonferroni's post hoc analysis was used to determine significance for mechanical thresholds, thermal latencies, gene expression, burrowing, open field testing, rotarod assessments, and CAP recordings. A Mann-Whitney U test was used for nesting behaviors. All statistical analyses were carried out using GraphPad Prism version 9 (GraphPad Software, San Diego, CA). Data presented as mean \pm SEM unless otherwise indicated with $p < 0.05$ considered statistically significant.

Results

Adcy1 mRNA expression is increased in the dorsal root ganglia and spinal cord in mice after chronic administration of morphine

Chronic agonist exposure of the MOR decreases inhibitory intracellular responses and increases adenylyl cyclase/cyclic-AMP activity (Williams et al., 2013). We attempted to confirm these

findings by analyzing the change in mRNA expression of various *Adcy* isoforms in nervous system tissues of morphine tolerant mice. Of the isoforms examined, an increased expression of *Adcy1* is seen in DRG and spinal cord (Figure 1). This suggests AC1 may play a role in morphine tolerance in both the central and peripheral nervous systems. *Adcy3*, *Adcy5*, and *Rapgef4* (protein: Epac2) mRNA were also elevated in dorsal root ganglia, while *Rapgef3* (protein: Epac1) was also elevated in the spinal cord.

Systemic ST034307 administration attenuates morphine tolerance and withdrawal

To further understand the physiological role of AC1 during tolerance and withdrawal with chronic morphine administration, pharmacological and gene knock-down strategies were implemented with behavioral assays. Previous research demonstrated ST034307 acts as an AC1 inhibitor and as an analgesic in a mouse chronic inflammatory pain model (Brust et al., 2017). In both

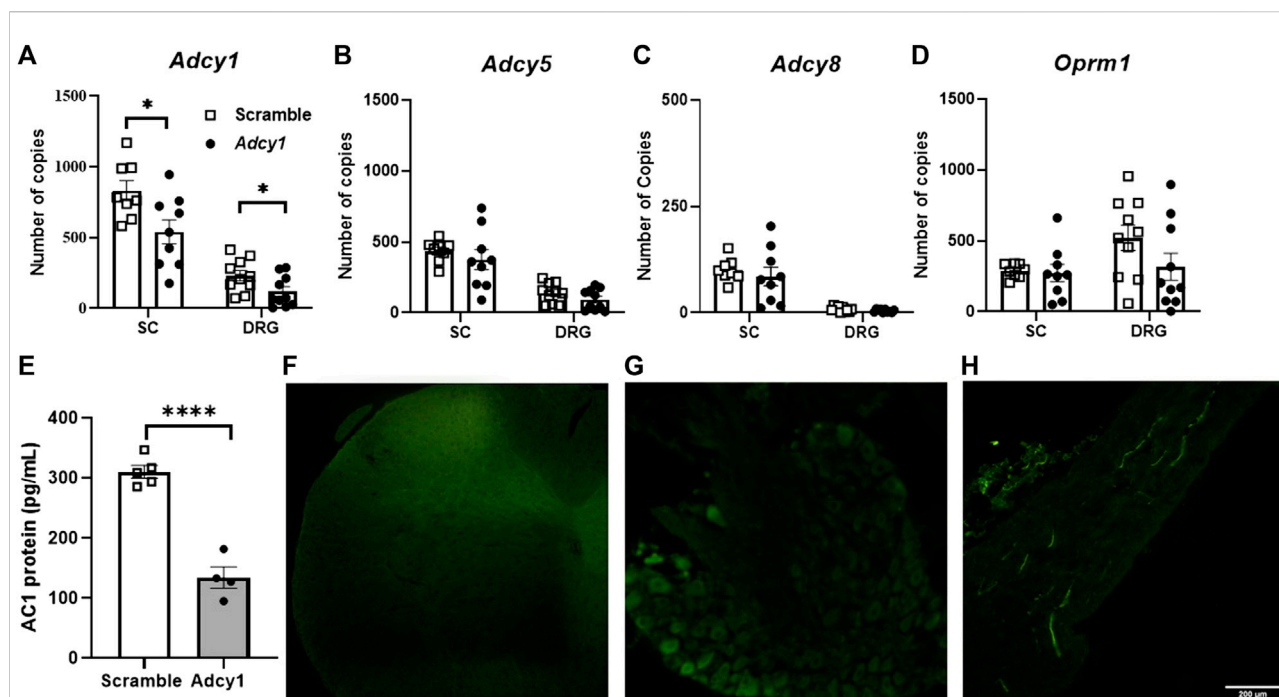


FIGURE 3

Intrathecal injection of small interfering RNA sequences targeting AC1 reduces *Adcy1* mRNA in spinal cord and DRG of mice. (A) Significant reduction of *Adcy1* mRNA copies present in mice injected with AAV9-*Adcy1*-shRNA-GFP (Adcy1) vs. AAV9-Scrambl-shRNA-GFP (Scramble; unpaired *t*-tests, **p* < 0.05). No significant changes are seen in *Adcy5* (B), *Adcy8* (C), or *Oprm1* (D) mRNA expression. *n* = 8–10/group. (E) Protein levels of AC1 collected from spinal cord are lower in AAV9-*Adcy1*-shRNA-GFP (Adcy1) vs. AAV9-Scrambl-shRNA-GFP injected mice (unpaired *t*-test, *p* < 0.0001), *n* = 4–5/group. Injections were verified by Immunofluorescence analysis in the spinal cord (F), DRG (G), and sciatic nerves (H). Scale bar = 200 μm. Data presented as mean ± SEM.

mechanical and thermal nociceptive tests, the peak threshold and latency measurements increased after intraperitoneal administration of ST034307 (Figures 2A,B). A significant increase in thermal latency was seen between vehicle and ST034307 over time (Figure 2B). The peak antinociceptive action of ST034307 occurred around ~15 min post-injection, but this effect is still fairly weak in naïve mice.

To determine if ST034307 attenuates morphine tolerance and opioid-induced hypersensitivity *in vivo*, mice were subjected to twice daily morphine injections (10 mg/kg on day one increasing 10 mg/kg each day to a final concentration of 40 mg/kg, sc) in combination with either an injection of vehicle or ST034307 (Figure 2C). Mechanical thresholds were measured before the start of injections and 30 min post morphine injection to measure opioid-induced hypersensitivity and morphine tolerance, respectively. ST034307 increased paw withdrawal thresholds pre-morphine administration, compared to vehicle injected animals, indicating the pharmacological inhibition of AC1 can decrease morphine-induced hyperalgesia. A mild effect on morphine tolerance was also observed as ST034307 increased paw withdrawal thresholds after morphine administration on Day 5 compared to vehicle controls.

Intrathecal knockdown of *Adcy1* attenuates morphine tolerance and opioid-induced hypersensitivity

A shRNA targeting *Adcy1* was used to reduce *Adcy1* expression within the peripheral nervous system and spinal cord via intrathecal injection. To ensure the shRNA knockdown strategy of the AAV9-*Adcy1* was successful, spinal cords and DRG were collected for qPCR after the conclusion of behavioral tests. The mRNA copy numbers of *Adcy1* were significantly reduced in AAV9-*Adcy1* mice in both the spinal cord (Figure 3A, unpaired *t*-test, *p* = 0.0201) and DRG (Figure 3A, unpaired *t*-test, *p* = 0.0370) compared to the AAV9-scramble mice. Changes to the expression levels of *Adcy5*, *Adcy8*, and *Oprm1* were also analyzed, but no significant differences were seen for any of these genes in either tissue (Figures 3B–D). Protein levels of AC1 in the spinal cord were also confirmed to be decreased using an ELISA assay (Figure 3E). Florescence microscopy also indicates the injection location was successful in these experiments (Figures 3F–H).

Since continued agonist stimulation of the MOR increases AC activity, the *Adcy1* knockdown model was hypothesized to show an

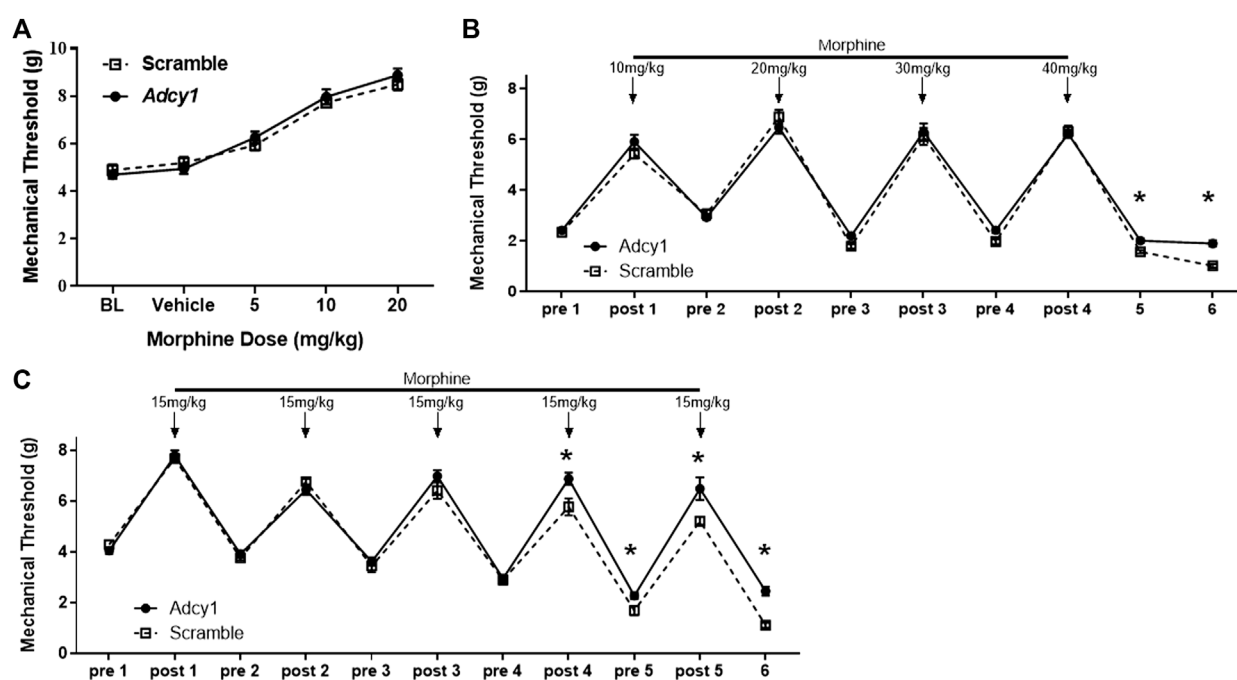


FIGURE 4

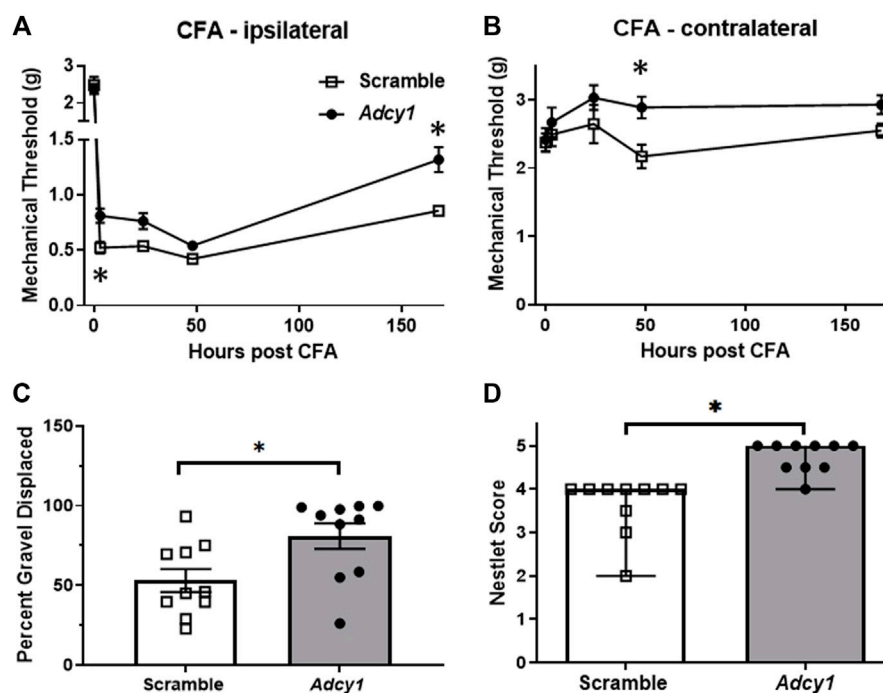
AC1 knockdown via intrathecal delivery of AAV9-Adcy1-shRNA partially attenuates morphine induced hyperalgesia in mice. (A) Knockdown of Adcy1 mRNA does not impact acute morphine antinociception (5–20 mg/kg, sc, measurements taken 30 min after morphine injection). (B) Twice daily escalating injections of morphine (10 mg/kg on day 1 increasing to 40 mg/kg by day 4, sc, 100 μ l) induce hyperalgesia that is attenuated in AAV9-Adcy1-shRNA compared to AAV9-Scrambl-shRNA injected mice on Days 5 and 6, ~18 and ~42 h after last morphine injection, respectively (repeated measures ANOVA, $F(1, 18) = 3.928$, $p = 0.00630$). (C) Morphine tolerance and hyperalgesia established by twice daily injections of morphine for 5 days (15 mg/kg, sc) are reduced in AAV9-Adcy1-shRNA compared to AAV9-Scrambl-shRNA injected mice ($F(1, 18) = 17.61$, $p = 0.0005$). Asterisk indicates statistical significance at each individual time point ($p < 0.05$). Data presented as mean \pm SEM with an $n = 10$ /group.

attenuation of morphine tolerance and opioid-induced hypersensitivity, but not necessarily acute morphine antinociception. An acute morphine dose-response curve indicated AAV9-Adcy1 and AAV9-scramble mice had similar antinociceptive effects of morphine (Figure 4A). Using an escalating morphine tolerance model, mice were subjected to mechanical testing while given twice daily injections of increasing doses of morphine in saline, starting with 10 mg/kg on day 1 and increasing by 10 mg/kg daily until reaching 40 mg/kg on day 4. AAV9-Adcy1 mice exhibited significantly higher mechanical thresholds than AAV9-scramble mice pre-morphine administration on days 5 and 6 (Figure 4B). In an alternative model of morphine tolerance, morphine was administered twice daily in saline (15 mg/kg, SQ), and on day 6 mechanical thresholds were taken ~18 h after the last morphine injection. AAV9-Adcy1 mice had significantly higher mechanical thresholds compared to AAV9-scramble mice pre-morphine administration on day 5 and day 6, indicating that loss of AC1 reduced morphine-induced hypersensitivity (Figure 4C). Collectively, these data show the knockdown of Adcy1 not only attenuates the development of morphine tolerance but also the development of opioid-induced hypersensitivity.

Intrathecal knockdown of Adcy1 improves mechanical hypersensitivity and non-evoked behaviors after complete freund's adjuvant injection in mice

Previous research has demonstrated pharmacological inhibition of AC1 via ST034307 could provide analgesia in a mouse model of chronic inflammatory pain (Brust et al., 2017). We performed a similar test to examine CFA analgesic efficacy after Adcy1-shRNA treatment 7 weeks after inoculation. AAV9-Adcy1 mice had significantly higher mechanical thresholds than AAV9-scramble mice on both the CFA injected paw (Figure 5A) and the uninjected hind paw (Figure 5B). This data indicates knockdown of Adcy1 does provide some analgesic efficacy in the chronic inflammatory pain model one-week post-CFA administration.

A significant increase in gravel displacement was seen between the AAV9-Adcy1 and control mice (Figure 5C). A significant increase in nesting scores was also seen in AAV9-Adcy1 compared to AAV9-scramble mice (Figure 5D). Altogether, this data indicates the level of ongoing pain or discomfort produced by CFA may be decreased after

**FIGURE 5**

Intrathecal delivery of AAV9-Adcy1-shRNA reduces mechanical hypersensitivity following intraplantar CFA. Mechanical paw withdrawal thresholds were measured before and after a unilateral hind paw injection of 20 μ l CFA. (A) AAV9-Adcy1 (●) mice had significantly higher MPW thresholds than AAV9-scramble mice (□) on the injected paw (repeated measures ANOVA with Bonferroni's *post hoc* test, $F(1, 18) = 6.157$, $p = 0.0232$), (B) and on the CFA uninjected paw (repeated measures ANOVA with Bonferroni's *post hoc* test, $F(1, 18) = 9.148$, $p = 0.0073$). (C) AAV9-Adcy1 mice have increased burrowing (unpaired *t*-test, $p = 0.0188$) (D) and higher nest building scores compared to control mice (Mann Whitney test, $p < 0.0001$). Asterisk indicates statistical significance at each individual time point ($p < 0.05$), $n = 10$ /group. Data in A–C presented as mean \pm SEM, data in D presented as median \pm 95% confidence interval.

AC1 knockdown and the loss of AC1 signaling may contribute to greater functional motility during chronic pain.

Knockdown of *Adcy1* does not alter mobility, thermal nociception, or sciatic nerve conduction in mice

Mice were subjected to rotarod and thermal paw withdrawal testing 3-weeks post virus injections and open field assessments 4-weeks post virus injections, before CFA administration. For rotarod testing, the total time on rotarod (Figure 6A) were not significantly different between AAV9-scramble and AAV9-Adcy1 mice. No significant difference was seen between AAV9-scramble and AAV9-Adcy1 mice during thermal testing (Figure 6B). In open field tests, no significant difference was seen between AAV9-scramble and AAV9-Adcy1 mice in distance traveled (Figure 6C), velocity (Figure 6D) or change in orientation angle (Figure 6E). However, a small yet significant difference was seen in time spent immobile (Figure 6F; unpaired *t*-test, $p = 0.0433$) indicating AAV9-Adcy1 mice spent less time stationary compared to

AAV9-scramble injected mice. This data indicates the AAV9-Adcy1 shRNA does not cause any major mobility changes in mice. Lastly, the downregulation of *Adcy1* did not have any impact on thresholds, amplitude, or conduction velocity of C-fiber CAPs (Figures 7A–D).

Discussion

The present study investigated the role of AC1 with regard to opioid tolerance, opioid-induced hyperalgesia, and inflammatory pain in mouse models. In our study, *Adcy1* was elevated in the DRG and spinal cord of mice after chronic morphine exposure. Our behavioral results indicate pharmaceutical inhibition of AC1 using ST034307 reduced opioid tolerance and attenuated morphine-induced hypersensitivity after increasing opioid administration. Intrathecal knockdown of *Adcy1* using a viral strategy was also effective at reducing morphine-induced hyperalgesia and withdrawal. The loss of *Adcy1* expression increased mechanical paw withdrawal thresholds, and improved burrowing and nesting behaviors after CFA intraplantar injection.

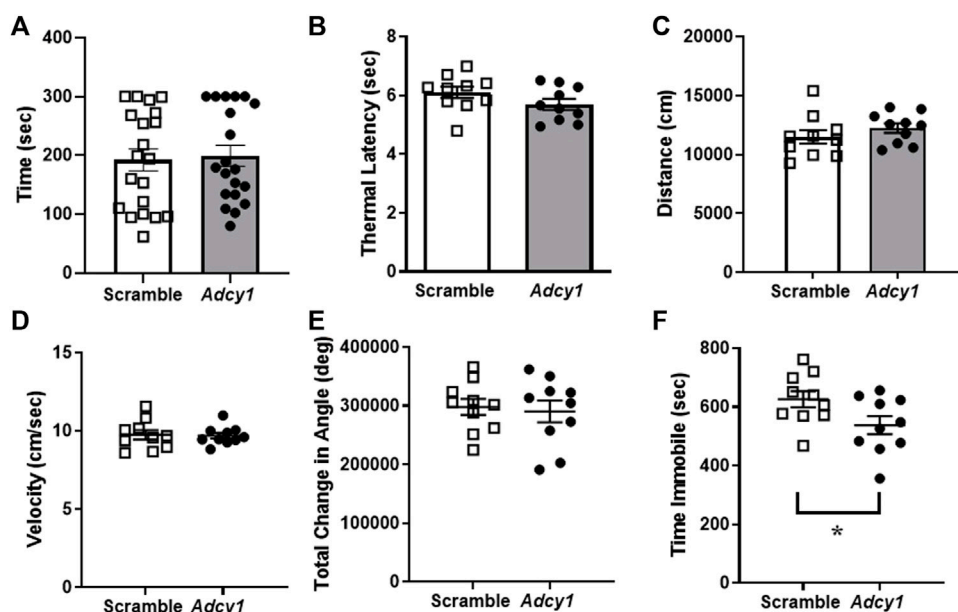


FIGURE 6

Animal mobility, thermal sensitivity and open field behaviors are not affected in mice with intrathecal knockdown of *Adcy1*. Mice underwent behavioral assessments to gauge mobility and the presence of behavioral deficits after intrathecal injection of AAV9-GFP-U6-m-*Adcy1*-shRNA (●) or AAV9-GFP-U6-scramble-shRNA (□) intrathecal injections. The (A) maximum time spent on a rotating rod, (B) thermal paw withdrawal latency, open field assessments including the (C) distance traveled, (D) velocity, and (E) total change in angular orientation were not significantly different between treatment groups. (F) The time spent immobile in seconds was significantly decreased in AAV9-*Adcy1* compared to AAV9-scramble mice (unpaired *t*-test, $p = 0.0433$, $n = 10$ /group).

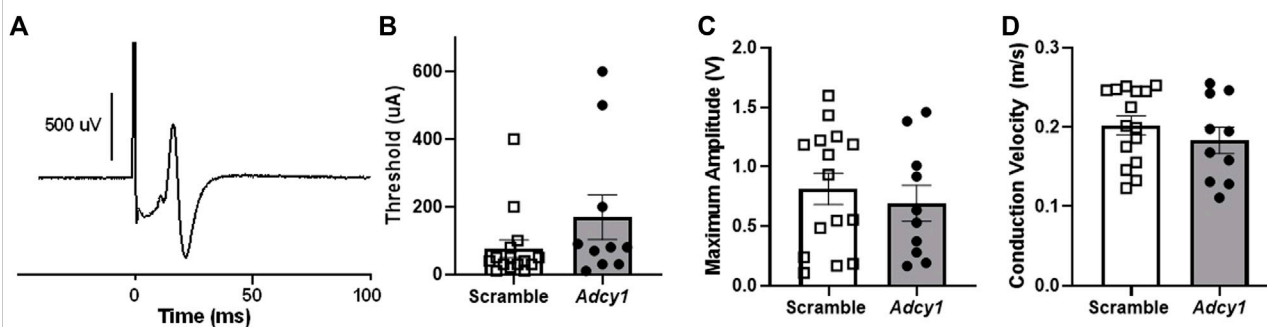


FIGURE 7

Intrathecal administration of AAV9-GFP-U6-m-*Adcy1*-shRNA (●) or AAV9-GFP-U6-scramble-shRNA (□) does not alter sciatic nerve C-fiber conduction properties. (A) Example of a compound action potential (CAP) recording from sciatic nerve of mouse. The (B) electrical thresholds, (C) maximum CAP amplitude, and (D) conduction velocity, were not significantly different between groups. Data presented as mean \pm SEM with $n = 10$ –20/group.

The mechanisms driving chronic pain are thought to be associated with opioid tolerance as both phenomena may arise from similar changes in intracellular signaling pathways in the peripheral and/or central nervous systems (Joseph et al., 2010). The rationale for using both morphine and inflammatory pain models in our study were that 1)

Chronic morphine treatment has been previously shown to produce a hypertrophied state of AC1, AC6, and AC8 *in vitro* (Avidor-Reiss et al., 1997) and 2) Several AC isoform-selective pharmacological inhibitors have been developed, particularly for AC1, and appear to attenuate chronic pain in mice (Brust et al., 2017; X.-H. Li et al., 2020; Vadakkan et al., 2006; H.

Wang et al., 2011). In chronic pain and opioid-tolerant states, increased AC activity is thought to contribute to enhanced neurotransmission of nociceptive circuits at several levels including the brain (Liauw et al., 2005; Zachariou et al., 2008), spinal cord (Wei et al., 2006), and primary afferents (Yue et al., 2008; Bavencoffe et al., 2016). Opioid tolerance and dependence can be enhanced in several mouse models after CFA treatment, indicating that some synergy is occurring between these two conditions (Liang et al., 2006). In our current and previous studies, systemic administration of ST034307, a small molecule inhibitor of AC1, did not greatly increase mechanical or thermal paw withdrawal thresholds in naïve animals, yet reduced morphine tolerance and hyperalgesia in CFA treated mice. (Brust et al., 2017). This further corroborates the idea that adenylyl cyclase activity in uninjured or morphine-naïve animals may be fairly low.

Hypersensitivity and hyperalgesia seen in chronic pain and drug-induced hypersensitivity most likely occur on multiple levels along sensory transmission pathways, from peripheral afferents, spinal cord synapses, and connectivity across midbrain and cortical cells. To determine if localized downregulation of AC1 in the spinal cord and primary afferent neurons could attenuate opioid tolerance and inflammatory chronic pain, an intrathecal viral knockdown approach was used with shRNA specifically targeted to *Adcy1*. Static dosing of morphine (15 mg/kg, 2x daily, 5 days) and escalating doses of morphine over 4 days (10–40 mg/kg, 2x daily) both resulted in enhanced baseline mechanical sensitivity. After intrathecal administration of AAV9-*Adcy1*, mice had higher mechanical paw withdrawal thresholds before (pre) and after (post) morphine administration compared to control mice. Our data agree with previous studies, as a global loss of either/both AC1 or AC8, appear to have a role in attenuating morphine tolerance and withdrawal (Villacres et al., 1998; Wang and Zhang, 2012). Additionally, AC1 and AC8 knockout mice have increased thermal latencies during the first few days of morphine tolerance testing as well as decreased withdrawal behaviors (Li et al., 2006; Zachariou et al., 2008).

In contrast, baseline mechanical sensitivity and acute morphine antinociception were not changed in AAV9-*Adcy1* mice compared to control mice. This distinction between a lack of antinociception after acute morphine delivery and a significant enhancement of paw withdrawal thresholds after chronic morphine administration is important, indicating adenylyl cyclase hypertrophy occurs after repeated stimulation of the MOR, and not after a single dose of an opioid, which has been a proposed paradigm for many years (Williams et al., 2001). Collectively, this suggests a reduction in the activity or function of AC1 may represent a novel analgesic target in addition to improving opioid withdrawal in patients taking chronic opioids.

AC1 and AC8 have also been linked to the development of both acute and chronic persistent inflammatory pain (Vadakkan et al., 2006; Wei et al., 2006; Griggs et al., 2017; Griggs et al., 2019). Baseline thermal and mechanical sensitivities are not altered in AC1^{-/-} mice, but responses after formalin and CFA are decreased compared to wild-type mice (Wei et al., 2002). In a separate study, the loss of AC1, but not AC8, decreased nocifensive responses to formalin (Vadakkan et al., 2006). Systemic delivery of pharmacological inhibitors of AC1 reduces hypersensitivity in neuropathic and inflammatory pain models in mice (Brust et al., 2017; Wang et al., 2011), consistent with knock-out mouse studies. In a mouse model of inflammatory pain, AAV9-*Adcy1* mice also had higher mechanical paw withdrawal thresholds compared to control mice 3 h and 7 days after CFA injection. The lack of analgesia seen during the initial phases after CFA administration (24–48 h), could be due the deferred hypertrophy of adenylyl cyclases after tissue injury, or the delayed role of adenylyl cyclases in enhanced transcription of pro-inflammatory molecules, taking several days to manifest (Tarnawski et al., 2018). The initial change in mechanical thresholds seen at 3 h post-CFA was surprising, as a previous study failed to demonstrate a pre-emptive effect in a rodent model of neuropathic pain with adenylyl cyclase inhibitor administered before injury (Liou et al., 2009). Another previous study using the AC1-specific inhibitor NB001 indicates that inhibition of hyperalgesia after CFA administration was seen 3 days after inoculation (Zhou et al., 2021).

It is possible after tissue damage, stimulation of cAMP and PKA due to adenylyl cyclase activation, promotes hyperalgesia by initially increasing levels of molecules such as PGE₂ in the early phases of injury (Aley and Levine, 1999). Activation of protein kinase A (PKA) in chronic pain has also been associated with subsequent phosphorylation of a transcription factor, cAMP response element-binding protein (CREB). CREB is responsible for the transcriptional regulation of a large number of proteins and peptides implicated in heightened nervous system activity (e.g. c-Fos, BDNF, tyrosine hydroxylase, etc.) during inflammation and during chronic opioid administration. The impact of AC1 inhibition could be delayed due to the role of CREB or other transcription factors involved in pain chronification that take a much longer time to develop (Tao et al., 2019). Attenuation of mechanical hyperalgesia was also seen on the contralateral (uninjected) hind paws. During chronic pain states, anatomical sites nearby also become sensitized to painful or non-painful stimulation (Chen et al., 2014; Griffioen et al., 2015). The inhibition of AC1 could also help attenuate pain sensitization beyond the primary zone of injury through changes in functional plasticity that occurs in contralateral sensory nerves following the induction of inflammation (Kelly et al., 2007) that may not follow the same time course as the ipsilateral side. AC1 inhibition most likely does not impact the progression of inflammation directly, as other studies have shown that NB001, does not impact CFA-

induced knee joint structural destruction nor mono-sodium urate-induced edema of the ankle joint (Tian et al., 2015; Liu et al., 2021). Alternatively, those results may be explained by the smaller overall level of the *Adcy1* knockdown in our studies when compared to global AC1 knockout mice (Wei et al., 2002).

Spontaneous pain and animal wellbeing after initiation of chronic pain are less frequently investigated than evoked measures, so our studies incorporated alternative testing measures including burrowing and nesting behaviors innate to rodents. Burrowing and nesting tests have been used to evaluate spontaneous pain or tonic pain in several models of chronic pain in rodents (Gaskill et al., 2013; Muralidharan et al., 2016). We found small differences between AAV9-*Adcy1* and AAV9-scramble mice in burrowing behaviors after CFA injection. A similar difference was also seen in the nesting scores after CFA induction, as AAV9-*Adcy1* mice demonstrated significantly higher nesting scores than control mice. In previous studies, burrowing behavior is reduced in CFA inflammatory pain models in rats and can be reversed by ibuprofen (Andrews et al., 2012). Nesting behaviors are reportedly attenuated after CFA injection in mice which can be reversed by ketoprofen or low doses of morphine (Negus et al., 2015). Notably, no significant differences were detected between AAV9-*Adcy1* and AAV9-scramble mice in either the rotarod, thermal paw withdrawal latencies, or open field-testing parameters, indicating intrathecal knockdown of AC1 does not affect acute thermal pain thresholds or affect general ambulatory behaviors. Transcriptional knockdown of AC1 in the sciatic nerves of mice was not specifically measured, however, there were no significant changes in C-fiber compound action potential properties. These data indicate behavioral changes seen in the AAV9-*Adcy1* animals may be restricted to the spinal cord and/or DRG, or loss of AC1 function does not impact axonal propagation of C-fiber action potentials.

Opioids are one of the most common analgesics used to alleviate pain in the clinic and function by inhibiting neuronal signal transmission. Individuals with chronic pain, including inflammatory pain, use opioids daily for pain management, causing the development of analgesic tolerance, leading to dosage escalation. Whether the increased opioid requirement is caused by the decreasing analgesic efficacy of the drug (i.e., tolerance), or an increase in spontaneous pain, or lowering the nociceptive threshold, the clinical effect is the same (Hayhurst and Durieux, 2016). Furthermore, if the patient ceases therapy, there is a possibility of withdrawal and hypersensitivity, increasing the likelihood of opioid dependence and abuse situations. New therapies that target the interaction of nociceptive signaling and opioid exposure have not emerged, but would provide an opportunity to not only reduce chronic pain but also potentially ease opioid tolerance and/or dependence. In conclusion, this study suggests AC1 may represent a novel pharmaceutical target for the reduction of chronic pain and the attenuation of

opioid-mediated adverse effects. Further research exploring the intracellular targets of AC1 may provide opportunities for new therapeutics in the future.

Data availability statement

The raw data supporting the conclusions of this article will be made available by the authors, without undue reservation.

Ethics statement

The animal study was reviewed and approved by University of Minnesota Institutional Animal Care and Use Committee.

Author contributions

Performed experiments and analyzed data: KJ, AD, AE, AV, RM, SH, AF, and AK. Conceived experiments, designed and directed the studies: AK and VW. Wrote the manuscript: KJ, AD, VW, and AK.

Funding

This work was supported by grants from the National Institute of Drug Abuse (K01DA042902, R01 DA051876; AK), the summer Undergraduate Research Program, and the Undergraduate Research Opportunity Program from the University of Minnesota (AD), The Biology Undergraduate Research summer Training program from the University of Minnesota (AV), the TRIO McNair Scholars Program from the College of St. Scholastica (AE), and the Purdue University College of Pharmacy (VW).

Conflict of interest

The authors declare that the research was conducted in the absence of any commercial or financial relationships that could be construed as a potential conflict of interest.

Publisher's note

All claims expressed in this article are solely those of the authors and do not necessarily represent those of their affiliated organizations, or those of the publisher, the editors and the reviewers. Any product that may be evaluated in this article, or claim that may be made by its manufacturer, is not guaranteed or endorsed by the publisher.

References

- Aley, K. O., and Levine, J. D. (1999). Role of protein kinase A in the maintenance of inflammatory pain. *J. Neurosci.* 19 (6), 2181–2186. doi:10.1523/jneurosci.19-06-02181.1999
- Andrews, N., Legg, E., Lisak, D., Issop, Y., Richardson, D., Harper, S., et al. (2012). Spontaneous burrowing behaviour in the rat is reduced by peripheral nerve injury or inflammation associated pain. *Eur. J. Pain* 16 (4), 485–495. doi:10.1016/j.ejpain.2011.07.012
- Avidor-Reiss, T., Nevo, I., Saya, D., Bayewitch, M., and Vogel, Z. (1997). Opiate-induced adenylyl cyclase superactivation is isozyme-specific. *J. Biol. Chem.* 272 (8), 5040–5047. doi:10.1074/jbc.272.8.5040
- Bavencoffe, A., Li, Y., Wu, Z., Yang, Q., Herrera, J., Kennedy, E. J., et al. (2016). Persistent electrical activity in primary nociceptors after spinal cord injury is maintained by scaffolded adenylyl cyclase and protein kinase A and is associated with altered adenylyl cyclase regulation. *J. Neurosci.* 36 (5), 1660–1668. doi:10.1523/JNEUROSCI.0895-15.2016
- Brust, T. F., Alongkronrusmee, D., Soto-Velasquez, M., Baldwin, T. A., Ye, Z., Dai, M., et al. (2017). Identification of a selective small-molecule inhibitor of type 1 adenylyl cyclase activity with analgesic properties. *Sci. Signal.* 10 (467), eaah5381. doi:10.1126/scisignal.aah5381
- Chen, K. H., Yang, C. H., Juang, S. E., Huang, H. W., Cheng, J. K., Sheen-Chen, S. M., et al. (2014). Pulsed radiofrequency reduced complete Freund's adjuvant-induced mechanical hyperalgesia via the spinal c-Jun N-terminal kinase pathway. *Cell. Mol. Neurobiol.* 34 (2), 195–203. doi:10.1007/s10571-013-0003-z
- Collier, H. O. J., and Francis, D. L. (1975). Morphine abstinence is associated with increased brain cyclic AMP. *Nature* 255, 159–162. doi:10.1038/255159b0
- Corder, G., Doolen, S., Donahue, R. R., Winter, M. K., Jutras, B. L., He, Y., et al. (2013). Constitutive μ -opioid receptor activity leads to long-term endogenous analgesia and dependence. *Science* 341 (6152), 1394–1399. doi:10.1126/science.1239403
- Crain, S. M., and Makman, M. H. (1987). Electrophysiologic responses and adenylate cyclase activities of mouse spinal cord-dorsal root ganglion explants rendered tolerant by chronic exposure to morphine or pertussis toxin. *Adv. Exp. Med. Biol.* 221, 331–344. doi:10.1007/978-1-4684-7618-7_23
- Crispin Junior, C. F., Pederiva, C. N., Bose, R. C., Garcia, V. A., Lino-de-Oliveira, C., and Marino-Neto, J. (2012). ETHOWATCHER: validation of a tool for behavioral and video-tracking analysis in laboratory animals. *Comput. Biol. Med.* 42 (2), 257–264. doi:10.1016/j.combiomed.2011.12.002
- Deacon, R. (2012). Assessing burrowing, nest construction, and hoarding in mice. *J. Vis. Exp.* 59, e2607. doi:10.3791/2607
- Defer, N., Best-Belpomme, M., and Hanoune, J. (2000). Tissue specificity and physiological relevance of various isoforms of adenylyl cyclase. *Am. J. Physiol. Ren. Physiol.* 279 (3), F400–F416. doi:10.1152/ajprenal.2000.279.3.F400
- Fairbanks, C. A. (2003). Spinal delivery of analgesics in experimental models of pain and analgesia. *Adv. Drug Deliv. Rev.* 55 (8), 1007–1041. doi:10.1016/s0169-409x(03)00101-7
- Gaskill, B. N., Karas, A. Z., Garner, J. P., and Pritchett-Corning, K. R. (2013). Nest building as an indicator of health and welfare in laboratory mice. *J. Vis. Exp.* 82, 51012. doi:10.3791/51012
- Griffioen, M. A., Dernetz, V. H., Yang, G. S., Griffith, K. A., Dorsey, S. G., and Renn, C. L. (2015). Evaluation of dynamic weight bearing for measuring nonevoked inflammatory hyperalgesia in mice. *Nurs. Res.* 64 (2), 81–87. doi:10.1097/NNR.0000000000000082
- Griggs, R. B., Laird, D. E., Donahue, R. R., Fu, W., and Taylor, B. K. (2017). Methylglyoxal requires AC1 and TRPA1 to produce pain and spinal neuron activation. *Front. Neurosci.* 11, 679. doi:10.3389/fnins.2017.00679
- Griggs, R. B., Santos, D. F., Laird, D. E., Doolen, S., Donahue, R. R., Wessel, C. R., et al. (2019). Methylglyoxal and a spinal TRPA1-AC1-Epac cascade facilitate pain in the db/db mouse model of type 2 diabetes. *Neurobiol. Dis.* 127, 76–86. doi:10.1016/j.nbd.2019.02.019
- Hargreaves, K., Dubner, R., Brown, F., Flores, C., and Joris, J. (1988). A new and sensitive method for measuring thermal nociception in cutaneous hyperalgesia. *Pain* 32 (1), 77–88. doi:10.1016/0304-3959(88)90026-7
- Haupt, C., Langhoff, J., and Huber, A. B. (2010). Adenylate Cyclase 1 modulates peripheral nerve branching patterns. *Mol. Cell. Neurosci.* 45 (4), 439–448. doi:10.1016/j.mcn.2010.08.003
- Hayhurst, C. J., and Durieux, M. E. (2016). Differential opioid tolerance and opioid-induced hyperalgesia: A clinical reality. *Anesthesiology* 124 (2), 483–488. doi:10.1097/ALN.0000000000000963
- Joseph, E. K., Reichling, D. B., and Levine, J. D. (2010). Shared mechanisms for opioid tolerance and a transition to chronic pain. *J. Neurosci.* 30 (13), 4660–4666. doi:10.1523/JNEUROSCI.5530-09.2010
- Kelly, S., Dunham, J. P., and Donaldson, L. F. (2007). Sensory nerves have altered function contralateral to a monoarthritis and may contribute to the symmetrical spread of inflammation. *Eur. J. Neurosci.* 26 (4), 935–942. doi:10.1111/j.1460-9568.2007.05737.x
- Klein, A. H., Mohammad, H. K., Ali, R., Peper, B., Wilson, S. P., Raja, S. N., et al. (2018). Overexpression of μ -opioid receptors in peripheral afferents, but not in combination with enkephalin, decreases neuropathic pain behavior and enhances opioid analgesia in mouse. *Anesthesiology* 128 (5), 967–983. doi:10.1097/ALN.0000000000002063
- Li, S., Lee, M. L., Bruchas, M. R., Chan, G. C., Storm, D. R., and Chavkin, C. (2006). Calmodulin-Stimulated adenylyl cyclase gene deletion affects morphine responses. *Mol. Pharmacol.* 70 (5), 1742–1749. doi:10.1124/mol.106.02573
- Li, X.-H., Chen, Q.-Y., and Zhuo, M. (2020). Neuronal adenylyl cyclase targeting central plasticity for the treatment of chronic pain. *Neurotherapeutics* 17, 861–873. doi:10.1007/s13311-020-00927-1
- Liang, D. Y., Guo, T., Liao, G., Kingery, W. S., Peltz, G., and Clark, D. J. (2006). Chronic pain and genetic background interact and influence opioid analgesia, tolerance, and physical dependence. *Pain* 121 (3), 232–240. doi:10.1016/j.pain.2005.12.026
- Liang, D. Y., Li, X., and Clark, J. D. (2011). 5-hydroxytryptamine type 3 receptor modulates opioid-induced hyperalgesia and tolerance in mice. *Anesthesiology* 114 (5), 1180–1189. doi:10.1097/ALN.0b013e31820efb19
- Liauw, J., Wu, L. J., and Zhuo, M. (2005). Calcium-stimulated adenylyl cyclases required for long-term potentiation in the anterior cingulate cortex. *J. Neurophysiol.* 94 (1), 878–882. doi:10.1152/jn.01205.2004
- Liou, J. T., Liu, F. C., Mao, C. C., Hsin, S. T., and Lui, P. W. (2009). Adenylate cyclase inhibition attenuates neuropathic pain but lacks pre-emptive effects in rats. *Can. J. Anaesth.* 56 (10), 763–769. doi:10.1007/s12630-009-9149-z
- Liu, R. H., Shi, W., Zhang, Y. X., Zhuo, M., and Li, X. H. (2021). Selective inhibition of adenylyl cyclase subtype 1 reduces inflammatory pain in chicken of gouty arthritis. *Mol. Pain* 17, 17448069211047863. doi:10.1177/17448069211047863
- Makman, M. H., Dvorkin, B., and Crain, S. M. (1988). Modulation of adenylate cyclase activity of mouse spinal cord-ganglion explants by opioids, serotonin and pertussis toxin. *Brain Res.* 445 (2), 303–313. doi:10.1016/0006-8993(88)91193-6
- Muralidharan, A., Kuo, A., Jacob, M., Lourdesamy, J. S., Carvalho, L. M., Nicholson, J. R., et al. (2016). Comparison of burrowing and stimuli-evoked pain behaviors as end-points in rat models of inflammatory pain and peripheral neuropathic pain. *Front. Behav. Neurosci.* 10, 88. doi:10.3389/fnbeh.2016.00088
- Negus, S. S., Neddenriep, B., Altarifi, A. A., Carroll, F. I., Leidl, M. D., and Miller, L. L. (2015). Effects of ketoprofen, morphine, and kappa opioids on pain-related depression of nesting in mice. *Pain* 156 (6), 1153–1160. doi:10.1097/j.pain.0000000000000171
- Schuster, D. J., Dykstra, J. A., Riedl, M. S., Kitto, K. F., Honda, C. N., McIvor, R. S., et al. (2013). Visualization of spinal afferent innervation in the mouse colon by AAV8-mediated GFP expression. *Neurogastroenterol. Motil.* 25 (2), e89–100. doi:10.1111/nmo.12057
- Sharma, S., Klee, W., and Nirenberg, M. (1975). Dual regulation of adenylate cyclase accounts for narcotic dependence and tolerance. *Proc. Natl. Acad. Sci. U. S. A.* 72 (8), 3092–3096. doi:10.1073/pnas.72.8.3092
- Sunahara, R. K., Dessauer, C. W., and Gilman, A. G. (1996). Complexity and diversity of mammalian adenylyl cyclases. *Annu. Rev. Pharmacol. Toxicol.* 36, 461–480. doi:10.1146/annurev.pa.36.040196.002333
- Tao, T., Wei, M. Y., Guo, X. W., Zhang, J., Yang, L. Y., and Zheng, H. (2019). Modulating cAMP responsive element binding protein 1 attenuates functional and behavioural deficits in rat model of neuropathic pain. *Eur. Rev. Med. Pharmacol. Sci.* 23 (6), 2602–2611. doi:10.26355/eurrev_201903_17410

- Tarnawski, L., Reardon, C., Caravaca, A. S., Rosas-Ballina, M., Tusche, M. W., Drake, A. R., et al. (2018). Adenylyl cyclase 6 mediates inhibition of TNF in the inflammatory reflex. *Front. Immunol.* 9, 2648. doi:10.3389/fimmu.2018.02648
- Tian, Z., Wang, D. S., Wang, X. S., Tian, J., Han, J., Guo, Y. Y., et al. (2015). Analgesic effects of NB001 on mouse models of arthralgia. *Mol. Brain* 8 (1), 60. doi:10.1186/s13041-015-0151-9
- Vadakkan, K., Wang, H., Ko, S., Zastepa, E., Petrovic, M., Sluka, K., et al. (2006). Genetic reduction of chronic muscle pain in mice lacking calcium/calmodulin-stimulated adenylyl cyclases. *Mol. Pain* 2, 7. doi:10.1186/1744-8069-2-7
- Villacres, E. C., Wong, S. T., Chavkin, C., and Storm, D. R. (1998). Type I adenylyl cyclase mutant mice have impaired mossy fiber long-term potentiation. *J. Neurosci.* 18 (9), 3186–3194. doi:10.1523/jneurosci.18-09-03186.1998
- Vulchanova, L., Schuster, D. J., Belur, L. R., Riedl, M. S., Podetz-Pedersen, K. M., Kitto, K. F., et al. (2010). Differential adeno-associated virus mediated gene transfer to sensory neurons following intrathecal delivery by direct lumbar puncture. *Mol. Pain* 6, 31. doi:10.1186/1744-8069-6-31
- Wang, H., Xu, H., Wu, L. J., Kim, S. S., Chen, T., Koga, K., et al. (2011). Identification of an adenylyl cyclase inhibitor for treating neuropathic and inflammatory pain. *Sci. Transl. Med.* 3 (65), 65ra3. doi:10.1126/scitranslmed.3001269
- Wang, H., and Zhang, M. (2012). The role of Ca^{2+} -stimulated adenylyl cyclases in bidirectional synaptic plasticity and brain function. *Rev. Neurosci.* 23 (1), 67–78. doi:10.1515/revneuro-2011-0063
- Wei, F., Qiu, C. S., Kim, S. J., Muglia, L., Maas, J. W., Pineda, V. V., et al. (2002). Genetic elimination of behavioral sensitization in mice lacking calmodulin-stimulated adenylyl cyclases. *Neuron* 36 (4), 713–726. doi:10.1016/s0896-6273(02)01019-x
- Wei, F., Vadakkan, K. I., Toyoda, H., Wu, L. J., Zhao, M. G., Xu, H., et al. (2006). Calcium calmodulin-stimulated adenylyl cyclases contribute to activation of extracellular signal-regulated kinase in spinal dorsal horn neurons in adult rats and mice. *J. Neurosci.* 26 (3), 851–861. doi:10.1523/JNEUROSCI.3292-05.2006
- Williams, J. T., Christie, M. J., and Manzoni, O. (2001). Cellular and synaptic adaptations mediating opioid dependence. *Physiol. Rev.* 81 (1), 299–343. doi:10.1152/physrev.2001.81.1.299
- Williams, J. T., Ingram, S. L., Henderson, G., Chavkin, C., von Zastrow, M., Schulz, S., et al. (2013). Regulation of μ -opioid receptors: desensitization, phosphorylation, internalization, and tolerance. *Pharmacol. Rev.* 65 (1), 223–254. doi:10.1124/pr.112.005942
- Wu, Z. L., Thomas, S. A., Villacres, E. C., Xia, Z., Simmons, M. L., Chavkin, C., et al. (1995). Altered behavior and long-term potentiation in type I adenylyl cyclase mutant mice. *Proc. Natl. Acad. Sci. U. S. A.* 92 (1), 220–224. doi:10.1073/pnas.92.1.220
- Yue, X., Tumati, S., Navratilova, E., Strop, D., St John, P. A., Vanderah, T. W., et al. (2008). Sustained morphine treatment augments basal CGRP release from cultured primary sensory neurons in a Raf-1 dependent manner. *Eur. J. Pharmacol.* 584 (2–3), 272–277. doi:10.1016/j.ejphar.2008.02.013
- Zachariou, V., Liu, R., LaPlant, Q., Xiao, G., Renthal, W., Chan, G. C., et al. (2008). Distinct roles of adenylyl cyclases 1 and 8 in opiate dependence: behavioral, electrophysiological, and molecular studies. *Biol. Psychiatry* 63 (11), 1013–1021. doi:10.1016/j.biopsych.2007.11.021
- Zhou, Z., Shi, W., Fan, K., Xue, M., Zhou, S., Chen, Q. Y., et al. (2021). Inhibition of calcium-stimulated adenylyl cyclase subtype 1 (AC1) for the treatment of neuropathic and inflammatory pain in adult female mice. *Mol. Pain* 17, 17448069211021698. doi:10.1177/17448069211021698



OPEN ACCESS

EDITED BY

Heike Wulff,
University of California, United States

REVIEWED BY

Lonny Ray Levin,
Cornell University, United States
Huaiyu Yang,
East China Normal University, China

*CORRESPONDENCE

David L. Roman,
david-roman@uiowa.edu
Val J. Watts,
wattsv@purdue.edu

[†]These authors have contributed equally
to this work

SPECIALTY SECTION

This article was submitted to
Experimental Pharmacology and Drug
Discovery,
a section of the journal
Frontiers in Pharmacology

RECEIVED 24 June 2022

ACCEPTED 08 August 2022

PUBLISHED 06 September 2022

CITATION

Dwyer TS, O'Brien JB, Ptak CP,
LaVigne JE, Flaherty DP, Watts VJ and
Roman DL (2022), Protein-protein
interaction-based high throughput
screening for adenylyl cyclase
1 inhibitors: Design, implementation,
and discovery of a novel chemotype.
Front. Pharmacol. 13:977742.
doi: 10.3389/fphar.2022.977742

COPYRIGHT

© 2022 Dwyer, O'Brien, Ptak, LaVigne,
Flaherty, Watts and Roman. This is an
open-access article distributed under
the terms of the [Creative Commons
Attribution License \(CC BY\)](#). The use,
distribution or reproduction in other
forums is permitted, provided the
original author(s) and the copyright
owner(s) are credited and that the
original publication in this journal is
cited, in accordance with accepted
academic practice. No use, distribution
or reproduction is permitted which does
not comply with these terms.

Protein-protein interaction-based high throughput screening for adenylyl cyclase 1 inhibitors: Design, implementation, and discovery of a novel chemotype

Tiffany S. Dwyer^{1†}, Joseph B. O'Brien^{2†}, Christopher P. Ptak³,
Justin E. LaVigne¹, Daniel P. Flaherty^{1,4,5}, Val J. Watts^{1,4,5*} and
David L. Roman^{2,6,7*}

¹Department of Medicinal Chemistry and Molecular Pharmacology, College of Pharmacy, Purdue University, West Lafayette, IN, United States, ²Department of Pharmaceutical Sciences & Experimental Therapeutics, The University of Iowa College of Pharmacy, Iowa City, IA, United States, ³Nuclear Magnetic Resonance Facility, The University of Iowa Carver College of Medicine, Iowa City, IA, United States, ⁴Iowa Neuroscience Institute, Iowa City, IA, United States, ⁵Purdue Institute for Drug Discovery, West Lafayette, IN, United States, ⁶Purdue Institute for Integrative Neuroscience, West Lafayette, IN, United States, ⁷Holden Comprehensive Cancer Center, The University of Iowa Hospitals & Clinics, Iowa City, IA, United States

Genetic and preclinical studies have implicated adenylyl cyclase 1 (AC1) as a potential target for the treatment of chronic inflammatory pain. AC1 activity is increased following inflammatory pain stimuli and AC1 knockout mice show a marked reduction in responses to inflammatory pain. Previous drug discovery efforts have centered around the inhibition of AC1 activity in cell-based assays. In the present study, we used an *in vitro* approach focused on inhibition of the protein-protein interaction (PPI) between Ca²⁺/calmodulin (CaM) and AC1, an interaction that is required for activation of AC1. We developed a novel fluorescence polarization (FP) assay focused on the PPI between an AC1 peptide and CaM and used this assay to screen over 23,000 compounds for inhibitors of the AC1-CaM PPI. Next, we used a cellular NanoBiT assay to validate 21 FP hits for inhibition of the AC1-CaM PPI in a cellular context with full-length proteins. Based on efficacy, potency, and selectivity for AC1, hits **12**, **13**, **15**, **18**, **20**, and **21** were prioritized. We then tested these compounds for inhibition of AC1 activity in cyclic AMP (cAMP) accumulation assays, using HEK293 cells stably expressing AC1. Hit **15** contained a dithiophene scaffold and was of particular interest because it shared structural similarities with our recently reported benzamide series of AC1 inhibitors. We next tested a small set of 13 compounds containing the dithiophene scaffold for structure-activity relationship studies. Although many compounds were non-selective, we observed trends for tuning AC1/AC8 selectivity based on heterocycle type and substituents. Having an ethyl on the central thiophene caused the scaffold to be more selective for AC8. Cyclization of the alkyl substituent fused to the thiophene significantly reduced activity and also shifted selectivity toward AC8. Notably, combining the fused

cyclohexane-thiophene ring system with a morpholine heterocycle significantly increased potency at both AC1 and AC8. Through designing a novel FP screen and NanoBiT assay, and evaluating hits in cAMP accumulation assays, we have discovered a novel, potent, dithiophene scaffold for inhibition of the AC1- and AC8-CaM PPI. We also report the most potent fully efficacious inhibitor of AC8 activity known to-date.

KEYWORDS

inflammatory pain, adenylyl cyclase, cAMP signaling, high throughput screen (HTS), Ca²⁺, calmodulin (CaM), drug discovery

Introduction

Adenylyl Cyclase Type 1 (AC1) is a promising target for treating chronic inflammatory pain. The overlapping neuronal expression of membrane-bound AC proteins prioritizes obtaining selectivity when targeting a single isoform (Dessauer et al., 2017). Studies with adenylyl cyclase knockout (KO) mice further emphasize this point. In mice lacking AC1, behavioral responses to inflammatory stimuli were nearly abolished, and memory deficits were nearly absent. Conversely, AC1/AC8 double KO mice exhibited reduced behavioral responses to inflammatory stimuli as expected but also displayed significant memory deficits (Ferguson & Storm, 2004; Liauw et al., 2005; Chen et al., 2014). Moreover, chronic inflammatory pain stimuli increases AC1 activity in mice, while AC1 KO mice had significantly less chronic pain (Wei et al., 2002; Vadakkan et al., 2006; Corder et al., 2013). Studies have also reported that pharmacologic inhibition of AC1 also elicits a reduction in responses to inflammatory pain stimuli (Wang et al., 2011; Brust et al., 2017; Kaur et al., 2019; Scott et al., 2022). The combination of these findings support AC1 as a promising target for treating chronic inflammatory pain conditions; however, they also emphasize the importance of selectively targeting AC1 over other AC isoforms, most notably AC8, which is co-localized in the same neuronal tissues (Defer et al., 2000).

AC1 signaling centers around its ability to synthesize the second-messenger cyclic adenosine monophosphate (cAMP) from ATP, and this primary function of AC1 is regulated by several signaling proteins. G $\alpha_{i/o}$ and G $\beta\gamma$ subunits inhibit the activity of AC1, whereas G α_s and Ca²⁺/calmodulin (CaM) stimulate AC1 activity, with Ca²⁺/CaM exhibiting particularly robust stimulation (Sadana & Dessauer, 2009; Dessauer et al., 2017). Therefore, inhibition of the AC1/CaM protein-protein interaction (PPI) would, in theory, inhibit Ca²⁺/CaM-mediated activation of AC1, thus diminishing cAMP production mediated through AC1. AC8 is also stimulated by Ca²⁺/CaM, although the binding interactions between the Ca²⁺/CaM complex with AC8 differs from how it interacts with AC1. Specifically, Ca²⁺/CaM interacts with the C1b regulatory domain of AC1 to activate the enzyme, but interacts with both the N-terminal and AC8-C2b regulatory domains of AC8 for activation (Simpson et al., 2006; Willoughby & Cooper, 2007; Masada et al., 2009; Mou et al., 2009; Masada et al., 2012; Herbst et al., 2013). These differences

in Ca²⁺/CaM binding interactions between the isoforms provides the basis for developing a novel biochemical fluorescence polarization assay that focuses on the CaM binding regions of AC1 and AC8. Additionally, the different interactions of AC1 and AC8 with CaM may provide a basis for selectively targeting inhibition of the AC1-CaM PPI in a more focused approach. The research described here provides evidence that this focused approach, which incorporates small AC peptides correlated to the respective CaM binding domains can identify compounds with novel chemotypes capable of selectively inhibiting the full-length AC/CaM PPIs. Here we report the screening design, implementation, and characterization of hit compounds from this high-throughput screen. In addition, we show the characterization of initial hits in terms of binding, via protein NMR, cell-based protein-protein interaction inhibition, and selectivity between adenylyl cyclase 1 and adenylyl cyclase 8. Furthermore, we present additional cell-based cAMP accumulation data for a novel dithiophene scaffold discovered through our screen as well as preliminary structure-activity relationship (SAR) studies. Collectively, this demonstrates the utility and robustness of these methods to identify novel inhibitor scaffolds that target the AC/CaM PPIs.

Materials and methods

DNA cloning

The human CaM (hCaM) bacterial expression vector was constructed as previously described (Hayes et al., 2018). Briefly, the protein-coding sequence of hCaM (residues 1–149, Addgene plasmid #47598) was cloned into pET-His6-GST-TEV-LIC (Addgene plasmid #29655) using ligation independent cloning. Then, this bacterial expression vector was used to generate hCaM with an N-terminal 6X-His-GST tag with a tobacco etch virus (TEV) protease recognition site between the GST and CaM regions.

The NanoBiT PPI TK/BiT MCS vectors were purchased from Promega (Madison, WI) for cell-based NanoBiT experiments. The hCaM residues 1–149, residues 1–1,248 of rat AC8 (rAC8), and the human AC1 (hAC1) residues 1–1,118 were cloned into the NanoBiT vectors per manufacturers' protocols, using the restriction sites NheI/XhoI for hCaM and BglII/XhoI. All DNA

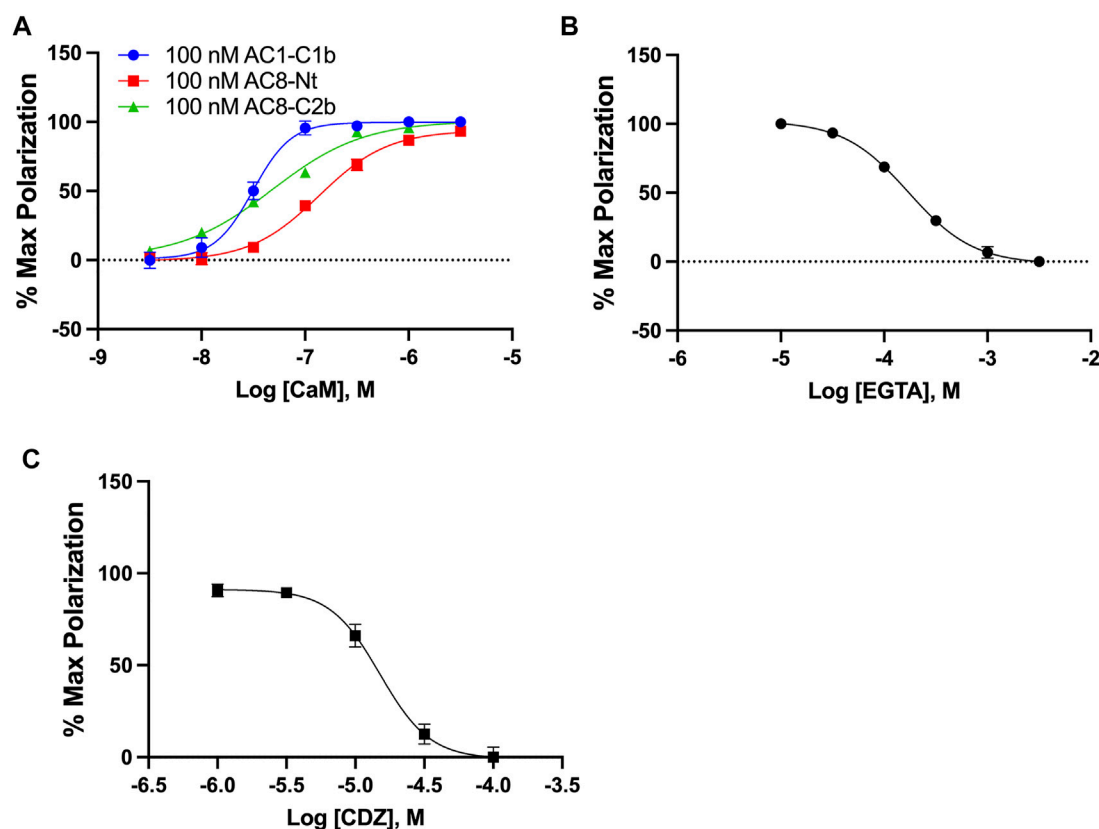


FIGURE 1

AC1/CaM FP Assay development. (A) 100 nM AC1-C1b (Blue), AC8-NT (Red), or AC8-C2b (Green) peptide with increasing concentrations of GST-CaM. Saturation is reached at ~100 nM GST-CaM. (B) 100 nM AC1 peptide and 100 nM GST-CaM with increasing concentrations of EGTA. (C) CRC for CDZ with 100 nM AC1-C1b and 100 nM GST-CaM, with 1% DMSO in the buffer. The AC1/CaM IC_{50} value for CDZ was ~15 μ M and the IC_{90} was ~100 μ M, which was used in the final assay. Calmidazolium CAS number: 57265-65-3. All data represents $n = 3$ experiments \pm SEM.

sequences were confirmed with Sanger sequencing (Iowa Institute of Human Genetics, Iowa City, IA).

Protein purification

hCaM was expressed and purified as described previously with minor modifications (Hayes et al., 2018). Briefly, hCaM was transformed into BL21-CodonPlus (DE3)-RIPL *E. Coli* and incubated at 37°C with shaking at 275–300 RPM until the OD_{600} reached 2.0. The bacterial culture was placed on ice with gentle mixing before protein production induction with isopropyl- β -D-1-thiogalactoside (RPMI) at a final concentration of 1.0 mM. Protein production continued for an additional 16 h at 18°C with shaking at 300 RPM. The bacterial culture was pelleted and resuspended in 50 ml of resuspension buffer (50 mM Tris pH 8.0, 150 mM NaCl, 10 mM imidazole, and a protease inhibitor cocktail consisting of leupeptin, E64, and phenylmethylsulfonyl fluoride) per 1 L of original bacterial culture. The resuspended bacterial cells were then subjected to

a freeze-thaw cycle using LN₂. The resuspended cells were thawed, supplemented with 1 mg/ml chicken egg lysozyme (Sigma-Aldrich, St. Louis, MO), and agitated on a tube rotator for 1 h before being subjected to two more freeze-thaw cycles with LN₂. After cell lysis was complete, 100 μ g DNase (Roche) was added to reduce viscosity and prepare the sample for centrifugation. The lysed cells were then subjected to ultracentrifugation at 100,000 \times g to clear the lysate from the supernatant. The separated supernatant was purified as described previously with minor modifications (Hayes et al., 2018). Briefly, using an AKTA FPLC (GE Life Sciences, Chicago, IL) the lysate was loaded onto NIS6FF resin and purified using a gradient elution over 20 column volumes of resuspension buffer with 400 mM imidazole. Peak fractions were pooled, diluted in 50 mM Tris pH 7.5, 1 mM CaCl₂, and loaded onto a glutathione sepharose 4FF column (GE Life Sciences, Chicago, IL). Purified GST-CaM was eluted using a gradient elution over 10 column volumes of 50 mM Tris pH 7.5, 1 mM CaCl₂, and 10 mM glutathione. Peak fractions were collected and analyzed with SDS-PAGE gel electrophoresis to assess their purity.

TABLE 1 AC1/CaM FP assay conditions for the pilot screen. The table indicates the concentrations for all AC1/CaM FP assay components. The order of addition for the AC1/CaM FP assay was vehicle, compound, or the positive control (CDZ) followed by GST-CaM and AC1-C1b after a 30-min incubation at RT.

Final volume	GST-CaM	AC1-C1b	Vehicle	Positive control	% DMSO	Time
60 μ l	100 nM (20 μ l)	100 nM (20 μ l)	FP buffer (20 μ l)	100 μ M CDZ (20 μ l)<	1–2.5	2

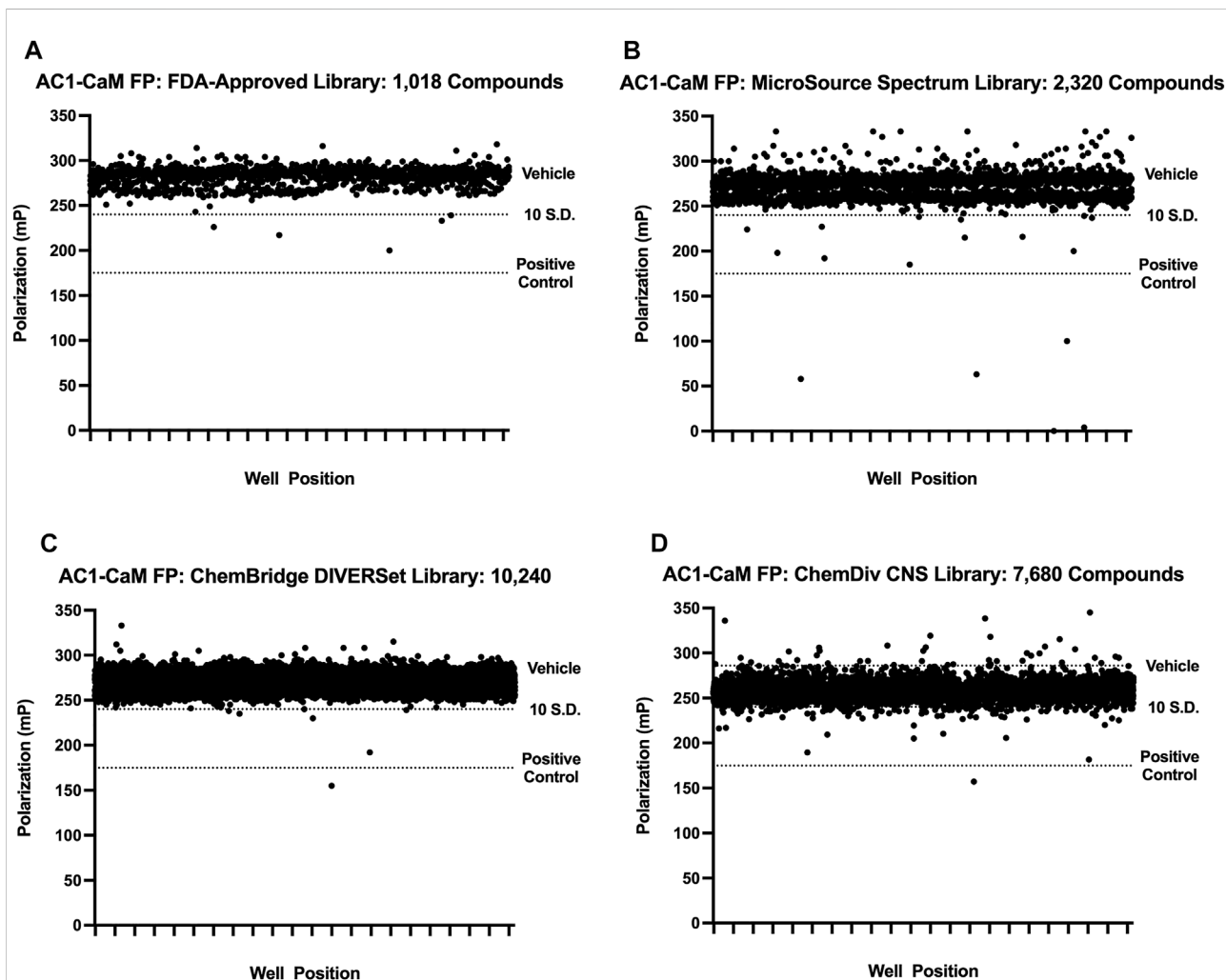


FIGURE 2

Pilot screen individual library results. All pilot screen assays used concentrations of AC1 and CaM shown in Table 1. The dotted line representing the vehicle is beneath the cluster of compounds screened (black circles). 100 μ M CDZ is shown as the dotted line labeled as positive control. Polarization values correspond to well positions for plates within the library tested. (A) FDA-approved library, (B) MicroSource Spectrum (MMSP) library, (C) ChemBridge DIVERSet library, (D) ChemDiv CNS library.

Fractions greater than 90% pure were pooled and exhaustively dialyzed against 20 mM HEPES pH 7.4, 100 mM KCl, at 4°C to remove Ca^{2+} , before samples were aliquoted, flash-frozen in LN_2 , and stored at -80°C . To purify tag-free CaM, we incubated GST-CaM with His-tagged TEV protease at a 20:1 M ratio (GST-CaM/TEV) while dialyzing the sample against 20 mM HEPES pH 7.4, 100 mM KCl, 1 mM CaCl_2 . Dialysis and TEV treatment proceeded

overnight at 4°C. The TEV treated CaM sample was then loaded onto an IMAC to separate 6XHis-tagged GST and TEV from CaM. The resulting flow-through fractions were collected and analyzed with SDS-PAGE and Coomassie staining. Fractions determined to be 95% pure CaM were concentrated to >10 mg/ml using an Amicon centrifugal concentrator with a 3kD cutoff (Amicon, EMD Millipore, Billerica, MA). Samples of pure CaM were

TABLE 2 AC1/CaM FP pilot screen summary. The AC1/CaM FP pilot screen included four chemical libraries. The Z' values are the ranges obtained for the designated libraries. A total of 54 validated hits were obtained from the pilot screen and through duplicate hits, unfavorable structures or potency/inhibition profiles a total of 25 compounds were advanced for concentration response curve assessment in the AC1/CaM and AC8/CaM FP assays.

Library	Compounds screened	Z'	Validated hits	Advanced to CRC
FDA-Approved	1,018	0.70–0.77	7	7
MMSP	2,320	0.69–0.77	13	7
ChemBridge DIVERSet	10,240	0.68–0.77	2	2
ChemDiv	7,680	0.69–0.76	32	9
Total	21,258	~0.69–0.77	54	25

aliquoted, flash-frozen in LN₂, and stored at -80°C. Production of ¹⁵N-labeled CaM for NMR experiments was accomplished as described above, with the only modification being that bacterial culturing was completed in M9 minimal media supplemented with 1 g of ¹⁵NH₄Cl per L.

Fluorescence polarization assays

Peptides for adenylyl cyclase proteins, AC1 and AC8, were generated based on the residues or domains known to interact with CaM (Vorherr et al., 1993; Levin & Reed, 1995; Masada et al., 2012). The peptide corresponding to residues 492–520 of human AC1 was obtained from Genemed Synthesis (San Antonio, Texas). Peptides corresponding to human AC8 residues 30–54 (N-Terminal) and 1,191–1,214 (C2b regulatory domain) were purchased from Genscript (Piscataway, NJ). Each peptide was designed to contain an additional N-terminal residue labeled with the fluorophore Cy5. This additional residue for the AC8 peptides was cysteine, while the AC1 peptide has an additional isoleucine. The FP experiments were completed in black 384-well microplates (Corning #3575), and fluorescence was monitored using a BioTek Synergy 2 (Winooski, VT) equipped with excitation 620/40 nm and emission 680/30 nm filters, and a 660 nm dichroic mirror with polarizers. The addition of individual components was done as follows. First, 20 µl of 3X test compound in FP assay buffer (20 mM HEPES pH 7.4, 100 mM KCl, and 50 µM CaCl₂), 3X calmidazolium (CDZ) in FP assay buffer, or 3X DMSO in FP assay buffer was added to their respective wells. Next, 20 µl of 3X GST-CaM in FP assay buffer was added to all wells, and the plate was incubated at room temperature for 30 min. Lastly, 20 µl of 3X AC peptide in FP assay buffer was added to all wells, and the plate was incubated in the dark at room temperature for either the amount of time indicated for the assay optimization experiments or 2 h for the high-throughput screening experiments. Fluorescence was then measured, and the polarization output was calculated using the measured intensities of emitted light parallel and perpendicular to the excitation light, shown in Equation 1 below. The final concentrations for all Cy5-labeled AC peptides (AC1 C1b, AC8 Nt, AC8 C2b) were 100 nM, the final concentration of

CDZ was 100 µM, and the final concentration of DMSO was 0.15–1%, depending on the compound library that was being tested. Data represents a mean of three independent experiments (N = 3) ± SEM for potency and selectivity profiling for AC-CaM FP. Data were analyzed using GraphPad Prism 8 and TIBCO Spotfire.

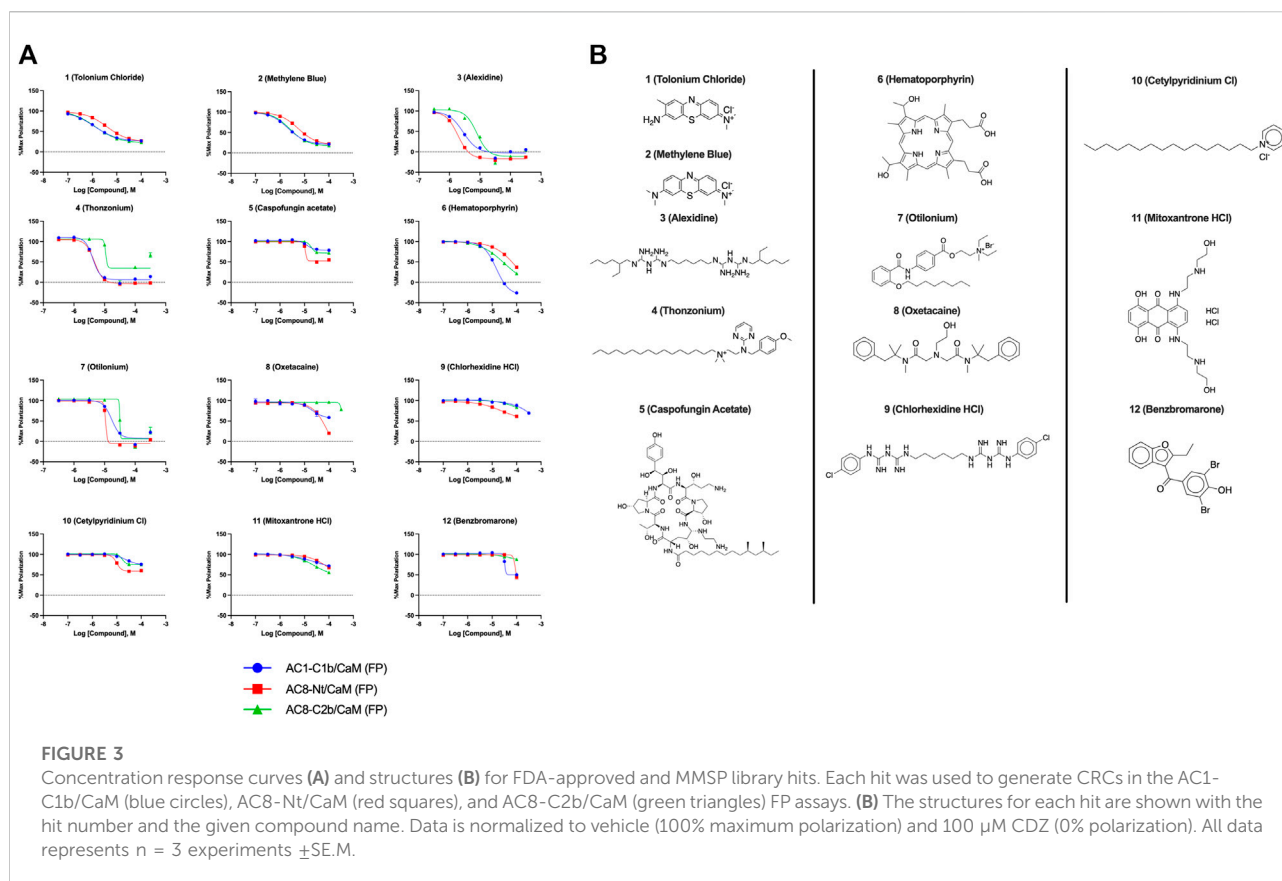
$$\text{Polarization} = \frac{\text{Intensity}_{\text{parallel}} - \text{Intensity}_{\text{perpendicular}}}{\text{Intensity}_{\text{parallel}} + \text{Intensity}_{\text{perpendicular}}} \quad (1)$$

FDA-approved library FP screen

The FDA-approved library (Selleck Chemical, Houston, TX) was screened at a final concentration of 14.5 µM (0.72% DMSO). On the day of the assay, a “middle” plate (ThermoFisher #264574) was created to simplify the addition of 20 µl of 3X compound to the final assay plate. First, using a Hamilton MircroLab Star liquid-handling robot, 2 µl of 2 mM compound from the FDA stock plate was added to the middle plate containing 90 µl of FP assay buffer. Next, 20 µl of 3X compound from the middle plate was added to the assay plate (Corning #3575). Controls were then added to empty wells (32 wells DMSO control, 32 wells CDZ positive control). Next, 20 µl of 3X GST-CaM (100 nM GST-CaM final for the screen with AC1 C1b peptide) was added to the entire plate, and the assay mixture was incubated for 30 min at room temperature. Finally, 20 µl of 3X AC1 C1b Cy5 labeled peptide (100 nM final AC1 C1b) was added to the entire plate, and the assay mixture was incubated at room temperature in the dark for 2 h before polarization was measured as described above.

Microsource spectrum collection FP screen

The Microsource spectrum collection (MMSP) (Microsource Discovery Systems, Gaylordsville, CT) was screened as outlined above for the FDA-approved library with some minor differences. First, the stock concentration of compounds was 10 mM. Therefore, the middle plate contains 1 µl of MMSP compounds with 90 µl of FP assay buffer (concentration of



the compound in the middle plate: 109.8 μ M). To achieve the desired 3X concentration in the test plate, 12 μ l of FP assay buffer was added to the test plate before adding 8 μ l of the compound from the middle plate (3X compound in test plate: 43.9 μ M). After compounds were added to the test plates addition of controls, GST-CaM, and Cy5-labeled AC1 C1b peptide were completed as described for the FDA-approved library. The test plate's final concentration of MMSP compounds was 14.64 μ M (0.147% DMSO).

ChemBridge DIVERSet library FP screen

The screening protocol for the ChemBridge DIVERSet library (San Diego, CA) of compounds as described for the FDA-approved library with the same minor differences as the MMSP library described above. The test plate's final concentration of ChemBridge DIVERSet compounds was 14.64 μ M (0.147% DMSO).

ChemDiv CNS targeted library FP screen

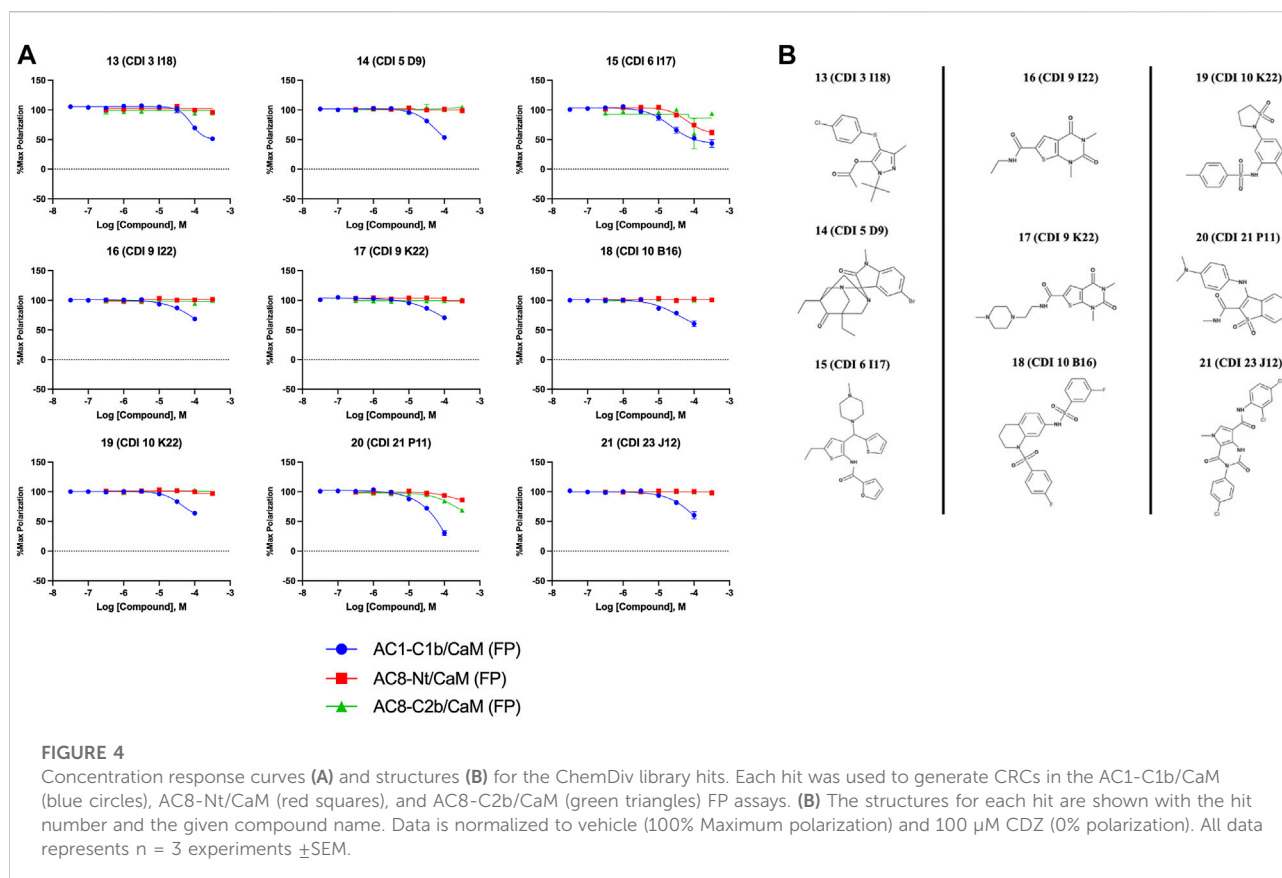
For the ChemDiv CNS targeted library (ChemDiv, San Diego, CA) of compounds, the protocol is the same as that

outlined for the FDA-approved library, with minor differences as the MMSP and ChemBridge DIVERSet libraries. The test plate's final ChemDiv CNS targeted compounds' concentration was 14.64 μ M (0.147% DMSO).

AC-CaM NanoBiT assays

The AC8/CaM NanoBiT assays were performed mainly as previously described (Hayes et al., 2018). The AC1/CaM NanoBiT assays were performed similarly to the AC8/CaM NanoBiT assays with some differences. Briefly, HEK293T cells were cultured in Gibco DMEM supplemented with 10% FBS (Gibco) and 1% Penicillin/Streptomycin at 37°C and 5% CO₂. Cells were plated at 25,000 cells/well in 96-well half area plates (Corning #3885) pretreated with poly-d-lysine. Cells were cultured for 16 h before transfection with Lipofectamine 3,000 (ThermoFisher Scientific, Waltham, MA) and the designated AC-CaM NanoBiT DNA constructs described above. Transfections were performed according to the manufacturer's protocol, and transfected cells were incubated for 40–44 h before compound treatment.

On the day of the assay, the culture medium was removed and replaced with 50 μ l of 1X Compound, BAPTA-AM (50 μ M final) (Sigma-Aldrich), or vehicle in HBSS (ThermoFisher Scientific, Waltham MA) supplemented with 20 mM HEPES



pH 7.4. The assay plate was then incubated at 37°C for 30 min before 12.5 μ l of 5X NanoGlo Live-cell substrate (Promega, Madison, WI), prepared according to the manufacturer's protocol, was added to each well. Next, the plate was read on a BioTek Synergy 2 plate reader at 37°C in luminescence mode for 30 min to establish a baseline for the protein-protein interaction. Next, 12.5 μ l of 6X Thapsigargin (ThermoFisher Scientific, Waltham, MA) was added to each well, and luminescence was read for an additional 60 min. The area under the curve (AUC) analysis quantified the AC-CaM association for vehicle, BAPTA-AM, and compound-treated cells. Using the AUC for compound-treated cells, the data were normalized to vehicle with 1 μ M thapsigargin added (100%) and 50 μ M BAPTA-AM (0%). Data were analyzed using GraphPad Prism 8, with each data set representing a mean of three independent experiments ($N = 3$) \pm SEM.

CellTiter-glo 2.0 cell viability assay

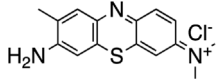
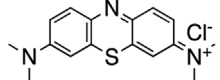
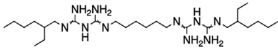
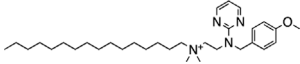
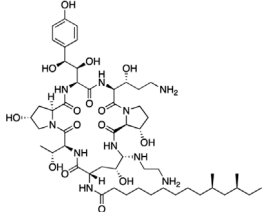
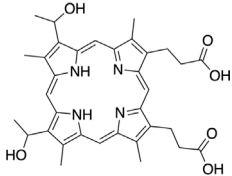
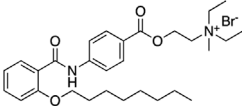
Cell viability measurements were performed using a BioTek Synergy 2 plate reader luminescence mode. HEK293T cells were cultured in Gibco DMEM supplemented with 10% FBS (Gibco) and 1% Penicillin/Streptomycin at 37°C and 5% CO₂. Cells were

plated at 25,000 cells/well in 96-well half area plates (Corning #3885) coated with poly-d-lysine and allowed to incubate for 40–44 h. On the day of the assay, culture media was aspirated and replaced with 25 μ l of 2X compound in HBSS supplemented with 20 mM HEPES pH 7.4 or 2X vehicle (HBSS supplement with 20 mM HEPES pH 7.4). After adding the compound or vehicle, the plate was incubated at 37°C for 30 min. Next, 25 μ l of 2X CellTiter-Glo 2.0 reagent (Promega, Madison, WI) was added, and the plate was mixed on an orbital shaker for 30 min to induce cell lysis and equilibrate the plate to room temperature. Luminescence was then measured for 30 min to establish a stable signal. The final three luminescence values from the 30-min read were averaged and used to assess cell viability. Cell viability for tested compounds was normalized relative to vehicle (100%) and wells containing buffer with no cells (0%). Data represent the mean of three independent experiments ($N = 3$) \pm SEM.

cAMP accumulation assay

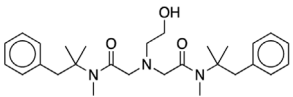
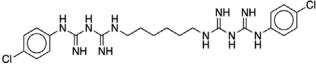
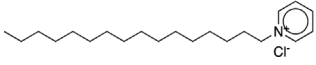
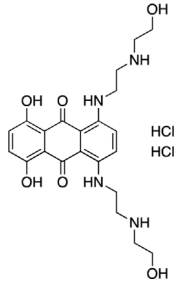
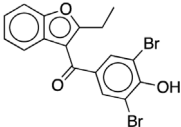
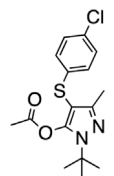
Cryopreserved HEK293 cells with AC3 and AC6 knocked out, and stably expressing AC1, AC2, AC5, or AC8 (AC1-HEK Δ 3/6 KO, AC2-HEK Δ 3/6 KO, AC5-HEK Δ 3/6 KO, or AC8-HEK Δ 3/6 KO cells, respectively; *Soto-Velasquez et al., 2018*)

TABLE 3 AC1/CaM pilot screen CRC analysis. IC₅₀ and % inhibition relative to 100 μ M CDZ (100% inhibition) obtained for each compound in the AC1/CaM FP assay. The K_i values obtained with experimentally determined K_D values for each AC/CaM FP assay and the IC₅₀ values obtained for each compound in the designated AC/CaM FP assay. The final two columns show the K_i ratios obtained for either AC8-NT/CaM or AC8-C2b/CaM over AC1/CaM. Values with K_i ratios greater than 1 were more potent in the AC1/CaM FP assay over the designated AC8/CaM FP assay. All data represents n = 3 experiments, \pm CI for AC1/CaM IC₅₀ values.

#	Compound name	Structure	Compound library (Plate, well position)	AC1-CaM FP		K _i (μ M)			K _i ratio (AC8 NT/AC1)	K _i ratio (AC8-C2b/AC1)
				IC ₅₀ , μ M (95% CI)	% inhib	AC1	C1b	AC8 C2b		
1	Tolonium Chloride		MMSP (Plate 5, N13)	1.24 (0.8–1.65)	75	0.29	2.3	0.44	7.9	1.5
2	Methylene Blue		MMSP (Plate 3, D10)	2.18 (2.1–2.3)	80	0.51	3.2	0.82	6.3	1.6
3	Alexidine		FDA-Approved (Plate 3, L11)	2.8 (2.4–3.3)	103	0.67	1.1	2.6	1.6	3.9
4	Thonzonium		FDA-Approved (Plate 4, E17)	4.14 (1.3–4.6)	94	1.0	2.7	3.6	2.7	3.7
5	Caspofungin Acetate		FDA-Approved (Plate 2, N18)	12.7 (10–15.7)	20	3.0	6.3	6.2	2.1	2.1
6	Hematoporphyrin		MMSP (Plate 6, O6)	14.7 (13.9–15.5)	131	3.5	61.7	10.1	17.8	2.9
7	Otilonium		FDA-Approved (Plate 2, L16)	17.1 (14.5–20)	92	4.1	6.3	10.3	1.6	2.5

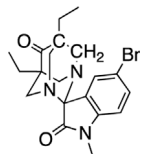
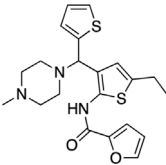
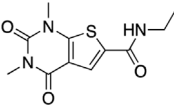
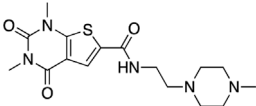
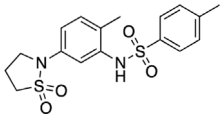
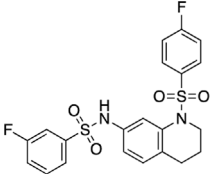
(Continued on following page)

TABLE 3 (Continued) AC1/CaM pilot screen CRC analysis. IC₅₀ and % inhibition relative to 100 μM CDZ (100% inhibition) obtained for each compound in the AC1/CaM FP assay. The K_i values obtained with experimentally determined K_D values for each AC/CaM FP assay and the IC₅₀ values obtained for each compound in the designated AC/CaM FP assay. The final two columns show the K_i ratios obtained for either AC8-NT/CaM or AC8-C2b/CaM over AC1/CaM. Values with K_i ratios greater than 1 were more potent in the AC1/CaM FP assay over the designated AC8/CaM FP assay. All data represents n = 3 experiments, ± CI for AC1/CaM IC₅₀ values.

#	Compound name	Structure	Compound library (Plate, well position)	AC1-CaM FP		K _i (μM)				K _i ratio (AC8 NT/AC1)	K _i ratio (AC8-C2b/AC1)
				IC ₅₀ , μM (95% CI)	% inhib	AC1	C1b	AC8 NT	AC8 C2b		
8	Oxetacaine		N/A	20 (11.5–32)	38	4.7		38	33.5	8.0	7.1
9	Chlorhexidine HCl		MMSP (Plate 1, P16)	22 (8.6–32)	15	5.2		13.8	20.8	2.7	4.0
10	Cetylpyridinium Cl		FDA-Approved (Plate 3, E18)	23.4 (16.1–31)	25	5.6		5.7	5.5	1.0	1.0
11	Mitoxantrone HCl			27.5 (17–42)	40	6.5		41.1	8.2	6.3	1.3
12	Benzbromarone			33 (17–54)	47	7.8		52.1	23.8	6.7	3.1
13	CDI 3 I18			73.5 (Wide)	34	17.4	n/i	n/i		AC1 Selective	AC1 Selective

(Continued on following page)

TABLE 3 (Continued) AC1/CaM pilot screen CRC analysis. IC₅₀ and % inhibition relative to 100 μM CDZ (100% inhibition) obtained for each compound in the AC1/CaM FP assay. The K_i values obtained with experimentally determined K_D values for each AC/CaM FP assay and the IC₅₀ values obtained for each compound in the designated AC/CaM FP assay. The final two columns show the K_i ratios obtained for either AC8-Nt/CaM or AC8-C2b/CaM over AC1/CaM. Values with K_i ratios greater than 1 were more potent in the AC1/CaM FP assay over the designated AC8/CaM FP assay. All data represents n = 3 experiments, ± CI for AC1/CaM IC₅₀ values.

#	Compound name	Structure	Compound library (Plate, well position)	AC1-CaM FP		K _i (μM)				K _i ratio (AC8 NT/AC1)	K _i ratio (AC8-C2b/AC1)
				IC ₅₀ , μM (95% CI)	% inhib	AC1	C1b	AC8 NT	AC8 C2b		
14	CDI 5 D9			58.2 (34.3–80)	69	13.8		n/i	n/i	AC1 Selective	AC1 Selective
15	CDI 6 I17			22.1 (14–43.4)	58	5.2		n/i	n/i	AC1 Selective	AC1 Selective
16	CDI 9 I22			24.2 (8.5–48)	25	5.7		n/i	n/i	AC1 Selective	AC1 Selective
17	CDI 9 K22			75.4 (19–132)	53	17.8		n/i	n/i	AC1 Selective	AC1 Selective
18	CDI 10 B16			38.4 (15.1–52)	54	9.1		n/i	n/i	AC1 Selective	AC1 Selective
19	CDI 10 K22			43.4 (27–59)	46	10.3		n/i	n/i	AC1 Selective	AC1 Selective

(Continued on following page)

TABLE 3 (Continued) AC1/CaM pilot screen CRC analysis. IC₅₀ and % inhibition relative to 100 μ M CDZ (100% inhibition) obtained for each compound in the AC1/CaM FP assay. The K_i values obtained with experimentally determined K_D values for each AC/CaM FP assay and the IC₅₀ values obtained for each compound in the designated AC/CaM FP assay. The final two columns show the K_i ratios obtained for either AC8-NT/CaM or AC8-C2b/CaM over AC1/CaM. Values with K_i ratios greater than 1 were more potent in the AC1/CaM FP assay over the designated AC8/CaM FP assay. All data represents n = 3 experiments, \pm CI for AC1/CaM IC₅₀ values.

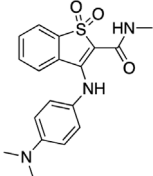
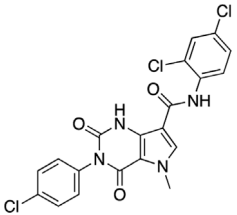
#	Compound name	Structure	Compound library (Plate, well position)	AC1-CaM FP		K _i (μ M)				K _i ratio (AC8 NT/AC1)	K _i ratio (AC8-C2b/AC1)
				IC ₅₀ , μ M (95% CI)	% inhib	AC1	C1b	AC8 NT	AC8 C2b		
20	CDI 21 P11			43 (Wide)	70	10.2		5.9	4.5	0.58	0.44
21	CDI 23 J12			9.9 (5.8–13.2)	59	13.1		n/i	n/i	AC1 Selective	AC1 Selective

TABLE 4 Results for AC1/CaM pilot screen hits in the NanoBIT and cell viability assay. Data are reported as IC₅₀ values with standard error of the mean for the AC1/CaM and AC8/CaM NanoBIT assays. All data represent the average \pm SEM of three individual experiments. The final column shows the % cell viability in the presence of each compound at it is AC1/CaM NanoBIT IC₅₀ concentration, using the CellTiter Glo-2.0 cell viability assay as previously described. All data represent the average \pm SEM of three individual experiments.

#	Compound	Nanobit: AC1-CaM IC ₅₀ (μ M \pm SEM)	Nanobit: AC8-CaM IC ₅₀ (μ M \pm SEM)	% Viable Cells at AC1 IC ₅₀
1	Tolonium Chloride	32.9 \pm 1.01	8.4 \pm 1.19	80
2	Methylene Blue	98 \pm 1.14	80.3 \pm 1.14	86
3	Alexidine	17.9 \pm 1.15	16.5 \pm 1.15	75
4	Thonzonium	29.1 \pm 1.2	18.5 \pm 1.26	100
6	Hematoporphyrin	38.4 \pm 1.17	11.6 \pm 1.24	95
7	Otilonium	18.8 \pm 1.16	12.8 \pm 1.22	96
8	Oxetacaine	40 \pm 1.15	34.6 \pm 1.32	93.3
9	Chlorhexidine	111 \pm 1.23	47.1 \pm 1.35	80
10	Cetylpyridinium Cl	30.4 \pm 1.1	14.4 \pm 1.29	96
11	Mitoxantrone	44 \pm 1.15	29.8 \pm 1.18	87
12	Benzbromarone	1.7 \pm 1.17	4.16 \pm 1.15	90
13	CDI 3 I18	16.1 \pm 1.13	13.1 \pm 1.19	96
14	CDI 5 D9	84 \pm 1.7	N/A	100
15	CDI 6 I17	26.1 \pm 1.17	33.3 \pm 1.18	100
18	CDI 10 B16	16.1 \pm 1.12	5.71 \pm 1.22	100
20	CDI 21 P11	63 \pm 1.34	70.3 \pm 1.13	100
21	CDI 23 J12	25.6 \pm 1.42	6.8 \pm 1.19	100

were plated at 5,000 cells/well. Cells were then incubated for 1 h at 37°C and 5% CO₂. Cells were then treated with varying concentrations of inhibitors for 30 min, followed by treatment with calcium ionophore A23187 (3 μ M) in 500 μ M 3-isobutyl-1-methylxanthine (IBMX), a phosphodiesterase inhibitor, for 1 h at RT (Sigma Aldrich, St. Louis, MO). Finally, Cisbio HTRF detection reagents were added and incubated for 1–24 h at RT. Plates were read according to manufacturer's protocol on an HTRF-compatible plate reader at 620 and 665 nm cAMP concentrations were interpolated from a cAMP standard curve. Data represents the mean \pm SEM of IC₅₀ values or percent of maximum A23187 inhibition from the mean of three independent experiments (N = 3). For cytotoxicity assays, compounds were tested at 30 μ M and this protocol was used with the exception of detection reagents; CellTiter-Glo 2.0 reagent was used according to manufacturer's protocol and luminescence was read on the Synergy Neo2 plate reader. Data are normalized to cells treated with vehicle (100%) or 2% tween (0%) and are represented as the percent of vehicle, from the average of three independent experiments (N = 3).

Nuclear magnetic resonance

All NMR samples contained 100 μ M ¹⁵N-CaM in 20 mM HEPES pH 7.4, 100 mM KCl, 10 mM CaCl₂, 10% D₂O, and 5% DMSO. Initial spectra were collected for CaM alone before individual

compounds were titrated to observe chemical shift perturbations. All spectra were acquired at 298 K using a 600 MHz Bruker Avance NEO NMR spectrometer with a triple resonance gradient cryoprobe. NMR spectra were processed using NMRPipe and analyzed using NMRFAM-SPARKY.

Results

Fluorescence polarization assays

Intending to identify small molecule inhibitors that selectively target the AC1/CaM PPI, we developed and optimized an FP assay for a high-throughput screening (HTS) campaign. For simplicity, peptides will be denoted AC1-C1b, AC8-Nt, and AC8-C2b, all containing an N-terminal Cy5 fluorophore label. The FP assays for AC8-Nt and AC8-C2b, established previously (Hayes et al., 2018), were used as counter screens for compounds identified in the HTS campaign and served as a guide for AC1/CaM assay development. The assay buffer used in all FP experiments consisted of 20 mM HEPES pH 7.4, 100 mM KCl and 50 μ M CaCl₂. At fixed concentrations of peptide and increasing concentrations of CaM, the dissociation constants (K_d) for AC1-C1b, AC8-Nt, and AC8-C2b were quantified to be 31.5, 136.5, and 48.5 nM, respectively (Figure 1A). The nature of CaM as a calcium-binding protein offered an opportunity to probe the calcium

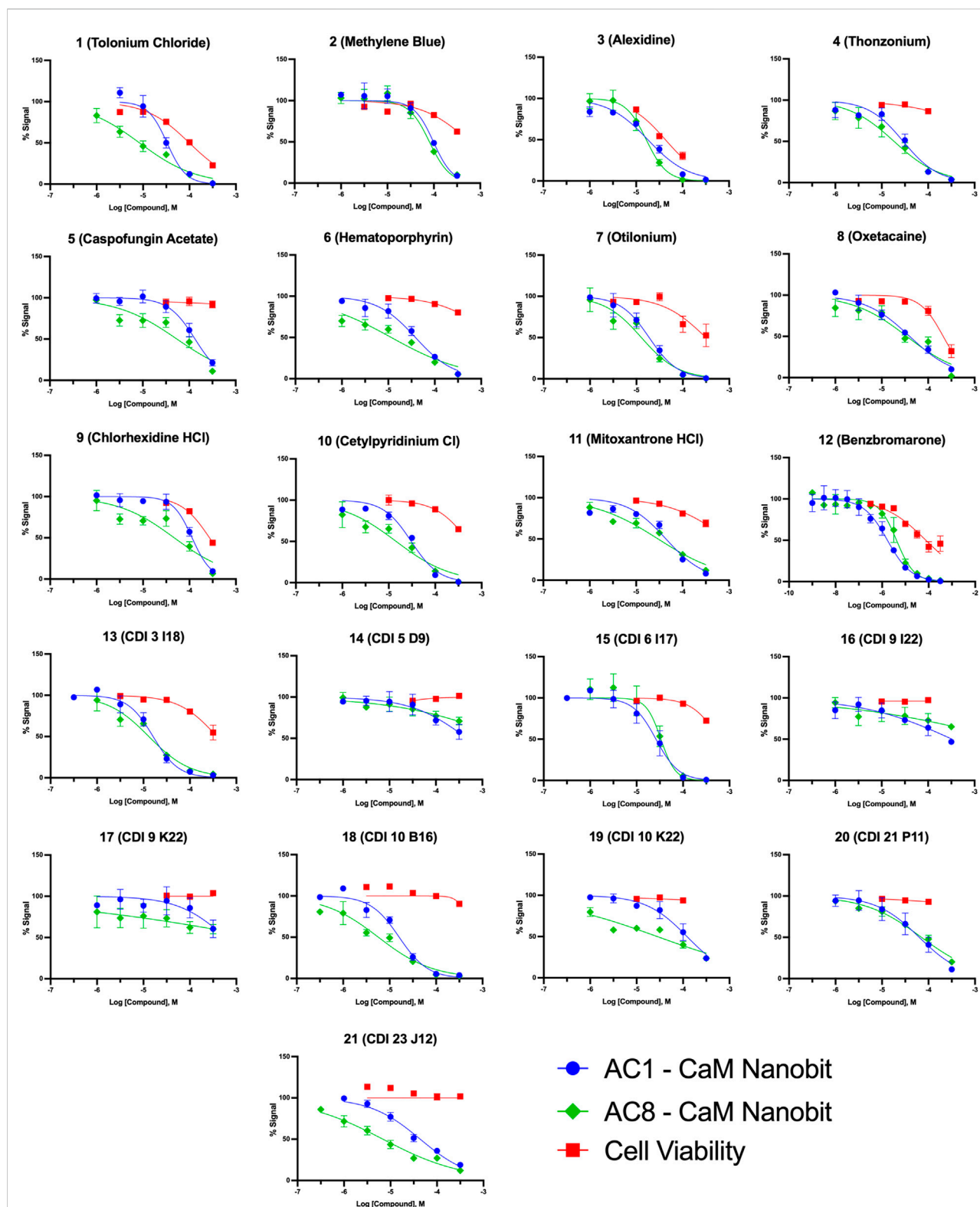
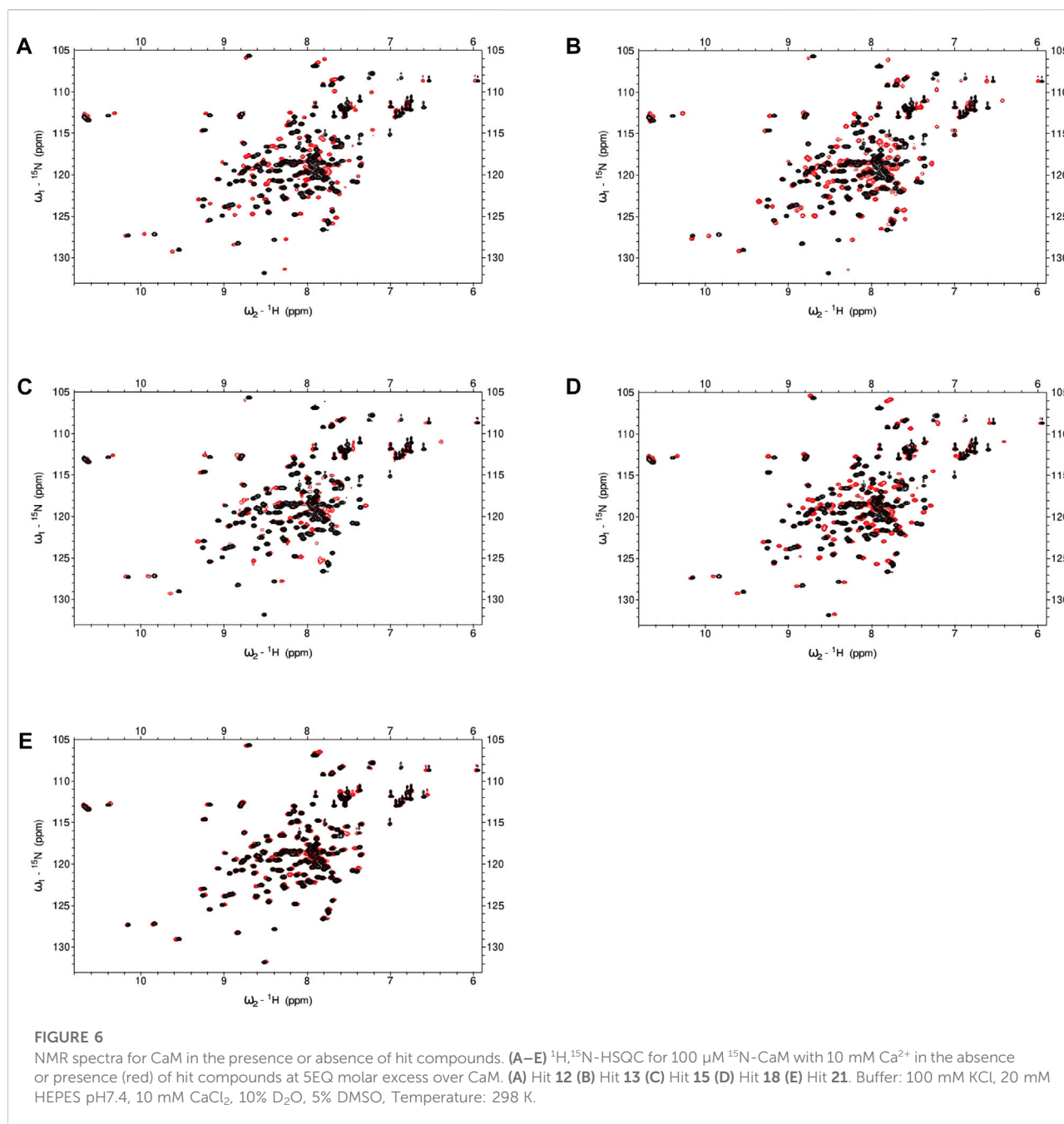


FIGURE 5

Concentration response curves for AC1/CaM pilot screen hits in NanoBt assay and CellTiter Glo-2.0 cell viability assay. NanoBt results are shown as blue circles for AC1/CaM, green squares for AC8/CaM, and red squares for cell viability (CellTiter Glo-2.0) assay results. The baseline corrected AUC values are normalized to vehicle in the presence of thapsigargin (100%) or vehicle pre-treated with BAPTA-AM (0%) for the NanoBt assay. The cell viability data is normalized to the cells treated with vehicle (100%) or cell free wells with vehicle added (0%). Data represents $n = 3$ experiments \pm SEM.



sensitivity of the AC1-C1b/CaM FP assay. Investigating the AC1-C1b/CaM interaction with EGTA (Ca^{2+} chelator) showed the interaction to be Ca^{2+} dependent, which was expected (Figure 1B). Incorporating EGTA as a positive control worked well for the AC8/CaM FP assay but did not provide a sufficient signal window for the AC1/CaM FP assays. Calmidazolium (CDZ), a compound known to bind CaM and previously identified in an AC8/CaM inhibitor screen, served as the positive control with an IC_{50} of 15.1 μM (Figure 1C) (Gietzen et al., 1981; Ahljianian & Cooper, 1987; Lubker & Seifert, 2015).

The AC1-C1b/CaM assay stability was assessed in the presence of 0–5% DMSO, with measurements taken at 1, 2, 4, and 6 h (Supplementary Figure S1 and Table 1). Throughout these experiments, Z' values were calculated using Equation 2 (Zhang et al., 1999) shown below to assess the assay for rigor and reproducibility in an HTS campaign (Table 2). With a Z' value cutoff of >0.65 , the AC1-C1b/CaM FP assay tolerated up to 2.5% DMSO, and the signal was stable after 4 h of incubation at RT. The final assay conditions for the AC1-C1b/CaM are described in Table 1, with $\sigma_{p,n}$ representing the standard

TABLE 5 Initial examination of selected hits against Ca^{2+} -stimulated AC1 activity in cAMP accumulation assays. AC1-HEK $\Delta 3/6$ KO cells plated at 10,000 cells per well. Compounds were added to wells and cAMP accumulation was stimulated with $3 \mu\text{M}$ A23187 for 1 h at RT. IC_{50} values \pm SEM generated from 3-parameter nonlinear regression from three independent experiments ($N = 3$).

Compound #	AC1 $\text{IC}_{50} \pm \text{SEM}$
12	4.09 ± 2.41
13	31.0 ± 6.63
15	4.88 ± 2.14
18	6.70 ± 0.70
20	66.3 ± 33.3
21	8.77 ± 4.47

deviation (SD) of positive and negative control, and $\mu_{p,n}$ representing the mean of the positive and negative control.

$$Z' = 1 - \frac{(3\sigma_p + 3\sigma_n)}{|\mu_p - \mu_n|} \quad (2)$$

AC1/CaM FP high throughput screen

A high-throughput screen of 21,258 compounds was completed using the AC1/CaM FP assay described above. Hit compounds identified in the initial HTS were verified by retesting with the primary AC1/CaM FP assay before advancing hit compounds to concentration-response curve (CRC) assessment in the AC1/CaM and AC8/CaM FP assays. Compounds were assessed based on their inhibition constants (K_i), calculated using the Cheng-Prusoff equation (Equation 3) shown below (Cheng & Prusoff, 1973), and selectivity ratios for AC1 over the AC8 peptide interactions with CaM in the FP assays. In the equation below, K_i = The inhibitor constant, IC_{50} = observed IC_{50} in AC/CaM FP assay, K_d = AC/CaM dissociation constant, AC = Concentration of AC peptide.

$$\text{Cheng - Prusoff Equation } K_i = \frac{\text{IC}_{50}}{1 + \frac{[\text{AC}]}{K_d}} \quad (3)$$

FDA-approved library FP screen: AC1/CaM

First, a pilot screen was performed on 1,018 compounds from the FDA-approved library (Selleck Chemical, Houston, TX) using the AC1/CaM FP assay. Compounds were screened individually at a single concentration of $14.5 \mu\text{M}$. The results of screening the FDA-approved library are shown in Figure 2A and summarized in Table 2. The calculated Z' remained above the lower threshold for an acceptable HTS screen (>0.5) (Zhang et al., 1999), with Z' ranging from 0.70–0.77. Hit criteria was

established at compounds that exhibited a signal 5 SD below the mean value of the vehicle control (1% DMSO). This cutoff corresponded to $\sim 30\%$ inhibition relative to $100 \mu\text{M}$ CDZ (100% inhibition) positive control. Finally, reproducibility experiments were conducted to assess assay variability over multiple screening days. The results of the variability testing showed that the compounds identified as hits on 1 day were identified again on the next day of screening (Supplementary Figure S2). Seven hits were validated at the screening concentration ($14.5 \mu\text{M}$), tested in triplicate. The hit rate for molecules that met the hit criteria and were validated as hits for the FDA-approved compounds was 0.7%.

Microsource spectrum collection FP screen: AC1/CaM

We screened 2,320 compounds from the Microsource Spectrum Collection (MMSP, Gaylordsville, CT) at a single concentration of $14.6 \mu\text{M}$. Hits were identified using a 5 SD. below the mean of the vehicle control (1% DMSO) cutoff and validated with a single concentration in the AC1/CaM FP assay as outlined for the FDA-Approved library. The results of screening the MMSP library are shown in Figure 2B and summarized in Table 2. The Z' ranged from 0.69–0.77 for the MMSP library screen, and 13 compounds were validated as hits, yielding a hit rate of 0.56%. However, due to library duplication, three of the validated hits from the FDA-Approved library were re-identified as hits in the MMSP library (Mitoxantrone HCl, Alexidine, and Thonzonium). Interestingly, this served as a validation of these compounds as hits and as additional evidence for the reliability of this HTS assay. In addition, three of our initial hit compounds contained structures that were deemed unfavorable for optimization or further characterization (Chicago Sky blue, Protoporphyrin IX, and Chlorophyllide Cu complex) and were therefore excluded from further testing.

ChemBridge DIVERSet library FP screen: AC1/CaM

The ChemBridge DIVERSet Library (ChemBridge Corp, San Diego, CA) is comprised of a compound collection that has been stringently filtered *in silico* to retain only compounds with desirable drug-like properties ($\text{MW} \leq 500$, $\text{cLogP} \leq 5$, H-Bond acceptors ≤ 10 , H-Bond donors ≤ 5). A total of 10,240 compounds were screened and hits identified using the same 5 SD. Hits were validated with a single concentration in the AC1/CaM FP assay as outlined for the FDA-Approved library. The results of screening the ChemBridge DIVERSet library can be seen in Figure 2C, and the summary of the results is shown in Table 2. The Z' for the ChemBridge DIVERSet library screen ranged from 0.68–0.77. Two compounds were validated as hits, yielding a hit rate of 0.02%.

ChemDiv CNS targeted library FP screen: AC1/CaM

The ChemDiv CNS targeted library (CDI, ChemDiv, San Diego, CA) is comprised of compounds selected for CNS protein targets (98 protein sub-families/unit targets) based on literature searches (ranging from 2014-present) as well as novel X-ray and Cryo-EM structures deposited in the PDB. These searches are designed to identify chemical structures and substructures more likely to penetrate the blood-brain barrier due to their physicochemical properties and known activities. The criteria for evaluating the screening data produced with the CDI library were the same as for the previous libraries screened. 7,680 compounds from the CDI library were screened against the AC1/CaM FP assay. The results of screening the CDI library are shown in Figure 2D and the summary of the results is shown in Table 2. The Z' ranged from 0.69–0.76, and hits were identified using the 5 SD cutoff and validated with a single concentration in the AC1/CaM FP assay as outlined for the FDA-Approved library. Screening the CDI library against the AC1/CaM FP assay yielded 32 validated hits, with a hit rate of 0.42%. To evaluate the potency of initial hits, concentration-response curves in the AC1/CaM FP assay were generated for the validated hits using the CDI library stocks. Of the 32 validated CDI hits, 9 compounds were advanced to the

next phase of evaluation based on their magnitude of inhibition and K_i values for the AC1/CaM FP assay.

Characterization of HTS hits: AC1/CaM and AC8/CaM FP

In total, 21,258 compounds from four compound libraries were screened in the AC1/CaM FP assay. From these screens, 25 validated hits were repurchased as a powder for CRC analysis. CRCs were generated for hits in the AC1/CaM primary assay and AC8/CaM counterscreen assays. Data were normalized to the vehicle (1% DMSO; 0% inhibition) and the 100 μ M CDZ positive control (100% inhibition). However, as CDZ is not a complete inhibitor of the AC-CaM interaction, it did not abolish the FP signal altogether. As a result, several hit compounds inhibited the FP signal greater than 100%, using CDZ inhibition as a comparator. The CRCs and structures of the hit compounds for the FDA-approved, MMSP, and ChemBridge libraries are shown in Figure 3, and the CDI library hits are shown in Figure 4. The calculated AC1/CaM and AC8/CaM K_i values for all hit compounds are summarized in Table 3.

The most potent compound identified in the AC1/CaM FP screen was **1** (tolonium chloride) from the MMSP library, with a K_i of 0.29 μ M for AC1-C1b/CaM (IC_{50} = 1.24 μ M), 2.3 μ M for

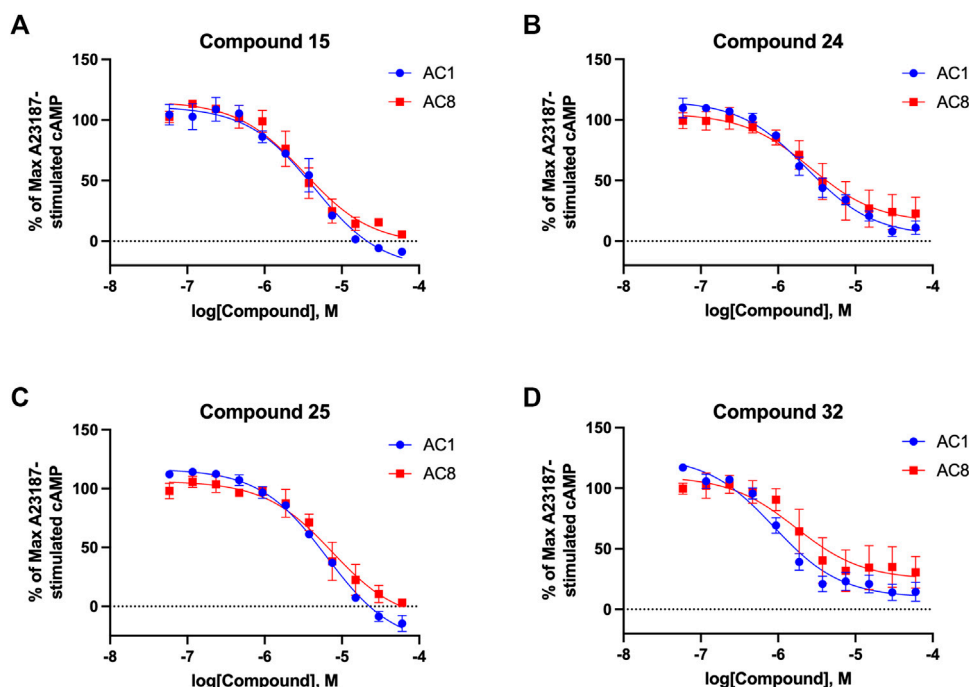
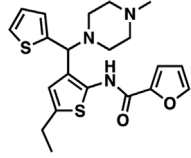
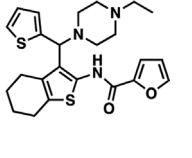
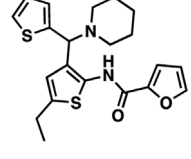
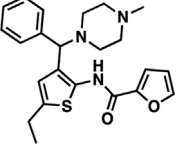
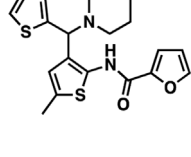
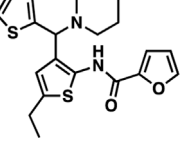
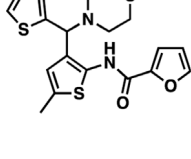
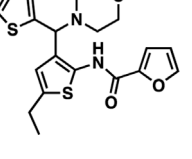
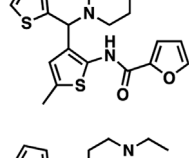
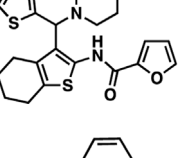
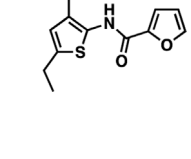
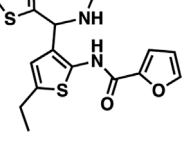
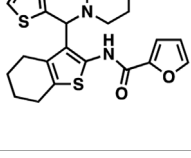


FIGURE 7
cAMP accumulation CRCs of CDI compounds at AC1 and AC8. cAMP accumulation data of select CDI compounds 15 (A), 24 (B), 25 (C), 32 (D), in AC1- or AC8-HEK Δ 3/6 KO cells. Points in representative summary curve displays the mean \pm SEM of the percent of 3 μ M A23187 inhibition from the averages of three independent experiments ($N = 3$).

TABLE 6 CDI analog structures, IC₅₀ values from cAMP accumulation assays in AC1- and AC8-HEK Δ3/6KO cells, and cell viability in AC1-HEK Δ3/6KO cells. IC₅₀ values were generated from a 3-parameter nonlinear regression of the averages of 3 independent experiments (N = 3).

#	Structure	IC ₅₀ (μM) ± SEM			% Viable Cells at AC1	#	Structure	IC ₅₀ (μM) ± SEM			% Viable Cells at AC1
15		AC1	AC8	30 μM		28		AC1	AC8	30 μM	
		4.36 ± 0.32	3.90 ± 1.83	43				20.0 ± 5.23	11.6 ± 1.82	88	
22		2.48 ± 0.39	3.23 ± 0.57	97		29		10.3 ± 1.45	14.4 ± 4.10	65	
23		3.08 ± 0.25	4.21 ± 1.01	100		30		10.6 ± 2.72	4.99 ± 1.10	100	
24		2.75 ± 0.82	2.70 ± 0.24	77		31		5.25 ± 1.07	1.49 ± 0.38	37	
25		6.39 ± 0.89	8.85 ± 2.70	94		32		0.89 ± 0.04	1.86 ± 0.32	100	
26		4.39 ± 0.44	2.92 ± 1.36	61		33		3.58 ± 2.26	2.70 ± 1.92	88	
27		34.8 ± 13.0	25.6 ± 6.77	48							

AC8-Nt/CaM, and 0.44 μM for AC8-C2b/CaM. The second most potent hit, **2**, also from the MMSP library, has an almost identical structure to **1**, differing by the addition of a methyl group on the tricyclic scaffold. The K_i values for **2**, 0.51 μM for AC1-C1b/CaM (IC₅₀ = 2.18 μM), 3.2 μM for AC8-Nt/CaM, and 0.82 μM for AC8-C2b/CaM, are nearly identical to those obtained for **1**.

Further, **1** and **2** achieved 75–80% inhibition relative to the positive control (100 μM CDZ) in the AC1 and AC8/CaM FP assays at the highest concentration tested (100 μM). These two compounds did not exhibit a significant selectivity for the AC1/CaM interaction versus either AC8/CaM interaction, evidenced by similar K_i values. These compounds share a phenothiazine

TABLE 7 Percent inhibition of CDI compounds (30 μ M) in AC2-HEK Δ 3/6KO and AC5-HEK Δ 3/6KO cells. Data reported as averages of % inhibition values at 30 μ M from three independent cAMP accumulation assays (N = 3) \pm SEM.

Compound #	% Inhibited at AC2 \pm SEM	% Inhibited at AC5 \pm SEM
15	59 \pm 14	47 \pm 10
24	15 \pm 11	16 \pm 11
25	52 \pm 11	46 \pm 5
32	10 \pm 8	3 \pm 3

scaffold present in the known CaM binder, trifluoperazine (TFP, StelazineTM) and will be discussed below (Ahlijanian & Cooper, 1987; Hayes et al., 2018). It should also be noted that compound 2 (methylene blue) is a known nonspecific PPI inhibitor, although it was identified as a hit against AC1 (Chuang et al., 2022).

The next most potent hits were 3 and 4, with K_i values of 0.67 and 1.0 μ M for AC1-C1b/CaM (IC_{50} = 2.8 and 4.14 μ M), respectively. Hits 3, 4, and 7 (K_i for AC1/CaM FP = 4.1 μ M) were the duplicate hits identified in the FDA-approved and MMSP library screens. These three hits have been previously identified as AC8/CaM inhibitors (Hayes et al., 2018). Hits 3, 4, and 7 inhibited nearly 100% of the AC1/CaM FP signal; however, they exhibited only modest selectivity for AC1 over the AC8 constructs. The hits 5, 6, and 8–11 had K_i values ranging from 3.0–7.8 μ M in the AC1/CaM FP assay. Hit 5 inhibited the AC1/CaM interaction with a K_i value of 3.0 μ M in the FP assay and exhibited slight selectivity (2-fold) for AC1 over AC8 in the FP assays. Hit 6 inhibited the AC1/CaM FP assay to 131% relative to the positive control due to CDZ's incomplete inhibition of the FP signal. Only hits 6 and 3 outperformed the positive control in the AC1/CaM FP assay. Hits 6 and 8 were the only non-CDI library compounds tested that preferentially inhibited AC1/CaM over AC8/CaM in the FP assays (Table 3; Figure 3). Hit 9 is structurally similar to 3 as both contain biguanidine scaffolds; however, 9 was a poor inhibitor of the AC1/CaM interaction in the FP assay, reaching only 15% inhibition, relative to the positive control, at the highest concentration tested.

The nine CDI CNS library hits 13–21 are from the original 32 confirmed hits from this library. After confirmation, we selected these nine hits for additional characterization based on the K_i and percent inhibition values gathered from CRCs in the AC1/CaM FP assay. In the FP assays, hits 13–19 and 21 exhibited selectivity for AC1/CaM over both AC8-Nt and AC8-C2b/CaM. The only exception was 20, which was slightly more selective for AC8 over AC1 in the FP assays. The most potent CDI library hits in the AC1/CaM FP assay were 15 and 16, with K_i values of 5.2 and 5.7 μ M, respectively. However, 15 and 16 were less efficacious, achieving only 58 and 25% inhibition of the AC1/CaM PPI in the FP assay, less than several more potent hits from the FDA-Approved or MMSP libraries. From the CDI CNS library, the maximal inhibition in the AC1/CaM FP assay was

~70% for 20 and 14, with three compounds displaying less than 50% inhibition (13, 16, and 19). However, we placed an equal priority on potent compounds and those that exhibit selectivity for inhibition of AC1-CaM over AC8-CaM. We, therefore, moved forward with 21 (Table 3) of the original 25 hits identified in the pilot screens for assessment with full-length proteins in the NanoBiT assay.

NanoBiT assay development: AC1/CaM

We used the NanoBiT PPI system (Promega, Madison, WI) as a cell-based orthogonal assay to test the hits identified in the AC1/CaM FP pilot screen. The NanoBiT assay provides a cellular context to examine compound activity and utilizes full-length adenylyl cyclase. We have applied this system in a prior study to assess the AC8/CaM PPI (Hayes et al., 2018). In the NanoBiT system, proteins are tagged on their N- or C-terminus with large or small BiT (LgBiT or SmBiT) fragments. As the proteins associate in cells, the BiT fragments complement to form a functional luciferase enzyme (NanoLuc) capable of producing luminescence when the substrate (NanoGlo reagent) is present. As the two interacting proteins can be tagged with the LgBiT or SmBiT on their N- or C-termini, there are eight total NanoBiT vector combinations for a PPI pair. Further, the relative sizes of the BiT fragments, with LgBiT at 17 kD and SmBiT at only 11 amino acids, necessitate testing of each NanoBiT vector combination to assess any impact the BiT fragment presence has on the PPI due to steric hindrance (Supplementary Figure S3). These vectors were generated as described above, and transient transfection methods were used to express the vector pairs in HEK293T cells. In addition to the vectors listed above, a Halo-SmBiT control was used as a non-specific protein to establish baseline luminescence from LgBiT activity, which is typically negligible in the absence of the SmBiT (168). The Ca^{2+} -dependent nature of the AC1/CaM PPI allowed use of controls for the NanoBiT assay which modulate the level of intracellular Ca^{2+} . The AC1/CaM PPI response to calcium mobilizers was assessed for all vector combinations. Several assay conditions were used to determine the most promising vector combinations under varying levels of intracellular Ca^{2+} . Briefly, BAPTA-AM was added 30 min before the addition of the NanoBiT substrate

(NanoGlo Reagent) to enter cells and chelate free Ca^{2+} . After this initial treatment, NanoBiT substrate was added, and baseline luminescence was measured continuously for 30 min. Finally, cells were treated with buffer, thapsigargin, or calcium ionophore A23187, and luminescence was monitored continuously for an additional 60 min. The response to vehicle or Ca^{2+} regulating mobilizing agents (Thapsigargin or A23187) in the absence or presence BAPTA-AM was assessed using the area under the curve (AUC) for the 25 min following the baseline luminescence read. Initial optimization efforts revealed poor results for the combinations with LgBiT attached to AC1 and SmBiT attached to CaM. This result is likely either the result of the LgBiT occluding CaM binding to the AC1 protein or the BiT fragments being too distant to associate and form functional NanoLuc enzyme. These Ca^{2+} sensitivity experiment results prompted us to use SmBiT-AC1 with LgBiT-CaM (both N-terminal attachments) to assess our initial hits using NanoBiT. This vector combination showed the most robust increase in luminescence with thapsigargin compared to A23187. In addition, the SmBiT-AC1 and LgBiT-CaM fusion protein combination was responsive to thapsigargin in terms of reversal of the decrease in luminescence from pre-incubation with BAPTA-AM (Supplementary Figure S3B).

NanoBiT assay: AC1/CaM FP hits in cells

Pairing the NanoBiT assay with the Cell-Titer Glo 2.0 assay allowed us to monitor a decrease in the NanoBiT signal and ensure this signal loss was not a result of cell death or loss of membrane integrity. The CRCs for hit compounds in the NanoBiT and cell viability assays are shown in Figure 5 and summarized in Table 4. One of the most promising hit compounds was **12** (Benzbromarone). In the NanoBiT assay, **12** was the most potent hit with an IC_{50} of $1.70 \pm 1.17 \mu\text{M}$ and $4.53 \pm 1.15 \mu\text{M}$ for the AC1/CaM and AC8/CaM PPI, respectively. Cell viability at the AC1/CaM IC_{50} was at 90% for **12**. Despite performing well in the NanoBiT assay, **12** was not the most potent hit in the AC1/CaM FP assay with an IC_{50} of $33 \mu\text{M}$ and a K_i of $7.8 \mu\text{M}$. In the FP assay, **12** was approximately 7- and 3-fold selective for AC1-C1b/CaM over AC8-Nt/CaM and AC8-C2b/CaM, respectively. This selectivity is not entirely lost in the NanoBiT assay but is a theme observed for several hit compounds tested.

The next most potent hits in cells were **3**, **7**, **13**, and **18**, with IC_{50} values below $20 \mu\text{M}$ for the AC1/CaM and AC8/CaM NanoBiT assays. These compounds were moderately selective for AC1 in the FP assays, but selectivity was lost in the NanoBiT assay. Interestingly, the AC selectivity of **18** flipped from what was observed in the FP assay, where **18** was selective for AC1-C1b/CaM over both the AC8/CaM FP constructs; in the NanoBiT assay, **18** was ~3-fold selective for AC8 over AC1.

This phenomenon was not specific to **18**. For example, the hit compounds **6** and **21** were 2- to 4-fold selective for AC8 over AC1 in the NanoBiT assay but exhibited near total selectivity for AC1-C1b/CaM over the AC8/CaM constructs in the FP assays. We will discuss possible explanations for this reversal of selectivity below.

With respect to cell viability, amongst all the pilot screen hits, **3** had the greatest decrease in cell viability of 25% at its AC1/CaM IC_{50} ($17.9 \pm 1.15 \mu\text{M}$) and 70% at $100 \mu\text{M}$. For hits **7**, **13**, and **18**, cell viability was between 96–100% at their respective AC1/CaM IC_{50} values. For **7** and **13**, cell viability was reduced by ~50% at the highest concentration tested ($316 \mu\text{M}$), but 90% cell viability was observed for **18** at this concentration. From the remaining pilot screen, only hits **1**, **2**, **9**, and **11** exhibited a reduction in cell viability greater than 10% at their respective AC1/CaM IC_{50} values. Although **1** was the most potent in the FP assays, this was not the case in the NanoBiT assay. **1** was more potent in the AC8/CaM NanoBiT assay, with IC_{50} values of 8.4 and $32.9 \mu\text{M}$ in the AC8 and AC1/CaM NanoBiT assay, respectively. The remainder of the pilot screen hits tested *in vitro* had AC1/CaM IC_{50} values between 20 and $\sim 100 \mu\text{M}$ or did not inhibit the AC/CaM PPI in the NanoBiT assay. For simplicity, the remaining sets were separated by a range of IC_{50} values from the AC1/CaM NanoBiT assay: Set A— IC_{50} values from 1 to $20 \mu\text{M}$: **3**, **7**, **12**, **13**, and **18**; Set B— IC_{50} values from 21 to $30 \mu\text{M}$: **4**, **15**, and **21**; Set C— IC_{50} values from 30 to $40 \mu\text{M}$: **1**, **6**, and **10**; Set D— IC_{50} values from 41 to $150 \mu\text{M}$: **2**, **5**, **8**, **9**, **11**, **14**, and **20**; Set E—No Inhibition in NanoBiT assay: **16**, **17**, and **19**.

Nuclear magnetic resonance: CaM binding

To ascertain if certain compounds were imparting inhibition through direct binding to calmodulin, we collected ^1H - ^{15}N HSQC spectra of ^{15}N -CaM in the presence or absence of the compound. We tested hit compounds **12**, **13**, **15**, **18**, and **21** at 5 equivalent molar excess of CaM concentration and observed chemical shift perturbations (CSP) for multiple CaM residues (Figure 6). Ligand-induced CSPs indicate binding as observed by backbone amides on ^{15}N -CaM. Hits **12** and **13** exhibited the largest CSPs in the AC1 set with CaM likely to be fully saturated or in fast exchange at 5EQ molar excess over CaM. Hits **18** and **21** exhibit modest chemical shift changes at 5EQ. Only compound **15** exhibited chemical shift changes where several peaks were broadened by intermediate exchange and disappeared. The disappearance of peaks in intermediate exchange occurs near the equilibrium between free and bound states that are on a time scale typical for conformational dynamics. At 5EQ molar excess of **15**, CaM is not fully saturated. The somewhat unique binding properties of **15** to CaM may provide opportunities for AC1 vs. and AC8 selectivity.

Characterization of FP and NanoBiT hits in AC1 cAMP accumulation assays

From the hits identified among FP screens and NanoBiT assays, six were selected for characterization of activity against AC1, based on their potency and selectivity profiles as well as favorable drug-like properties. Hits from the CDI library (**12**, **13**, **15**, **18**, **20**, and **21**; Table 5) were AC1-selective in the FP assays with moderate efficacy and displayed modest potency against AC1 and/or AC8 in cellular NanoBiT assays. Hit **12** was identified in the AC1 FP screens but was not identified as a hit against AC8, indicating possible selectivity for AC1. Furthermore, **12** displayed the highest potency at inhibiting the PPI between AC1-CaM and AC8-CaM in NanoBiT assays. For initial characterization of these six compounds, we utilized HEK-293 cell lines where endogenous AC3 and AC6 were knocked out to reduce the background cAMP signal and subsequently transfected with AC1 (AC1-HEK Δ 3/6 KO cells; (Soto-Velasquez et al., 2018). cAMP accumulation is measured as a direct output of AC inhibition via a Cisbio homogenous time-resolved fluorescence (HTRF) assay. The data shown in Table 5 and represent the mean \pm SEM of the IC₅₀ values (μ M) for each compound, in AC1-HEK Δ 3/6 KO cells. Hit **12** displayed the highest potency against AC1 at 4.09 μ M, with **15** following closely at 4.89 μ M; both of these compounds were equally efficacious, displaying ~75% inhibition of AC1 activity (data not shown). Hits **18** and **21** were slightly less potent at 6.70 and 8.77 μ M, respectively. **18** and **21** also displayed lower efficacies, at ~70 and ~50%, respectively. Finally, hits **13** and **20** were significantly less potent at AC1 than other hits evaluated, at 31.0 and 66.3 μ M, respectively.

Structure-activity relationship (SAR) studies of dithiophene CDI compounds in AC1/AC8 cAMP accumulation assays

Among the hits that were identified and characterized for AC1 activity inhibition, the dithiophene scaffold of compound **15** from the CDI library was prioritized for initial SAR evaluation for several reasons: 1) the combined potency and selectivity in the FP assays, 2) efficacy for PPI inhibition in the NanoBiT assay, and 3) drug-like physicochemical properties. To accomplish this, we utilized HEK Δ 3/6 KO cells expressing AC1 or AC8. The data shown in Table 6 represent the mean \pm SEM of the IC₅₀ values (μ M) for each compound, in AC1- and AC8-HEK Δ 3/6 KO cells, respectively. Testing of the dithiophene compounds, referred to hereafter as CDI analogs (Table 6), with A23187-stimulated AC1 and AC8 activity yielded a unique SAR profile, focused on the cyclic amine ring of the dithiophenes as well as substituents from this ring and to the thiophene heterocycles. For this assessment, 12 additional CDI analogs (**22–33**) were purchased from ChemDiv, along with the original dithiophene

hit **15**. For the first piperidine series (**22–24**), SAR was relatively flat with modest changes to either the piperidine or alkyl group on the thiophene leading to equipotent analogs. **24** was the most potent of this cohort versus AC1 with an IC₅₀ value of 2.75 μ M. This molecule also was equipotent against AC8 with an IC₅₀ values of 2.70 μ M. Moving from a piperidine to the matched molecular pair *N*-alkylated piperazine analogs (**15**, **25**, **26**) provides a slight reduction in AC1 activity (2–3-fold) compared to the piperidine containing counterpart. The piperazine modification also had varying effects on AC8, particularly with the ethyl-thiophene derivatives (**15**, **26**) slightly favoring AC8 over AC1. The next two analogs (**27**, **28**) contained a fused cyclic alkane to the central thiophene of the scaffold, as opposed to methyl or ethyl substitution. Each exhibited marked reduction of activity against both AC1 and AC8 compared to nearest neighbor analogs non-cyclic analog. The reduction was greater against AC1, thus making these analogs more selective for AC8, with **28** being 2-fold more potent at AC8. In both AC1- and AC8-overexpressing HEK cells, several of these compounds displayed approximately 100% inhibition of cAMP accumulation, as well as low-micromolar IC₅₀ values at both AC1 and AC8. **29** maintained the *N*-methylpiperazine and ethyl substituent off the central thiophene, but swapped the second thiophene heterocycle for a phenyl ring. When compared to its matched molecular pair in **15**, **29** exhibited about a 2- and 3-fold reduction in AC1 and AC8 potency, respectively. **30–32** swapped the piperazine for a morpholine moiety. Notably, this modification decreased both AC1 and AC8 potency for the matched molecular pairs that incorporated either the piperazine or piperidine with one exception. **32** actually displayed an improved potency against A23187-stimulated cAMP accumulation in AC1-HEK cells with an IC₅₀ at AC1 of 0.89 μ M. This molecule was also modestly selective over AC8 with an IC₅₀ of 1.86 μ M. Interestingly, although **32** is slightly more potent against AC1, the AC8 potency makes this compound the most potent AC8 inhibitor known to date. The final analog in this SAR set was **33**, which moved from the *N*-cyclic alkane substituent and incorporated a 2-aminopyridine. This compound displayed similar potency to the piperidine series (**22–24**), with modest selectivity for AC8. Concentration-response curves for selected analogs (**15**, **24**, **25**, and **32**) are presented in Figure 7. Among these four compounds are some of the most potent inhibitors at AC1 and AC8, also displaying 100% inhibition of AC1 activity and 70–100% inhibition of AC8 activity (Table 6 and Figure 7).

Isoform selectivity of CDI compounds at AC2 and AC5

To determine whether these compounds were selective for AC1 and AC8 over other isoforms, we tested **15**, **24**, **25**, and **32** in

cAMP assays against AC2 and AC5 as representative isoforms from Groups II and III, respectively, of AC isoforms. We used AC2-HEK $\Delta 3/6$ KO and AC5-HEK $\Delta 3/6$ KO cells and tested each of the four compounds at 30 μM , assessing percent inhibition, shown in Table 7. Surprisingly, hit compound **15** displayed modest inhibition at AC2 and AC5 (59 and 47%, respectively). Compound **25** also partially inhibited AC2 and AC5 activity (52 and 46%, respectively). **15** and **25** are structurally almost identical, differing only in the substituent on the central thiophene (ethyl on **15** versus methyl on **25**), which may explain why these had similar activity against AC2 and AC5. On the other hand, compounds **24** and **32**, having a piperidine and morpholine heterocycle, respectively, showed very little inhibition against AC2 and AC5 (<16%). Interestingly, in our previous studies we have observed AC1 inhibitors to modestly potentiate AC2 at 10 and 30 μM , thus, the inhibition at 30 μM was a bit unexpected but may be a result of the different mode of action for this scaffold. This will be investigated in future studies.

Discussion

The FP assay developed for this work allowed us to measure the interaction between CaM and an AC1-C1b peptide. In our FP assay, we utilized peptides labeled with the fluorescent dye cyanine-5 (Cy5) that incorporated the residues on AC1 or AC8 where Ca^{2+} dependent CaM binding has been previously established (Masada et al., 2012; Herbst et al., 2013). In the AC-CaM FP assays, the Cy5-AC peptides are approximately 4 kD (AC1-C1b: 3,868 g/mol, AC8-Nt: 3,746 g/mol, AC8-C2b: 3,549 g/mol) and GST-CaM is 39 kD (His6-GST: 25 kD, CaM: 14 kD). The addition of the GST-tag to CaM improved the degree of polarization for the AC peptide when it was bound to GST-CaM and increased the FP signal window necessary for HTS. After our optimization efforts, the AC1/CaM FP assay proved to be robust, evidenced by Z' values ranging from 0.68–0.77 throughout the compound screen, consistently above the lower threshold of 0.5 for assays to be considered robust and suitable for HTS hit identification (Zhang et al., 1999). Further, the assay tolerated up to 2.5% DMSO and was stable from 1 to 6 h (Supplementary Figure S1). Therefore, we prioritized optimizing our HTS approach to incorporate assays that were sensitive to Ca^{2+} , a key mediator of the AC/CaM interaction. We were pleased to find that the interaction between CaM and the Cy5 labeled AC peptides was dependent on Ca^{2+} in the FP assays, as evidenced by the response observed when EGTA was present in the assay (Figure 1B). A drawback to this approach was the potential for metal chelators; we, therefore, assessed compounds that contained structures or exhibited inhibitory behavior that suggests the ability to chelate Ca^{2+} . Our optimization process centered around our goal of identifying

compounds that would perform well in a calcium-rich environment where the PPI occurs.

Approximately 21,000 compounds from 4 different chemical libraries were screened using the AC1/CaM FP assay. The pilot screen identified 54 compounds (FDA-Approved: 7 hits, MMSP: 13 hits, DIVERSet: 2 hits, and ChemDiv: 32 hits). However, due to library duplication, three compounds (Alexidine, Otilonium, and Thonzonium) were identified as hits in the FDA-Approved and MMSP libraries. An additional three compounds, Chicago Sky blue, Protoporphyrin IX, and Chlorophyllide Cu complex, were removed after their chemical structures were unfavorable for further development. The availability of ChemDiv CNS library stocks permitted initial concentration-response curve assessments to be made before ordering powder stocks. From the original 32 ChemDiv hits, 9 were advanced to the next phase of screening based on their approximate IC_{50} and percent inhibition relative to the positive control (100 μM CDZ = 100% inhibition) in the AC1/CaM FP assay. In addition to the reduction in hits from the CDI library (32–9), five compounds identified in the FDA-approved MMSP and ChemBridge library screens did not exhibit significant inhibition of AC1/CaM in the FP assay after fresh powder stocks were ordered. Two of those compounds were from the ChemBridge DIVERSet library, two were from the Microsource spectrum collection (ethyl quinine and rivastigmine tartrate), and one was from the FDA-approved library (nicotine ditartrate). Compounds that exhibited poor potency or inhibition in the AC1/CaM FP assay were tested in the AC8/CaM FP assays to gather information about what chemical scaffolds/structures tended to be more selective for the AC8/CaM interaction(s) over the AC1/CaM interaction. As a result, 25 of the original 54 hit compounds were advanced for further characterization.

Characterization of hits centered around CRC analysis of the primary AC1/CaM FP assay, with counter screening efforts to identify hit compounds that selectively inhibited the AC1/CaM interaction over the AC8/CaM interaction(s). The two most potent hits identified in the FP pilot screen, **1** and **2**, contain a phenothiazine structure. These hits have the same phenothiazine scaffold as the known CaM antagonist trifluoperazine (TFP). This common substructure could indicate that the AC/CaM inhibition observed for **1** and **2** results from CaM binding rather than AC binding. However, TFP poorly inhibited AC1/CaM in the FP assay with only 30% inhibition at 100 μM for AC1/CaM. Further, our prior testing with TFP in the AC8/CaM FP assays found that it could inhibit AC8-Nt/CaM (~85% at 100 μM) but did not inhibit AC8-C2b/CaM (**3**). Despite their structural similarities, **2** has been found to reduce pain caused by cancer treatment as an oral rinse, alleviate the pain that accompanies a propofol injection, and reduce lower back pain as an intradiscal injection (Salman et al., 2011; Kallewaard et al., 2016; Roldan et al., 2017). Although the mechanism of **2** is not fully understood, the predominant

proposed mechanisms involve the inhibition of monoamine oxidase A, nitric oxide synthase, guanylate cyclase (GC), and blockade of the GABA receptor (Alda, 2019; Bistas & Sanghavi, 2020). Acting in the CNS on a GC would suggest **2** could reach AC1 at the very least. However, this finding prompts further structural optimization of compounds with a phenothiazine scaffold to avoid off-target effects. Another structural feature shared by several hits (**3–5**, **7**, **9**, and **10**) is a long carbon chain or linker (6 carbons or more). As these linkers will afford flexibility to these compounds, it may be possible that these aliphatic “tails” allow for more significant inhibition by binding to a hydrophobic pocket. However, further studies examining the binding site would need to confirm this notion. Apart from **20**, all the validated hits from the CDI library inhibited the AC1/CaM FP assay but could not inhibit both AC8/CaM FP assays. However, the hits from the CDI library exhibited a lower degree of inhibition in the AC1/CaM FP assay as compared to the hits from the FDA-approved or the MMSP libraries.

Of the 25 compounds, 21 were advanced for testing in NanoBiT assays. The goal of this AC1/CaM FP HTS was to identify novel structures capable of disrupting the AC1-C1b/CaM and AC1/CaM interactions. In pursuit of this goal, two assays were developed to detect this interaction in both a biochemical setting and in a living cellular environment. Screening ~22,000 compounds from four unique chemical libraries has yielded small molecule inhibitors with interesting and novel chemical scaffolds that can disrupt the AC1/CaM interaction.

The NanoBiT assay was used an approach for assessing the ability of the hit compounds to inhibit the full-length AC/CaM proteins in a live cell format. As mentioned above, **12** was the most potent compound in the AC1/CaM NanoBiT assay. **12** (Benzbromarone) contains a 1-Benzofuran scaffold with an ethyl group substituted at the C-2 position and a 3,5-dibromo-4-hydroxybenzyl group at the C-3 position. Although **12** is labeled as a uricosuric agent and a known xanthine oxidase inhibitor, **12** was never approved by the FDA due to reports of acute liver toxicity (Chen et al., 2011; Chen et al., 2016). Compounds **1** and **2**, the most potent hits in the AC1/CaM FP assay, exhibited a significant loss of activity in the NanoBiT assay. Compounds **3** and **4**, which preferentially inhibited AC1 in the FP assays, displayed a reduced AC1 selectivity in the NanoBiT assays. Previous work has found that **3** and **4** exhibit CaM binding (Hayes et al., 2018). This observation could indicate that these compounds do not exert their AC1/CaM inhibition by binding to the C1b domain of AC1 but rather bind to CaM. While this mechanism may challenge AC selectivity, the interactions of CaM with AC1 and AC8 are not identical, and thus binding to CaM does not entirely undermine the ability of compounds to be selective.

In the transition from biochemical to cell-based assays, a loss in potency is not uncommon. Further, as the AC/CaM PPI is occurring not at the cell surface but inside the cell, a loss in

potency could be attributed to a compounds inability to cross the cell membrane or a high degree of non-specific protein binding (Strelow et al., 2004). Finally, mechanistic insights into the AC/CaM interaction provide an additional rationale for compounds exhibiting a loss in potency when transitioning from the peptide-based FP assay to the NanoBiT assay. The NanoBiT assays assessed the ability of the compounds to inhibit the full-length PPI, which for AC8 incorporates two CaM binding domains that are believed to work in unison. Although the activity of both AC1 and AC8 is stimulated by Ca^{2+} /CaM binding, their sensitivity to Ca^{2+} and binding mechanisms with CaM are distinct. For example, the activity of AC8 responds rapidly to transient fluxes of Ca^{2+} levels, while AC1 exhibits an increase in activity in response to Ca^{2+} flux that is sustained for a prolonged period (Masada et al., 2009; Masada et al., 2012). Although CaM has a higher affinity for AC1 relative to AC8, CaM must be fully saturated with Ca^{2+} before binding AC1 (Masada et al., 2009; Masada et al., 2012). On the other hand, the rapid response of AC8 to Ca^{2+} levels has been attributed in part to the presence of the two CaM binding domains, with a mechanism that is believed to involve tethering CaM to the N-Terminus of AC8 (Simpson et al., 2006; Masada et al., 2009; Masada et al., 2012). When Ca^{2+} levels increase, CaM is tethered to the N-terminus of AC8 and rapidly associates with the C2b domain of AC8, and an autoinhibitory mechanism is alleviated. Our FP approach does not fully capture this dynamic interplay between AC8 and CaM. As a result, several compounds exhibited a loss of selectivity for AC1 over AC8 in the NanoBiT assay relative to the FP assay. For example, the hits from the CDI library, apart from **20**, did not exhibit any degree of inhibition in either AC8/CaM FP assay, but were found to inhibit both the AC1 and AC8/CaM NanoBiT signal. Another aspect of the hits from the CDI library was their lack of toxicity, with only **13** and **15** exhibiting a decrease in cell viability at ~300 μM .

Of the 21 compounds we advanced from the FP characterization, only 5 were advanced through further testing. The hits **12**, **13**, **15**, **18**, **20**, and **21** were selected based on their criteria as AC/CaM inhibitors in both the FP and NanoBiT assays. Although **3**, **4**, and **7** displayed similar potencies, these compounds have been assessed in a previous report (Hayes et al., 2018). Further, the selected hits contained chemical scaffolds amenable to further structural optimization.

As we characterized the hits from our FP screen, we began to focus on the unique chemotypes we identified in the process. Among the AC1-selective hits with regard to disruption of the AC1 peptide-CaM interaction in the FP assay was hit **15** (58% efficacy at AC1, $\text{IC}_{50} = 22.1 \mu\text{M}$). **15** was then confirmed as an AC1/AC8 non-selective hit against full-length AC1- and AC8-CaM in the NanoBiT assay (100% inhibition of both AC1- and AC8-CaM interactions; AC1-CaM $\text{IC}_{50} = 26.1 \mu\text{M}$, AC8-CaM $\text{IC}_{50} = 33.4 \mu\text{M}$). Compound **15** also had a number of favorable drug like properties (molecular weight = 415 g/mol and LogP = 0.53) and possessed multiple sites amenable to explore SAR.

Lastly, we observed that compound **15** shared some structural overlap with a benzamide series of compounds that are known inhibitors of AC1 activity with selectivity vs. AC8 (Scott et al., 2022). We selected 13 dithiophene analogs including **15** for cellular testing against inhibition of Ca^{2+} /CaM-stimulated AC1 and/or AC8 activity. This scaffold contains a central thiophene ring linked to an aromatic ring (furan) via an amide, which directly overlaps with the benzamide series (Scott et al., 2022). The central thiophene is also linked to a central carbon bound to the second aromatic ring (usually thiophene), with a variation of different heterocycles (piperazine, piperidine, morpholine, or pyridine). In our cAMP accumulation assays, we found that the piperazine analogs slightly reduced AC1 activity, 2- to 3-fold. We noticed a trend in which changing the methyl to an ethyl on the central thiophene caused the analog to be more selective for AC8. Cyclization of the alkyl substituent to the thiophene significantly reduced activity at both AC1 and AC8, and also shifted selectivity toward AC8. This suggests that more hydrophobic groups, or perhaps more rigidity, at the central thiophene may cause analogs to be more potent at AC8. Notably, combining the fused cyclohexane-thiophene ring system with a morpholine heterocycle significantly increased potency at both AC1 and AC8 (**32**). Importantly, **32** is the most potent inhibitor of AC8 activity known to-date, although this compound also potently inhibits AC1 activity. Overall, the limited SAR on this series suggests that AC1 and AC8 potency and selectivity can be tuned individually. AC1 activity was favored more by a methyl-substituent on the thiophene ring, whereas AC8 activity was favored more so by the ethyl in the same position. The cyclohexane-fused thiophene selectivity was highly dependent on the nature of the N-heterocycle with piperazine favoring AC8 activity and morpholine favoring AC1. These preliminary SAR data points will now inform design of future analogs to tune both AC1 and AC8 selectivity inhibitors from within the same series. As previously mentioned, some differences in potency and selectivity in cellular assays may be attributed to the differential interactions of AC1 and AC8 with CaM. Additionally, it is possible that other proteins within the cellular environment may affect the activity of these compounds.

Some degree of CaM binding was observed for all compounds tested in the NMR experiments. The ^1H - ^{15}N HSQC spectra obtained for **12**, **18**, and **21** at 5EQ molar excess showed CaM was fully saturated or in fast exchange. To be in fast exchange, peaks exhibiting chemical shifts in the presence of a compound must move smoothly from free to bound (red) (Figure 6). In intermediate exchange, peaks will regain their original “free state” shape when saturation is reached but will exhibit broadened shape when in equilibrium between free and saturated, which was the case for **15**. Despite significant chemical shifts observed for **12** and **13**, we could not accurately predict a

binding site on CaM. The abundance of residues exhibiting CSP made it difficult to accurately determine binding sites for these compounds without multidimensional NMR experiments, which was outside of the scope of this study.

Through development of a novel fluorescence polarization assay, screening of over 21,000 compounds for inhibition of AC1 and/or AC8, and validation of activity in novel NanoBiT assays, we have discovered a novel dithiophene scaffold. Interestingly, the dithiophene scaffold shares structural similarities with the AC1 inhibitor benzamide series (Scott et al., 2022). Unlike the benzamide series, however, many compounds among this small dithiophene set were not selective for AC1 over AC8. This may be attributed to differences in AC1- or AC8-CaM interactions, since CaM has one mode of interaction with the C1b domain of AC1, whereas it can interact with the N-terminal domain and the C2b domain of AC8. Although we screened and selected for AC1-selective inhibitors, it is possible that AC8 inhibition could be beneficial for anxiety associated with various chronic and inflammatory pain states in humans and rodents (see (Shiers et al., 2022) and references therein). Multiple studies have reported that AC8 knockout mice exhibited reduced anxiety-like behaviors in the elevated plus maze test (Schaefer et al., 2000; Bernabucci & Zhuo, 2016). Furthermore, Shiers et al. showed that *Adcy8* mRNA expression increased in the anterior cingulate cortex (ACC) in a mouse model of neuropathic pain, although AC8 knockout does not play a role in mechanical hypersensitivity after inflammation (Wei et al., 2002; Shiers et al., 2022). This suggests a potential role of AC8 in anxiety-like behaviors. Thus, a non-selective AC1/AC8 inhibitor may be desirable for treating both chronic pain and the associated anxiety. In future studies, it would be interesting to determine how these non-selective dithiophene compounds affect the interactions of AC1 and AC8 with CaM. Further characterization should also be done on these compounds, such as assessment of their activity against different AC activators such as $\text{G}\alpha_s$ and forskolin. This dithiophene scaffold provides a novel AC1/AC8 inhibitor scaffold which is highly potent and may potentially be useful for treatment of chronic pain and anxiety.

Data availability statement

The raw data supporting the conclusions of this article will be made available by the authors, without undue reservation.

Author contributions

TD completed experiments, analyzed data, and wrote the paper. JO completed experiments, analyzed data, and wrote the

paper. CP performed experiments and analyzed data. JL performed experiments and analyzed data. DF analyzed data and edited the paper. VW analyzed data and edited the paper. DR analyzed data and edited the paper.

Funding

This work was supported by funds from the Rick and Anne Borch Research Award, Department of Medicinal Chemistry and Molecular Pharmacology, NIH NS111070 and 119917, NCI P30CA086862, 5T32GM008365. Partial support was received from the Purdue University Libraries Open Access Publishing Fund.

Acknowledgments

We also acknowledge the personnel and instrumentation in the University of Iowa Carver College of Medicine NMR Facility, supported by the Roy J. and Lucille A. Carver College of Medicine and grants from the Roy J. Carver Charitable Trust.

References

- Ahlijanian, M. K., and Cooper, D. M. (1987). Antagonism of calmodulin-stimulated adenylate cyclase by trifluoperazine, calmidazolium and W-7 in rat cerebellar membranes. *J. Pharmacol. Exp. Ther.* 241 (2), 407–414.
- Alda, M. (2019). Methylene blue in the treatment of neuropsychiatric disorders. *CNS Drugs* 33 (8), 719–725. doi:10.1007/s40263-019-00641-3
- Bernabucci, M., and Zhuo, M. (2016). Calcium activated adenylyl cyclase AC8 but not AC1 is required for prolonged behavioral anxiety. *Mol. Brain* 9 (1), 60. doi:10.1186/s13041-016-0239-x
- Bistas, E., and Sanghavi, D. (2020). *Methylene blue*. Treasure Island, FL: StatPearls.
- Brust, T. F., Alongkronrusmee, D., Soto-Velasquez, M., Baldwin, T. A., Ye, Z., Dai, M., et al. (2017). Identification of a selective small-molecule inhibitor of type 1 adenylyl cyclase activity with analgesic properties. *Sci. Signal.* 10 (467), eaah5381. doi:10.1126/scisignal.aah5381
- Chen, M., Suzuki, A., Thakkar, S., Yu, K., Hu, C., and Tong, W. (2016). DILIrank: The largest reference drug list ranked by the risk for developing drug-induced liver injury in humans. *Drug Discov. Today* 21 (4), 648–653. doi:10.1016/j.drudis.2016.02.015
- Chen, M., Vijay, V., Shi, Q., Liu, Z., Fang, H., and Tong, W. (2011). FDA-approved drug labeling for the study of drug-induced liver injury. *Drug Discov. Today* 16 (15–16), 697–703. doi:10.1016/j.drudis.2011.05.007
- Chen, T., O'Den, G., Song, Q., Koga, K., Zhang, M. M., and Zhuo, M. (2014). Adenylyl cyclase subtype 1 is essential for late-phase long term potentiation and spatial propagation of synaptic responses in the anterior cingulate cortex of adult mice. *Mol. Pain* 10, 65. doi:10.1186/1744-8069-10-65
- Cheng, Y., and Prusoff, W. H. (1973). Relationship between the inhibition constant (K_i) and the concentration of inhibitor which causes 50 per cent inhibition (I₅₀) of an enzymatic reaction. *Biochem. Pharmacol.* 22 (23), 3099–3108. doi:10.1016/0006-2952(73)90196-2
- Chuang, S. T., Papp, H., Kuczmog, A., Eells, R., Condor Capcha, J. M., Shehadeh, L. A., et al. (2022). Methylene blue is a nonspecific protein-protein interaction inhibitor with potential for repurposing as an antiviral for COVID-19. *Pharm. (Basel)* 15 (5), 621. doi:10.3390/ph15050621
- Corder, G., Doolen, S., Donahue, R. R., Winter, M. K., Jutras, B. L., He, Y., et al. (2013). Constitutive mu-opioid receptor activity leads to long-term endogenous analgesia and dependence. *Science* 341 (6152), 1394–1399. doi:10.1126/science.1239403
- Defer, N., Best-Belpomme, M., and Hanoune, J. (2000). Tissue specificity and physiological relevance of various isoforms of adenylyl cyclase. *Am. J. Physiol. Ren. Physiol.* 279 (3), F400–F416. doi:10.1152/ajprenal.2000.279.3.F400
- Dessauer, C. W., Watts, V. J., Ostrom, R. S., Conti, M., Dove, S., and Seifert, R. (2017). International union of basic and clinical Pharmacology. CI. Structures and small molecule modulators of mammalian adenylyl cyclases. *Pharmacol. Rev.* 69 (2), 93–139. doi:10.1124/pr.116.013078
- Ferguson, G. D., and Storm, D. R. (2004). Why calcium-stimulated adenylyl cyclases? *Physiol. (Bethesda)* 19, 271–276. doi:10.1152/physiol.00010.2004
- Gietzen, K., Wuthrich, A., and Bader, H. (1981). R 24571: A new powerful inhibitor of red blood cell Ca⁺⁺-transport ATPase and of calmodulin-regulated functions. *Biochem. Biophys. Res. Commun.* 101 (2), 418–425. doi:10.1016/0006-291x(81)91276-6
- Hayes, M. P., Soto-Velasquez, M., Fowler, C. A., Watts, V. J., and Roman, D. L. (2018). Identification of FDA-approved small molecules capable of disrupting the calmodulin-adenylyl cyclase 8 interaction through direct binding to calmodulin. *ACS Chem. Neurosci.* 9 (2), 346–357. doi:10.1021/acscchemneuro.7b00349
- Herbst, S., Masada, N., Pfennig, S., Ihling, C. H., Cooper, D. M., and Sinz, A. (2013). Structural insights into calmodulin/adenylyl cyclase 8 interaction. *Anal. Bioanal. Chem.* 405 (29), 9333–9342. doi:10.1007/s00216-013-7358-3
- How, H. Y., Khoury, J. C., and Sibai, B. M. (2009). Cervical dilatation on presentation for preterm labor and subsequent preterm birth. *Am. J. Perinatol.* 26 (1), 1–6. doi:10.1055/s-0028-1090586
- Kallewaard, J. W., Geurts, J. W., Kessels, A., Willems, P., van Santbrink, H., and van Kleef, M. (2016). Efficacy, safety, and predictors of intradiscal methylene blue injection for discogenic low back pain: Results of a multicenter prospective clinical series. *Pain Pract.* 16 (4), 405–412. doi:10.1111/papr.12283
- Kaur, J., Soto-Velasquez, M., Ding, Z., Ghanbarpour, A., Lill, M. A., van Rijn, R. M., et al. (2019). Optimization of a 1,3,4-oxadiazole series for inhibition of Ca(2+)/calmodulin-stimulated activity of adenylyl cyclases 1 and 8 for the treatment of chronic pain. *Eur. J. Med. Chem.* 162, 568–585. doi:10.1016/j.ejmech.2018.11.036
- Levin, L. R., and Reed, R. R. (1995). Identification of functional domains of adenylyl cyclase using *in vivo* chimeras. *J. Biol. Chem.* 270 (13), 7573–7579. doi:10.1074/jbc.270.13.7573
- Liauw, J., Wu, L. J., and Zhuo, M. (2005). Calcium-stimulated adenylyl cyclases required for long-term potentiation in the anterior cingulate cortex. *J. Neurophysiol.* 94 (1), 878–882. doi:10.1152/jn.01205.2004

Conflict of interest

The authors declare that the research was conducted in the absence of any commercial or financial relationships that could be construed as a potential conflict of interest.

Publisher's note

All claims expressed in this article are solely those of the authors and do not necessarily represent those of their affiliated organizations, or those of the publisher, the editors and the reviewers. Any product that may be evaluated in this article, or claim that may be made by its manufacturer, is not guaranteed or endorsed by the publisher.

Supplementary material

The Supplementary Material for this article can be found online at: <https://www.frontiersin.org/articles/10.3389/fphar.2022.977742/full#supplementary-material>

- Lubker, C., and Seifert, R. (2015). Effects of 39 compounds on calmodulin-regulated adenylyl cyclases AC1 and Bacillus anthracis edema factor. *PLoS One* 10 (5), e0124017. doi:10.1371/journal.pone.0124017
- Masada, N., Ciruela, A., Macdougall, D. A., and Cooper, D. M. (2009). Distinct mechanisms of regulation by Ca²⁺/calmodulin of type 1 and 8 adenylyl cyclases support their different physiological roles. *J. Biol. Chem.* 284 (7), 4451–4463. doi:10.1074/jbc.M807359200
- Masada, N., Schaks, S., Jackson, S. E., Sinz, A., and Cooper, D. M. (2012). Distinct mechanisms of calmodulin binding and regulation of adenylyl cyclases 1 and 8. *Biochemistry* 51 (40), 7917–7929. doi:10.1021/bi300646y
- Mou, T. C., Masada, N., Cooper, D. M., and Sprang, S. R. (2009). Structural basis for inhibition of mammalian adenylyl cyclase by calcium. *Biochemistry* 48 (15), 3387–3397. doi:10.1021/bi802122k
- Roldan, C. J., Nouri, K., Chai, T., and Huh, B. (2017). Methylene blue for the treatment of intractable pain associated with oral mucositis. *Pain Pract.* 17 (8), 1115–1121. doi:10.1111/papr.12566
- Sadana, R., and Dessauer, C. W. (2009). Physiological roles for G protein-regulated adenylyl cyclase isoforms: Insights from knockout and overexpression studies. *Neurosignals* 17 (1), 5–22. doi:10.1159/000166277
- Salman, A. E., Salman, M. A., Saricaoglu, F., Akinci, S. B., and Aypar, U. (2011). Pain on injection of propofol: A comparison of methylene blue and lidocaine. *J. Clin. Anesth.* 23 (4), 270–274. doi:10.1016/j.jclinane.2010.09.008
- Schaefer, M. L., Wong, S. T., Wozniak, D. F., Muglia, L. M., Liauw, J. A., Zhuo, M., et al. (2000). Altered stress-induced anxiety in adenylyl cyclase type VIII-deficient mice. *J. Neurosci.* 20 (13), 4809–4820. doi:10.1523/jneurosci.20-13-04809.2000
- Scott, J. A., Soto-Velasquez, M., Hayes, M. P., LaVigne, J. E., Miller, H. R., Kaur, J., et al. (2022). Optimization of a pyrimidinone series for selective inhibition of Ca(2+)/calmodulin-stimulated adenylyl cyclase 1 activity for the treatment of chronic pain. *J. Med. Chem.* 65 (6), 4667–4686. doi:10.1021/acs.jmedchem.1c01759
- Shiers, S., Elahi, H., Hennen, S., and Price, T. J. (2022). Evaluation of calcium-sensitive adenylyl cyclase AC1 and AC8 mRNA expression in the anterior cingulate cortex of mice with spared nerve injury neuropathy. *Neurobiol. Pain* 11, 100081. doi:10.1016/j.ynpai.2021.100081
- Simpson, R. E., Ciruela, A., and Cooper, D. M. (2006). The role of calmodulin recruitment in Ca²⁺ stimulation of adenylyl cyclase type 8. *J. Biol. Chem.* 281 (25), 17379–17389. doi:10.1074/jbc.M510992200
- Soto-Velasquez, M., Hayes, M. P., Alpsoy, A., Dykhuizen, E. C., and Watts, V. J. (2018). A novel CRISPR/Cas9-Based cellular model to explore adenylyl cyclase and cAMP signaling. *Mol. Pharmacol.* 94 (3), 963–972. doi:10.1124/mol.118.111849
- Strelow, J., Dewe, W., Iversen, P. W., Brooks, H. B., Radding, J. A., McGee, J., et al. (2004). “Mechanism of action assays for enzymes,” in *Assay guidance manual*. Editors S. Markossian, G. S. Sittampalam, A. Grossman, K. Brimacombe, M. Arkin, D. Auld, et al. (Bethesda, MD: Eli Lilly & Company).
- Vadakkan, K. I., Wang, H., Ko, S. W., Zastepa, E., Petrovic, M. J., Sluka, K. A., et al. (2006). Genetic reduction of chronic muscle pain in mice lacking calcium/calmodulin-stimulated adenylyl cyclases. *Mol. Pain* 2, 7. doi:10.1186/1744-8069-2-7
- Vorherr, T., Knopfel, L., Hofmann, F., Mollner, S., Pfeuffer, T., and Carafoli, E. (1993). The calmodulin binding domain of nitric oxide synthase and adenylyl cyclase. *Biochemistry* 32 (23), 6081–6088. doi:10.1021/bi00074a020
- Wang, H., Xu, H., Wu, L. J., Kim, S. S., Chen, T., Koga, K., et al. (2011). Identification of an adenylyl cyclase inhibitor for treating neuropathic and inflammatory pain. *Sci. Transl. Med.* 3 (65), 65ra3. doi:10.1126/scitranslmed.3001269
- Wei, F., Qiu, C. S., Kim, S. J., Muglia, L., Maas, J. W., Pineda, V. V., et al. (2002). Genetic elimination of behavioral sensitization in mice lacking calmodulin-stimulated adenylyl cyclases. *Neuron* 36 (4), 713–726. doi:10.1016/s0896-6273(02)01019-x
- Willoughby, D., and Cooper, D. M. (2007). Organization and Ca²⁺ regulation of adenylyl cyclases in cAMP microdomains. *Physiol. Rev.* 87 (3), 965–1010. doi:10.1152/physrev.00049.2006
- Zhang, J. H., Chung, T. D., and Oldenburg, K. R. (1999). A simple statistical parameter for use in evaluation and validation of high throughput screening assays. *J. Biomol. Screen.* 4 (2), 67–73. doi:10.1177/108705719900400206



OPEN ACCESS

EDITED BY
Rennolds S. Ostrom,
Chapman University, United States

REVIEWED BY
Muhammad Aslam,
University of Giessen, Germany
Ferenc Antoni,
University of Edinburgh,
United Kingdom

*CORRESPONDENCE
Hongbing Wang,
wangho@msu.edu

SPECIALTY SECTION
This article was submitted to
Experimental Pharmacology and
Drug Discovery,
a section of the journal
Frontiers in Pharmacology

RECEIVED 20 May 2022
ACCEPTED 05 September 2022
PUBLISHED 16 September 2022

CITATION
Chen J, Ding Q, An L and Wang H
(2022), Ca^{2+} -stimulated adenylyl
cyclases as therapeutic targets for
psychiatric and
neurodevelopmental disorders.
Front. Pharmacol. 13:949384.
doi: 10.3389/fphar.2022.949384

COPYRIGHT
© 2022 Chen, Ding, An and Wang. This is
an open-access article distributed
under the terms of the [Creative
Commons Attribution License \(CC BY\)](#).
The use, distribution or reproduction in
other forums is permitted, provided the
original author(s) and the copyright
owner(s) are credited and that the
original publication in this journal is
cited, in accordance with accepted
academic practice. No use, distribution
or reproduction is permitted which does
not comply with these terms.

Ca^{2+} -stimulated adenylyl cyclases as therapeutic targets for psychiatric and neurodevelopmental disorders

Jiao Chen, Qi Ding, Lulu An and Hongbing Wang*

Department of Physiology, Michigan State University, East Lansing, MI, United States

As the main secondary messengers, cyclic AMP (cAMP) and Ca^{2+} trigger intracellular signal transduction cascade and, in turn, regulate many aspects of cellular function in developing and mature neurons. The group I adenylyl cyclase (ADCY, also known as AC) isoforms, including ADCY1, 3, and 8 (also known as AC1, AC3, and AC8), are stimulated by Ca^{2+} and thus functionally positioned to integrate cAMP and Ca^{2+} signaling. Emerging lines of evidence have suggested the association of the Ca^{2+} -stimulated ADCYs with bipolar disorder, schizophrenia, major depressive disorder, post-traumatic stress disorder, and autism. In this review, we discuss the molecular and cellular features as well as the physiological functions of ADCY1, 3, and 8. We further discuss the recent therapeutic development to target the Ca^{2+} -stimulated ADCYs for potential treatments of psychiatric and neurodevelopmental disorders.

KEYWORDS

autism, Ca^{2+} -stimulated adenylyl cyclase, bipolar disorder, schizophrenia, major depressive disorder, post-traumatic stress disorder, therapeutics

Introduction

Adenylyl cyclase (ADCY) activity accounts for the basal level as well as activity-dependent production of cAMP, which is a main second messenger and regulates a wide spectrum of intracellular signaling molecules (Figure 1). In the nervous system, extracellular stimuli lead to functional responses and activity-dependent plasticity through the activation of surface neurotransmitter receptors followed by activation/inhibition of intracellular signaling molecules. With its enzymatic activity directly regulated by the G protein coupled neurotransmitter receptors (GPCR) on cell membrane, ADCY contributes to the dynamic intracellular cAMP transient following extracellular stimulation. The outcome of the cAMP-mediated signal transduction has broad impact on cellular functions including gene transcription and translation (Figure 1), the precise regulation of which is essential for neurodevelopment and activity-dependent modification of neuronal function. Thus, it is envisioned that appropriate ADCY activity is critical for neurodevelopment and neuroplasticity. Further, in addition to GPCRs, many other intracellular signaling molecules also

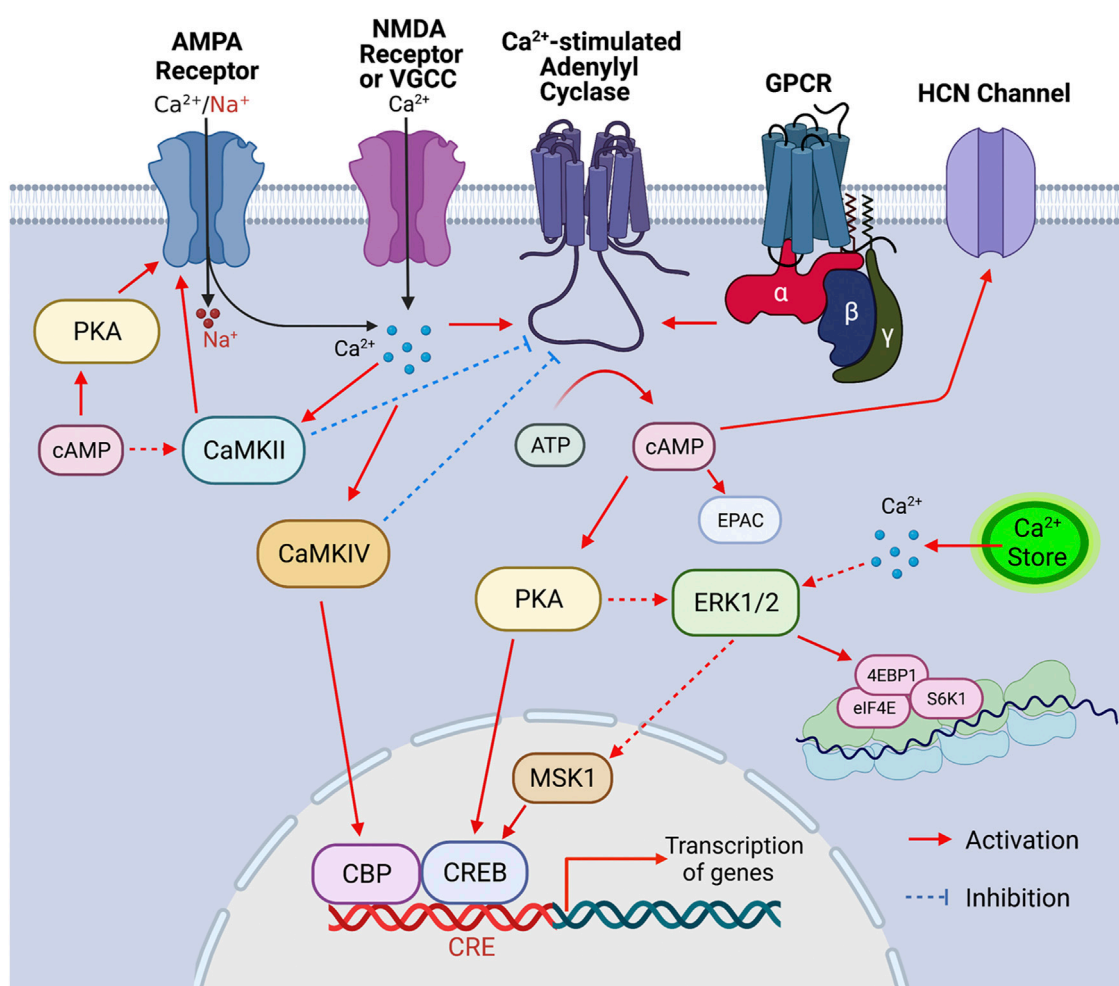


FIGURE 1

Signaling cascade triggered by the activation of Ca^{2+} -stimulated ADCYs. Upon the activation of GPCR, Ca^{2+} influx through Ca^{2+} channels (such as VGCC, NMDAR, and Ca^{2+} -permeable AMPAR) and/or Ca^{2+} release from internal store, the Ca^{2+} -stimulated ADCYs are activated, leading to increased production of cAMP. The upregulation of cAMP activates PKA, which causes phosphorylation of CREB, ERK_{1/2} (indirectly), CaMKII (indirectly) and GluR1 (at S845), leading to activation of these molecules. Increase of intracellular Ca^{2+} leads to activation of ERK_{1/2} (indirectly), CaMKII, and CaMKIV, which, in turn, activate MSK1/CREB, GluR1 phosphorylation (at S831), and CBP (CREB binding protein), respectively. The activated CBP/CREB triggers CRE (cAMP responsive element)-mediated gene transcription. The ERK_{1/2}-mediated activation of eIF4E, 4EBP1, and S6K1 may enhance ribosome activity and lead to increase of protein translation. The Ca^{2+} -stimulated CaMKIV and CaMKII may lead to feedback inhibition of ADCY1 and ADCY3, respectively. Other main aspects of cAMP effect include the cAMP-mediated EPAC (exchange protein directly activated by cAMP) activation and cAMP-facilitated opening of the HCN (hyperpolarization-activated cyclic nucleotide-gated) channels.

dynamically regulate ADCY activity (Figure 1), leading to fine tuning of cAMP signaling in a task-specific manner. With regards to their physiological function, specific isoforms of ADCY have been shown to regulate distinct aspects of neuroplasticity and behavior that are essential for survival and adaptation. Emerging lines of animal study and human genome data have also suggested association of ADCY with a variety of dysfunction in the central nervous system (CNS) and the peripheral systems.

To date, ten isoforms of mammalian ADCY have been identified. Nine ADCYs (i.e., ADCYs 1-9) are membrane-

bound proteins and share similar structures with a short N-terminal cytoplasmic domain (the C1 domain) two transmembrane domains (i.e., TM1 and TM2) connected by the C1 cytoplasmic loop, and the C2 cytoplasmic domain at the C-terminus (Cooper, 2003) (Figure 1). Through the C1 and C2 domains, ADCYs 1-9 confer the catalytic activity and can be regulated by GPCRs and intracellular protein kinases and phosphatases (Cooper, 2003) (Figure 1). Based on structure and regulatory properties, five groups of ADCY are defined. In general, the group I ADCYs includes ADCY1, 3, and 8. They are stimulated by G_s and Ca^{2+} and inhibited by G_i . The group II

ADCYs include ADCY2, 4, and 7. They are stimulated by G_s and not responsive to Ca^{2+} and G_i . The group III ADCYs include ADCY5 and 6. They are stimulated by G_s and inhibited by Ca^{2+} and G_i . The group IV ADCY includes ADCY9, which is only stimulated by G_s and, unlike other ADCYs, not responsive to the general ADCY activator forskolin. The group V ADCY includes ADCY10, which is a structurally distinct soluble cytoplasmic protein whose activity is regulated by Ca^{2+} and bicarbonate but not GPCRs (Buck et al., 1999; Litvin et al., 2003; Kleinboelting et al., 2014). ADCY10 is mainly expressed in the liver and testes but not in the central nervous system. Among these ADCYs, the group I Ca^{2+} -stimulated ADCYs are functionally positioned to couple the two main small molecule messengers Ca^{2+} and cAMP in neurons (Figure 1). Human genetic studies and animal models suggest emerging roles of the Ca^{2+} -stimulated ADCYs in regulating distinct aspects of pathology in psychiatric disorders. In this review, we focus on the Ca^{2+} -stimulated ADCYs and discuss their potential as therapeutic targets to treat neurodevelopment and psychiatric disorders.

Regulation and molecular targets of the Ca^{2+} -stimulated adenylyl cyclases

Regulation by Ca^{2+} and G proteins

The existence of the calmodulin (CaM)-binding domain in the C1 or C2 region of some ADCYs suggests that certain isoforms can be regulated by Ca^{2+} (Wang and Storm, 2003). Affinity purification with the CaM-sepharose chromatography aided the cloning of ADCY1 followed by discovering other CaM-binding ADCYs (Krupinski et al., 1989). Among all the Ca^{2+} -sensitive ADCYs, the group I isoforms consists of the Ca^{2+} -stimulated ADCY1, ADCY3 and ADCY8 (Cooper, 2003). As cAMP and Ca^{2+} are the main second messengers in neurons, it is postulated and the Ca^{2+} -stimulated ADCYs are at the converging hub to integrate the cAMP and Ca^{2+} signaling (Figure 1).

ADCY1 activity is stimulated by Ca^{2+} (Tang et al., 1991) with an EC₅₀ of ~100 nM (Fagan et al., 1996), which is slightly lower than the free Ca^{2+} level in resting neurons (Berridge et al., 2003). This indicates that ADCY1 is constitutively stimulated by the basal Ca^{2+} in resting neurons and further activated by transient increase of Ca^{2+} in stimulated neurons. Distinct amino acid mutations in the CaM-binding domain either reduce or abolish the Ca^{2+} stimulation of ADCY1 (Wu et al., 1993). Although GTPγS can directly increase ADCY1 activity (Tang et al., 1991), G_{as} only stimulates ADCY1 in the presence of Ca^{2+} (Wayman et al., 1994); G_{ai} (Nielsen et al., 1996) and $G_{\beta\gamma}$ (Tang et al., 1991) cause inhibition of ADCY1. Intriguingly, CaMKIV (CaM-dependent kinase IV) can directly phosphorylate ADCY1, leading to activity inhibition (Wayman et al., 1996). It is conceivable that, depending on subcellular micro-environment, Ca^{2+} /CaM may exert dichotomy effects on

ADCY1. While Ca^{2+} may predominantly stimulate ADCY1 in sub-cellular regions that are devoid of CaMKIV, a compromised or even inhibitory effect may be observed in the CaMKIV-enriched regions. CaMKIV may also function as a molecular break to prevent over-stimulation of ADCY1 by sustained Ca^{2+} elevation (Figure 1).

ADCY3 shares the most structural similarity with ADCY1 and ADCY8. However, *in vitro* assays with membrane preparation reveal that Ca^{2+} alone is not sufficient to stimulate ADCY3 activity (Choi et al., 1992; Wayman et al., 1995). When paired with the general ADCY activator forskolin or G protein activator GppNHp, high level of Ca^{2+} stimulates ADCY3 with an EC₅₀ of ~5,000 nM (Choi et al., 1992). Considering that the intracellular Ca^{2+} varies in the 1–10,000 nM range (Smith and Augustine, 1988), Ca^{2+} stimulation of ADCY3 may occur in specific subcellular domains with high Ca^{2+} transients in stimulated neurons. Notably, Wayman et al. found that, in the presence of GppNHp or glucagon, Ca^{2+} at a much lower concentration (e.g., 200 nM) can cause ~2-fold increase of ADCY3 activity *in vitro* (Wayman et al., 1995). Counterintuitively, cAMP accumulation assay with live cells reveal that increase of intracellular Ca^{2+} (at ~100–300 nM) significantly inhibits hormone- and G_{as} -stimulated ADCY3 *in vivo* (Wayman et al., 1995). It is further identified that CaMKII (CaM-dependent protein kinase II) phosphorylates and inhibits ADCY3, suggesting an indirect inhibition effect of Ca^{2+} (Wei et al., 1996) (Figure 1). Although the physiological relevance of the Ca^{2+} -stimulated regulation of ADCY3 remains to be elucidated, the Ca^{2+} /CaMKII-mediated inhibition is likely to ensure a transient rather than persistent increase of cAMP increase in olfactory cilia, leading to the temporal attenuation of sensation following odor detection (Wei et al., 1998).

ADCY8 possesses a CaM-binding domain and is directly stimulated by Ca^{2+} with an EC₅₀ of ~500–800 nM (Fagan et al., 1996; Nielsen et al., 1996). Considering that ADCY8 is moderately sensitive to Ca^{2+} , it is speculated that Ca^{2+} released from the internal store may not be sufficient to stimulate ADCY8. However, Martin et al. (2009) suggest that the capacitative Ca^{2+} entry (CCE), which is triggered by Ca^{2+} depletion from the internal store, may lead to more robust Ca^{2+} increase and stimulate ADCY8. In the non-neuronal HEK293 cells, when ADCY8 and the CCE functional molecules STIM1 and Orai1 are over-expressed, they colocalize in lipid raft domains of the cell membrane. Functionally, while Ca^{2+} store depletion alone fails to activate ADCY8, over-expression of STIM1 and Orai1 along with Ca^{2+} store depletion leads to ADCY8 activation (Martin et al., 2009). Given that there is high expression level of STIM and Orai isoforms in the central nervous system (e.g., STIM2 and Orai2 in hippocampus), it is likely that CCE activates ADCY8 as well as ADCY1 and ADCY3 in neurons (Zhang and Hu, 2020). *In vitro* assays with membrane preparations from ADCY8-expressing HEK293 cells detect that the Ca^{2+} -stimulated

ADCY activity can be further increased in the presence of activated G_{as} (i.e., GTP γ S bound G_{as}) (Cali et al., 1994). However, the *in vivo* cAMP accumulation assay fails to detect any effect in HEK293 cells following pharmacological activation of the G_s -coupled adrenergic receptors (Cali et al., 1994; Nielsen et al., 1996). Further, the *in vivo* cAMP accumulation assay with the ADCY8-expressing HEK293 cells fails to detect the inhibition effects following the activation of the G_i -coupled somatostatin and dopaminergic receptors (Nielsen et al., 1996). Thus, these lines of evidence suggest that ADCY8 is exclusively regulated by Ca^{2+} but not by G proteins *in vivo*. However, overexpression of a constitutively active $G_{\alpha/olf}$ causes robust activation of both ADCY1 and ADCY8 (Regnaud et al., 2002). Regarding whether and how GPCRs can regulate ADCY8 activity, examination with neurons (rather than the heterologous HEK293 cells) and activation of full spectrum of GPCRs (in addition to adrenergic, dopaminergic and somatostatin receptors) is required.

Molecular targets

Through the Ca^{2+} -stimulated ADCYs, cAMP and Ca^{2+} signaling may converge and tune specific signaling networks and, in turn, regulate cellular functions relevant to neurotransmitter receptor activity, gene transcription, and translation (Figure 1). With regards to the function of Ca^{2+} -stimulated ADCYs in neuroplasticity, neurodevelopment and psychiatric disorders, we focus on the Ca^{2+} /cAMP-PKA (cAMP-dependent protein kinase)/ERK $_{1/2}$ (extracellular signal-regulated kinases 1/2)-MSK1 (mitogen- and stress-activated protein kinase-1)-CREB (cAMP responsive element binding protein), the Ca^{2+} /cAMP-ERK $_{1/2}$ -eIF4E (eukaryotic translation initiation factor 4E)/4EBP1 (Eukaryotic translation initiation factor 4E-binding protein 1)/S6K1 (ribosome protein S6 kinase 1), and the Ca^{2+} /cAMP-PKA/CaMKII-GluR1 (glutamate ionotropic AMPA type subunit 1) cascades (Figure 1).

The definitive function of ADCY1 and ADCY8 in regulating the Ca^{2+} /cAMP-mediated signaling is mainly examined with brain samples collected from mutant mice. The Ca^{2+} -stimulated ADCY activity is reduced by ~50% and ~30% in the hippocampus of *Adcy1* knockout (KO) and *Adcy8* KO mice, respectively (Wong et al., 1999). The cAMP level is reduced by ~25% in the *Adcy1* KO hippocampus (Sethna et al., 2017). Although lack of both ADCY1 and ADCY8 surprisingly increases the basal ERK1/2 activity, the contextual fear learning- and cocaine-triggered upregulation of the ERK $_{1/2}$ -MSK1-CREB signaling is abolished in the *Adcy1/Adcy8* double knockout (DKO) mice (Sindreu et al., 2007; DiRocco et al., 2009). The *Adcy1/Adcy8* DKO mice also do not display diurnal oscillation of ERK $_{1/2}$ phosphorylation in the hippocampus (Eckel-Mahan et al., 2008), suggesting lack of molecular circadian rhythm. In primary cortical neurons,

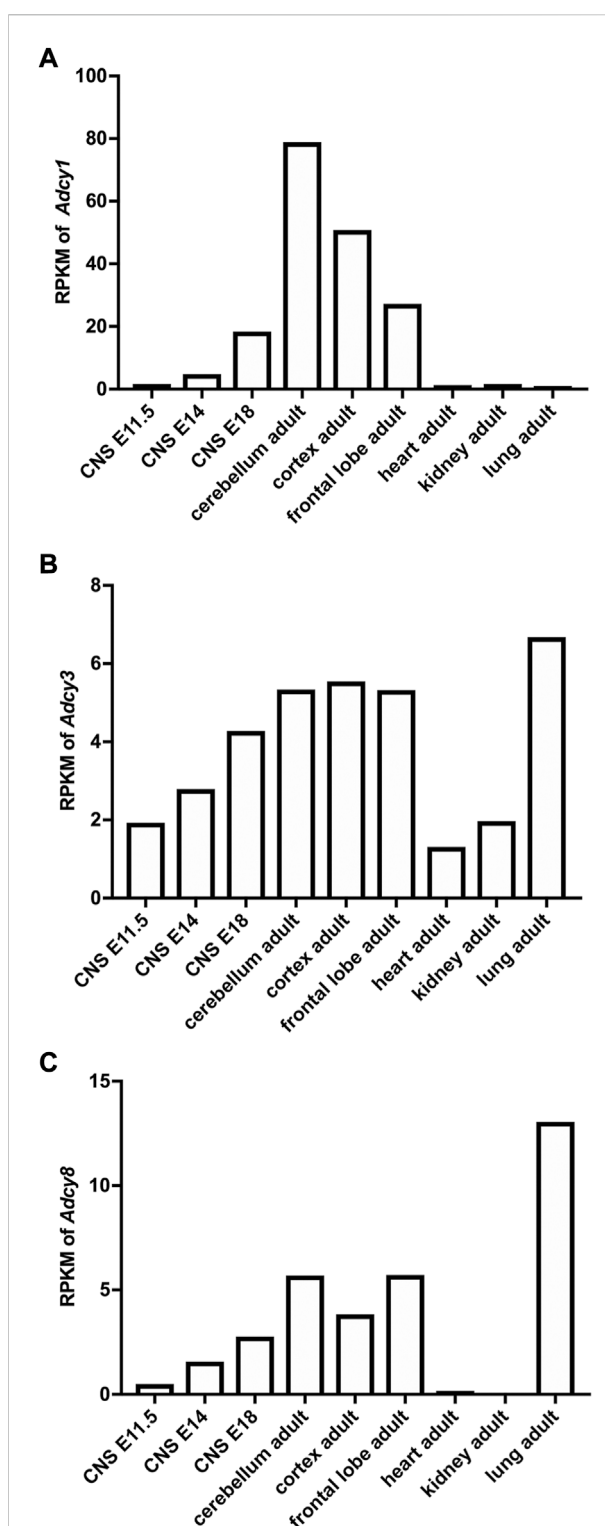


FIGURE 2

Developmental and tissue-specific expression of Ca^{2+} -stimulated *Adcy* mRNA transcripts in mouse. The RNAseq study by the Mouse ENCODE Consortium (Yue et al., 2014) revealed the expression of *Adcy1* (A), *Adcy3* (B), and *Adcy8* (C) mRNA in different tissues and in CNS at different developmental stages. RPKM: Reads Per kilobase of transcript per Million mapped reads. CNS: central nervous system. E11.5, E14, and E18: embryonic day 11.5, 14, and 18.

ADCY1 deficiency impairs the glutamate-induced upregulation of CREB activity (Wang et al., 2007). Consistent with the function of ERK_{1/2}-CREB in regulating the Ca²⁺/CRE (cAMP-responsive element)-mediated transcription of *bdnf* (brain-derived neurotrophic factor) (Zheng et al., 2011), mice lacking ADCY1 and ADCY8 fail to show learning- and exercise-induced up-regulation of *bdnf* mRNA (Zheng et al., 2012; Zheng et al., 2016). Conversely, overexpression of ADCY1 results in increase of Ca²⁺-stimulated ADCY activity, cAMP level, PKA activity, and basal as well as learning-induced upregulation of ERK_{1/2}-CREB activity in the hippocampus (Wang et al., 2004). Overexpression of ADCY1 also blocks the stress-induced downregulation of *bdnf* transcription in hippocampus and prefrontal cortex (Yang et al., 2020).

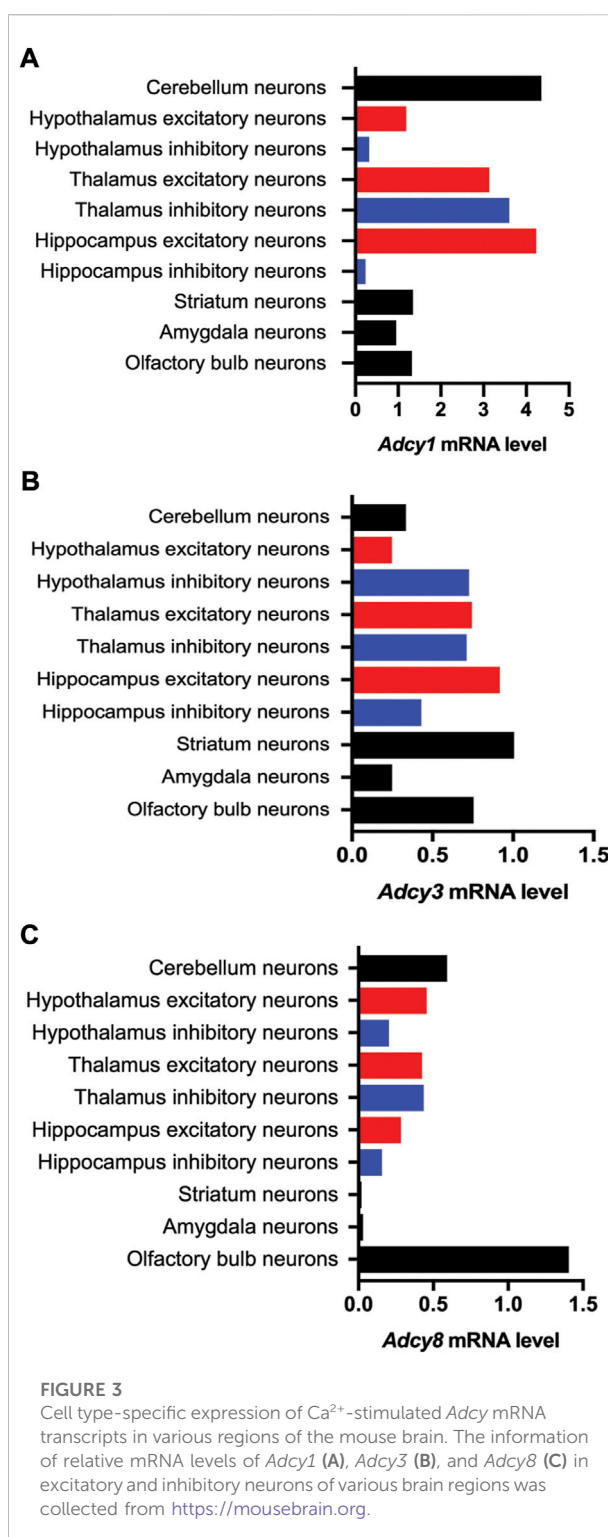
With regards to gene expression, the cAMP-regulated ERK_{1/2} may impinge on ribosome activity and, in turn, regulate protein synthesis. *In vitro* and *in vivo* studies demonstrate that inhibition of ERK_{1/2} leads to impairments of activity-dependent upregulation of eIF4E, 4EBP1, and S6K1 phosphorylation (Kelleher et al., 2004; Zhou et al., 2010). Inhibition of ERK_{1/2} also suppresses various forms of protein synthesis-dependent synaptic plasticity (Gallagher et al., 2004; Kelleher et al., 2004). Whether and how the Ca²⁺-stimulated ADCYs regulate basal and activity-dependent changes of ribosome activity remain to be determined.

The cAMP signaling may also regulate neuronal function on cell surface. Two main phosphorylation sites (i.e., Serine 845 and 831) of GluR1 are targets of PKA and CaMKII/PKC (protein kinase C), respectively (Figure 1), and functionally involved to regulate receptor trafficking and channel conductance (Malinow, 2003). The phosphorylation of GluR1 at S845 and S831 is dynamically altered after the induction of long-term potentiation (LTP), long-term depression (LTD), and synaptic depotentiation (Lee et al., 2000; Huang et al., 2001). Although S831 phosphorylation can be suppressed by PKC and CaMKII inhibitors, it may also be regulated indirectly through the cAMP-enhanced CaMKII activation (Makhinson et al., 1999). In mice with a natural loss-of-function mutation in *Adcy1*, phosphorylation of GluR1 (pGluR1) at S845, AMPAR-mediated EPSCs, and surface GluR1 are decreased at the thalamocortical synapses (Lu et al., 2003).

Expression pattern and cellular function of the Ca²⁺-stimulated adenylyl cyclases

Adenylyl cyclase1

The mRNA transcript of *Adcy1*, detected by Northern blot and *in situ* hybridization, is predominantly expressed in the nervous system tissues including brain, adrenal gland, and retina (Figure 2A) (Xia et al., 1993; Yue et al., 2014). Within the central



nervous system (CNS), *Adcy1* mRNA expression is developmentally regulated (Figure 2A) and detected in distinct regions at various levels (Figures 2A, 3A) (Yue et al., 2014) (<https://brainrnaseq.org>). Notably, *Adcy1* mRNA level is

overwhelmingly higher in excitatory neurons than inhibitory neurons in the hippocampus but not in other regions (Figure 3A). Although RNA-sequencing has detected *Adcy1* mRNA in neurons and glial cells (<https://brainrnaseq.org>), Western blot with a validated antibody (Sethna et al., 2017) detects ADCY1 protein expression only in neuron-enriched but not glial cell-enriched primary cultures (Ding et al., 2020).

The subcellular distribution of endogenous ADCY1, due to the lack of antibody for histochemistry, is largely unknown. With expression of the epitope-tagged recombinant protein, it is found that the HA (hemagglutinin)-ADCY1 is expressed in both dendrite and axon. The punctate and discrete HA-ADCY1 colocalizes with synaptophysin and synapsin I in cerebellar neurons, indicating enrichment in the synaptic compartment (Wang et al., 2002). Western blot analysis with synaptosome fractions detects that the endogenous ADCY1 in hippocampus is enriched in postsynaptic density and extrasynaptic fractions (Conti et al., 2007).

Consistent with the high expression level of *Adcy1* mRNA in cortex, hippocampus, and cerebellum, studies with the *Adcy1* KO mice have found that activity-dependent potentiation of synaptic efficacy in these brain regions requires ADCY1 (Storm et al., 1998; Liauw et al., 2005; Zheng et al., 2016). It is also evident that ADCY1 supports long-term potentiation (LTP) at both presynaptic (Villacres et al., 1998; Miao et al., 2019) and postsynaptic sites (Liauw et al., 2005; Zheng et al., 2016). It is demonstrated that ADCY1 in presynaptic neurons is required for sensory input and neurodevelopment of postsynaptic neurons. Brain region-specific knockout of *Adcy1* in thalamus causes disruptive barrel patterning in layer 4 of the somatosensory cortex (Suzuki et al., 2015). Further, ADCY1 deficiency in the presynaptic RGC (retinal ganglion cell) causes map disruption of the postsynaptic tissues SC (superior colliculus) and LGN (lateral geniculate nucleus) (Dhande et al., 2012).

Adenylyl cyclase3

ADCY3 was initially identified as the major ADCY in olfactory epithelium (Bakalyar and Reed, 1990). Following the molecular cloning of *Adcy3* gene, Northern blot and semiquantitative RT-PCR detected broad expression of the *Adcy3* mRNA in both CNS and peripheral tissues (Xia et al., 1992; Yang et al., 1999; Yue et al., 2014) (Figure 2B). The expression level is high in brain, placenta, lung, and skeletal muscle. Intermediate expression is detected in heart, kidney, and pancreas (Yang et al., 1999; Yue et al., 2014). Within the CNS, *Adcy3* mRNA and ADCY3 protein are found in many brain regions, including olfactory bulb, cortex, hippocampus, amygdala, nucleus accumbens, thalamus, hypothalamus and cerebellum (Bishop et al., 2007) (Figures 2B, 3B). It is expressed in both excitatory and inhibitory neurons (Figure 3B) as well as in glia cells (Bishop et al., 2007).

Interestingly, *Adcy3* mRNA level is higher in inhibitory neurons than excitatory neurons in hypothalamus (Figure 3B).

Within the olfactory epithelium, ADCY3 is predominantly localized in olfactory cilia, which is the main organelle of sensory neuron to conduct the sensation of smell. Upon activation of the G_{olf} -coupled odorant receptors, cAMP is generated by the G_{olf} -activated ADCY3. Binding of cAMP to the cyclic nucleotide-gated (CNG) channels causes the influx of Na^+ and Ca^{2+} , leading to sensory neuron activation and the subsequent olfactory detection process. Deficiency of ADCY3, which is the only ADCY in olfactory cilia, causes anosmia (i.e., loss of smell) (Wong et al., 2000).

In brain neurons, ADCY3 is localized in the primary cilium (Bishop et al., 2007), which is a solitary microtubule-based 2–12 μm projection from the cell surface. In contrast to typical synaptic structures, primary cilia are devoid of ionotropic neurotransmitter receptors and thought to mediate neuronal signaling via metabotropic GPCRs (Green and Mykityn, 2014). The co-existence of ADCY3 and certain GPCRs (e.g., melanocortin 4 receptor, somatostatin receptor 3, and type 6 serotonin receptor) suggests activity-dependent cAMP signaling in primary cilia (Wang et al., 2011b; Guadiana et al., 2013; Siljee et al., 2018). Although how cilia signaling affects neuronal function is largely unknown, disruption of the cilia-enriched proteins causes alteration of neuron development and synaptic function. Notably, ADCY3 deficiency leads to reduced dendritic outgrowth and arborization, hippocampus atrophy, reduced neural transmission and impaired LTP at the schaffer collateral-CA1 synapses (Chen et al., 2016).

Adenylyl cyclase8

Adcy8 is expressed in both the CNS and the peripheral non-neuronal tissues (Muglia et al., 1999; Yue et al., 2014) (Figure 2C). Within the CNS, *Adcy8* mRNA shows the highest levels in olfactory bulb, thalamus, hypothalamus and brain stem (Muglia et al., 1999; Schaefer et al., 2000) (Figure 3C). In these brain regions, ADCY8 but not ADCY1 accounts for most of the Ca^{2+} -stimulated ADCY activity. In olfactory bulb and hypothalamus of the *Adcy8* KO mice, there is no significant Ca^{2+} -stimulated upregulation of ADCY activity (Schaefer et al., 2000). Moderately high level of *Adcy8* mRNA is detected in hippocampus, in which ADCY8 deficiency causes ~25% reduction of Ca^{2+} -stimulated ADCY activity (Schaefer et al., 2000). In contrast to *Adcy1* mRNA, robust *Adcy8* mRNA is detected in both excitatory and inhibitory neurons in hippocampus (Figure 3C). This suggests that the Ca^{2+} -stimulated cAMP signaling may be co-regulated by ADCY1 and ADCY8 in excitatory neurons, and predominantly regulated by ADCY8 in inhibitory neurons in the hippocampus.

The subcellular distribution of ADCY8 has been examined with neurons expressing the recombinant HA-ADCY8. The HA-ADCY8 displays punctate staining in both dendrites and axons of cortical and hippocampal neurons and colocalizes with both presynaptic (i.e., synaptophysin and synapsin I) and postsynaptic marker (i.e., PSD95) proteins (Wang et al., 2003). The endogenous hippocampal ADCY8 is preferentially enriched in the presynaptic active zone and also detected in extrasynaptic fractions (Conti et al., 2007). The presynaptic cellular function of ADCY8 is implicated by that the mossy fiber-CA3 LTP, which mainly relies on presynaptic Ca^{2+} /cAMP signaling, is defective in the *Adcy8* KO mice (Wang et al., 2003). The postsynaptic function of ADCY8 is implicated by that the schaffer collateral-CA1 LTD (long-term depression) is defective in the *Adcy8* KO mice (Schaefer et al., 2000).

Association of the Ca^{2+} -stimulated adenylyl cyclases with psychiatric and neurodevelopment disorders

Alteration of Ca^{2+} /cAMP-mediated signaling has been detected as molecular outcomes that are associated with various aspects of psychiatric and neurodevelopment disorders. Within the Ca^{2+} /cAMP signaling network (Figure 1), abnormal function of GPCR (Grace, 2016), ion channel (Lee et al., 2016; Zanos and Gould, 2018; Nakazawa and Sapkota, 2020), and protein kinase (Wang et al., 2012; Robison, 2014; Gross et al., 2019) is associated with distinct malfunction and maladaptation of the brain. Here, we discuss the emerging roles of Ca^{2+} -stimulated ADCY as risk and causal factors in regulating the cellular pathology and behavioral symptoms associated with psychiatric and neurodevelopment disorders.

Adenylyl cyclase1

Hyper-expression of ADCY1 has been identified in a mouse model of Fragile X syndrome (FXS) (Sethna et al., 2017), which is predominantly caused by mutations in the *FMR1* (Fragile X messenger ribonucleoprotein 1) gene and deficient expression of its gene product FMRP (FMR1 protein). FXS is a neurodevelopment disorder and leading cause of intellectual disability and autism (Sethna et al., 2014). Among various functions of FMRP (Richter and Zhao, 2021), the RNA binding activity has been demonstrated to be directly related to the main symptoms in FXS. High-throughput screenings have revealed that FMRP binds 800–6,000 distinct mRNA targets and may suppress their translation (Brown et al., 2001; Darnell et al., 2011; Ascano et al., 2012). Along with general elevation of mRNA translation, abnormally increased expression of

specific FMRP targets is linked to exaggerated signaling in FXS neurons (Wang et al., 2012; Gross et al., 2015). Mining and analysis of the multiple high-throughput screening data identified *Adcy1* mRNA as a top-ranked FMRP target. Consistently, ADCY1 protein expression level is abnormally higher in the brain of *Fmr1* knockout (KO) mice (Sethna et al., 2017). The enhanced ADCY1 expression is associated with the exaggerated $\text{ERK}_{1/2}$ /PI3K (phosphoinositide 3-kinases)-S6K1 signaling in FXS (Wang et al., 2012; Gross et al., 2015). The causal function of the elevated ADCY1 expression is supported by that genetic reduction of ADCY1 in the *Fmr1* KO mice rescues the key aspects of pathology, including the exaggerated overall protein synthesis and $\text{ERK}_{1/2}$ /PI3K-S6K1 activity, higher dendritic spine density, audiogenic seizure, repetitive behavior and social deficits (Sethna et al., 2017). Interestingly, enhanced ADCY1 expression also results in certain behavioral abnormalities associated with FXS and autism. Forebrain overexpression of ADCY1 in transgenic mice causes hyper locomotion and social deficits (Chen et al., 2015).

Alteration of *Adcy1* gene, as suggested by the human genome-wide association study (GWAS), is a potential genetic risk factor for schizophrenia (Sundararajan et al., 2018). A recent study analyzed a combined list of schizophrenia-risk genes that are collected from published GWAS data, meta-analysis data, and the OMIM and GeneCards databases (Butler et al., 2016a; Butler et al., 2016b; Wu et al., 2017). By using the GeneAnalytics program, Sundararajan et al. (2018) suggest that the schizophrenia genes have significant impact on Ca^{2+} signaling pathway, CREB pathway, and monoamine GPCRs. Integration analysis of the schizophrenia gene and the phenotype database (<http://www.informatics.jax.org/>; <http://human-phenotype-ontology.github.io/>) identifies an association of schizophrenia genes with reduced LTP, abnormal spatial learning, and neurodevelopment (Sundararajan et al., 2018). Based on biochemical data and functional studies with mutant mice, it is evident that ADCY1 directly regulates the CREB pathway and integrates Ca^{2+} and GPCR signaling. Although how ADCY1 regulates the hallmark schizophrenia symptoms remains unclear, ADCY1 deficiency leads to impaired LTP (Villacres et al., 1998; Zheng et al., 2016) and spatial memory (Wu et al., 1995) and maldevelopment of the sensory cortex (Suzuki et al., 2015). It is interesting to note that ADCY1 shows high level in cerebellum, cerebral cortex, and thalamus, which are where the schizophrenia risk genes predominantly express (Sundararajan et al., 2018). As defective cortico-cerebellar-thalamic-cortical circuit is suggested as an emerging etiological factor for schizophrenia (Andreassen and Pierson, 2008; Dorph-Petersen and Lewis, 2017), the region-specific function of ADCY1 needs to be studied.

Alterations of *Adcy1* gene may affect the therapeutic efficacy of lithium in bipolar disorder (International Consortium on Lithium Genetics et al., 2018). Although bipolar disorder and schizophrenia shares significant number of genetic risk factors, patient responses to pharmacological interventions are dramatically different. While the mood stabilizer lithium is used as the first line medication in bipolar disorder, it is not effective for schizophrenia patients. Further, a significant population of bipolar disorder patients also does not show therapeutic outcome following lithium treatment. A cross-trait meta-analysis of the GWAS of schizophrenia and Consortium on Lithium Genetics has found an interesting reverse association of polygenic schizophrenia load and lithium response in bipolar disorder (International Consortium on Lithium Genetics et al., 2018). Bipolar disorder patients with low polygenic schizophrenia load show better therapeutic response to lithium. Regarding whether and how ADCY1 activity impinges on pharmacological and molecular outcome of lithium treatment, validations with *in vitro* cellular assays and *in vivo* behavioral examinations may be needed. With the available ADCY1 inhibitors and mouse models (e.g., the *Adcy1* KO and overexpression mice), it is feasible to detect whether the lithium effects are attenuated or potentiated.

Adenylyl cyclase3

Although there are debates on the significance of genetic risk factors in human major depressive disorder, a GWAS study with 2,431 major depressive disorder and 3,673 control samples revealed a suggestive association of *Adcy3* polymorphism with depression (Wray et al., 2012). Notably, lower PKA expression and ADCY activity (Perez et al., 2001; Hines et al., 2005) in platelets, which express only *Adcy3* but not other *Adcy* isoforms (Katsel et al., 2003), are detected in major depressive disorder subjects and attenuated by the use of various drugs including antidepressants, analgesics, and addictive drugs (Hines et al., 2005). Consistently, *Adcy3* mRNA level is reduced in the blood samples of major depressive disorder (Redei et al., 2014). Brain transcriptome analysis of human postmortem samples has also found altered level of *Adcy3* transcript in autism spectrum disorder (Guan et al., 2019).

The functional relevance of *Adcy3* mutations to major depressive disorder and autism spectrum disorder has been examined with the KO and knock-in mice. The conventional whole body *Adcy3* KO mice display a wide spectrum of symptoms including increased REM (rapid eye movement) sleep, hypo-locomotion, neophobia, higher immobility in the tail suspension and forced swimming test, impaired nesting behavior and impaired sociability (Chen et al., 2016). The forebrain-specific pyramidal neuron conditional *Adcy3* KO mice recapitulates many aspects of the major depressive disorder- and autism spectrum disorder-associated

symptoms, but intriguingly display normal social interaction (Chen et al., 2016). The conventional and the conditional forebrain-specific *Adcy3* KO mice show defective spatial memory and object recognition memory (Wang et al., 2011b; Chen et al., 2016). Whole body *Adcy3* deficiency also causes impairments in passive avoidance memory and fear memory extinction (Wang et al., 2011b). Intriguingly, the region-specific knock-down of *Adcy3* in the main olfactory epithelium not only leads to anosmia but also causes depression-like behavior (Liu et al., 2020a) and cognitive defects (Liu et al., 2020b). The results suggest a role of olfactory cAMP signaling in the association of olfaction deficiency and depression (Kohli et al., 2016); further understanding of how ADCY3 mediates the functional cross-talk among brain circuitry networks of olfaction, emotion and cognition is critical.

Further, *Adcy3* loss-of-function variants are identified as a risk factor of obesity (Grarup et al., 2018), which often co-occurs with depression (Carey et al., 2014; Mannan et al., 2016). Whole body KO or knockdown of *Adcy3* in ventromedial hypothalamus causes obesity (Wang et al., 2009; Yang et al., 2022). In contrast, mice overexpressing the human ADCY3 gene (Yang et al., 2022) and mice harboring a point mutation, which causes elevated enzymatic activity of ADCY3, (Pitman et al., 2014) are resistant to high fat diet-induced obesity.

Adenylyl cyclase8

Genetic variants of *Adcy8* gene, as suggested by the human genetics studies, may be associated with bipolar disorder, schizophrenia, autism spectrum disorder, obsessive-compulsive disorder, and posttraumatic stress disorder. A linkage study with microsatellite markers reported an association of bipolar disorder with the genetic loci on chromosome 8q24, which covers three candidate risk genes including *Adcy8* (Avramopoulos et al., 2004). Two follow-up studies using more SNP (single nucleotide polymorphism) markers revealed a finer mapping of the bipolar disorder-associated region on 8q24 and also suggest *Adcy8* as a potential risk gene (Zandi et al., 2008; Zhang et al., 2010). Brain transcriptome analysis of human postmortem samples has found altered level of *Adcy8* transcript in bipolar disorder and schizophrenia (Guan et al., 2019).

Clinical data have found that significant population of autism spectrum disorder and obsessive-compulsive disorder patients show overlapping pathological features (Gross-Isseroff et al., 2001; van Steensel et al., 2011). GWAS data also reveal genetic variants commonly associated with autism spectrum disorder and obsessive-compulsive disorder (Liu et al., 2019). Further, an integrative analysis of brain transcriptome in autism spectrum disorder and genomic variants in obsessive-compulsive disorder identifies *Adcy8* as a common risk factor for autism

spectrum disorder and obsessive-compulsive disorder (Liu et al., 2019).

Regarding functional relevance of ADCY8 alteration to symptoms associated with psychiatric and neurodevelopmental disorders, supporting data are mostly collected from mice with *Adcy8* mutations. In mice with a QTL (quantitative trait loci) on a chromosome region that is homologous to human 8q24, increased *Adcy8* mRNA level is detected in ventral hypothalamus and piriform cortex and associated with avoidance behavior (i.e., preference of the sheltered feeding platform over the exposed feeding platform) (de Mooij-van Malsen et al., 2009). In contrast, the *Adcy8* KO mice display risk-taking traits, as indicated by more occupancy in the center area of the open field and open arm of the elevated plus maze (Schaefer et al., 2000). The *Adcy8* KO mice are also hyperactive in their home cage and during the forced swimming test (Razzoli et al., 2010).

The high expression level of *Adcy8* in hypothalamus suggests potential functions in regulating stress responses through the HPA (hypothalamic-pituitary-adrenal) axis. A GWAS study implicates a suggestive association of *Adcy8* with posttraumatic stress disorder (Wolf et al., 2014). *Adcy8* deficiency in the KO mice causes adrenal hypertrophy but normal basal plasma corticosterone level (Schaefer et al., 2000; Razzoli et al., 2010). Intriguingly, following chronic stress, the *Adcy8* KO mice display higher elevation of corticosterone (than wild type mice) along with more risk-taking rather than anxiogenic behavior (Schaefer et al., 2000; Razzoli et al., 2010).

Development of therapeutic compounds

To achieve the therapeutic potential of targeting the Ca^{2+} -stimulated ADCYs, it is necessary to develop pharmacological reagents. To date, several small molecule inhibitors against ADCY1 have been developed and tested in certain animal models. Drugs showing specific regulatory activity for ADCY3 and ADCY8 have not been reported yet.

By using a structure-based rational design compound library, Wang et al. (2011a) characterized and identified NB001 as a preferential inhibitor against ADCY1 over other ADCY isoforms. The peripherally administered NB001 can cross the blood-brain-barrier and have a half-life of about 2 h in the brain (Sethna et al., 2017). Although NB001 has a modest IC₅₀ of 10 μM , a reasonably low dose at 1–3 mg/kg shows analgesic effect in preclinical models of neuropathic and inflammatory pain (Wang et al., 2011a). In a mouse model of FXS, NB001 at 1 mg/kg attenuates the abnormally elevated ERK_{1/2}/Akt-S6K1 signaling and rescues repetitive behaviors and social deficits (Sethna et al., 2017).

Although NB001 is currently tested for safety in human clinical trials (Wang et al., 2022), it is not yet approved by

FDA. The promising efficacy of NB001 with the FXS mouse model has motivated repurposing of the existing FDA-approved drugs. Ding et al. (2020) examined the effects of carbamazepine, which is an FDA-approved anticonvulsant and also shows pharmacological inhibition action against ADCY1 (Mann et al., 2009). It is demonstrated that carbamazepine attenuates the elevated ERK_{1/2}/Akt activity and protein synthesis in the *Fmr1* KO neurons. Peripheral administration of carbamazepine corrects hyperlocomotion and social deficits and improves learning and memory in the *Fmr1* KO mice (Ding et al., 2020).

Another ADCY1 inhibitor has been identified by screening a natural product derivatives library. ST034307 shows an IC₅₀ of 2.3 μM against ADCY1 and no detectable inhibition against other ADCYs (Brust et al., 2017). Interestingly, ST034307 at higher concentration (e.g., 30 μM) causes potentiation effect on ADCY2, 3, 5, and 6 (Brust et al., 2017). Consistent with the potential role of ADCY1 in pain (Li et al., 2020), intrathecal injection of ST034307 relieves pain in a mouse model of inflammatory pain (Brust et al., 2017).

As the backbone structures of the adenosine-based NB001 and chromone-based ST034307 predict limitation and drawback of these compounds as practical therapeutic reagents, recent effort aims to identify ADCY1 inhibitors with different structures. The oxadiazole-based AC10065 at micromolar concentrations can suppress both ADCY1 and ADCY8 (Kaur et al., 2019). New drug screening followed by structure optimization has revealed several pyrimidinone-based compounds that show selectivity of ADCY1 over other ADCYs with an IC₅₀ at the sub-micromolar level (Scott et al., 2022). As these newly identified ADCY1 inhibitors show moderate therapeutic efficacy in an inflammatory pain model (Scott et al., 2022), further optimization may be needed.

Conclusion and future directions

In summary, previous studies have demonstrated the function of Ca^{2+} -stimulated ADCYs in regulating various aspects of neuronal property and behavior. It is evident that a distinct ADCY isoform, rather than general and overall cAMP level, may specifically control an isoform-specific cellular and physiological function. Elucidation of Ca^{2+} -stimulated ADCY function in distinct brain regions and distinct cell types may help to develop precise intervention of the disorder-specific pathology. Development of high affinity isoform-specific drugs with favorable pharmacokinetics and toxicity profile will lead to practical intervention to promote mental health and alleviate symptoms associated with certain psychiatric and neurodevelopment disorders. Further, interpretation with the current animal models should consider non-specific effects of global gene deficiency, complication of different genetic

backgrounds and validity of the behavior outcome. Precision preclinical models with more direct face and construct validity need to be developed.

Author contributions

JC, QD, and LA wrote the first draft of the manuscript. HW wrote the manuscript and obtained funding.

Funding

This research was supported by NIH grants R01MH124992 and R01MH119149 (to HW).

References

- Andreasen, N. C., and Pierson, R. (2008). The role of the cerebellum in schizophrenia. *Biol. Psychiatry* 64 (2), 81–88. doi:10.1016/j.biopsych.2008.01.003
- Ascano, M., Jr., Mukherjee, N., Bandaru, P., Miller, J. B., Nusbaum, J. D., Corcoran, D. L., et al. (2012). FMRP targets distinct mRNA sequence elements to regulate protein expression. *Nature* 492 (7429), 382–386. doi:10.1038/nature11737
- Avramopoulos, D., Willour, V. L., Zandi, P. P., Huo, Y., MacKinnon, D. F., Potash, J. B., et al. (2004). Linkage of bipolar affective disorder on chromosome 8q24: Follow-up and parametric analysis. *Mol. Psychiatry* 9 (2), 191–196. doi:10.1038/sj.mp.4001388
- Bakalyar, H. A., and Reed, R. R. (1990). Identification of a specialized adenylyl cyclase that may mediate odorant detection. *Science* 250 (4986), 1403–1406. doi:10.1126/science.2255909
- Berridge, M. J., Bootman, M. D., and Roderick, H. L. (2003). Calcium signalling: Dynamics, homeostasis and remodelling. *Nat. Rev. Mol. Cell Biol.* 4 (7), 517–529. doi:10.1038/nrm1155
- Bishop, G. A., Berbari, N. F., Lewis, J., and Mykityn, K. (2007). Type III adenylyl cyclase localizes to primary cilia throughout the adult mouse brain. *J. Comp. Neurol.* 505 (5), 562–571. doi:10.1002/cne.21510
- Brown, V., Jin, P., Ceman, S., Darnell, J. C., O'Donnell, W. T., Tenenbaum, S. A., et al. (2001). Microarray identification of FMRP-associated brain mRNAs and altered mRNA translational profiles in fragile X syndrome. *Cell* 107 (4), 477–487. doi:10.1016/s0092-8674(01)00568-2
- Brust, T. F., Alongkronrusmee, D., Soto-Velasquez, M., Baldwin, T. A., Ye, Z., Dai, M., et al. (2017). Identification of a selective small-molecule inhibitor of type 1 adenylyl cyclase activity with analgesic properties. *Sci. Signal.* 10 (467), eaah5381. doi:10.1126/scisignal.aah5381
- Buck, J., Sinclair, M. L., Schapal, L., Cann, M. J., and Levin, L. R. (1999). Cytosolic adenylyl cyclase defines a unique signaling molecule in mammals. *Proc. Natl. Acad. Sci. U. S. A.* 96 (1), 79–84. doi:10.1073/pnas.96.1.79
- Butler, M. G., McGuire, A. B., Masoud, H., and Manzardo, A. M. (2016a). Currently recognized genes for schizophrenia: High-resolution chromosome ideogram representation. *Am. J. Med. Genet. B Neuropsychiatr. Genet.* 171B (2), 181–202. doi:10.1002/ajmg.b.32391
- Butler, M. G., Rafi, S. K., McGuire, A., and Manzardo, A. M. (2016b). Currently recognized clinically relevant and known genes for human reproduction and related infertility with representation on high-resolution chromosome ideograms. *Gene* 575 (1), 149–159. doi:10.1016/j.gene.2015.08.057
- Cali, J. J., Zwaagstra, J. C., Mons, N., Cooper, D. M., and Krupinski, J. (1994). Type VIII adenylyl cyclase. A Ca²⁺/calmodulin-stimulated enzyme expressed in discrete regions of rat brain. *J. Biol. Chem.* 269 (16), 12190–12195. doi:10.1016/s0021-9258(17)32700-x
- Carey, M., Small, H., Yoong, S. L., Boyes, A., Bisquera, A., and Sanson-Fisher, R. (2014). Prevalence of comorbid depression and obesity in general practice: A cross-sectional survey. *Br. J. Gen. Pract.* 64 (620), e122–127. doi:10.3399/bjgp14X677482
- Chen, X., Cao, H., Saraf, A., Zweifel, L. S., and Storm, D. R. (2015). Overexpression of the type 1 adenylyl cyclase in the forebrain leads to deficits of behavioral inhibition. *J. Neurosci.* 35 (1), 339–351. doi:10.1523/JNEUROSCI.2478-14.2015
- Chen, X., Luo, J., Leng, Y., Yang, Y., Zweifel, L. S., Palmiter, R. D., et al. (2016). Ablation of type III adenylyl cyclase in mice causes reduced neuronal activity, altered sleep pattern, and depression-like phenotypes. *Biol. Psychiatry* 80 (11), 836–848. doi:10.1016/j.biopsych.2015.12.012
- Choi, E. J., Xia, Z., and Storm, D. R. (1992). Stimulation of the type III olfactory adenylyl cyclase by calcium and calmodulin. *Biochemistry* 31 (28), 6492–6498. doi:10.1021/bi00143a019
- Conti, A. C., Maas, J. W., Jr., Muglia, L. M., Dave, B. A., Vogt, S. K., Tran, T. T., et al. (2007). Distinct regional and subcellular localization of adenylyl cyclases type 1 and 8 in mouse brain. *Neuroscience* 146 (2), 713–729. doi:10.1016/j.neuroscience.2007.01.045
- Cooper, D. M. (2003). Regulation and organization of adenylyl cyclases and cAMP. *Biochem. J.* 375 (3), 517–529. doi:10.1042/BJ20031061
- Darnell, J. C., Van Driesche, S. J., Zhang, C., Hung, K. Y., Mele, A., Fraser, C. E., et al. (2011). FMRP stalls ribosomal translocation on mRNAs linked to synaptic function and autism. *Cell* 146 (2), 247–261. doi:10.1016/j.cell.2011.06.013
- de Mooij-van Malsen, A. J., van Lith, H. A., Oppelaar, H., Hendriks, J., de Wit, M., Kostrzewa, E., et al. (2009). Interspecies trait genetics reveals association of Adcy8 with mouse avoidance behavior and a human mood disorder. *Biol. Psychiatry* 66 (12), 1123–1130. doi:10.1016/j.biopsych.2009.06.016
- Dhande, O. S., Bhatt, S., Anishchenko, A., Elstrott, J., Iwasato, T., Swindell, E. C., et al. (2012). Role of adenylyl cyclase 1 in retinofugal map development. *J. Comp. Neurol.* 520 (7), 1562–1583. doi:10.1002/cne.23000
- Ding, Q., Zhang, F., Feng, Y., and Wang, H. (2020). Carbamazepine restores neuronal signaling, protein synthesis, and cognitive function in a mouse model of fragile X syndrome. *Int. J. Mol. Sci.* 21 (23), E9327. doi:10.3390/ijms21239327
- DiRocco, D. P., Scheiner, Z. S., Sindreu, C. B., Chan, G. C., and Storm, D. R. (2009). A role for calmodulin-stimulated adenylyl cyclases in cocaine sensitization. *J. Neurosci.* 29 (8), 2393–2403. doi:10.1523/JNEUROSCI.4356-08.2009
- Dorph-Petersen, K. A., and Lewis, D. A. (2017). Postmortem structural studies of the thalamus in schizophrenia. *Schizophr. Res.* 180, 28–35. doi:10.1016/j.schres.2016.08.007
- Eckel-Mahan, K. L., Phan, T., Han, S., Wang, H., Chan, G. C., Scheiner, Z. S., et al. (2008). Circadian oscillation of hippocampal MAPK activity and cAMP: Implications for memory persistence. *Nat. Neurosci.* 11 (9), 1074–1082. doi:10.1038/nn.2174
- Fagan, K. A., Mahey, R., and Cooper, D. M. (1996). Functional co-localization of transfected Ca(2+)-stimulable adenylyl cyclases with capacitative Ca²⁺ entry sites. *J. Biol. Chem.* 271 (21), 12438–12444. doi:10.1074/jbc.271.21.12438
- Gallagher, S. M., Daly, C. A., Bear, M. F., and Huber, K. M. (2004). Extracellular signal-regulated protein kinase activation is required for metabotropic glutamate

Conflict of interest

The authors declare that the research was conducted in the absence of any commercial or financial relationships that could be construed as a potential conflict of interest.

Publisher's note

All claims expressed in this article are solely those of the authors and do not necessarily represent those of their affiliated organizations, or those of the publisher, the editors and the reviewers. Any product that may be evaluated in this article, or claim that may be made by its manufacturer, is not guaranteed or endorsed by the publisher.

- receptor-dependent long-term depression in hippocampal area CA1. *J. Neurosci.* 24 (20), 4859–4864. doi:10.1523/JNEUROSCI.5407-03.2004
- Grace, A. A. (2016). Dysregulation of the dopamine system in the pathophysiology of schizophrenia and depression. *Nat. Rev. Neurosci.* 17 (8), 524–532. doi:10.1038/nrn.2016.57
- Grarup, N., Moltke, I., Andersen, M. K., Dalby, M., Vitting-Seerup, K., Kern, T., et al. (2018). Loss-of-function variants in ADCY3 increase risk of obesity and type 2 diabetes. *Nat. Genet.* 50 (2), 172–174. doi:10.1038/s41588-017-0022-7
- Green, J. A., and Mykytyn, K. (2014). Neuronal primary cilia: An underappreciated signaling and sensory organelle in the brain. *Neuropsychopharmacology* 39 (1), 244–245. doi:10.1038/npp.2013.203
- Gross, C., Banerjee, A., Tiwari, D., Longo, F., White, A. R., Allen, A. G., et al. (2019). Isoform-selective phosphoinositide 3-kinase inhibition ameliorates a broad range of fragile X syndrome-associated deficits in a mouse model. *Neuropsychopharmacology* 44 (2), 324–333. doi:10.1038/s41386-018-0150-5
- Gross, C., Chang, C. W., Kelly, S. M., Bhattacharya, A., McBride, S. M., Danielson, S. W., et al. (2015). Increased expression of the PI3K enhancer PIKE mediates deficits in synaptic plasticity and behavior in fragile X syndrome. *Cell Rep.* 11 (5), 727–736. doi:10.1016/j.celrep.2015.03.060
- Gross-Isseroff, R., Hermesh, H., and Weizman, A. (2001). Obsessive compulsive behaviour in autism—towards an autistic-obsessive compulsive syndrome? *World J. Biol. Psychiatry* 2 (4), 193–197. doi:10.3109/15622970109026809
- Guadiana, S. M., Semple-Rowland, S., Daroszewski, D., Madorsky, I., Breunig, J. J., Mykytyn, K., et al. (2013). Arborization of dendrites by developing neocortical neurons is dependent on primary cilia and type 3 adenylyl cyclase. *J. Neurosci.* 33 (6), 2626–2638. doi:10.1523/JNEUROSCI.2906-12.2013
- Guan, J., Cai, J. J., Ji, G., and Sham, P. C. (2019). Commonality in dysregulated expression of gene sets in cortical brains of individuals with autism, schizophrenia, and bipolar disorder. *Transl. Psychiatry* 9 (1), 152. doi:10.1038/s41398-019-0488-4
- Hines, L. M., Tabakoff, B., and State, W. I. S. (2005). Trait markers of alcohol, U., and dependence, IPlatelet adenylyl cyclase activity: A biological marker for major depression and recent drug use. *Biol. Psychiatry* 58 (12), 955–962. doi:10.1016/j.biopsych.2005.05.040
- Huang, C. C., Liang, Y. C., and Hsu, K. S. (2001). Characterization of the mechanism underlying the reversal of long term potentiation by low frequency stimulation at hippocampal CA1 synapses. *J. Biol. Chem.* 276 (51), 48108–48117. doi:10.1074/jbc.M106388200
- International Consortium on Lithium Genetics. Amare, A. T., Schubert, K. O., Hou, L., Clark, S. R., Papiol, S., et al. (2018). Association of polygenic score for schizophrenia and hla antigen and inflammation genes with response to lithium in bipolar affective disorder: A genome-wide association study. *JAMA Psychiatry* 75 (1), 65–74. doi:10.1001/jamapsychiatry.2017.3433
- Katsel, P. L., Tagliente, T. M., Schwarz, T. E., Craddock-Royal, B. D., Patel, N. D., and Maayani, S. (2003). Molecular and biochemical evidence for the presence of type III adenylyl cyclase in human platelets. *Platelets* 14 (1), 21–33. doi:10.1080/0953710021000062905
- Kaur, J., Soto-Velasquez, M., Ding, Z., Ghanbarpour, A., Lill, M. A., van Rijn, R. M., et al. (2019). Optimization of a 1, 3, 4-oxadiazole series for inhibition of Ca(2+)/calmodulin-stimulated activity of adenylyl cyclases 1 and 8 for the treatment of chronic pain. *Eur. J. Med. Chem.* 162, 568–585. doi:10.1016/j.ejmech.2018.11.036
- Kelleher, R. J., 3rd, Govindarajan, A., Jung, H. Y., Kang, H., and Tonegawa, S. (2004). Translational control by MAPK signaling in long-term synaptic plasticity and memory. *Cell* 116 (3), 467–479. doi:10.1016/s0092-8674(04)00115-1
- Kleinboelting, S., Diaz, A., Moniot, S., van den Heuvel, J., Weyand, M., Levin, L. R., et al. (2014). Crystal structures of human soluble adenylyl cyclase reveal mechanisms of catalysis and of its activation through bicarbonate. *Proc. Natl. Acad. Sci. U. S. A.* 111 (10), 3727–3732. doi:10.1073/pnas.1322778111
- Kohli, P., Soler, Z. M., Nguyen, S. A., Muus, J. S., and Schlosser, R. J. (2016). The association between olfaction and depression: A systematic review. *Chem. Senses* 41 (6), 479–486. doi:10.1093/chemse/bjw061
- Krupinski, J., Coussen, F., Bakalyar, H. A., Tang, W. J., Feinstein, P. G., Orth, K., et al. (1989). Adenylyl cyclase amino acid sequence: Possible channel- or transporter-like structure. *Science* 244 (4912), 1558–1564. doi:10.1126/science.2472670
- Lee, H. K., Barbarosie, M., Kameyama, K., Bear, M. F., and Haganir, R. L. (2000). Regulation of distinct AMPA receptor phosphorylation sites during bidirectional synaptic plasticity. *Nature* 405 (6789), 955–959. doi:10.1038/35016089
- Lee, K., Goodman, L., Fourie, C., Schenk, S., Leitch, B., and Montgomery, J. M. (2016). AMPA receptors as therapeutic targets for neurological disorders. *Adv. Protein Chem. Struct. Biol.* 103, 203–261. doi:10.1016/bs.apcsb.2015.10.004
- Li, X. H., Chen, Q. Y., and Zhuo, M. (2020). Neuronal adenylyl cyclase targeting central plasticity for the treatment of chronic pain. *Neurotherapeutics* 17 (3), 861–873. doi:10.1007/s13311-020-00927-1
- Liauw, J., Wu, L. J., and Zhuo, M. (2005). Calcium-stimulated adenylyl cyclases required for long-term potentiation in the anterior cingulate cortex. *J. Neurophysiol.* 94 (1), 878–882. doi:10.1152/jn.01205.2004
- Litvin, T. N., Kamenetsky, M., Zarifyan, A., Buck, J., and Levin, L. R. (2003). Kinetic properties of "soluble" adenylyl cyclase. Synergism between calcium and bicarbonate. *J. Biol. Chem.* 278 (18), 15922–15926. doi:10.1074/jbc.M212475200
- Liu, D., Cao, H., Kural, K. C., Fang, Q., and Zhang, F. (2019). Integrative analysis of shared genetic pathogenesis by autism spectrum disorder and obsessive-compulsive disorder. *Biosci. Rep.* 39 (12), BSR20191942. doi:10.1042/BSR20191942
- Liu, X., Zhou, Y., Li, S., Yang, D., Jiao, M., Liu, X., et al. (2020a). Type 3 adenylyl cyclase in the main olfactory epithelium participates in depression-like and anxiety-like behaviours. *J. Affect. Disord.* 268, 28–38. doi:10.1016/j.jad.2020.02.041
- Liu, X., Zhou, Y., Yang, D., Li, S., Liu, X., and Wang, Z. (2020b). Type 3 adenylyl cyclase in the MOE is involved in learning and memory in mice. *Behav. Brain Res.* 383, 112533. doi:10.1016/j.bbr.2020.112533
- Lu, H. C., She, W. C., Plas, D. T., Neumann, P. E., Janz, R., and Crair, M. C. (2003). Adenylyl cyclase I regulates AMPA receptor trafficking during mouse cortical 'barrel' map development. *Nat. Neurosci.* 6 (9), 939–947. doi:10.1038/nn1106
- Makhinson, M., Chotiner, J. K., Watson, J. B., and O'Dell, T. J. (1999). Adenylyl cyclase activation modulates activity-dependent changes in synaptic strength and Ca2+/calmodulin-dependent kinase II autophosphorylation. *J. Neurosci.* 19 (7), 2500–2510. doi:10.1523/jneurosci.19-07-02500.1999
- Malinow, R. (2003). AMPA receptor trafficking and long-term potentiation. *Philos. Trans. R. Soc. Lond. B Biol. Sci.* 358 (1432), 707–714. doi:10.1098/rstb.2002.1233
- Mann, L., Heldman, E., Bersudsky, Y., Vatner, S. F., Ishikawa, Y., Almog, O., et al. (2009). Inhibition of specific adenylyl cyclase isoforms by lithium and carbamazepine, but not valproate, may be related to their antidepressant effect. *Bipolar Disord.* 11 (8), 885–896. doi:10.1111/j.1399-5618.2009.00762.x
- Mannan, M., Mamun, A., Doi, S., and Clavarino, A. (2016). Prospective associations between depression and obesity for adolescent males and females—A systematic review and meta-analysis of longitudinal studies. *PLoS One* 11 (6), e0157240. doi:10.1371/journal.pone.0157240
- Martin, A. C., Willoughby, D., Ciruela, A., Ayling, L. J., Pagano, M., Wachten, S., et al. (2009). Capacitative Ca2+ entry via Orail and stromal interacting molecule 1 (STIM1) regulates adenylyl cyclase type 8. *Mol. Pharmacol.* 75 (4), 830–842. doi:10.1124/mol.108.051748
- Miao, H. H., Li, X. H., Chen, Q. Y., and Zhuo, M. (2019). Calcium-stimulated adenylyl cyclase subtype 1 is required for presynaptic long-term potentiation in the insular cortex of adult mice. *Mol. Pain* 15, 1744806919842961. doi:10.1177/1744806919842961
- Muglia, L. M., Schaefer, M. L., Vogt, S. K., Gurtner, G., Imamura, A., and Muglia, L. J. (1999). The 5'-flanking region of the mouse adenylyl cyclase type VIII gene imparts tissue-specific expression in transgenic mice. *J. Neurosci.* 19 (6), 2051–2058. doi:10.1523/jneurosci.19-06-02051.1999
- Nakazawa, K., and Sapkota, K. (2020). The origin of NMDA receptor hypofunction in schizophrenia. *Pharmacol. Ther.* 205, 107426. doi:10.1016/j.pharmthera.2019.107426
- Nielsen, M. D., Chan, G. C., Poser, S. W., and Storm, D. R. (1996). Differential regulation of type I and type VIII Ca2+-stimulated adenylyl cyclases by Gi-coupled receptors *in vivo*. *J. Biol. Chem.* 271 (52), 33308–33316. doi:10.1074/jbc.271.52.33308
- Perez, J., Tardito, D., Racagni, G., Smeraldi, E., and Zanardi, R. (2001). Protein kinase A and Rap1 levels in platelets of untreated patients with major depression. *Mol. Psychiatry* 6 (1), 44–49. doi:10.1038/sj.mp.4000795
- Pitman, J. L., Wheeler, M. C., Lloyd, D. J., Walker, J. R., Glynne, R. J., and Gekakis, N. (2014). A gain-of-function mutation in adenylate cyclase 3 protects mice from diet-induced obesity. *PLoS One* 9 (10), e110226. doi:10.1371/journal.pone.0110226
- Razzoli, M., Andreoli, M., Maraia, G., Di Francesco, C., and Arban, R. (2010). Functional role of calcium-stimulated adenylyl cyclase 8 in adaptations to psychological stressors in the mouse: Implications for mood disorders. *Neuroscience* 170 (2), 429–440. doi:10.1016/j.neuroscience.2010.07.022
- Redei, E. E., Andrus, B. M., Kwasny, M. J., Seok, J., Cai, X., Ho, J., et al. (2014). Blood transcriptomic biomarkers in adult primary care patients with major depressive disorder undergoing cognitive behavioral therapy. *Transl. Psychiatry* 4, e442. doi:10.1038/tp.2014.66
- Regnault, K. L., Leteurtre, E., Gutkind, S. J., Gespach, C. P., and Emami, S. (2002). Activation of adenylyl cyclases, regulation of insulin status, and cell survival by

- G(alpha)olf in pancreatic beta-cells. *Am. J. Physiol. Regul. Integr. Comp. Physiol.* 282 (3), R870–R880. doi:10.1152/ajpregu.00374.2001
- Richter, J. D., and Zhao, X. (2021). The molecular biology of FMRP: New insights into fragile X syndrome. *Nat. Rev. Neurosci.* 22 (4), 209–222. doi:10.1038/s41583-021-00432-0
- Robison, A. J. (2014). Emerging role of CaMKII in neuropsychiatric disease. *Trends Neurosci.* 37 (11), 653–662. doi:10.1016/j.tins.2014.07.001
- Schaefer, M. L., Wong, S. T., Wozniak, D. F., Muglia, L. M., Liauw, J. A., Zhuo, M., et al. (2000). Altered stress-induced anxiety in adenylyl cyclase type VIII-deficient mice. *J. Neurosci.* 20 (13), 4809–4820. doi:10.1523/jneurosci.20-13-04809.2000
- Scott, J. A., Soto-Velasquez, M., Hayes, M. P., LaVigne, J. E., Miller, H. R., Kaur, J., et al. (2022). Optimization of a pyrimidinone series for selective inhibition of Ca(2+)/calmodulin-stimulated adenylyl cyclase 1 activity for the treatment of chronic pain. *J. Med. Chem.* 65 (6), 4667–4686. doi:10.1021/acs.jmedchem.1c01759
- Sethna, F., Feng, W., Ding, Q., Robison, A. J., Feng, Y., and Wang, H. (2017). Enhanced expression of ADCY1 underlies aberrant neuronal signalling and behaviour in a syndromic autism model. *Nat. Commun.* 8, 14359. doi:10.1038/ncomms14359
- Sethna, F., Moon, C., and Wang, H. (2014). From FMRP function to potential therapies for fragile X syndrome. *Neurochem. Res.* 39 (6), 1016–1031. doi:10.1007/s11064-013-1229-3
- Siljee, J. E., Wang, Y., Bernard, A. A., Ersoy, B. A., Zhang, S., Marley, A., et al. (2018). Subcellular localization of MC4R with ADCY3 at neuronal primary cilia underlies a common pathway for genetic predisposition to obesity. *Nat. Genet.* 50 (2), 180–185. doi:10.1038/s41588-017-0020-9
- Sindreu, C. B., Scheiner, Z. S., and Storm, D. R. (2007). Ca2+ -stimulated adenylyl cyclases regulate ERK-dependent activation of MSK1 during fear conditioning. *Neuron* 53 (1), 79–89. doi:10.1016/j.neuron.2006.11.024
- Smith, S. J., and Augustine, G. J. (1988). Calcium ions, active zones and synaptic transmitter release. *Trends Neurosci.* 11 (10), 458–464. doi:10.1016/0166-2236(88)90199-3
- Storm, D. R., Hansel, C., Hacker, B., Parent, A., and Linden, D. J. (1998). Impaired cerebellar long-term potentiation in type I adenylyl cyclase mutant mice. *Neuron* 20 (6), 1199–1210. doi:10.1016/s0896-6273(00)80500-0
- Sundararajan, T., Manzardo, A. M., and Butler, M. G. (2018). Functional analysis of schizophrenia genes using GeneAnalytics program and integrated databases. *Gene* 641, 25–34. doi:10.1016/j.gene.2017.10.035
- Suzuki, A., Lee, L. J., Hayashi, Y., Muglia, L., Itoharu, S., Erzurumlu, R. S., et al. (2015). Thalamic adenylyl cyclase 1 is required for barrel formation in the somatosensory cortex. *Neuroscience* 290, 518–529. doi:10.1016/j.neuroscience.2015.01.043
- Tang, W. J., Krupinski, J., and Gilman, A. G. (1991). Expression and characterization of calmodulin-activated (type I) adenylyl cyclase. *J. Biol. Chem.* 266 (13), 8595–8603. doi:10.1016/s0021-9258(18)93016-4
- van Steensel, F. J., Bogels, S. M., and Perrin, S. (2011). Anxiety disorders in children and adolescents with autistic spectrum disorders: A meta-analysis. *Clin. Child. Fam. Psychol. Rev.* 14 (3), 302–317. doi:10.1007/s10567-011-0097-0
- Villacres, E. C., Wong, S. T., Chavkin, C., and Storm, D. R. (1998). Type I adenylyl cyclase mutant mice have impaired mossy fiber long-term potentiation. *J. Neurosci.* 18 (9), 3186–3194. doi:10.1523/jneurosci.18-09-03186.1998
- Wang, H., Chan, G. C., Athos, J., and Storm, D. R. (2002). Synaptic concentration of type-I adenylyl cyclase in cerebellar neurons. *J. Neurochem.* 83 (4), 946–954. doi:10.1046/j.1471-4159.2002.01206.x
- Wang, H., Ferguson, G. D., Pineda, V. V., Cundiff, P. E., and Storm, D. R. (2004). Overexpression of type-I adenylyl cyclase in mouse forebrain enhances recognition memory and LTP. *Nat. Neurosci.* 7 (6), 635–642. doi:10.1038/nn1248
- Wang, H., Gong, B., Vadakkan, K. I., Toyoda, H., Kaang, B. K., and Zhuo, M. (2007). Genetic evidence for adenylyl cyclase 1 as a target for preventing neuronal excitotoxicity mediated by N-methyl-D-aspartate receptors. *J. Biol. Chem.* 282 (2), 1507–1517. doi:10.1074/jbc.M607291200
- Wang, H., Pineda, V. V., Chan, G. C., Wong, S. T., Muglia, L. J., and Storm, D. R. (2003). Type 8 adenylyl cyclase is targeted to excitatory synapses and required for mossy fiber long-term potentiation. *J. Neurosci.* 23 (30), 9710–9718. doi:10.1523/jneurosci.23-30-09710.2003
- Wang, H., and Storm, D. R. (2003). Calmodulin-regulated adenylyl cyclases: Cross-talk and plasticity in the central nervous system. *Mol. Pharmacol.* 63 (3), 463–468. doi:10.1124/mol.63.3.463
- Wang, H., Xu, H., Wu, L. J., Kim, S. S., Chen, T., Koga, K., et al. (2011a). Identification of an adenylyl cyclase inhibitor for treating neuropathic and inflammatory pain. *Sci. Transl. Med.* 3 (65), 65ra3. doi:10.1126/scitranslmed.3001269
- Wang, W., Chen, Q. Y., Zhao, P., Zhong, J., Wang, Y., Li, X., et al. (2022). Human safety study of a selective neuronal adenylyl cyclase 1 inhibitor NB001 which relieves the neuropathic pain and blocks ACC in adult mice. *Mol. Pain* 2022, 17448069221089596. doi:10.1177/17448069221089596
- Wang, X., Snape, M., Klann, E., Stone, J. G., Singh, A., Petersen, R. B., et al. (2012). Activation of the extracellular signal-regulated kinase pathway contributes to the behavioral deficit of fragile x-syndrome. *J. Neurochem.* 121 (4), 672–679. doi:10.1111/j.1471-4159.2012.07722.x
- Wang, Z., Li, V., Chan, G. C., Phan, T., Nudelman, A. S., Xia, Z., et al. (2009). Adult type 3 adenylyl cyclase-deficient mice are obese. *PLoS One* 4 (9), e6979. doi:10.1371/journal.pone.0006979
- Wang, Z., Phan, T., and Storm, D. R. (2011b). The type 3 adenylyl cyclase is required for novel object learning and extinction of contextual memory: Role of cAMP signaling in primary cilia. *J. Neurosci.* 31 (15), 5557–5561. doi:10.1523/JNEUROSCI.6561-10.2011
- Wayman, G. A., Impey, S., and Storm, D. R. (1995). Ca2+ inhibition of type III adenylyl cyclase *in vivo*. *J. Biol. Chem.* 270 (37), 21480–21486. doi:10.1074/jbc.270.37.21480
- Wayman, G. A., Impey, S., Wu, Z., Kindsvogel, W., Prichard, L., and Storm, D. R. (1994). Synergistic activation of the type I adenylyl cyclase by Ca2+ and Gs-coupled receptors *in vivo*. *J. Biol. Chem.* 269 (41), 25400–25405. doi:10.1016/s0021-9258(18)47263-8
- Wayman, G. A., Wei, J., Wong, S., and Storm, D. R. (1996). Regulation of type I adenylyl cyclase by calmodulin kinase IV *in vivo*. *Mol. Cell. Biol.* 16 (11), 6075–6082. doi:10.1128/MCB.16.11.6075
- Wei, J., Wayman, G., and Storm, D. R. (1996). Phosphorylation and inhibition of type III adenylyl cyclase by calmodulin-dependent protein kinase II *in vivo*. *J. Biol. Chem.* 271 (39), 24231–24235. doi:10.1074/jbc.271.39.24231
- Wei, J., Zhao, A. Z., Chan, G. C., Baker, L. P., Impey, S., Beavo, J. A., et al. (1998). Phosphorylation and inhibition of olfactory adenylyl cyclase by CaM kinase II in neurons: A mechanism for attenuation of olfactory signals. *Neuron* 21 (3), 495–504. doi:10.1016/s0896-6273(00)80561-9
- Wolf, E. J., Rasmusson, A. M., Mitchell, K. S., Logue, M. W., Baldwin, C. T., and Miller, M. W. (2014). A genome-wide association study of clinical symptoms of dissociation in a trauma-exposed sample. *Depress. Anxiety* 31 (4), 352–360. doi:10.1002/da.22260
- Wong, S. T., Athos, J., Figueroa, X. A., Pineda, V. V., Schaefer, M. L., Chavkin, C. C., et al. (1999). Calcium-stimulated adenylyl cyclase activity is critical for hippocampus-dependent long-term memory and late phase LTP. *Neuron* 23 (4), 787–798. doi:10.1016/s0896-6273(01)80036-2
- Wong, S. T., Trinh, K., Hacker, B., Chan, G. C., Lowe, G., Gaggari, A., et al. (2000). Disruption of the type III adenylyl cyclase gene leads to peripheral and behavioral anosmia in transgenic mice. *Neuron* 27 (3), 487–497. doi:10.1016/s0896-6273(00)00060-x
- Wray, N. R., Pergadia, M. L., Blackwood, D. H., Penninx, B. W., Gordon, S. D., Nyholt, D. R., et al. (2012). Genome-wide association study of major depressive disorder: New results, meta-analysis, and lessons learned. *Mol. Psychiatry* 17 (1), 36–48. doi:10.1038/mp.2010.109
- Wu, Y., Yao, Y. G., and Luo, X. J. (2017). Szdb: A database for schizophrenia genetic research. *Schizophr. Bull.* 43 (2), 459–471. doi:10.1093/schbul/sbw102
- Wu, Z. L., Thomas, S. A., Villacres, E. C., Xia, Z., Simmons, M. L., Chavkin, C., et al. (1995). Altered behavior and long-term potentiation in type I adenylyl cyclase mutant mice. *Proc. Natl. Acad. Sci. U. S. A.* 92 (1), 220–224. doi:10.1073/pnas.92.1.220
- Wu, Z., Wong, S. T., and Storm, D. R. (1993). Modification of the calcium and calmodulin sensitivity of the type I adenylyl cyclase by mutagenesis of its calmodulin binding domain. *J. Biol. Chem.* 268 (32), 23766–23768. doi:10.1016/s0021-9258(20)80447-5
- Xia, Z., Choi, E. J., Wang, F., Blazynski, C., and Storm, D. R. (1993). Type I calmodulin-sensitive adenylyl cyclase is neural specific. *J. Neurochem.* 60 (1), 305–311. doi:10.1111/j.1471-4159.1993.tb05852.x
- Xia, Z., Choi, E. J., Wang, F., and Storm, D. R. (1992). The type III calcium/calmodulin-sensitive adenylyl cyclase is not specific to olfactory sensory neurons. *Neurosci. Lett.* 144 (1–2), 169–173. doi:10.1016/0304-3940(92)90742-p
- Yang, B., He, B., Abdel-Halim, S. M., Tibell, A., Brendel, M. D., Bretzel, R. G., et al. (1999). Molecular cloning of a full-length cDNA for human type 3 adenylyl cyclase and its expression in human islets. *Biochem. Biophys. Res. Commun.* 254 (3), 548–551. doi:10.1006/bbrc.1998.9983
- Yang, D., Wu, X., Wang, W., Zhou, Y., and Wang, Z. (2022). Ciliary type III adenylyl cyclase in the VMH is crucial for high-fat diet-induced obesity

mediated by autophagy. *Adv. Sci.* 9 (3), e2102568. doi:10.1002/advs.202102568

Yang, M., Ding, Q., Zhang, M., Moon, C., and Wang, H. (2020). Forebrain overexpression of type 1 adenylyl cyclase promotes molecular stability and behavioral resilience to physical stress. *Neurobiol. Stress* 13, 100237. doi:10.1016/j.yynstr.2020.100237

Yue, F., Cheng, Y., Breschi, A., Vierstra, J., Wu, W., Ryba, T., et al. (2014). A comparative encyclopedia of DNA elements in the mouse genome. *Nature* 515 (7527), 355–364. doi:10.1038/nature13992

Zandi, P. P., Zollner, S., Avramopoulos, D., Willour, V. L., Chen, Y., Qin, Z. S., et al. (2008). Family-based SNP association study on 8q24 in bipolar disorder. *Am. J. Med. Genet. B Neuropsychiatr. Genet.* 147B (5), 612–618. doi:10.1002/ajmg.b.30651

Zanos, P., and Gould, T. D. (2018). Mechanisms of ketamine action as an antidepressant. *Mol. Psychiatry* 23 (4), 801–811. doi:10.1038/mp.2017.255

Zhang, I., and Hu, H. (2020). Store-operated calcium channels in physiological and pathological States of the nervous system. *Front. Cell. Neurosci.* 14, 600758. doi:10.3389/fncel.2020.600758

Zhang, P., Xiang, N., Chen, Y., Sliwerska, E., McInnis, M. G., Burmeister, M., et al. (2010). Family-based association analysis to finemap bipolar linkage peak on chromosome 8q24 using 2, 500 genotyped SNPs and 15, 000 imputed SNPs. *Bipolar Disord.* 12 (8), 786–792. doi:10.1111/j.1399-5618.2010.00883.x

Zheng, F., Zhang, M., Ding, Q., Sethna, F., Yan, L., Moon, C., et al. (2016). Voluntary running depreciates the requirement of Ca²⁺-stimulated cAMP signaling in synaptic potentiation and memory formation. *Learn. Mem.* 23 (8), 442–449. doi:10.1101/lm.040642.115

Zheng, F., Zhou, X., Luo, Y., Xiao, H., Wayman, G., and Wang, H. (2011). Regulation of brain-derived neurotrophic factor exon IV transcription through calcium responsive elements in cortical neurons. *PLoS One* 6 (12), e28441. doi:10.1371/journal.pone.0028441

Zheng, F., Zhou, X., Moon, C., and Wang, H. (2012). Regulation of brain-derived neurotrophic factor expression in neurons. *Int. J. Physiol. Pathophysiol. Pharmacol.* 4 (4), 188–200.

Zhou, X., Lin, D. S., Zheng, F., Sutton, M. A., and Wang, H. (2010). Intracellular calcium and calmodulin link brain-derived neurotrophic factor to p70S6 kinase phosphorylation and dendritic protein synthesis. *J. Neurosci. Res.* 88 (7), 1420–1432. doi:10.1002/jnr.22321



OPEN ACCESS

EDITED BY

Val J. Watts,
Purdue University, United States

REVIEWED BY

Ferenc Antoni,
University of Edinburgh,
United Kingdom
Hartmut Kuhn,
Charité Universitätsmedizin Berlin,
Germany

*CORRESPONDENCE

Joachim E. Schultz,
joachim.schultz@uni-tuebingen.de

SPECIALTY SECTION

This article was submitted to
Experimental Pharmacology and Drug
Discovery,
a section of the journal
Frontiers in Pharmacology

RECEIVED 02 August 2022

ACCEPTED 06 September 2022

PUBLISHED 27 September 2022

CITATION

Schultz JE (2022), The evolutionary
conservation of eukaryotic membrane-
bound adenylyl cyclase isoforms.
Front. Pharmacol. 13:1009797.
doi: 10.3389/fphar.2022.1009797

COPYRIGHT

© 2022 Schultz. This is an open-access
article distributed under the terms of the
[Creative Commons Attribution License](https://creativecommons.org/licenses/by/4.0/)
(CC BY). The use, distribution or
reproduction in other forums is
permitted, provided the original
author(s) and the copyright owner(s) are
credited and that the original
publication in this journal is cited, in
accordance with accepted academic
practice. No use, distribution or
reproduction is permitted which does
not comply with these terms.

The evolutionary conservation of eukaryotic membrane-bound adenylyl cyclase isoforms

Joachim E. Schultz*

Department Pharmaceutical Biochemistry, Pharmazeutisches Institut der Universität, Tübingen, Germany

The nine membrane-delimited eukaryotic adenylyl cyclases are pseudoheterodimers with an identical domain order of seven (nine) distinct subdomains. Bioinformatics show that the protein evolved from a monomeric bacterial progenitor by gene duplication and fusion probably in a primordial eukaryotic cell around 1.5 billion years ago. Over a timespan of about 1 billion years, the first fusion product diverged into nine highly distinct pseudoheterodimeric isoforms. The evolutionary diversification ended approximately 0.5 billion years ago because the present isoforms are found in the living fossil coelacanth, a fish. Except for the two catalytic domains, C1 and C2, the mAC isoforms are fully diverged. Yet, within each isoform a high extent of conservation of respective subdomains is found. This applies to the C- and N-termini, a long linker region between the protein halves (C1b), two short cyclase-transducing-elements (CTE) and notably to the two hexahelical membrane domains TM1 and TM2. Except for the membrane anchor all subdomains were previously implicated in regulatory modalities. The bioinformatic results unequivocally indicate that the membrane anchors must possess an important regulatory function specifically tailored for each mAC isoform.

KEYWORDS

adenylyl cyclase, isozyme, domain structure, evolution, bioinformatics, regulation, cyclic AMP, conservation

Introduction

Isozymes are ubiquitous throughout all kingdoms of life. They either are splice variants of a “master” gene or are encoded by separate genes. Often, they share stretches of conserved amino acid sequences pointing to gene duplication events during evolution followed by subsequent divergence restricted by functional requirements. Frequently, this results in the evolution of new regulatory features in individual isoforms whereas the functional catalytic center is preserved. A textbook example is hexokinase 1 on chromosome 10 and glucokinase on chromosome 7 (human), both catalyzing glucose phosphorylation generating glucose-6-phosphate. Hexokinase is subject to product inhibition and glucokinase is not. Expression of these isozymes is tissue specific. Thus, regulation differs in two important aspects, different kinetics and cellular

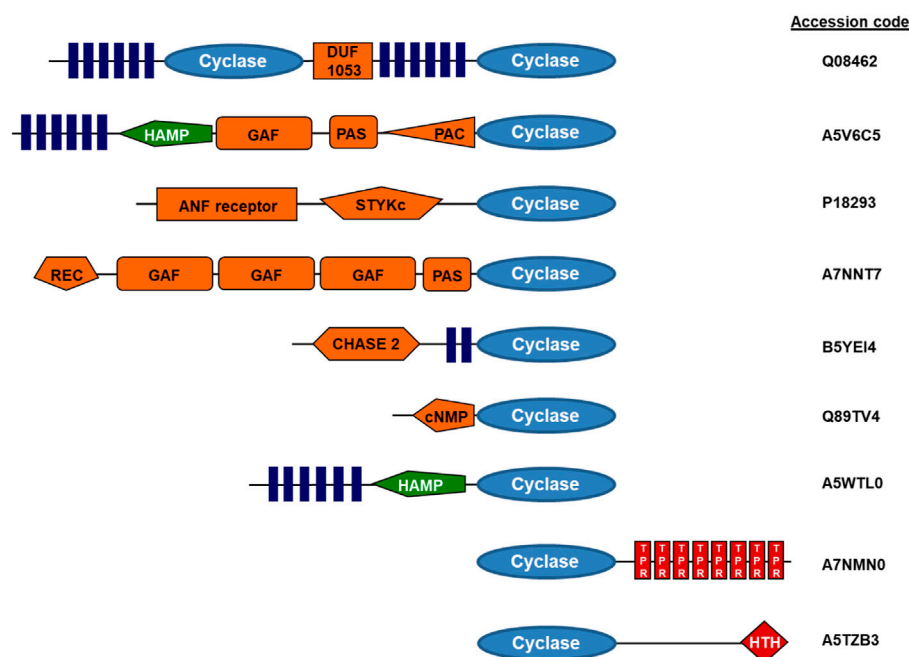


FIGURE 1

Examples of modular adenylyl cyclase proteins (domain symbols adapted from EMBL-SMART). Q08462, human adenylyl cyclase, type 2; A5V6C5, adenylyl cyclase from *Sphingomonas wittichii*; A7NNT7, *Roseiflexus castenholzii* adenylyl cyclase with GAF and PAS/PAC sensors; B5YEI4, *Dictyoglomus thermophilum* adenylyl cyclase; Q89TV4, *Bradyrhizobium japonicum* adenylyl cyclase; A5WTL0, mycobacterial adenylyl cyclase Rv3645; A7NMN0, *Roseiflexus castenholzii* adenylyl cyclase with terminal TPR repeats; A5TZB3, mycobacterial adenylyl cyclase Rv0386 with a helix-turn-helix terminal transcriptional regulator (figure adapted from ref. Schultz and Natarajan, 2013).

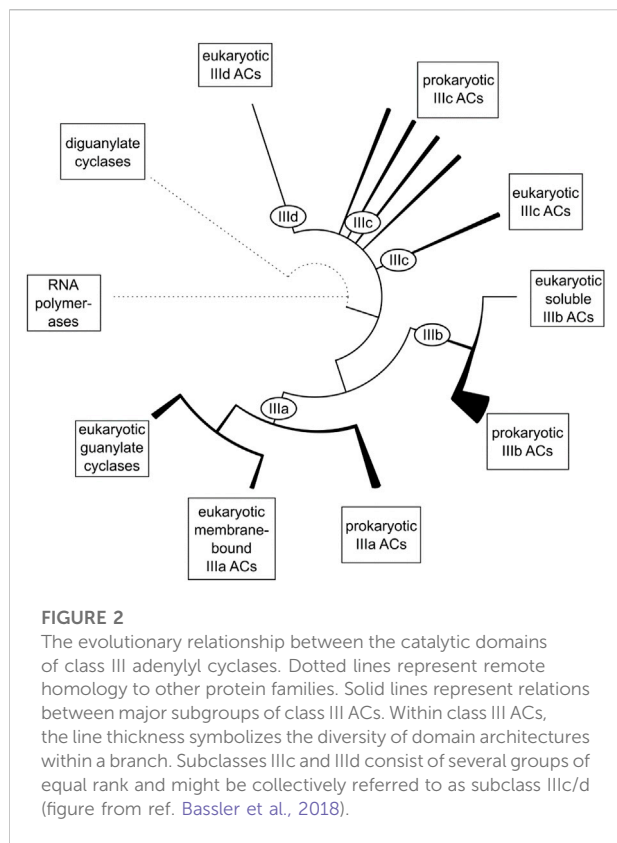
localization. Numerous other examples show similar patterns, i.e., identical reaction yet different regulation.

A most interesting family of multiple isozymes are class III adenylyl cyclases (AC) which are present in pro- as well as in eukaryotes. In the latter, only class IIIa isozymes are present whereas in bacteria classes IIIa to IIId forms exist (Linder and Schultz, 2003). These ACs catalyze the cyclization of ATP to the universal second messenger cyclic 3', 5'-AMP by an essentially identical reaction mechanism in an endothermic reaction driven by the hydrolysis of the product pyrophosphate (Hayaishi et al., 1971). In all instances, the active centers are dimeric.

Bacterial class III ACs are monomeric proteins, which homodimerize to form a catalytic center at the dimer interface. It is unknown whether this is of regulatory importance. In individual bacterial strains up to 30 class III AC isozymes have been identified, all containing highly similar catalytic domains (https://www.ncbi.nlm.nih.gov/Complete_Genomes/SignalCensus.html) (Bassler et al., 2018). A different picture emerges regarding associated domains which are not required for activity. In bacterial ACs numerous diverse N-terminal domains have been identified, among them membrane anchors of two, four or six predicted α -helices, and several distinct domains located between membrane anchor and catalytic domain (Linder and Schultz, 2003; Schultz and

Natarajan, 2013; Beltz et al., 2016; Bassler et al., 2018; Wissig et al., 2019). Thus, each of these bacterial AC isoforms probably is endowed with unique molecular features, which confer peculiar regulatory modalities, almost completely unexplored at this time (for representative samples see Figure 1 and (Bassler et al., 2018)). Another interesting question is why many bacteria contain multiple class III AC isozymes, e.g., 16 in *Mycobacterium tuberculosis* or 28 in *Sinorhizobium meliloti*. Notably, the AC CyaC from *Sinorhizobium* is regulated by its hexahelical membrane domain which contains a di-heme-B entity integrated in its membrane domain enabling regulation by oxidation-reduction processes (Wissig et al., 2019). The regulation of other bacterial ACs with hexahelical membrane domains is unknown. In general, very little is known about how the expression of multiple class III ACs in bacteria is coordinated. It is reasonable to assume that bacteria use the regulatory diversity of ACs to specifically respond to biochemical or biophysical cues when encountering variant environments. This area deserves further study in the future.

In contrast, the regulation of the nine membrane-delimited vertebrate AC isoforms (mACs) has been explored extensively, has often been reviewed over the years and this shall not be recapitulated here (Sinha and Sprang, 2006; Dessauer et al., 2017; Ostrom et al., 2022). The current canonical view is that



mammalian mACs are indirectly regulated via GPCR-receptor stimulation and subsequent cytosolic release of and activation by the G α s subunit of the trimeric G-proteins. Other regions have been implicated to different extents such as the N- and C-termini, and the long C1b loop connecting both halves of mAC proteins. In contrast, the extensive AC membrane anchors usually have not been implicated in direct regulatory processes of eukaryotic mACs. Since 2010, evidence emerged in our laboratory that the membrane domains might directly affect regulation of vertebrate mACs, i.e., may operate as receptors for yet unknown ligands (Kanchan et al., 2010; Winkler et al., 2012; Beltz et al., 2016; Seth et al., 2020).

Here, I present very extensive comparisons of eukaryotic mAC protein sequences, either comprising mACs of all nine AC isoforms together or of individual isoforms alone. Bioinformatics indicate that all domains, N-terminus, both hexahelical membrane anchor domains and C-terminal domains most likely have isoform-specific physiological roles which are distinct for every mAC isoform and subdomain. The existence of conserved cyclase-transducing elements (CTEs) between the exits of the two TM domains and the adjoining catalytic C1 and C2 domains strongly argues for a regulatory input *via* the membrane domains. This evidence is derived from evolutionary and genetic considerations, from sequence

and functional comparisons, from structural work and from our own ongoing experimental work. In this perspective these data are compiled and presented in easily comprehensible diagrams in which individual aa are hidden by respective shading.

The evolution of pseudoheterodimeric adenylyl cyclases

Bacterial and eukaryotic class III ACs including eukaryotic guanylyl cyclases have a common evolutionary root as reported earlier [Figure 2; (Bassler et al., 2018)]. Obviously, the eukaryotic mAC isoforms are the result of an early gene duplication and subsequent fusion event of one of the bacterial progenitor ACs. Many bacterial ACs have a single hexahelical membrane domain and an inactive catalytic domain which requires complementation by dimerization for enzymatic activity as exemplified by the mycobacterial AC Rv1625c (Guo et al., 2001). Both bacterial monomers participate equally in forming two productive active centers (Guo et al., 2001; Reddy et al., 2001; Sinha et al., 2005; TewsFindeisen et al., 2005). The first gene-duplication-fusion event most likely occurred early after the emergence of eukaryotic cells around 1.5 billion years ago resulting in a linked homodimeric protein (Farquhar et al., 2007; Bobrovskiy et al., 2018; Tang et al., 2020). Subsequent gene duplications concomitant with mutational diversification finally resulted in nine distinct and, importantly, functionally indispensable eukaryotic mAC isoforms. This process appears to have ended rather abruptly after about one billion years of evolution, i.e., around 0.5 billion years ago. Around this time the nine mAC isoforms as we know them today had evolved in the coelacanth and elephant shark. Interestingly, in these fish also soluble and membrane-bound guanylyl cyclases were identified indicating that at this point of evolution, i.e., 0.5 billion years ago, the separation of ACs and GCs was probably evolutionarily established. Coelacanth and elephant shark have a stable 0.5-billion-year evolutionary history and the last eukaryotic common ancestor these fish shared with humans was alive about 450 million years ago. For example, the mAC5 isoforms from human and coelacanth, and elephant shark, share overall 66% and 59% sequence identity, respectively. These considerations bolster the claim that at this point in evolution each isoform had acquired molecular features which were functionally indispensable for regulation of eukaryotic cells and organisms. Any subsequent mutational diversification obviously did not result in an added evolutionary advantage, rather, we can suppose, was detrimental. It appears then fair to state that each mAC isoform appears to be exceedingly well conserved across all species independently of their evolutionary position. Probably in this aeon also GPCRs and G-proteins evolved which are absent in archaea and eubacteria (Noonan et al., 2004;

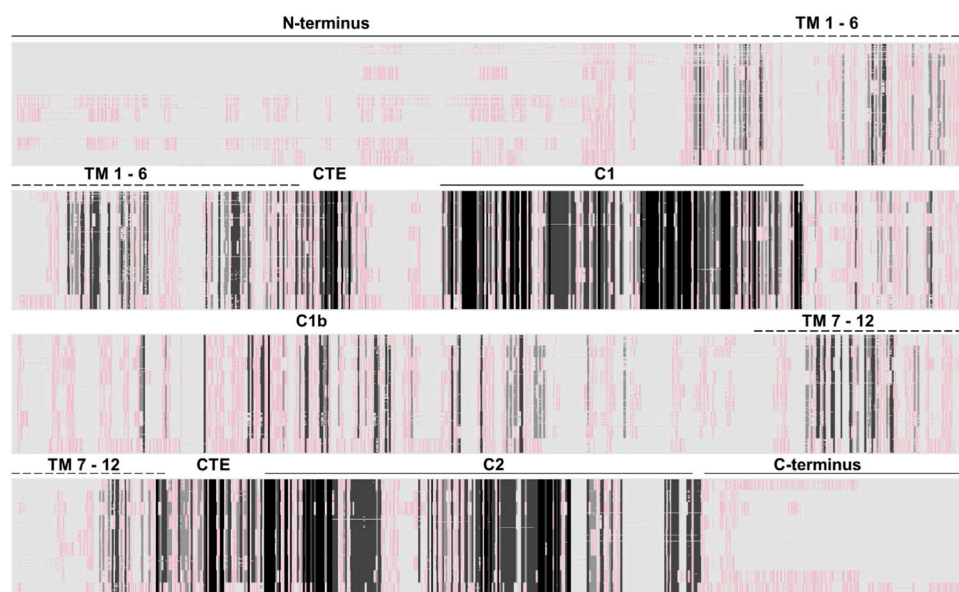


FIGURE 3

Alignment of 258 class III adenylyl cyclases about equally comprised of all nine isoforms (AC1 26 sequences; AC2, 25; AC3, 29; AC4, 30; AC5, 28; AC6, 30; AC7, 33; AC8, 28; AC9, 29). The approximate domain borders are indicated above. Clearly, the catalytic domains are cognizable as dark-shaded sections. All other domains, i.e., cytosolic N- and C-termini, the membrane domains and the cytosolic C1b linker are not conserved. The Clustal W alignment was adapted and shaded using the programme GeneDoc (<http://nrbsc.org/gfx/genedoc/>). Shading: black, invariant; dark grey, highly conserved; light grey, slightly conserved; whitish/reddish: fully diverged. A list of all mACs used for the alignment is attached at the end.

Anantharaman et al., 2011; Amemiya et al., 2013; Bradford et al., 2013).

In bacteria, a fused dimeric class III AC species is unknown. An open question is what is the advantage of a duplicated and fused AC protein compared to the bacterial monomer-dimer equilibrium? Conceivably, in a linked dimer the number and specificity of regulatory inputs could be considerably expanded (see below). Further, a physically linked dimer might respond to regulatory inputs more readily and reversibly.

Similarity of adenylyl cyclase isoforms

The genes of the human mAC isozymes are distributed over eight chromosomes, AC1 is on chromosome 7, AC2 on 5, AC3 on 2, AC4 on 14, AC5 on 3, AC6 on 12, AC7 on 16, AC8 on 8, and AC9 on 16. Probably, this suggests specific expression patterns, cellular localization, tissue distribution and specialized functions. No detailed studies are available on how expression of mAC isoforms is regulated in individual cells and tissues, and the question what induces and regulates the expression of a particular mAC isoform in a cell certainly needs further study. For a long time, it is known that several mAC isoforms can be simultaneously expressed in a single cell resulting in different mAC isozyme ratios. The physiological

mechanisms responsible for differential cellular expression patterns are unknown. Is the isozyme ratio in a cell stable over its lifetime or does it vary with development and aging? Distinct differences in cellular localization have been proposed and the concept of cAMP signaling compartmentation has been discussed in the past (Crossthwaite et al., 2005; Piggott et al., 2008; Ostrom et al., 2012; Scott et al., 2013; Cooper and Tabbasum, 2014; Johnstone et al., 2018). Another largely unanswered question is whether different mAC isozymes in a cell may be subject to distinct *direct* regulatory inputs, in addition to the well-established indirect activation *via* the GPCR axis. These findings and the number of unsolved questions suggests to consider that all mAC domains, cytosolic N- and C-termini, membrane anchors, catalytic domains, and the C1b linker regions which physically connect both halves of the protein, and possibly the C-termini are functionally indispensable, have distinct physiological roles and are required for regulating second messenger biosynthesis.

mACs are about similar in size, i.e., 1,065 (AC isoform 4)–1,353 amino acids long (AC isoform 9). A sequence alignment of 258 eukaryotic class III mAC isoforms shows that exclusively the two catalytic domains are conserved (Figure 3). All other domains are highly diverged. This is not surprising as mutations in the catalytic domains would have impaired enzyme activity and thus made the protein useless. In

contrast, mutational events in associated domains probably resulted in gain of additional functional features [see Figure 1 and (Schultz and Natarajan, 2013)]. Generally, the cytosolic N-termini which precede the first 6TM anchor domain differ with respect to length and sequence. Similarly, the subsequent first hexahelical membrane domain (TM1) is poorly conserved among isoforms beyond the general fact that the hydrophobic amino acids Ala, Val, Leu, Ile predominate in transmembrane helices. The extra- and intracellular stretches between the membranous α -helices are rather short (Beltz et al., 2016). The catalytic C1 domain is connected to TM1 by a linker of about 80 aa containing a conserved stretch of 19 amino acids which constitutes a cyclase-transducing-element, abbreviated CTE, by others termed helical domain (Ziegler et al., 2017; Qi et al., 2019). In all nine human isoforms it is positionally conserved with respect to the start of the first catalytic domain, C1. CTE_1 has an invariant center sequence of SxL/MP [(Ziegler et al., 2017) and see below]. The C1 domain is sequence and length conserved, and this extends to its bacterial progenitor isoforms [(Bassler et al., 2018), see below].

What follows is an extended cytosolic domain, termed C1b, which in mACs 1-8 is approximately 145 aa–174 aa long, in mAC9 it is 205 aa long. C1b is not conserved between isoforms. Upon C1b follows the second hexahelical membrane domain (TM2) which is diverged. The linker between the exit from α -helix 12 of TM2 to the second catalytic domain; C2 is shorter compared to the similarly positioned linker in the first half of the protein. It carries a second, conserved sequence of 19 aa, CTE_2, with an almost invariant center, NxLP, significantly deviating from the corresponding CTE_1 (Ziegler et al., 2017). The second catalytic domain is conserved. The C-terminal regions (7 to almost 100 aa) are diverged. Similar comparisons have been made in the past and have been presented in various alignment formats.

Examination of subdomain conservation in various categories of eukaryotic mAC isoforms

With the increasing number of fully sequenced vertebrate genomes comprehensive alignments allow valid predictions concerning potential mAC domain functions. Below I present exemplary samples of sequence comparisons of eukaryotic mAC domains using isoforms 1 to 9. In these alignments I span a huge evolutionary distance in each group with isoform sample sequences from the “living fossils” coelacanth and the elephant shark, birds, e.g., chicken, up to humans. The selected domain borders used for comparisons are uniform for all isoforms, however, due to inherent ambiguities should be considered as approximate borders. The presentation proceeds from N- to C-terminal.

The N-termini are isoform-specifically conserved

The N-termini of mACs are cytosolic. Potential bacterial progenitors have N-termini of variable length; sequence similarities are currently unknown. The biochemical and physiological functions of the N-termini of eukaryotic mACs have not been systematically investigated. An alignment of 258 N-termini (isoforms 1 through 9) shows no sequence conservation (see Figure 3). The N-termini vary in length from 6 aa to 240 aa. When examining N-termini of individual isoforms the situation changes profoundly (Figure 4). Most notably, the N-termini are isoform-specifically conserved for almost 0.5 billion years of evolution. Of note, all N-termini appear to have a short, invariant region ahead of the first α -helix of TM1. The length of the N-termini of mACs 3, 4, 6, 7, 8, and 9 is almost invariant (Figure 4). This suggests an indispensable physiological function which is currently unknown. Further to this point the isoform-singularity of the N-termini indicate that physiological functions of the N-termini vary with respect to isoform category. Presently, we can only speculate about potential functionalities, e.g., regulation of transcription, protein folding, targeted membrane insertion as reported for AC5 (Crossthwaite et al., 2005), cellular localization, and interactions with distinct regions of the catalytic dimer, possibly the C1b linker region or with other cellular proteins, as shown for the mAC2 and the A-kinase-anchoring protein Yotiao (Piggott et al., 2008).

The membrane anchors are fully diverged, yet isoform-specifically conserved

The AC membrane anchor consists of two separate hexahelical domains which were predicted at the time the first mAC sequence was reported (Krupinski et al., 1989). In 2019 this prediction was experimentally verified by the cryo-EM structure of an mAC9 holoenzyme (Qi et al., 2019). Structure predictions by AlphaFold uniformly indicate two intertwined hexahelical membrane domains forming an aggregated structural entity. Initially, the membrane anchors were suggested to possess a function as ion channel or transporter, properties which subsequently could not be experimentally demonstrated (Krupinski et al., 1989). Another physiological function of the membrane anchors beyond membrane-anchoring was never outright dismissed, yet it appears difficult to experimentally probe such a possibility (Schultz and Natarajan, 2013; Beltz et al., 2016).

The two hexahelical membrane domains show little conservation beyond the usual predominance of hydrophobic amino acids. The eukaryotic TM1 and TM2 membrane domains are dissimilar to their bacterial congeners (Beltz et al., 2016). After the primordial gene-duplication/fusion event which

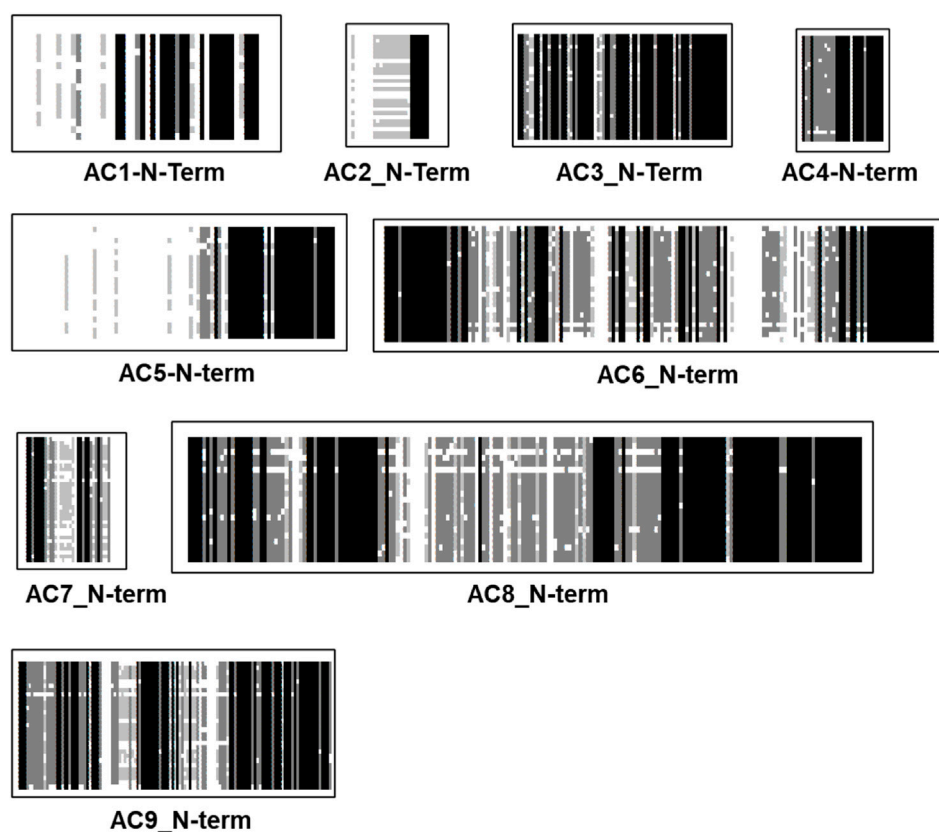


FIGURE 4

Alignment of N-termini of the nine mammalian mAC isoforms. mAC1: 19 isoforms were used, the N-terminus is 50 aa–60 aa long; mAC2: 27 isoforms; N-terminus rather variable between 6 aa and 50 aa. mAC3: 29 isoforms, length (77 aa) and sequence conserved. mAC4: 28 isoforms, length (28) and sequence conserved. mAC5: 28 isoforms of variable length (50 aa–240 aa); mAC6: 29 isoforms with an invariant 148 aa long, highly conserved N-terminus; mAC7: 34 isoforms, invariantly of 33 well conserved aa's; mAC8: 29 isoforms, highly conserved length of 180 aa. mAC9: 34 isoforms, uniform length of 120 highly conserved aa. Note the invariant region prior to TM1 in all isoforms except AC7. Shading: black, invariant; dark grey, conserved; light grey, slightly conserved; white: disparate.

involved a 6 TM bacterial AC progenitor mutational expansion of all domains except the catalytic domains progressed. Aligning TM1 and TM2 domains from 258 mACs isoforms 1 through 9 shows no sequence conservation (Figure 3). This demonstrates that in a time span of about 1 billion years of evolution the TM domains have isoform-specifically diverged beyond recognition from the supposed primordial bacterial fusion product with two identical membrane domains. Further, the TM1 and TM2 domains of every individual isoform when aligned against each other according to the α -helix predictions possess no sequence similarity.

Strikingly, different pictures emerge when TM1 or TM2 domains of individual isoforms from creatures of vastly different evolutionary positions are aligned. The results unequivocally demonstrate an almost complete sequence conservation for about 500 million years, confirming again the fact that most of mAC evolution stopped at around this point in

time. As an example, I present the alignment of TM1 of mAC3 (28 isoforms) and mAC8 (34 isoforms). mAC isoforms 3 and 8 are usually grouped together with mAC1 in one category because these isoforms are Ca^{2+} -stimulated (other categories comprise $\text{G}\beta\gamma$ -stimulated mAC2, 4, 7; $\text{Gi}\alpha/\text{Ca}^{2+}$ -inhibited AC5 and 6, and supposedly forskolin-insensitive mAC9 (Sadana and Dessauer, 2009)). An alignment of the TM1 domains from mAC3 and 8 illustrates how different they are from each other (Figure 5 top). Of note, the last α -helix of this membrane domain shows an invariant stretch of 4 aa (LY/FMC) and an exactly spaced Gly. However, when TM1 domains from either mAC3 or mAC8 alone are aligned the unique identity is evident (Figure 5, middle and bottom).

I have systematically carried out such comparative alignments using all nine eukaryotic mAC isoforms with identical results: all TM1 membrane regions are highly conserved in an isoform specific manner across all species, yet are highly diverged when aligned

pairwise in differing combinations or all together (see Figure 3). The same situation prevails when aligning the TM2 domains, i.e., in all animal species a high degree of sequence conservation within one isoform, yet no significant similarities when aligning TM2 domains from different mAC isoforms.

These sequence comparisons further confirm our earlier cluster analyses for mAC transmembrane domains. In these studies, the TM1 and TM2 domains clearly segregated according to isoform and the differences between TM1 and TM2 domains were resolved (Beltz et al., 2016). Previously, we had demonstrated, that it is impossible to generate chimeric mammalian mACs in which the membrane domains from different AC isoforms were combined (Seebacher et al., 2001). Thus, one can confidently conclude that TM1 and TM2 domains are not only highly isoform specific but share a pair-wise evolution, i.e., they are preserved as a functional pair for >450 million years. Clearly TM1 and TM2 domains evolved jointly to interact with each other. These observations indicate that the function of the dodeca-helical membrane domain of eukaryotic ACs is functionally not sufficiently described when attributing exclusively a simple anchoring function. We have proposed a receptor function for yet unknown ligands which directly modulate the extent of Gsa activation (Beltz et al., 2016; Ziegler et al., 2017; Seth et al., 2020).

The conserved cyclase-transducing-elements

Evidently, this view is considerably bolstered by an analysis of the 19 aa long Cyclase-Transducing-Elements [CTE, (Vercellino et al., 2017; Ziegler et al., 2017)]. The CTEs are positioned between the membrane exit of TM1 or TM2, respectively, and the start of the subsequent catalytic regions, C1 or C2. CTE₁ and CTE₂ sequences differ. In a chimeric construct consisting of the hexahelical quorum sensing receptor LqsS from *Legionella pneumophila* and the mycobacterial AC Rv1625c it was demonstrated that the mycobacterial CTE is indispensable for signal transmission (Ziegler et al., 2017). A high resolution cluster analysis of the CTEs of eukaryotic mAC isoforms unequivocally demonstrated that they are position - and isoform-specifically conserved during evolution (Figure 6). This is almost unequivocal evidence that these CTEs must have an essential role in transmembrane signaling. Obviously, the catalytic domains are subjects of regulation by membrane signals and the CTEs are crucially positioned at the intersection (Ziegler et al., 2017).

The catalytic domains C1 and C2

The vertebrate mACs are termed “pseudoheterodimers” which denotes the identical domain compositions and sequences. That the AC signaling system evolved from a

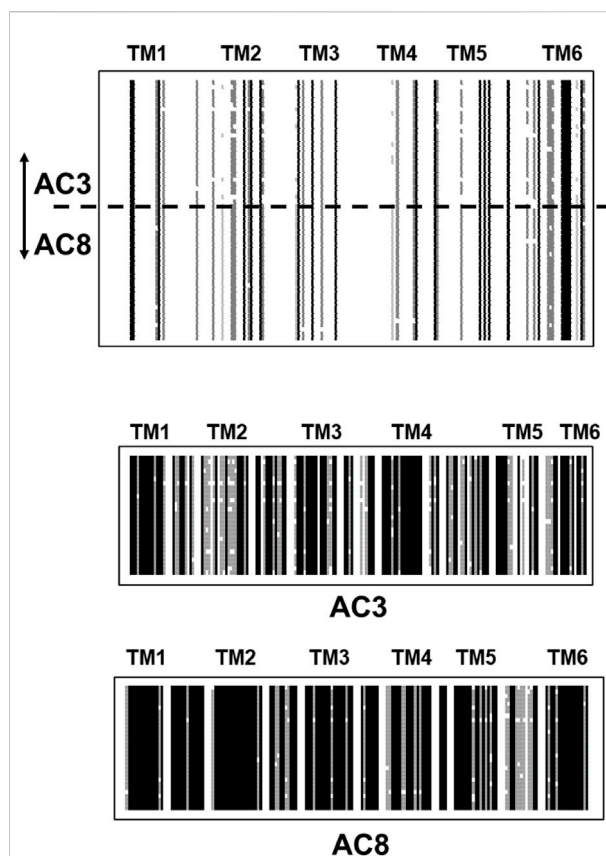


FIGURE 5

Top: Alignment of the first hexahelical membrane domains of mAC isoforms 3 (28 isoforms) and 8 (34 isoforms). The joint alignment shows scant conservation between the domains from mAC3 and 8. Single α -helices are indicated above the sequences. Below: alignments of the TM1 domains from mAC3 and mAC8. Note the high degree of conservation across a large variety of species. Shading: black, invariant; dark grey, conserved; light grey, slightly conserved; white: disparate. (Sequences used: AC3: *Callithrix jacchus*; alligator; antelope; *ceratotherium simum simum*; brown bat; chicken; chinchilla; desert mouse; dog; falcon; *Mustela putorius furo*; frog; goat; guinea pig; hog; horse; human; macaque; mouse; *Heterocephalus*; orca; coelacanth; rat; manatee; sheep; turtle; catfish. AC8: *myotis brandtii*; *Bos taurus*; camel; cat; chicken; dog; *Mustela putorius furo*; frog; gibbon; guinea pig; hog; human; hedgehog; lemur; macaque; monkey; mouse; *Heterocephalus*; rhino; orca; baboon; *Ochotona princeps*; pigeon; rat; manatee; sheep; *Melopsittacus undulatus*; squirrel; vicuna; walrus).

bacterial progenitor is most clearly shown by aligning the nine C1 or C2 catalytic domains \pm the single catalytic domain from the mycobacterial AC Rv1625c, a potential progenitor (Figure 7). Due to the evolutionary history from cyanobacteria to mammals it is unsurprising that to conserve enzymatic functionality the catalytic domains of class III ACs display pronounced sequence similarities (Linder and Schultz, 2003). In the physically linked vertebrate “AC-dimers” the two catalytic domains C1 and C2 diverged only slightly. The catalytic amino acids, positionally conserved, are distributed between the C1 and C2 domains (Tesmer and Sprang, 1998). Neither

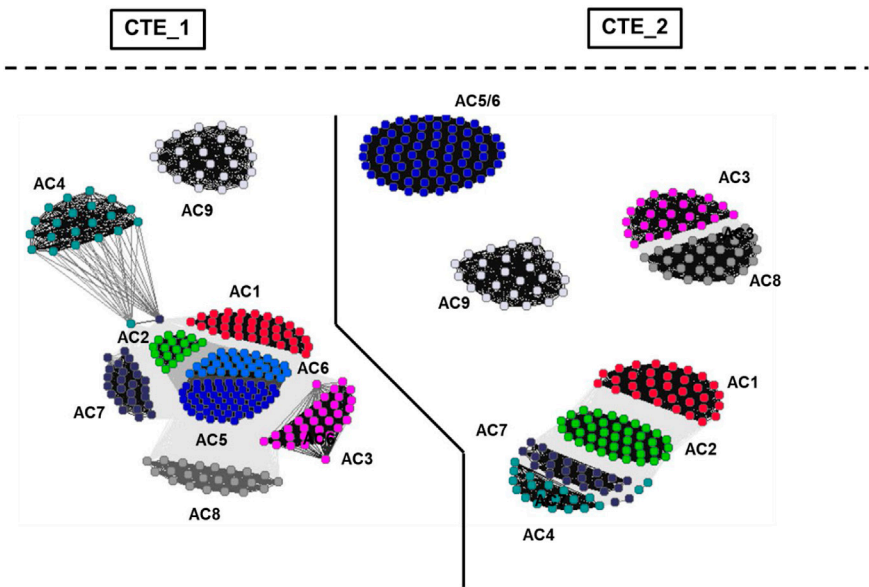


FIGURE 6
Cluster map of cyclase-transducing-elements (CTEs). For preparation of the figure, the data set from Ziegler et al. (2017) was used. The bacterial sequences were removed and vertebrate class IIIa CTEs were analyzed using CLANS (Frickey and Lupas, 2004). Each dot represents a single sequence. The CTE_1 and CTE_2 sectors are separated by a solid line. Cluster labeling indicates the mAC isoform. The segregation shows that CTEs from class IIIa ACs are highly specific for their C1- and C2-domain origins as well as for AC isoforms.

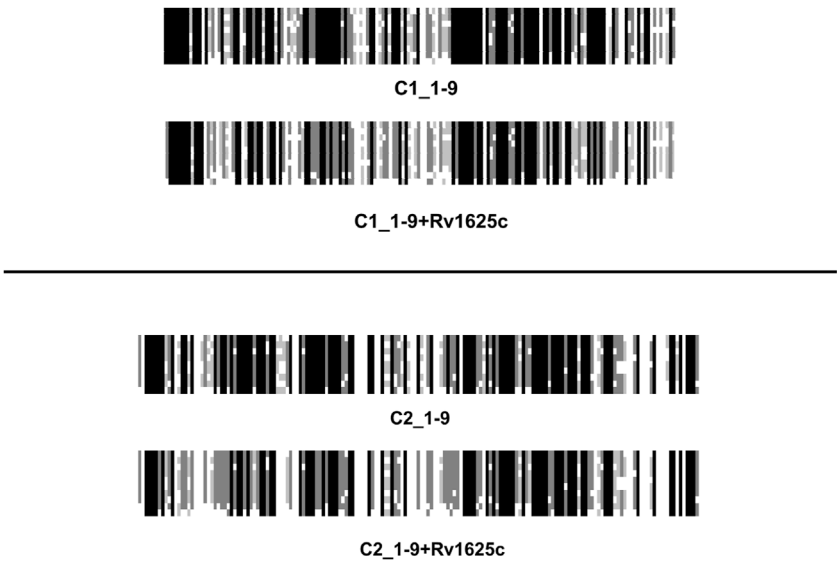


FIGURE 7
An alignment of the C1 and C2 catalytic domains from human adenylyl cyclases isoforms 1 through 9 ± the catalytic domain from the mycobacterial adenylyl cyclase Rv1625c.

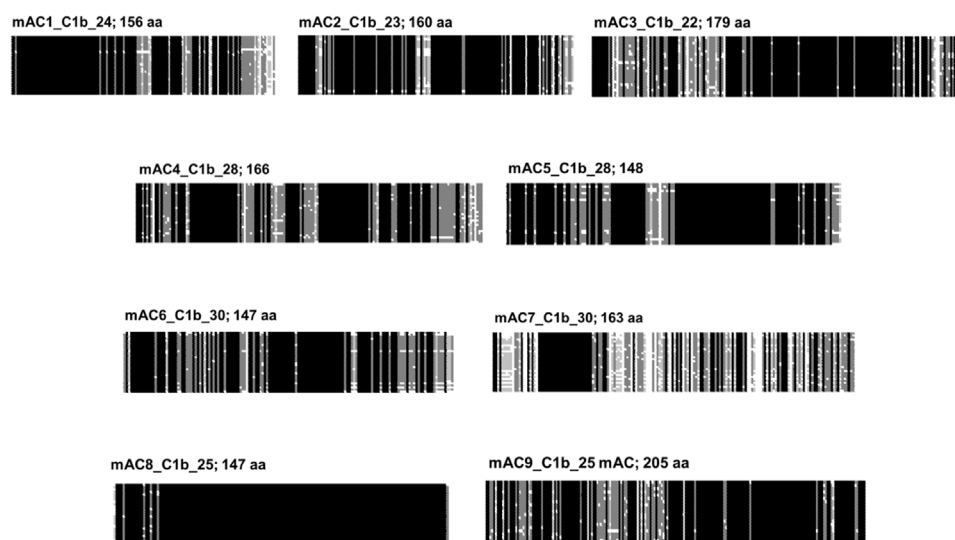


FIGURE 8

Alignment of the C1b subdomains of the mammalian mAC isoforms. The number of isozyms used for each alignment and the respective C-terminal lengths are indicated above. Shading: black, invariant; dark grey, conserved; light grey, slightly conserved; white: disparate.

C1 nor C2 by itself has catalytic activity. Extensive evolutionary mutations in the catalytic domains probably would have compromised activity and abolished system signaling capability. The major evolutionary gain in eukaryotic mACs then appears to be the acquisition regulation by G-proteins. Over the years we have been unable to unlock the molecular determinants which finally enable G-protein activation. We generated > 100 purposeful mutations in the mycobacterial mAC Rv1625c without attaining G-protein sensitivity (unpublished). The available structures of eukaryotic mACs obviously do not yet give a picture detailed enough to show exactly how G α -binds to and initiates the conformational changes leading to activation of the catalytic heterodimer (Tesmer et al., 1997; Dessauer et al., 1998; Tesmer and Sprang, 1998; Tesmer et al., 1999; Qi et al., 2019).

The C1b domain

C1b connects the halves of the pseudoheterodimer. Formally, one may assume that in the fusion event C1b originated from the C-terminus of the first half and the N-terminus of the second half. Resemblances to such partial sequences have not been identified, probably due to mutational adaptations during evolution. Combined alignments of C1b regions from 258 eukaryotic mAC isoforms show no similarity (see Figure 3). The conservation among any category of isoforms, however, is very high (Figure 8). This should be taken as an indication of an evolutionary functionalization of the C1b region fitting

each mAC isoform with a peculiar regulatory potential. In fact, in the past the C1b region has been studied as a calmodulin-binding region in mAC isoforms, target of phosphorylation and of Ca²⁺-binding modulating activity.

The C-terminal domains

Formally, the mAC C-terminal corresponds to the C1b region of the monomeric progenitor. Therefore, it is often termed C2b. Compared with C1b the sequences (148 aa–205 aa long) the C2b are shorter (25 aa–110 aa). No similarity is detected. The C-termini in general are diverged when compared as a set of 258 mACs (Figure 3), yet as with the other subdomains of mACs are highly conserved among isoforms (Figure 9). This would afford them distinct roles in mAC regulation. The general diversity and isoform conformity is indicative that no uniform functionality may be expected but functions tailored by evolution for each isoform.

Discussion

The establishment of conserved sequence patterns of the nine eukaryotic mACs is necessarily a reduction which simplifies the complexity of mAC regulation. Yet even as a superficial sequence analysis it proves beyond a reasonable doubt that the system evolved up to a point around 0.5 billion years ago at which it reached a final state of functionality and, concomitantly, importance in regulating essential life functions. Obviously, this

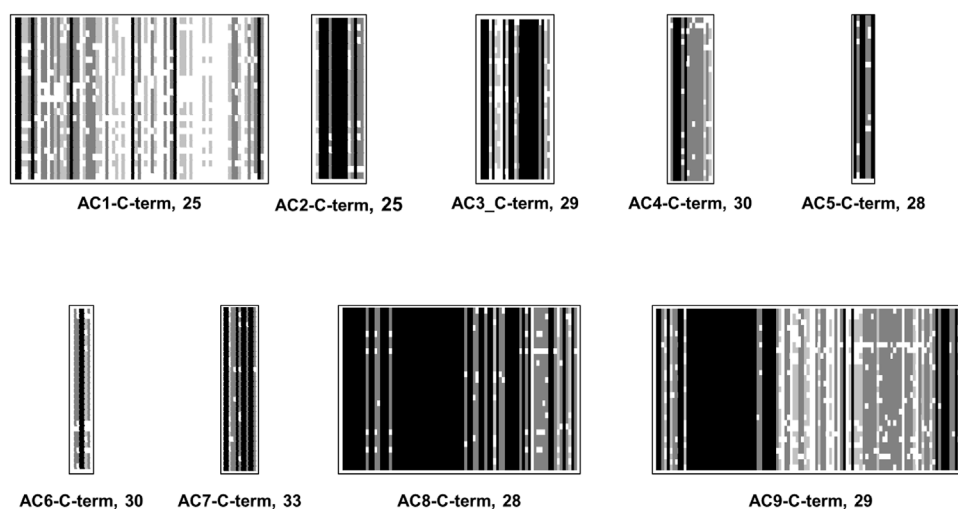


FIGURE 9

Alignment of C-termini of mammalian mAC isoforms. For each mAC isoform the number of analyzed proteins is indicated. mAC1: C-terminus is 65 aa–75 aa long. mAC2: C-terminus is uniformly 25 aa long. mAC3: C-terminus is 25 aa long. mAC4: length is 15 aa. AC5: length invariably 7 aa. mAC6: length 6 aa–7 aa. mAC7: 13 aa long; mAC8: highly conserved with a length of 81 aa. mAC9: uniform length of 110/111 aa's. Shading: black, invariant; dark grey, conserved; light grey, slightly conserved; white: disparate.

final evolutionary status of eukaryotic mAC isoforms was not visibly affected by subsequent events of whole-genome duplication in teleost's about 350 to 216 million years ago (Glasauer and Neuhauss, 2014; Davesne et al., 2021), or the genome duplication in salmonids around 95 million years ago (Robertson et al., 2017). So, a comprehensive comparative analysis of protein sequences of mAC isoforms is presented. As such, this does not permit specific predictions concerning regulatory modalities connected with a specific subdomain. However, it should be helpful to focus future questions and experimental approaches systematically for each isoform on rather distinct domains of a mAC isoform. The established patterns of mAC regulation, as reported in the past (Sunahara et al., 1996; Sadana and Dessauer, 2009) should now be centered on individual isoforms and particular subdomains thereof. Each domain, i.e., N-termini, TM1 and TM2, C1b and C-termini appear to be fine-tuned to a specific isoform. It appears likely that patterns of regulatory inputs presently attributed to several isoforms are only an approximation.

In fact, over the years essentially all subdomains except for the TM1 and TM2 membrane anchors were implicated in one way or the other in regulatory mechanisms. The N-terminus of mAC isoform 6 was implicated in Gai inhibition (Kao et al., 2004). The N-terminus of mAC8 was reported to bind protein phosphatase 2A (Crossthwaite et al., 2006; Simpson et al., 2006). The C1b region jointly with the N-terminus of mAC7 was implicated in the regulation by the G_{13} pathway (Jiang et al., 2013). The C-terminus of mAC2 has been implicated in regulation by phosphorylation (Levin and Reed, 1995; Böl et al., 1997a; Böl et al., 1997b; Pálvolgyi et al., 2018) and in mAC9 C2b region is implicated in autoinhibition (Vercellino

et al., 2017; Qi et al., 2019; Qi et al., 2022). In mAC8 C2b has been reported as autoinhibitory and to contribute to the stimulation of the enzyme with Ca^{2+} /calmodulin (Macdougall et al., 2009). An excellent example of the regulatory partition of the mAC subdomains may be the multiple mutations of mAC5 identified in humans. Thirteen point mutations have been identified. Affected are the N-terminus, the C1 domain, C1b domain, α -helix 7 of TM2, C2, and the C-terminus. Each mutation results in a distinct clinical pattern of hyperkinetic disorders (Ferrini et al., 2021).

A notable property of vertebrate mAC isozymes are the succinct differences of their 6TM membrane anchors. We can assume that after the early evolutionary dimerization event considerable diversification of the 6TM subdomains occurred. This fact may be interpreted in two ways: 1) the membrane domains may simply anchor the ACs into the cellular membrane and are otherwise physiologically inconsequential. The mutational diversifications may be fortuitous and of no further functional meaning. From this follows that one ascribes regulation of AC activity solely to the cytosolic portions of the proteins. 2) the succinct differences in membrane domains may be and, in the opinion of this author, should be taken as a sign of distinct regulatory properties affecting transmembrane signaling. One must ask why do nine vertebrate AC isoforms exist when these proteins anyway are uniformly activated by cytosolic Gsa, released upon GPCR activation and by forskolin, a non-physiologic activator of mAC isoforms (Seth et al., 2020)? To this author, signalling compartmentation appears a rather meager argument for disputing a regulatory functionality of the diverged membrane

anchor. To plausibly explain how cAMP levels are regulated in mammals it will be necessary to incorporate a major and highly specific functionality of the membrane anchors. Needless to state that the consequences for physiology, pharmacology and the potential for development of therapeutics is enormous. With no chemically identified ligand the acceptance of a receptor hypothesis is, however, currently depending on whether one is willing to accept bioinformatic data as solid evidence and guidance for further explorations.

Data availability statement

The datasets presented in this study can be found in online repositories. The names of the repository/repositories and accession number(s) can be found in the article/[Supplementary Material](#).

Author contributions

The author confirms being the sole contributor of this work and has approved it for publication.

Funding

Our work is supported by the Deutsche Forschungsgemeinschaft (Schu275/45) and institutional funds from the Max-Planck-Society. The funders had no role in writing this ms.

References

- Amemiya, C. T., Alföldi, J., Lee, A. P., Fan, S., Philippe, H., Maccallum, I., et al. (2013). The African coelacanth genome provides insights into tetrapod evolution. *Nature* 496, 311–316. doi:10.1038/nature12027
- Anantharaman, V., Abhiman, S., de Souza, R. F., and Aravind, L. (2011). Comparative genomics uncovers novel structural and functional features of the heterotrimeric GTPase signaling system. *Gene* 475, 63–78. doi:10.1016/j.gene.2010.12.001
- Bassler, J., Schultz, J. E., and Lupas, A. N. (2018). Adenylate cyclases: Receivers, transducers, and generators of signals. *Cell Signal* 46, 135–144. doi:10.1016/j.cellsig.2018.03.002
- Beltz, S., Bassler, J., and Schultz, J. E. (2016). Regulation by the quorum sensor from *Vibrio* indicates a receptor function for the membrane anchors of adenylate cyclases. *Elife* 5, e13098. doi:10.7554/eLife.13098
- Bobrovskiy, I., Hope, J. M., Ivantsov, A., Nettersheim, B. J., Hallmann, C., and Brocks, J. J. (2018). Ancient steroids establish the Ediacaran fossil Dickinsonia as one of the earliest animals. *Science* 361, 1246–1249. doi:10.1126/science.aat7228
- Böl, G. F., Gros, C., Hülster, A., Bösel, A., and Pfeuffer, T. (1997). Phorbol ester-induced sensitization of adenylate cyclase type II is related to phosphorylation of threonine 1057. *Biochem. Biophys. Res. Commun.* 237, 251–256. doi:10.1006/bbrc.1997.7123
- Böl, G. F., Hülster, A., and Pfeuffer, T. (1997). Adenylate cyclase type II is stimulated by PKC via C-terminal phosphorylation. *Biochim. Biophys. Acta* 1358, 307–313. doi:10.1016/s0167-4889(97)00073-6
- Bradford, W., Buckholz, A., Morton, J., Price, C., Jones, A. M., and Urano, D. (2013). Eukaryotic G protein signaling evolved to require G protein-coupled receptors for activation. *Sci. Signal* 6, ra37. doi:10.1126/scisignal.2003768
- Cooper, D. M., and Tabbasum, V. G. (2014). Adenylate cyclase-centred microdomains. *Biochem. J.* 462, 199–213. doi:10.1042/BJ20140560
- Crossthwaite, A. J., Ciruela, A., Rayner, T. F., and Cooper, D. M. (2006). A direct interaction between the N terminus of adenylate cyclase AC8 and the catalytic subunit of protein phosphatase 2A. *Mol. Pharmacol.* 69, 608–617. doi:10.1124/mol.105.018275
- Crossthwaite, A. J., Seebacher, T., Masada, N., Ciruela, A., Dufraux, K., Schultz, J. E., et al. (2005). The cytosolic domains of Ca²⁺-sensitive adenylate cyclases dictate their targeting to plasma membrane lipid rafts. *J. Biol. Chem.* 280, 6380–6391. doi:10.1074/jbc.M411987200
- Davesne, D., Friedman, M., Schmitt, A. D., Fernandez, V., Carnevale, G., Ahlberg, P. E., et al. (2021). Fossilized cell structures identify an ancient origin for the teleost whole-genome duplication. *Proc. Natl. Acad. Sci. U. S. A.* 118, e2101780118. doi:10.1073/pnas.2101780118
- Dessauer, C. W., Tesmer, J. J., Sprang, S. R., and Gilman, A. G. (1998). Identification of a G α binding site on type V adenylate cyclase. *J. Biol. Chem.* 273, 25831–25839. doi:10.1074/jbc.273.40.25831
- Dessauer, C. W., Watts, V. J., Ostrom, R. S., Conti, M., Dove, S., and Seifert, R. (2017). International union of basic and clinical pharmacology. CI. Structures and small molecule modulators of mammalian adenylate cyclases. *Pharmacol. Rev.* 69, 93–139. doi:10.1124/pr.116.013078
- Farquhar, J., Peters, M., Johnston, D. T., Strauss, H., Masterson, A., Wiechert, U., et al. (2007). Isotopic evidence for Mesozoic anoxia and changing atmospheric sulphur chemistry. *Nature* 449, 706–709. doi:10.1038/nature06202
- Ferrini, A., Steel, D., Barwick, K., and Kurian, M. A. (2021). An update on the phenotype, genotype and neurobiology of ADCY5-related disease. *Mov. Disord.* 36, 1104–1114. doi:10.1002/mds.28495
- Frickey, T., and Lupas, A. (2004). Clans: A java application for visualizing protein families based on pairwise similarity. *Bioinformatics* 20, 3702–3704. doi:10.1093/bioinformatics/bth444

Acknowledgments

Our work is supported by the Deutsche Forschungsgemeinschaft and institutional funds from the Max-Planck-Society.

Conflict of interest

The author declares that the research was conducted in the absence of any commercial or financial relationships that could be construed as a potential conflict of interest.

Publisher's note

All claims expressed in this article are solely those of the authors and do not necessarily represent those of their affiliated organizations, or those of the publisher, the editors and the reviewers. Any product that may be evaluated in this article, or claim that may be made by its manufacturer, is not guaranteed or endorsed by the publisher.

Supplementary material

The Supplementary Material for this article can be found online at: <https://www.frontiersin.org/articles/10.3389/fphar.2022.1009797/full#supplementary-material>

- Glasauer, S. M., and Neuhaus, S. C. (2014). Whole-genome duplication in teleost fishes and its evolutionary consequences. *Mol. Genet. Genomics* 289, 1045–1060. doi:10.1007/s00438-014-0889-2
- Guo, Y. L., Seebacher, T., Kurz, U., Linder, J. U., and Schultz, J. E. (2001). Adenylyl cyclase Rv1625c of *Mycobacterium tuberculosis*: A progenitor of mammalian adenylyl cyclases. *EMBO J.* 20, 3667–3675. doi:10.1093/emboj/20.14.3667
- Hayaishi, O., Greengard, P., and Colowick, S. P. (1971). On the equilibrium of the adenylate cyclase reaction. *J. Biol. Chem.* 246, 5840–5843. doi:10.1016/s0021-9258(18)61884-8
- Jiang, L. I., Wang, J. E., and Sternweis, P. C. (2013). Regions on adenylyl cyclase VII required for selective regulation by the G13 pathway. *Mol. Pharmacol.* 83, 587–593. doi:10.1124/mol.112.082446
- Johnstone, T. B., Agarwal, S. R., Harvey, R. D., and Ostrom, R. S. (2018). cAMP signaling compartmentation: Adenylyl cyclases as anchors of dynamic signaling complexes. *Mol. Pharmacol.* 93, 270–276. doi:10.1124/mol.117.110825
- Kanchan, K., Linder, J. U., Winkler, K., Hantke, K., Schultz, A., and Schultz, J. E. (2010). Transmembrane signaling in chimeras of the *Escherichia coli* aspartate and serine chemotaxis receptors and bacterial class III adenylyl cyclases. *J. Biol. Chem.* 285, 2090–2099. doi:10.1074/jbc.M109.051698
- Kao, Y. Y., Lai, H. L., Hwang, M. J., and Chern, Y. (2004). An important functional role of the N terminus domain of type VI adenylyl cyclase in Galphai-mediated inhibition. *J. Biol. Chem.* 279, 34440–34448. doi:10.1074/jbc.M401952200
- Krupinski, J., Coussen, F., Bakalyar, H. A., Tang, W. J., Feinstein, P. G., Orth, K., et al. (1989). Adenylyl cyclase amino acid sequence: Possible channel- or transporter-like structure. *Science* 244, 1558–1564. doi:10.1126/science.2472670
- Levin, L. R., and Reed, R. R. (1995). Identification of functional domains of adenylyl cyclase using *in vivo* chimeras. *J. Biol. Chem.* 270, 7573–7579. doi:10.1074/jbc.270.13.7573
- Linder, J. U., and Schultz, J. E. (2003). The class III adenylyl cyclases: Multi-purpose signalling modules. *Cell Signal* 15, 1081–1089. doi:10.1016/s0898-6568(03)00130-x
- Macdougall, D. A., Wachten, S., Ciruela, A., Sinz, A., and Cooper, D. M. (2009). Separate elements within a single IQ-like motif in adenylyl cyclase type 8 impart Ca^{2+} /calmodulin binding and autoinhibition. *J. Biol. Chem.* 284, 15573–15588. doi:10.1074/jbc.M809585200
- Noonan, J. P., Grimwood, J., Danke, J., Schmutz, J., Dickson, M., Amemiya, C. T., et al. (2004). Coelacanth genome sequence reveals the evolutionary history of vertebrate genes. *Genome Res.* 14, 2397–2405. doi:10.1101/gr.2972804
- Ostrom, K. F., LaVigne, J. E., Brust, T. F., Seifert, R., Dessauer, C. W., Watts, V. J., et al. (2022). Physiological roles of mammalian transmembrane adenylyl cyclase isoforms. *Physiol. Rev.* 102, 815–857. doi:10.1152/physrev.00013.2021
- Ostrom, R. S., Bogard, A. S., Gros, R., and Feldman, R. D. (2012). Choreographing the adenylyl cyclase signalosome: Sorting out the partners and the steps. *Naunyn-Schmiedeberg Arch. Pharmacol.* 385, 5–12. doi:10.1007/s00210-011-0696-9
- Pálvölgyi, A., Simpson, J., Bodnár, I., Bíró, J., Palkovits, M., Radovits, T., et al. (2018). Auto-inhibition of adenylyl cyclase 9 (AC9) by an isoform-specific motif in the carboxyl-terminal region. *Cell Signal* 51, 266–275. doi:10.1016/j.cellsig.2018.08.010
- Piggott, L. A., Bauman, A. L., Scott, J. D., and Dessauer, C. W. (2008). The A-kinase anchoring protein Yotiao binds and regulates adenylyl cyclase in brain. *Proc. Natl. Acad. Sci. U. S. A.* 105, 13835–13840. doi:10.1073/pnas.0712100105
- Qi, C., Lavriha, P., Mehta, V., Khanppanavar, B., Mohammed, I., Li, Y., et al. (2022). Structural basis of adenylyl cyclase 9 activation. *Nat. Commun.* 13, 1045. doi:10.1038/s41467-022-28685-y
- Qi, C., Sorrentino, S., Medalia, O., and Korkhov, V. M. (2019). The structure of a membrane adenylyl cyclase bound to an activated stimulatory G protein. *Science* 364, 389–394. doi:10.1126/science.aav0778
- Reddy, S. K., Kamireddy, M., Dhanireddy, K., Young, L., Davis, A., and Reddy, P. T. (2001). Eukaryotic-like adenylyl cyclases in *Mycobacterium tuberculosis* H37Rv: Cloning and characterization. *J. Biol. Chem.* 276, 35141–35149. doi:10.1074/jbc.M104108200
- Robertson, F. M., Gundappa, M. K., Grammes, F., Hvidsten, T. R., Redmond, A. K., Lien, S., et al. (2017). Lineage-specific rediploidization is a mechanism to explain time-lags between genome duplication and evolutionary diversification. *Genome Biol.* 18, 111. doi:10.1186/s13059-017-1241-z
- Sadana, R., and Dessauer, C. W. (2009). Physiological roles for G protein-regulated adenylyl cyclase isoforms: Insights from knockout and overexpression studies. *Neurosignals* 17, 5–22. doi:10.1159/000166277
- Schultz, J. E., and Natarajan, J. (2013). Regulated unfolding: A basic principle of intraprotein signaling in modular proteins. *Trends Biochem. Sci.* 38, 538–545. doi:10.1016/j.tibs.2013.08.005
- Scott, J. D., Dessauer, C. W., and Taskén, K. (2013). Creating order from chaos: Cellular regulation by kinase anchoring. *Annu. Rev. Pharmacol. Toxicol.* 53, 187–210. doi:10.1146/annurev-pharmtox-011112-140204
- Seebacher, T., Linder, J. U., and Schultz, J. E. (2001). An isoform-specific interaction of the membrane anchors affects mammalian adenylyl cyclase type V activity. *Eur. J. Biochem.* 268, 105–110. doi:10.1046/j.1432-1327.2001.01850.x
- Seth, A., Finkbeiner, M., Grischin, J., and Schultz, J. E. (2020). Gsa stimulation of mammalian adenylyl cyclases regulated by their hexahelical membrane anchors. *Cell Signal* 68, 109538. doi:10.1016/j.cellsig.2020.109538
- Simpson, R. E., Ciruela, A., and Cooper, D. M. F. (2006). The role of calmodulin recruitment in Ca^{2+} stimulation of adenylyl cyclase type 8. *J. Biol. Chem.* 281, 17379–17389. doi:10.1074/jbc.M510992200
- Sinha, S. C., and Sprang, S. R. (2006). Structures, mechanism, regulation and evolution of class III nucleotidyl cyclases. *Rev. Physiol. Biochem. Pharmacol.* 157, 105–140. doi:10.1007/112_0603
- Sinha, S. C., Wetterer, M., Sprang, S. R., Schultz, J. E., and Linder, J. U. (2005). Origin of asymmetry in adenylyl cyclases: Structures of *Mycobacterium tuberculosis* Rv1900c. *EMBO J.* 24, 663–673. doi:10.1038/sj.emboj.7600573
- Sunahara, R. K., Dessauer, C. W., and Gilman, A. G. (1996). Complexity and diversity of mammalian adenylyl cyclases. *Annu. Rev. Pharmacol. Toxicol.* 36, 461–480. doi:10.1146/annurev.pa.36.040196.002333
- Tang, Q., Pang, K., Yuan, X., and Xiao, S. (2020). A one-billion-year-old multicellular chlorophyte. *Nat. Ecol. Evol.* 4, 543–549. doi:10.1038/s41559-020-1122-9
- Tesmer, J. J. G., Sunahara, R. K., Johnson, R. A., Gosselin, G., Gilman, A. G., and Sprang, S. R. (1999). Two-metal-ion catalysis in adenylyl cyclase. *Science* 285, 756–760. doi:10.1126/science.285.5428.756
- Tesmer, J. J., and Sprang, S. R. (1998). The structure, catalytic mechanism and regulation of adenylyl cyclase. *Curr. Opin. Struct. Biol.* 8, 713–719. doi:10.1016/s0959-440x(98)80090-0
- Tesmer, J. J., Sunahara, R. K., Gilman, A. G., and Sprang, S. R. (1997). Crystal structure of the catalytic domains of adenylyl cyclase in a complex with G α TPgammaS. *Science* 278, 1907–1916. doi:10.1126/science.278.5345.1907
- TewsFindeisen, F., Findeisen, I., Sinning, A., Schultz, J. E., Schultz, J. U., and Linder, J. U. (2005). The structure of a pH-sensing mycobacterial adenylyl cyclase holoenzyme. *Science* 308, 1020–1023. doi:10.1126/science.1107642
- Vercellino, I., Rezabkova, L., Olieric, V., Polyhach, Y., Weinert, T., Kammerer, R. A., et al. (2017). Role of the nucleotidyl cyclase helical domain in catalytically active dimer formation. *Proc. Natl. Acad. Sci. U. S. A.* 114, E9821–E9828. doi:10.1073/pnas.1712621114
- Winkler, K., Schultz, A., and Schultz, J. E. (2012). The S-helix determines the signal in a Tsr receptor/adenylyl cyclase reporter. *J. Biol. Chem.* 287, 15479–15488. doi:10.1074/jbc.M112.348409
- Wissig, J., Grischin, J., Bassler, J., Schubert, C., Friedrich, J. E., Bähre, G., et al. (2019). CyaC, a redox-regulated adenylate cyclase of *Sinorhizobium meliloti* with a quinone responsive di-heme-B membrane anchor domain. *Mol. Microbiol.* 112, 16–28. doi:10.1111/mmi.14251
- Ziegler, M., Bassler, J., Beltz, S., Schultz, A., Lupas, A. N., and Schultz, J. E. (2017). Characterization of a novel signal transducer element intrinsic to class IIIa/b adenylate cyclases and guanylate cyclases. *FEBS J.* 284, 1204–1217. doi:10.1111/febs.14047



OPEN ACCESS

EDITED BY
Tarsis Brust,
aTyr Pharma, United States

REVIEWED BY
Carmen W. Dessauer,
University of Texas Health Science
Center at Houston, United States
Victoria Macht,
University of North Carolina at Chapel
Hill, United States

*CORRESPONDENCE
Boris Tabakoff,
boris.tabakoff@cuanschutz.edu

SPECIALTY SECTION
This article was submitted to
Experimental Pharmacology and Drug
Discovery,
a section of the journal
Frontiers in Pharmacology

RECEIVED 04 August 2022
ACCEPTED 07 October 2022
PUBLISHED 28 October 2022

CITATION
Tabakoff B and Hoffman PL (2022), The
role of the type 7 adenylyl cyclase
isoform in alcohol use disorder
and depression.
Front. Pharmacol. 13:1012013.
doi: 10.3389/fphar.2022.1012013

COPYRIGHT
© 2022 Tabakoff and Hoffman. This is an
open-access article distributed under
the terms of the [Creative Commons
Attribution License \(CC BY\)](#). The use,
distribution or reproduction in other
forums is permitted, provided the
original author(s) and the copyright
owner(s) are credited and that the
original publication in this journal is
cited, in accordance with accepted
academic practice. No use, distribution
or reproduction is permitted which does
not comply with these terms.

The role of the type 7 adenylyl cyclase isoform in alcohol use disorder and depression

Boris Tabakoff^{1,2*} and Paula L. Hoffman^{1,2,3}

¹Department of Pharmaceutical Sciences, Skaggs School of Pharmacy and Pharmaceutical Sciences, University of Colorado Anschutz Medical Campus, Aurora, CO, United States, ²Lohocla Research Corporation, Aurora, CO, United States, ³Department of Pharmacology, School of Medicine, University of Colorado Anschutz Medical Campus, Aurora, CO, United States

The translation of extracellular signals to intracellular responses involves a number of signal transduction molecules. A major component of this signal transducing function is adenylyl cyclase, which produces the intracellular “second messenger,” cyclic AMP. What was initially considered as a single enzyme for cyclic AMP generation is now known to be a family of nine membrane-bound enzymes, and one cytosolic enzyme. Each member of the adenylyl cyclase family is distinguished by factors that modulate its catalytic activity, by the cell, tissue, and organ distribution of the family members, and by the physiological/behavioral functions that are subserved by particular family members. This review focuses on the Type 7 adenylyl cyclase (AC7) in terms of its catalytic characteristics and its relationship to alcohol use disorder (AUD, alcoholism), and major depressive disorder (MDD). AC7 may be part of the inherited system predisposing an individual to AUD and/or MDD in a sex-specific manner, or this enzyme may change in its expression or activity in response to the progression of disease or in response to treatment. The areas of brain expressing AC7 are related to responses to stress and evidence is available that CRF1 receptors are coupled to AC7 in the amygdala and pituitary. Interestingly, AC7 is the major form of the cyclase contained in bone marrow-derived cells of the immune system and platelets, and in microglia. AC7 is thus, poised to play an integral role in both peripheral and brain immune function thought to be etiologically involved in both AUD and MDD. Both platelet and lymphocyte adenylyl cyclase activity have been proposed as markers for AUD and MDD, as well as prognostic markers of positive response to medication for MDD. We finish with consideration of paths to medication development that may selectively modulate AC7 activity as treatments for MDD and AUD.

KEYWORDS

type 7 adenylyl cyclase (AC7), alcohol use disorder, depression, disease markers, medication development

Introduction

“In the beginning. . .”, [Blenkinsopp \(2011\)](#) (which for cyclic adenosine 3'-5' monophosphate (cyclic AMP, cAMP) and adenylyl cyclase, by the Western calendar, was 1957), Sutherland and Rall identified a chemical which was produced during incubation of liver “particles” (homogenates) with ATP, magnesium, glucagon, and epinephrine ([Sutherland and Rall, 1957](#)). They reported that “similar or identical” compounds could be isolated from heart, skeletal muscle, and brain. This was the first identification of the “second messenger” ([Sutherland et al., 1968](#)) molecule formally known as adenosine 3'-5' monophosphate or cyclic AMP. In 1962, Sutherland, Rall, and Menon described “adenyl cyclase” the enzyme that catalyzed the synthesis of cyclic AMP from ATP ([Sutherland et al., 1962](#)). It soon became obvious that adenylyl cyclase (now referred to as adenylyl cyclase) and cyclic AMP were critical intermediaries in the actions of a plethora of hormones and other first messengers which interacted with their cognate receptors and modulated adenylyl cyclase activity. The receptors that can modulate adenylyl cyclase activity are within the family of G-protein-coupled receptors (GPCRs).

The discovery of guanine nucleotide binding proteins (G-proteins), which couple the GPCRs to adenylyl cyclase, is ascribed to Alfred Gilman and Martin Rodbell. Martin Rodbell showed in 1971 that the relay of a signal from a receptor on the exterior of a cell to the cell interior requires three functional units: 1) the receptor, 2) a “transducer” that utilizes GTP and, 3) an “amplifier” that generates a second messenger ([Rodbell et al., 1971a](#); [Rodbell et al., 1971b](#)). The character of the transducer that interacts with adenylyl cyclase (the “amplifier”) was then described by the laboratory of Alfred Gilman and colleagues in 1980 ([Schleifer et al., 1980](#)). They isolated trimeric proteins (“G proteins” consisting of α , β and γ subunits) from brain that could restore coupling of receptors to adenylyl cyclase in mutant leukemia cells which lacked such proteins ([Schleifer et al., 1980](#)). Through such reconstitution, one could restore the responses of the mutant cell to hormones. Interestingly, in the Nobel Lecture by Rodbell on the occasion of the Nobel Prize to Gilman and Rodbell in 1994, it was stated, “In some common disease states the amounts of G-proteins in cells are altered. There can be too much or too little of them. In for example diabetes and in alcoholism there may be some symptoms that are due to altered signaling *via* G-proteins” ([Rodbell, 1995](#)). This statement bears some truth, but there is more to the story.

Before proceeding, one should touch on how the second messenger cyclic AMP produces its effects within the cell. The initial discovery of an effector mediating the signal initiated by intracellular levels of cyclic AMP garnered yet another Nobel prize. This prize went to Edwin G. Krebs and Edward Fischer for their discovery and characterization of protein kinase A ([Krebs et al., 1964](#); [Walsh et al., 1968](#)), and the description of protein phosphorylation cascades that are the final mediators of much of

cellular function, from energy metabolism to gene transcription, to cell survival ([Ahn et al., 1991](#)). Although it was initially thought that protein kinase A was the sole mediator of cyclic AMP action, it is now evident that cyclic AMP acts through several effectors. The three most studied effectors are: 1) protein kinase A, 2) the exchange proteins activated by cyclic AMP (Epac) ([Robichaux and Cheng, 2018](#)), and 3) cyclic nucleotide-gated ion channels (CNG channels ([van der Horst et al., 2020](#)). More recently additional cAMP effector proteins have been identified including hyperpolarizing activated cyclic nucleotide-gated potassium channels (HCN1-4) ([Brand, 2019](#); [Santoro and Shah, 2020](#)); the Popeye domain-containing proteins (POPDC proteins) ([Brand, 2019](#)); and cyclic nucleotide receptors involved in sperm function (CRIS) ([Krähling et al., 2013](#)). In addition, some isoforms of phosphodiesterases (PDE) which degrade cAMP are also regulated allosterically by cAMP ([Omori and Kotera, 2007](#)).

In the late 1970s and early 1980s, the proposal that ethanol produced its neurobiological effects by perturbing the physical structure of neuronal membranes held dominance in the area of alcohol research. It struck us ([Tabakoff and Hoffman, 1979](#)) that the adenylyl cyclase system of brain would be a good test of how, and if, in neuronal membrane preparations, a disruption of membrane structure would translate into a perturbation of an important signal transduction system (i.e., adenylyl cyclase). By then the work of Sutherland, Rall and Gilman had demonstrated that at least three different membrane-bound protein components had to act in concert to modulate the production of cyclic AMP (this is not counting the fact that G-proteins were trimers of α , β and γ protein subunits). Thus we thought that the adenylyl cyclase system would be excellent for reflecting ethanol's lipid perturbing properties.

This review puts in historical context the work that established that ethanol, at concentrations found in the brain of inebriated individuals, can significantly alter adenylyl cyclase activity and the adaptive responses seen in the adenylyl cyclase signaling system with chronic exposure of the brain to ethanol. The discoveries of multiple isoforms of adenylyl cyclase disclosed that one particular isoform was most sensitive to ethanol's actions, and genetic manipulation of the expression of this isoform revealed the biological context for this isoform's actions within particular neuronal systems, such as the GABA neurons of the amygdala and nucleus accumbens, and the corticotropes of the pituitary. The effects of genetic manipulation of this isoform on the behavioral repertoire of a genetically modified animal, indicated that alcohol consumptive behavior, and behaviors associated with animal models of MDD, were related to the levels of expression of the alcohol sensitive adenylyl cyclase in brain, but these effects were influenced by the sex of the animal. Extrapolating from mouse to human, the levels of expression of the alcohol-sensitive adenylyl cyclase in brain or cells in blood, established that measures of this enzyme's expression or activity could be considered state or trait

markers of AUD or MDD. A more recent finding, demonstrating that the alcohol-sensitive adenylyl cyclase is the primary cyclase in cells of the immune system, opens another aspect in the biology of this enzyme isoform, and its relation to ethanol's action in humans. An added facet to this observation is the dominant presence of this isoform in microglia in brain, and the possible implications of this fact on microglial activation, and the effects of ethanol on this aspect of brain function. We finish with some observations on the prospects of isoform-specific modulators of adenylyl cyclase activity, and the possibility of their use as medications in treating AUD and MDD.

Ethanol's action on brain membrane-bound adenylyl cyclase

In our initial studies, we used cell membrane preparations of the striatum of mouse brain and measured the production of cyclic AMP (Luthin and Tabakoff, 1984). We found that concentrations of ethanol up to 500 mM had no effect on basal adenylyl cyclase activity. Only after the addition of Gpp (NH)p, the non-hydrolysable analog of GTP, to the assay mixture did ethanol, at concentrations as low as 50 mM, produce significant increases in production of cyclic AMP. This was the first indication that ethanol's actions on adenylyl cyclase were related to the presence of the activated G protein in the assay, but the low ethanol concentration necessary to produce the measurable effect did not well support the hypothesis that ethanol was acting by perturbing membrane lipid structure.

We followed these studies with the examination of the acute and chronic effects of ethanol administration on dopamine-stimulated adenylyl cyclase activity in striatal membrane preparations (Tabakoff and Hoffman, 1979). Ethanol, at concentrations of 50 mM, added to striatal membrane preparations from "ethanol naive" mice increased dopamine-stimulated adenylyl cyclase activity without changing the potency of dopamine. Mice were then chronically treated with ethanol to produce physical dependence, and sacrificed at various times over the ensuing 7 days following withdrawal. We noted that after ethanol was cleared from their systems (8–24 h), the response of striatal membrane adenylyl cyclase to dopamine was reduced in a time-dependent manner. The reduction in response became evident at a time when withdrawal signs were reaching their peak, and continued to decrease through the initial 24 h of the withdrawal period. The phenomenon was reversible, with the responsiveness to dopamine beginning to return to control levels by 36 h post withdrawal. The responsiveness to exogenously added ethanol remained intact during this period. Thus, ethanol could still increase the response of adenylyl cyclase to addition of dopamine, and at particular concentrations (50 mM), produce a response to dopamine that equaled the response to dopamine of the membranes from control mice, measured without the addition of ethanol. From these studies, we

surmised that the withdrawal from a chronic ethanol feeding paradigm generated the diminution of the response of striatal adenylyl cyclase to dopamine, and the reintroduction of ethanol could "normalize" this function of dopamine. Rabin and colleagues (Rabin et al., 1980; Rabin and Molinoff, 1981) followed with an attempt to replicate our results. Their work demonstrated that the addition of ethanol (≥ 68 mM) to incubations containing striatal homogenates increased dopamine stimulated adenylyl cyclase activity, but when they treated mice chronically with an ethanol-containing liquid diet to produce physical dependence, and isolated striatal membranes from control and ethanol-fed mice 24 h after withdrawal, they found no difference in response to dopamine between the preparations from the ethanol-treated and control mice (Rabin et al., 1980). Interestingly, they replicated additional aspects of our prior studies such as the increase in levels of muscarinic cholinergic receptors in the striatum of the ethanol-fed and withdrawn mice (Tabakoff et al., 1979). Further research using rats chronically treated with intraperitoneal (ip) injections of ethanol, produced ambiguous results regarding dopamine-stimulated adenylyl cyclase activity in striatum of the ethanol-treated rats during withdrawal. Seeber and Kuschinsky (1976) found that 15 h after withdrawal, there was a "slight postjunctional subsensitivity to dopamine," but the differences were not statistically significant. One of the variables contributing to the disparate findings regarding the effects of chronic treatment with ethanol and withdrawal on dopamine-stimulated adenylyl cyclase activity in the striatum, is the time of measurement of the enzyme activity after withdrawal. Our studies demonstrated that the differences become evident after some period after withdrawal, are evident during the first 24 h, and begin to disappear by 72 h after withdrawal (Tabakoff and Hoffman, 1979). The measurements at a single timepoint during the first 24 h after withdrawal in mice (Rabin et al., 1980), or rats (Seeber and Kuschinsky, 1976), may miss the optimal time to demonstrate the changes in the striatum. Such studies that will have to be better designed in the future, including a careful preparation of the cell membranes used in the analysis. As will be discussed later, the phosphorylation state of particular isoforms of the adenylyl cyclase is important in the measure of G-protein stimulated activity. Thus, a more careful assessment of the time course of changes in striatal dopamine-stimulated adenylyl cyclase activity, and more concern about factors that may contribute to ethanol-induced changes, continue to be warranted. It should be noted that there is consistent evidence that the changes in the dopamine-stimulated adenylyl cyclase activity in the striatum are not due to changes in the D1 dopamine receptors (Tabakoff and Hoffman, 1979; Rabin et al., 1980), and probably not due to changes in the quantity of the stimulatory G-protein α subunit (Tabakoff et al., 1995).

A reason for giving emphasis to changes in dopamine function in the striatum of ethanol withdrawn animals, is the currently popular concept regarding allostasis and reward deficit

that drive withdrawal-induced alcohol consumption (Koob and Volkow, 2016). If dopamine function in the striatum is compromised, and ethanol can normalize (increase) the response to dopamine effects, these factors could put biological context to the behavioral phenomena.

Receptor-activated adenylyl cyclase activity has also been measured in other brain areas of animals chronically treated with ethanol (Saito et al., 1987). Isoproterenol (β -adrenergic receptor agonist)-stimulated adenylyl cyclase activity in cerebral cortical membranes was shown to be reduced after chronic treatment of mice with ethanol. These changes were normalized within 24 h after withdrawal (Saito et al., 1987). Rabin (1990a), however, found that there were no differences in isoproterenol-stimulated adenylyl cyclase when measured 20 h after withdrawal. Again, the changes seen in the cortical tissue follow a particular time course, and studies of the changes need to include measurement at several time points after withdrawal. Interestingly, Rabin (1990a), Rabin (1990b) did find that ethanol treatment of cells (cerebellar granule cells and PC12 cells) in culture for several days decreased the maximum activation of adenylyl cyclase in these cells by isoproterenol or 2-chloroadenosine. Studies with HEL cells in cultures containing ethanol also demonstrated ethanol-dependent reduction in PGE1-stimulated adenylyl cyclase activity (Rabbani and Tabakoff, 2001). It may be concluded that a down-regulation of adenylyl cyclase activity in certain areas of brain, and in immune/platelet cell precursors, does take place in animals or cells chronically treated with ethanol, but a careful and more extensive monitoring of the time course of events is necessary to further substantiate such phenomena. Given this observation, the mechanism of this phenomenon becomes of interest.

Forskolin is a diterpene alkaloid which has been shown to bind to most forms of adenylyl cyclase, and radioactively-labeled forskolin has also been used to quantify adenylyl cyclase protein levels (Insel and Ostrom, 2003). Measurement of forskolin-stimulated adenylyl cyclase activity in cerebral cortical membranes of chronically ethanol-treated mice, demonstrated that the stimulation by forskolin had a similar potency in tissue from control and ethanol-treated mice, but the maximal effects were significantly lower in the ethanol-fed animals (Valverius et al., 1989). Autoradiographic analysis of ^3H -forskolin binding across the various areas of mouse brain revealed differences between control and ethanol-fed animals in several brain areas (Valverius et al., 1989). It should be noted that in these studies, the animals were sacrificed while still intoxicated. Lower levels of forskolin binding were found in areas such as the cortical areas, nucleus accumbens, amygdala, hippocampus, and globus pallidus, while no significant differences were noted in the caudate putamen or cerebellum at this point in time. One can come to a conclusion that chronic ethanol administration to rodents produces diminutions in the expression of adenylyl cyclase protein in certain areas of brain, and the physiological phenomena accompanying the withdrawal from ethanol may produce changes in adenylyl cyclase activity in other brain areas.

Overall, the early studies demonstrated that ethanol's stimulation of adenylyl cyclase activity was dependent on the presence of G protein, and chronic exposure of cells in culture to ethanol resulted in a down-regulation of GPCR-mediated activation of adenylyl cyclase. The results with brain tissue taken from animals that had been chronically treated with ethanol are somewhat ambiguous, but the ambiguity comes mainly from the fact that the diminution in GPCR-stimulated adenylyl cyclase activity after ethanol treatment and withdrawal follows a particular time course, and the phenomenon may be missed if only one timepoint after withdrawal is studied. The down-regulation of GPCR-stimulated adenylyl cyclase activity by chronic exposure of the organism to ethanol may well be related to ethanol craving and CNS hyperexcitability that occur during withdrawal.

The identification of adenylyl cyclase isoforms and the ethanol-sensitive adenylyl cyclase

The work described to this point was performed prior to the discovery that there were multiple forms of adenylyl cyclase. Gilman's laboratory (Krupinski et al., 1989; Tang et al., 1991) reported on the first isoform of adenylyl cyclase aptly named the Type 1 adenylyl cyclase. Soon after Type 2 adenylyl cyclase was described (Feinstein et al., 1991). Type 3 adenylyl cyclase was first described by Bakalyar and Reed (1990), Type 4 by Gao and Gilman (1991), Type 5 by Ishikawa et al. (1992), Type 6 by Katsushika et al. (1992), Yoshimura and Cooper (1992) and Krupinski et al. (1992), Type 8 by Cali et al. (1994), and Type 9 by Hacker and Storm (1998) and Premont et al. (1996). All of these were membrane-bound forms of adenylyl cyclase and there was one form of adenylyl cyclase that was found to be cytosolic (Type 10) (Buck et al., 1999). Soon after the findings regarding the Type 6 adenylyl cyclase, we isolated a sequence from human erythroleukemia (HEL) cells that showed sequence similarities to other adenylyl cyclases, but also displayed characteristic functional differences (Hellevuo et al., 1993). After cloning the full length sequence, expressing the protein, and characterizing its activity, it became clear that this adenylyl cyclase was unique and was named the Type 7 adenylyl cyclase (Hellevuo et al., 1995). At the same time, Watson et al. (1994), isolated and characterized a similar adenylyl cyclase from rat brain illustrating that the Type 7 adenylyl cyclase (AC7) was present in rodents, as well as in human tissues.

The characteristics of the discovered adenylyl cyclases were such that they could be fitted into 4 families (Devasani and Yao, 2022). AC7 joined the family containing the Type 2 and Type 4 adenylyl cyclases. This family was distinguished by its insensitivity to calcium with or without calmodulin, insensitivity to inhibition by the Gai protein and by the stimulatory effects of phorbol esters acting through PKC, as

well as the co-stimulation by the $\beta\gamma$ subunits of the G proteins acting simultaneously with the $G_{\alpha s}$ protein (Yoshimura et al., 1996). The $\beta\gamma$ subunits that act in concert with $G_{\alpha s}$ were found to be derived from G_i/o proteins coupled to GPCRs that are many times thought to be inhibitory to adenylyl cyclase activity (Yoshimura et al., 1996; Rhee et al., 1998). Thus, for example activation of opiate or cannabinoid receptors (coupled to G_i) simultaneously with activation of D1 dopamine receptors (coupled to G_s) further activates AC7 and the other members of its family.

We found another feature that distinguished the AC7, i.e., ethanol could stimulate the activity of AC7 to a two-to-three times greater extent than any of the other adenylyl cyclases (Yoshimura and Tabakoff, 1995; Yoshimura and Tabakoff, 1999). An activated $G_{\alpha s}$ protein was still necessary to witness this effect of ethanol (Yoshimura and Tabakoff, 1995). AC7 was also the most responsive to activation by phorbol esters, in comparison to the other members of its family (Type 2 and Type 4), and the stimulation of AC7 by phorbol esters involved the presence of an activated $G_{\alpha s}$ (Yoshimura and Cooper, 1993; Hellevuo et al., 1995). It became of interest to consider whether ethanol and phorbol esters may be utilizing a similar pathway to accomplish the activation of AC7. Phorbol esters are known activators of members of the protein kinase C (PKC) family (Reyland, 2009). There are 10 known PKCs and 8 of them are activated by phorbol esters (classical PKCs: α , β_1 , β_2 and γ , which are responsive to phorbol esters and diacylglycerol, and are dependent on calcium binding for their activity; novel PKCs: δ , θ , ϵ , η which are responsive to phorbol esters and diacylglycerol but insensitive to calcium; and atypical PKCs: ζ , λ , ι , which depend on binding of phosphatidylinositol 3, 4, 5-trisphosphate or ceramide for activation (Reyland, 2009; Newton and Brognard, 2017)). All of the PKC enzymes are processed by a series of ordered phosphorylations and conformational changes to attain a catalytically active form. The enzymes are maintained in an inactive state until the binding of the proper second messenger (in the case of PKC δ , for example, the second messenger is diacylglycerol) and a conformational change leading to a catalytically active, open, form of this enzyme is then attained (Newton and Brognard, 2017).

At the time that involvement of PKC in the action of ethanol on adenylyl cyclase was being studied, little of the detail of the activation process for PKCs was known. However, through a series of studies dependent on the process of elimination, the PKC most likely to interact with AC7, and increase its activity, was found to be PKC δ (Nelson et al., 2003). Nelson et al. (2003) using HEL cells which contain predominantly AC7 (Hellevuo et al., 1993), demonstrated that PKC δ could phosphorylate AC7 protein, with the likely site of phosphorylation being the C1b domain of AC7 (Nelson et al., 2003).

The catalytic conversion of ATP to cyclic AMP by adenylyl cyclases involves the juxtaposition of two domains of the enzyme

protein. The C1a region of the intracellular loop between the membrane spanning domains, M1 and M2 has to align with the C2 region of the C terminal tail of the adenylyl cyclase protein to form the catalytic domain. The addition of $G_{\alpha s}$ activated by GTP γ S to a mixture of the C1a region peptide of the Type 1 adenylyl cyclase and the C2 region peptide of the Type 2 adenylyl cyclase increased the enzymatic activity of this mixture (cyclic AMP production) well over a thousand-fold (Yan et al., 1996). The explanation for this increase in enzymatic activity is that the activated $G_{\alpha s}$ acts as a link between the two adenylyl cyclase fragments and aligns them into the proper conformation for catalysis. Analysis of the crystal structure of the C1a and C2 regions of adenylyl cyclase in combination with $G_{\alpha s}$ and forskolin demonstrated the binding of $G_{\alpha s}$ to the C2 region and interaction with C1a region resulting in a change in orientation of these regions to each other with the resultant increase in catalytic activity (Tesmer et al., 1997).

Interposed between the C1a region and the M2 transmembrane domains is a region referred to as C1b and this region has been considered to be important for conferring isoform-specific regulatory properties to members of the adenylyl cyclase family (see references in Beeler et al. (2004)). A particularly interesting function of the C1b region is to modulate the ability of activated $G_{\alpha s}$ to promote the catalytic function of the C1a•C2 dimers (Scholich et al., 1997). Beeler et al. (2004) generated a recombinant protein representing the C1b region from AC7 (aa 506–584) and examined its effects on the catalytic function of the mixture of C1a and C2 regions from AC7. It was found that the C1b peptide inhibited the activation by $G_{\alpha s}$ of the mixture of C1a and C2 peptides derived from the AC7. The inhibition was only evident at the lower concentrations of $G_{\alpha s}$ and no effect was evident at higher concentrations (>2 μ M) $G_{\alpha s}$.

The C1b region can be phosphorylated by PKC. Shen et al. (2012) demonstrated the phosphorylation of serine 490 and 543 in the C1b region of the Type 2 adenylyl cyclase (AC2) by PKC with resultant changes in response of the enzyme to $G_{\alpha i}$ and $\beta\gamma$. In the AC7 sequence, several PKC phosphorylation sites are evident in the C1b region, but serines 505 and 536 are most interesting since they exist in an area of alignment to a putative binding region for PKC δ on SRBC protein (a PKC δ binding protein) and phosphorylation of these serines by PKC δ (Izumi et al., 1997) in the SRBC protein has been demonstrated. The phosphorylation of serines 505 and 536 may well allow for a more productive interaction between the C1a and C2 domains.

One can speculate that the effect of ethanol on the activity of AC7 is mediated by phosphorylation of serines in the C1b region of the AC7 enzyme. The phosphorylation could reduce the inhibition of high affinity $G_{\alpha s}$ binding by the C1b region, resulting in a greater catalytic response of AC7 to binding of $G_{\alpha s}$ in the presence of ethanol (Figure 1).

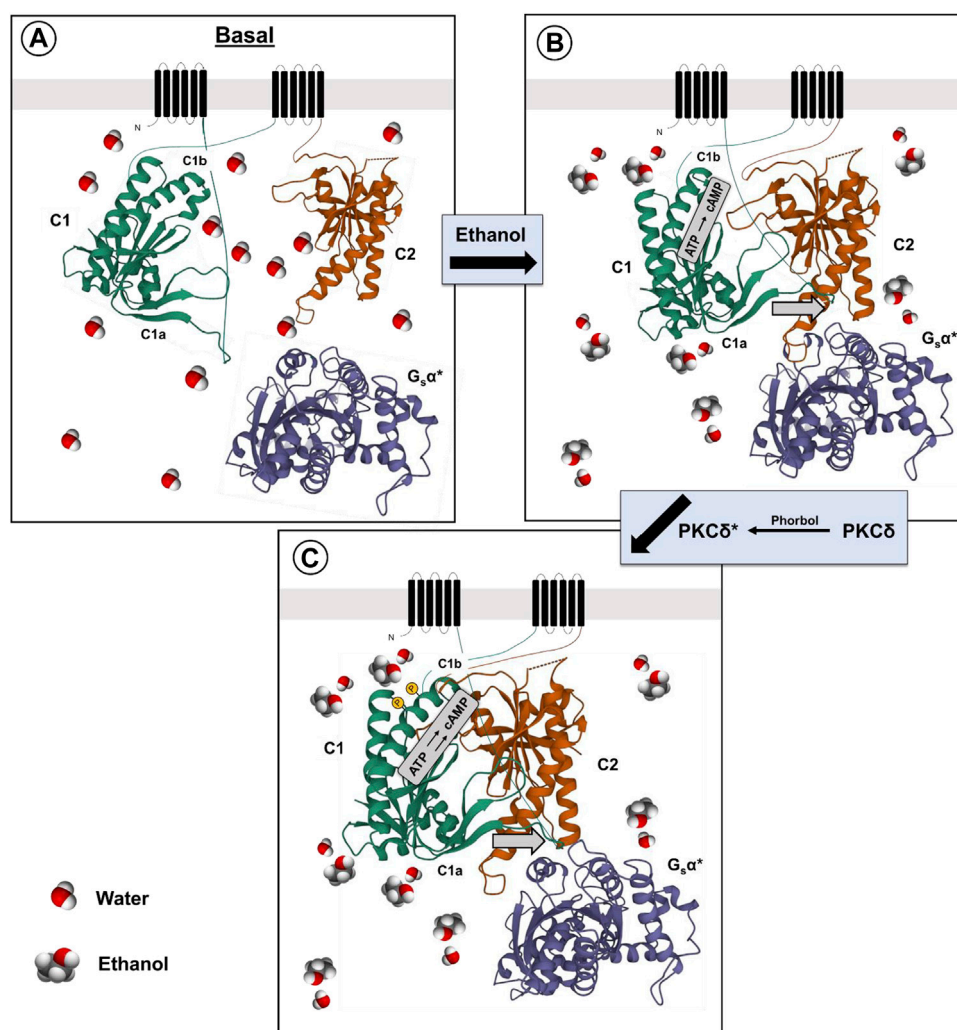


FIGURE 1

Proposed mechanism for ethanol potentiation of $G_{\alpha s}$ -mediated activation of AC7 (A,B). The presence of ethanol in the water layer immediately adjacent to the C1a, C1b and C2 domains (Bagchi, 2005) promotes the alignment of these domains and interaction with $G_{\alpha s}$ (Yan et al., 1996) (C). Further modification of the secondary or tertiary structure of the C1b domain can promote access to this region by PKC δ (protein-protein interaction) and phosphorylation of AC7, further enhancing $G_{\alpha s}$ -mediated activation of AC7 enzyme activity.

There is a caveat to this explanation of ethanol's actions on AC7. Yoshimura et al. (2006) produced chimeras of different regions of AC2 and AC7. When expressed in HEK 293 cells, which were also transfected with dopamine (D_1) receptors, the chimera containing the C1b and M2 region of AC7 with the C1a and C terminal region (C2) of AC2 responded to ethanol potentiation of dopamine-stimulated activity as would AC2, while the chimera containing the C1b and M2 region of AC2 with the C1a and C2 region of AC7 responded to ethanol as would be expected for AC7 (3–4 times greater response). These results led Yoshimura et al. (2006) to conclude that the C1b region of AC7 was not important for ethanol's action. This conclusion omits consideration of the fact

that ethanol's actions on AC7 are dependent on the presence of the activated form of $G_{\alpha s}$ and that the effects of the C1b region are not independent of the other domains of the adenylyl cyclase protein. The effect of the AC7 C1b may well be tuned to the specific sequences of the C1a and C2 regions which bind $G_{\alpha s}$ in particular adenylyl cyclases (Beeler et al., 2004; Shen et al., 2012). It was notable that the chimeras in which the C1b regions of AC7 and AC2 were combined with heterologous C1a and C2 regions of these enzymes had significantly lower (5–8 times lower) dopamine-stimulated activity than in their homologous environment, and the activity in the presence of ethanol was also low. In the end, Yoshimura et al. (2006) concluded that ethanol directly influences the interaction of

C1a and C2 regions of particular adenylyl cyclases, but the mechanism of this effect was left open. The control of Gas binding by phosphorylation of the C1b region of particular adenylyl cyclases, i.e., AC7, thus remains an attractive hypothesis.

Finally, it should be noted that there is evidence that ethanol is not simply activating PKC δ to produce its effects on AC7. Rabbani et al. (1999) utilized HEL cells which naturally express AC7 to demonstrate that the effects of phorbol esters and ethanol were additive even though both the ethanol and phorbol ester effects were blocked by PKC inhibitors. This brings forth the possibility that the phorbol esters and ethanol act in a complementary manner with phorbol esters activating PKC δ , and ethanol enhancing the phosphorylation of particular substrates such as AC7. The C1b region of AC7 may be particularly sensitive to ethanol's amphiphilic properties (Klemm, 1998) which could influence the secondary or tertiary structure of the C1b region (Beeler et al., 2004), and allow phosphorylation of serines in that region (Figure 1).

At this point, the best characterization of ethanol's action on AC7 is that it acts as a "conditional" stimulus, with its actions dependent on the presence of the activated Gas, and additional work needs to be performed to clarify the molecular events attendant to ethanol's potentiation of Gas activating properties. Ethanol's actions on AC7 activity are evident at concentrations of 50 mM (230 mg%) or higher in cell systems in which AC7 is naturally expressed (e.g., HEL cells), and such pharmacological considerations should be applied when evaluating the physiological implications of the effects of ethanol on adenylyl cyclase-related events. It can be noted that blood alcohol levels of 200 mg% and over are not unusual for individuals coming to emergency rooms or even driving (Maruschak, 1999; Allely et al., 2006). An important issue to consider when one is evaluating the physiological impact of the effects of ethanol on adenylyl cyclase activity is the fact that adenylyl cyclases exist in "microdomains" within a cell and it is the local concentration of cAMP that instigates the downstream consequences (Zaccolo et al., 2021). At this time, the effects of ethanol on levels of cAMP have not taken this fact into account, and the changes in cAMP concentrations have been measured on a whole cell level or within an incubation volume. Localized, and possibly quite significant effects of ethanol may be diluted by such experimental approaches.

Genetic manipulation of AC7 and the neurobiological phenotype

The generation of AC7 transgenic (TG) and heterozygous (HET) knock-down mice (Yoshimura et al., 2000; Hines et al., 2006), allowed for the qualitative assessment of the behavioral and physiological effects of AC7. The transgene used for generating the TG mice was the human form of AC7 under the control of a synapsin promoter (Yoshimura et al., 2000),

while the HET mice were generated by homologous recombination with the deletion of exon 3 of AC7 (Hines et al., 2006). We were not able to produce the homozygous knock-out because the fetuses bearing the homozygous deletion died *in utero* on GD11 (Hines et al., 2006). The phenomenon of the fetus bearing two copies of the disrupted AC7 gene dying *in utero* was also noted more recently by Duan et al. (2010), highlighting the importance of AC7 in development. The initial choice of the biological systems, and then the behaviors to be examined, were based on the known involvement of adenylyl cyclase as an effector for dopamine D1 and D2 receptors and the corticotropin-releasing factor (CRF) receptors. An elegant addition to the work on involvement of AC7 in the functions of CRF in brain and pituitary, was the work of Duan et al. (2010) who used genetic manipulation of AC7 expression in cells of the peripheral immune system to demonstrate that AC7 was integral to the innate and adaptive responses of the immune system.

AC7 and CRF receptor coupling in the amygdala

CRF acting within the amygdala has been linked to depression and anxiety disorders in humans (Binder and Nemeroff, 2010), and to anxiety-like, and alcohol consumptive behaviors in rodents (Agoglia and Herman, 2018). CRF and CRF1 receptors also appear to be involved in alcohol withdrawal-induced anxiety and increased alcohol consumption in alcohol-dependent animals after withdrawal (craving?) (Agoglia and Herman, 2018). Marissa Roberto and her colleagues have examined the effects of ethanol on CRF-sensitive neurons in the central amygdala (CeA) (Roberto et al., 2021). CRF acting through the CRF1 receptor, which is coupled to Gs protein, can increase GABA release, and activate post synaptic GABA-A receptors. The increased release of GABA can be measured by the increases in inhibitory post-synaptic potentials (IPSPs) (Roberto et al., 2021). Ethanol or CRF added to the CeA slice preparations were shown to significantly increase the GABA-mediated IPSPs (Roberto et al., 2021). Using the CeA slices from the WT and AC7 HET mice, Cruz et al. (2011), showed that the IPSPs measured in the presence of CRF or ethanol were reduced or absent, respectively, in the preparations from the HET mice compared to the WT mice (Cruz et al., 2011). This led to the suggestion that AC7, which in part is located presynaptically (Mons et al., 1998), can be involved in the signaling initiated by the CRF1 receptor and culminating in release of GABA. There is prior evidence that CRF1 receptors couple to both AC7 and Type 9 adenylyl cyclase (Antoni et al., 2003), and the significant diminution of AC7 in brains of the HET knock-down mice may be responsible for the reduced effects of CRF and ethanol in the CeA slice preparations. Work by Bajo et al. (2008), had demonstrated that PKC ϵ was also involved in CRF1 receptor-mediated and ethanol-potentiated GABA release in slices of the CeA. Recording of "basal" IPSP activity attributed to spontaneous GABA release was significantly increased in

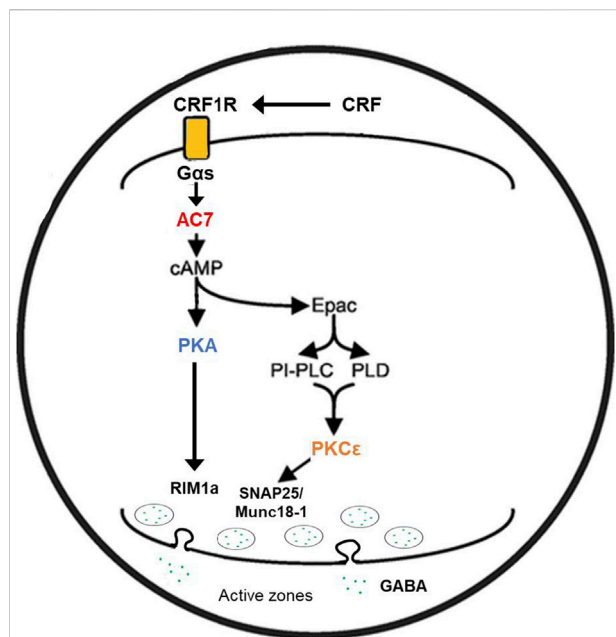


FIGURE 2

Proposed mechanism of ethanol potentiation of CRF-mediated GABA release in the central amygdala. In the pre-synaptic terminal CRF interacting with CRF1 receptors coupled to Gs protein acts to enhance the activity of AC7. Ethanol potentiates the Gs-mediated catalytic activity of AC7 and increases the generation of cAMP. cAMP can interact with two effector molecules, PKA and Epac (Hucho et al., 2005; Robichaux and Cheng, 2018; Wang et al., 2022a) to engage two distinct pathways (Gekel and Neher, 2008) modulating transmitter release (e.g., GABA). The exocytosis of the contents of vesicles requires fusion of the vesicle with the pre-synaptic membrane and positioning of the vesicle in proximity to N or P/Q-type Ca^{++} channels (Südhof and Rizo, 2011). cAMP has also been shown to modulate vesicle loading with neurotransmitter (Costa et al., 2017). The fusion of vesicles with the synaptic membrane, pore formation, and transmitter release requires the interaction of several proteins including RIM proteins, Munc 13–1, Munc 18–1, and SNAP proteins. These proteins can be phosphorylated by PKA or PKCε (Lonart et al., 2003; Sossin, 2007; Brockmann et al., 2020) and such phosphorylation modifies their function. The change in function of the transmitter release machinery can be measured by amplitude and frequency of post-synaptic mIPSPs or mEPSPs. Ethanol-induced potentiation of CRF-initiated GABA release in the central amygdala (Nie et al., 2009) was diminished by knockdown of AC7 or knockout of PKCε (see text), and this illustration provides a rendition of the interactive pathways by which the observed effects can be explained.

tissue from animals whose PKCε was disrupted by homologous recombination (PKCε^{-/-}) (Khasar et al., 1999). Additionally, the CRF1 receptor-mediated enhancement of GABA release, as well as ethanol-mediated GABA release in the CeA slices, was blocked in tissue from the PKCε^{-/-} mice (Bajo et al., 2008). There is a significant difference in the results obtained from AC7 HET mouse tissue *versus* the tissue from the PKCε^{-/-} mice (Bajo et al., 2008; Cruz et al., 2011). The basal GABA release in the slices of the PKCε^{-/-} mice was substantially increased, and thus the stores available for release by CRF or ethanol may have been depleted.

In AC7 HET mice, there was no change in the basal release of GABA and thus an explanation based on depletion of GABA stores would not resonate with reduced effects of CRF and ethanol in the HET mice. The evidence for mechanistic differences in PKCε effects and the effects of AC7, thus do not contradict the evidence for PKCδ mediation of the interaction of Gs and AC7 whether induced by receptor activation or by ethanol.

A parsimonious reconciliation (Figure 2) of the involvement of both PKCε and the adenylyl cyclase system can be considered by invoking a cAMP to PKCε communication link. Such a link has already been established for excitatory transmitter release in the CNS (Gekel and Neher, 2008). Hucho et al. (2005) presented evidence that Epac is central for the activation and translocation of PKCε in neurons of the dorsal root ganglion, and that adenylyl cyclase activation *via* Gs is the initiator of this cascade. Wang et al. (2022b) further elucidated the role of Epac-PKCε in the facilitation of docking and release of the contents of synaptic vesicles in parallel fibers of the cerebellum. If similar events are evident in GABAergic neurons (Robichaux and Cheng, 2018), then two related pathways (adenylyl cyclase/cAMP/PKA or PKCε-mediated) or one sequential pathway (adenylyl cyclase, Epac, PKC) could explain the effects of both AC7 and PKCε on modulation of CRF-mediated GABA release by ethanol.

AC7 and CRF receptor coupling in the pituitary

The effects of ethanol on CRF-mediated signaling (Figure 3) have been further investigated using CRF-mediated ACTH release in the pituitary of the HET knock-down and TG mice overexpressing AC7. Assessment of the forms of adenylyl cyclase present in the mouse pituitary indicated the presence of the Type 2, Type 3, Type 6, and Type 7 (Pronko et al., 2010). It should be noted that Type 9 adenylyl cyclase has been reported to be present in rodent corticotropes (Antoni et al., 2003), but was not found in the mouse pituitary using microarray analysis (Pronko et al., 2010).

In the WT, AC7 HET, and AC7 TG mice (Pronko et al., 2010), the most profound differences were noted in the plasma ACTH levels of the male and female mice after injection of ethanol (Pronko et al., 2010). Significant quantitative differences among WT, HET and TG mice were found in both the peak levels and AUC of the ACTH responses to injection of ethanol (these values well surpassed the levels seen after saline injection). The levels of corticosterone correlated in magnitude with plasma ACTH levels after ethanol injection. The rank order of the plasma ACTH and corticosterone levels after ethanol injection was AC7 HET < WT < TG. In all cases, female mice had higher levels of corticosterone than the males of that genotype (Pronko et al., 2010). The results of these studies again establish AC7 as an important component of the link between the CRF1 receptor, and the downstream consequences of its activation, but the differences in the corticosterone response between males and females are not explained by

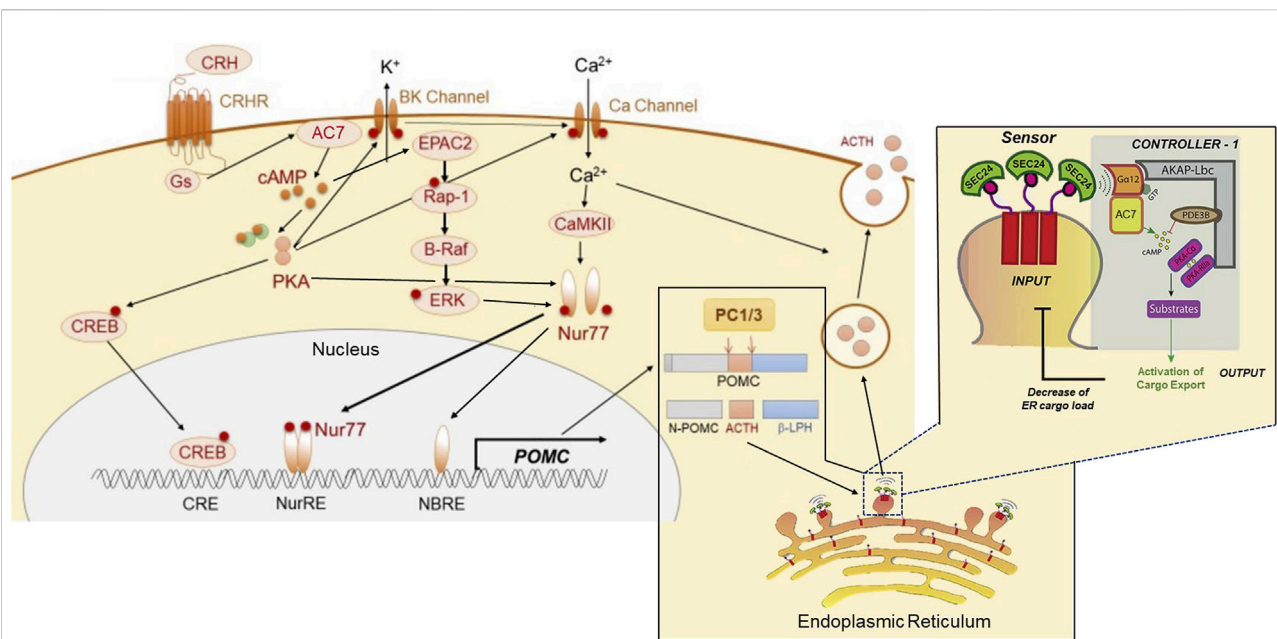


FIGURE 3

Proposed dual sites of action of AC7 in peptide (ACTH) synthesis and release. AC7 can participate in both the control of synthesis and release of ACTH. CRF (CRH) activates AC7 through a Gs-coupled mechanism and increases production of cAMP. The cAMP enhances the active state of both PKA and Epac2. PKA acts through its canonical CREB transcription activator pathway by phosphorylating CREB and translocating it to the nucleus to bind to its DNA promoter sequence. The binding of CREB to DNA is necessary but not sufficient to activate the transcription of POMC (the precursor to ACTH). The activation and DNA binding of Nur77 is a requirement for initiation of transcription. The phosphorylation and translocation of Nur77 to the nucleus, requires a coordinated interaction of ERK, PKA and CAMKII (Kovalovsky et al., 2002; Zhang and Heaney, 2020). Two sites for Nur77-binding exist upstream of the POMC transcription initiation site, a Nur77-binding response element (NBRE), and a Nur response element (NurRE), and both need to be occupied by Nur77 to initiate the transcription of POMC. Once the POMC RNA is produced, it is translocated to the endoplasmic reticulum for protein synthesis, and the processing of the pre-propeptide (POMC) by proprotein convertase (PC1/3) into ACTH and the other POMC derived peptides. The ACTH has to be loaded into dense core vesicles which are generated by "budding" of the endoplasmic reticulum, and the "cargo" of these vesicles (ACTH) is then readied for release by a calcium-dependent mechanism through fusion with the cellular membrane. AC7 is integral in the process of loading and preparing vesicles for release. AC7 is located on the endoplasmic reticulum membrane where it can be activated by Gα12. The activation of Gα12 by guanine nucleotide exchange is instigated by a sensor on the budding vesicle, SEC24. The cAMP produced by AC7 at this site can activate PKA (which is recruited to this site by an AKAP). PKA-dependent phosphorylation of an ill-defined substrate is then central to the process of release of the concentrated cargo by controlling the uncoating and separation of the maturing vesicles from the endoplasmic reticulum. This Figure was generated based on illustrations and information provided by Fukuoka et al. (2020), and Subramanian et al. (2019).

differences between sexes in expression of AC7 in the pituitary. The genetic manipulation of the *Adcy7* gene produced similar levels of AC7 RNA in the pituitary of the male and female mice of the HET or TG genotypes (Pronko et al., 2010), and the protein levels for AC7 followed the same pattern as the RNA levels with no statistically significant differences between males and females (Pronko et al., 2010). In the WT and AC7 HET mice, the higher levels of corticosterone in females may reflect higher ACTH levels. However, ACTH levels did not differ significantly between AC TG male and female mice. One explanation of the lack of sex differences in AC7 in the pituitary, but significant sex differences in the corticosterone response of AC7 TG mice, is the observation that the adrenal tissue of females may be more responsive to ACTH than that of males (Rao and Androulakis, 2017), and at a particular level of ACTH more corticosterone would be released from the adrenals of females.

The probable involvement of AC7 in the CRF1 receptor-mediated release of ACTH brings into further consideration the importance of microdomains in the actions of ethanol on AC7. AC7 is part of what was referred to as a "signalosome" consisting of Gα₁₂, AC7, PDE3B, PKA and other kinases organized around AKAP13 on the endoplasmic reticulum (Zaccolo et al., 2021). This type of signalosome has been shown to be important in the regulation of secretory function of the endoplasmic reticulum for recently synthesized and properly folded proteins (Subramanian et al., 2019). The presence of Gα₁₂ in this signalosome complex is consistent with the presence of AC7 since Jiang et al. (2008) demonstrated that AC7 is a specific downstream target of the Gα_{12/13} subunits that produce an increase in AC7 activity (Figure 3).

The involvement of the "ethanol sensitive" AC7 in the ACTH/corticosterone response to ethanol administered *in vivo*, helps explain a seeming enigma with regard to responses

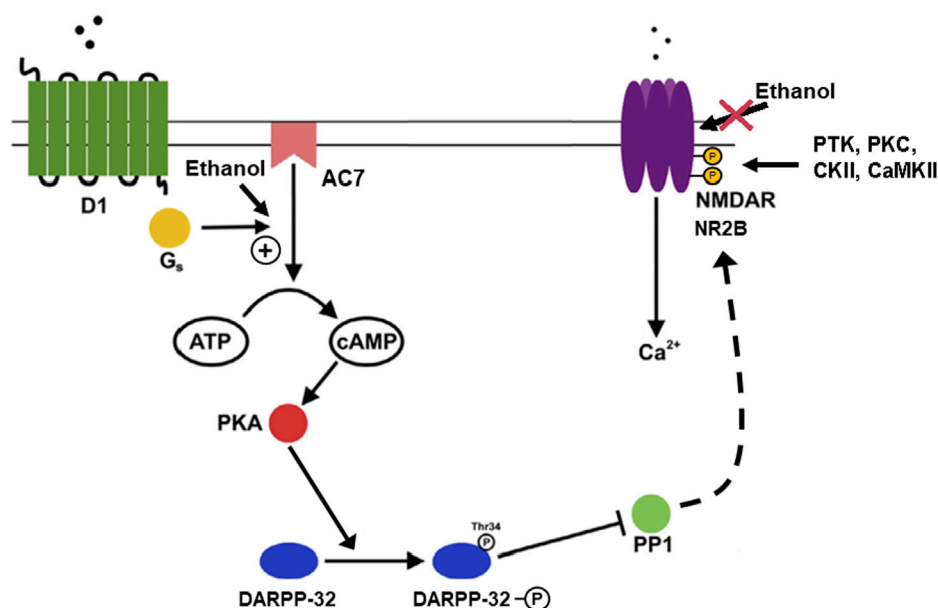


FIGURE 4

Phosphorylation of DARPP-32 mediated by dopamine through AC7 and actions of ethanol. The activity of medium spiny neurons (GABAergic neurons) in the nucleus accumbens and other areas of the striatum are important in the control of reward-related dopamine signals mediated via D1 and D2 dopamine receptors, with D1 receptors acting to enhance dendritic excitability (Surmeier et al., 2007). The increase in dendritic excitability is proposed to be dependent on modulation of cortico-striatal glutamatergic signaling via NMDA receptors located on the dendrites which also contain the D1 receptors. The link between the dopamine and glutamate signals is provided by the actions of PKA, DARPP-32, and protein phosphatase 1 (PP1) (Fernandez et al., 2006). The figure illustrates that ethanol, by acting on AC7, increases the production of cAMP which activates PKA, which in turn phosphorylates DARPP-32 on threonine 34. When phosphorylated on threonine 34, DARPP acts as an inhibitor of PP1, preventing dephosphorylation of the PP1 substrates. One of the PP1 substrates is the NMDA receptor which is a substrate for phosphorylation by protein tyrosine kinases (PTK), PKC, casein kinase (CKII), and calcium calmodulin kinase (CaMKII) (Chen and Roche, 2007). The NMDA receptor/channel is more active in its phosphorylated state (Nakazawa et al., 2001), and also resistant to the inhibitory effect of ethanol on the NMDA receptor/channel (Hoffman et al., 1989; Miyakawa et al., 1997). The overall result of these events is the sparing of the NMDA receptor from the inhibitory effects of ethanol in particular neuronal populations (Yaka et al., 2003). The implication is that ethanol can depress excitatory glutamatergic activity in certain types of cells and brain areas, but the reward-related neurons of the striatum would be spared from this inhibitory effect of ethanol by the action of DARPP-32 via PP1.

to imbibed ethanol. Ethanol is considered an anxiolytic drug, but several reports have provided evidence that ethanol ingestion generates an increase in the circulating levels of cortisol (stress hormone) in humans. Since the anxiolytic and the cortisol elevating effects of ethanol can arise by different mechanisms and involve different areas of brain (Pronko et al., 2010; Olsen and Liang, 2017), these results can be quite compatible.

AC7 mediation of dopamine effects on DARPP-32 and ethanol's actions

The DARPP-32 signaling pathway has been proposed as a therapeutic target for AUD medication development (Greener and Storr, 2022). The phosphorylation of glutamate receptors (NMDA, AMPA) on the medium spiny neurons of the nucleus accumbens is the major event which controls the strength of excitatory input to these neurons. The actions of DARPP-32 are integral in controlling the phosphorylation state of NMDA and AMPA receptors and DARPP-32 function is itself controlled by phosphorylation/dephosphorylation events (Nishi et al., 2005).

The medium spiny neurons of the nucleus accumbens are the integrators of dopaminergic signals from the ventral tegmentum and glutamatergic signals from the pre-frontal cortex (Figure 4) and play an important role in mediating the reinforcing/rewarding effects of addictive drugs (Surmeier et al., 2007; Allichon et al., 2021). An important component of this integration is dopamine D1 receptor-mediated generation of cyclic AMP, the activation of PKA, the phosphorylation of DARPP on residue threonine 34 (T34 Phospho-DARPP), the inhibition of protein phosphatase-1, and the maintenance of the ionotropic glutamate receptors in their phosphorylated state (see Figure 4). Donohue et al. (2005) used the AC7 TG mice to study the phosphorylation of the DARPP-32 protein on the threonine-34 residue in the nucleus accumbens, caudate/putamen, and amygdala. The effects of ethanol administered *in vivo* on tissue obtained from these brain areas were also examined. In the brains of AC7 TG mice and WT mice, no differences in total levels of the DARPP-32 protein were evident in any of the tested brain areas (Donohue et al., 2005). In the amygdala and caudate/

putamen of saline-treated (control) WT mice, the levels of T34 Phospho-DARPP were significantly lower than those in the saline-treated AC7 TG mice. Interestingly, just the opposite was true in the nucleus accumbens. The acute administration of ethanol, *in vivo*, increased the levels of T34-Phospho-DARPP in all brain areas of the WT mice. But, only in the amygdala was the effect of the transgene evident. In the amygdala of the TG mice, the administration of alcohol significantly increased the levels of T34-Phospho-DARPP beyond those produced by saline or by the same dose of ethanol in WT mice. A somewhat similar experiment was performed by Bjork et al. (2010), in which ethanol was administered to C57BL/6 mice and levels of T32-Phospho-DARPP were measured in the “striatum,” an area including the nucleus accumbens and amygdala. Ethanol administration produced a “robust” increase in T32-Phospho-DARPP which was blocked by the dopamine D₂ receptor antagonist, sulpiride. The effect of ethanol was also blocked by administration of naloxone given prior to the administration of ethanol. The results with the dopamine D₂ receptor antagonist, and the opiate receptor antagonist naloxone, do indicate more complexity to the phosphorylation of DARPP in the “striatum” than a simple activation of the D₁ dopamine receptor to initiate the phosphorylation cascade. A possibility not considered by Bjork et al. (2010) was that the presence of AC7 in the “striatum” would offer the opportunity for activation of dopamine D₂ or opiate receptors to potentiate the activity of AC7 through release of $\beta\gamma$ subunits from the Gi/Go trimers (Yoshimura et al., 1996). Naloxone administration would block the opiate/D₁ dopamine receptor additive effect (*via* G α and $\beta\gamma$) on AC7.

The contention that opiates are acting in the striatum by coupling to Gi/Go proteins to release $\beta\gamma$, and produce additional activation of AC7, is further supported by the work of Karlsson et al. (2016). In this work, the role of melanin-concentrating hormone in modulating ethanol-induced conditioned place preference (CPP) was investigated. This included measurement of DARPP-32 phosphorylation in WT and MCH1 receptor knock-out mice. Administration of ethanol produced a significant increase in T32-Phospho-DARPP in the shell region of the nucleus accumbens in the WT mice, but not in the MCH1 knock-out mice. The MCH1 knock-out mice also showed diminished propensity to develop ethanol-induced CPP compared to WT mice. The results seen with mice carrying the deletion of the MCH1 gene could be replicated in WT mice by the use of a MCH1 receptor antagonist (Karlsson et al., 2016). An important consideration in interpreting these results is that the MCH1 receptor is a Gi/Go-coupled receptor (Lembo et al., 1999), which is co-expressed with dopamine receptors on medium spiny neurons (Zhang et al., 2006). Again, the generation of $\beta\gamma$ subunits upon activation of the MCH1 receptor, could act in concert with G α to produce an accentuated activation of AC7, and more robust generation of cAMP.

An interesting conclusion can arise from data on ethanol's effects on DARPP phosphorylation, as well as the above-described studies on CRF-mediated GABA release in the central amygdala. One can speculate that, in neurons of the limbic system, AC7, which is responsive to both ethanol and to $\beta\gamma$ subunits, would be the mediator of ethanol and $\beta\gamma$ subunit effects on phosphorylation cascades in these neurons. The PKA- and Epac-mediated events downstream of the activity of AC7 would set the tone for both metabolic and neurotransmission functions in these neurons.

AC7 in the immune system

Duan and colleagues (Duan et al., 2010) bred mice in which one allele of the *Adcy7* gene was disrupted, and although most of the offspring that were double mutants (AC7^{-/-}) died *in utero*, approximately 2–3% survived through birth. The bone marrow from these AC7 knockout animals and bone marrow from their wild type littermates was isolated and transplanted into mice whose immune system had been destroyed by irradiation. The immune system of the recipient mice fully regenerated, producing chimeric mice bearing the donor bone marrow cells. The total number of splenocytes was reduced by more than half in the chimeric mice generated from the bone marrow of the AC7^{-/-} mice, indicating the importance of AC7 in proliferation of both B and T lymphocytes. On the other hand, when challenged with LPS, the chimeric mice with the AC7^{-/-} bone marrow generated a 3–4 times greater TNF α response compared to the mice which received the wild type bone marrow. LPS was also more lethal in the mice carrying the AC7-deficient bone marrow. Macrophages from the AC7-deficient mice produced significantly higher levels of TNF α when challenged with LPS *in vitro*, compared to mice carrying the wild type bone marrow (this response also involved yet-to-be-identified serum factors). Duan et al. (2010) also demonstrated that AC7 was necessary for an optimal antibody response when mice were exposed to antigens. The deficiency in the AC7^{-/-} chimeric mice was primarily due to AC7-dependent function of the T helper cells, even though B cell function was also disrupted in the animals with AC7^{-/-} bone marrow. In conclusion, Duan et al. (2010) state: “...AC7 is the key AC isoform in mediating cAMP response and its downstream physiological functions in the immune system”. Table 1 summarizes the neurobiological phenotypes elucidated in mice in which the expression of AC7 was manipulated.

Genetic manipulation of the type 7 adenylyl cyclase and the behavioral phenotype

Given the electrophysiological, neurochemical, and physiological results of studies with the HET, WT, and TG AC7 mice, these animals were used for behavioral measures of

ethanol consumption and measures of anxiety-like and depressive phenotypes.

In measures of alcohol consumption and preference, AC7 HET mice on two genetic backgrounds (C57BL/6 and 129/SvEv) were used. C57BL/6 mice normally show a high preference for alcohol-containing solutions, and using the HET mice on the C57BL/6 background, no statistically significant differences were found between the HET and WT mice in the quantities of ethanol consumed by males or females. When AC7 was knocked down in the 129/SvEv strain, which drinks low to moderate amounts of ethanol, the females of the HET genotype consumed more ethanol, particularly at the higher concentrations of 10 and 20%. This increase in ethanol consumption resulted in a higher calculated “preference” for ethanol when water intake was taken into account (Desrivieres et al., 2011). In the male HET mice on the 129/SvEv background, the amount of ethanol consumed at the highest concentration was actually less than that consumed by the WT mice, and there was no statistically significant change in the preference measure (Desrivieres et al., 2011). The measure of what is called “preference” has an important concept attached. A “preference” ratio of 0.5 indicates neutrality of choice between the alternatives of the ethanol solution or plain water, while a preference ratio above 0.5 indicates a greater desire for the ethanol solution, and a preference ratio of less than 0.5 indicates an aversion to the ethanol solution. In the case of the HET female mice on the C57BL/6 background and their corresponding WT littermates, all preference ratios were above 0.8, irrespective of the status of AC7 (even though there was an evident increase to almost 1.0 in the HET mice at the lower ethanol concentrations). In the WT females of the 129/SvEv background, the “preference” for the 10 or 20% ethanol solutions was approximately 0.15 and in the HET females the ratio increased to 0.3. These results can be interpreted as indicating that on the 129/SvEv background, the diminution of AC7 in female mice, diminishes the aversion to consuming ethanol solutions containing the higher concentrations of ethanol.

Measures of behavior which is interpreted as “depressive” or “learned helplessness” were also performed in HET, WT, and TG AC7 mice (Hines et al., 2006). Using the forced swim test (FST), female HET mice were shown to exhibit a significantly lesser time of being immobile during the duration of this test compared to the female WT mice (i.e., less “depression”). AC7 TG female mice were, on the other hand, found to exhibit longer periods of immobility than the female WT mice (more “depression”). There were no differences in the immobility time of male WT mice *versus* male TG, or male HET mice in the FST. In the tail suspension test (TST), female HET mice did not differ in immobility from WT mice, but the female TG mice showed greater periods of immobility. Again, there were no differences in immobility time in the TST between male HET, WT, and TG mice. These results indicate that in females, the overexpression of AC7 results in a higher level of “learned helplessness”

(depressive-like behavior), while a reduction in AC7 expression produces greater resilience to depressive-like behaviors. A major caveat to this simple explanation, is the fact that the knock-down of AC7 in the HET female mice resulted in significant changes in gene expression of 30 other transcripts, and there were no changes in other transcript expression in the male mice. One of these transcripts in female strains, peroxiredoxin, has been implicated in behavior in the FST and TST (Scotton et al., 2020).

Table 1 summarizes the behavioral and physiological phenotypes elucidated in mice in which the expression of AC7 was manipulated.

Genetic association of the ADCY7 gene with alcoholism and/or depression in humans

The results with genetic manipulation of AC7 expression in mice qualified this adenylyl cyclase as a possible candidate gene for a genetic contribution to human AUD (Boezio et al., 2017) and/or MDD. Desrivieres et al. (2011) examined single nucleotide polymorphisms (SNPs) within the ADCY7 gene in humans for association with alcohol dependence (defined by DSM-IV and ICD-10 criteria). The subjects consisted of 1,703 individuals classified as alcohol dependent and 1,347 controls, and both men and women were included in this Caucasian population. A SNP (rs2302717) that defined a haplotype across a portion of AC7 gene (ADCY7) was found to be associated with alcohol dependence, but this association was only significant in the females. The minor allele (T) at this locus reduced the risk to develop alcohol dependence (OR = 0.71). Desrivieres et al. (2011) noted that the haplotype identified by this SNP extended into the promoter region of ADCY7, and performed an analysis of the quantity of RNA for AC7 that was present in whole blood or adipose tissue from another large sample of Caucasian individuals. These studies revealed that the minor allele of rs2302717 correlated with lower ADCY7 expression in both tissues. This was seemingly at odds with the data from the studies with mice (Desrivieres et al., 2011), in which knock-down of *Adcy7* and resultant diminution of AC7 RNA in brains of females resulted in less aversion to drinking, while in humans, a polymorphism that was protective against alcohol dependence was also responsible for lower levels of AC7 RNA. An obvious caveat is that the RNA measures in the HET mice were made in brain tissue while the human AC7 RNA was measured in blood and adipose tissues (Desrivieres et al., 2011). The other caveat, already mentioned above, is the fact that the knock-down of *Adcy7* in female mice results in changes in expression of a number of other transcripts in brains of the HET female mice, and this phenomenon will have to be explored in future studies, possibly in postmortem tissue of humans.

TABLE 1 Phenotypes of WT, AC7 HET, and AC7 TG mice.

Behavioral phenotype			Neurobiological phenotype			
I. Alcohol consumption and preference			I. CRF- and ethanol-induced GABA release (IPSP) in CeA*			
	Alcohol consumption	Alcohol preference	WT (CRF)		⇧⇧	
AC7 HET (C57) vs. WT	=	=	AC7 HET (CRF)		⇧	
AC7 HET (129SvEv) vs. WT	M =	=	WT (EtOH)		⇧⇧	
	F ⇧	⇧	AC7 HET (EtOH)		NC	
II. Immobility in forced swim test (Depression)			II. Ethanol-mediated ACTH release (AUC)			
AC7 HET vs. WT	M =			HET	WT	TG
	F ⇩		M	⇧	⇧⇧	⇧⇧⇧
AC7 TG vs. WT	=		F	⇧⇧	⇧⇧⇧	⇧⇧⇧
	F ⇧					
III. Immobility in tail suspension test (Depression)			III. Ethanol-mediated increase (vs. Saline) in T34 pDARPP*			
AC7 HET vs WT	M =		NucAcc		Amygdala	
	F =			Caudate		
AC7 TG vs WT	M =		WT	AC7 TG	WT	AC7 TG
	F ⇧		⇧	⇧	⇧ =	⇧ ⇧⇧
			IV. Immune system function			
				Innate (Macrophages, TNFα)	Adaptive (Antibodies, B Cell/T-helper)	
			AC7 ^{-/-} Chimera vs. WT Chimera**	⇧⇧	⇩	

↑, Increase ↓, Decrease =, No Difference NC, No Change *, All males **, Chimeric mice carry WT or AC7/bone marrow

Given the finding that an allele that is protective against alcohol dependence in women, is also associated with lower levels of AC7 RNA in human blood, it is instructive to review a number of studies which measured adenylyl cyclase activity in human platelets and lymphocytes of alcoholics and control (non-alcoholic) subjects. The first of such studies (Tabakoff et al., 1988) included 95 alcoholic subjects and 33 controls, and the majority of the alcoholic subjects (all except 5 who had been abstinent by self-report for 12–48 months) were abstinent for 23 ± 16 days. All of the subjects were male. Measures of platelet adenylyl cyclase activity demonstrated no differences in basal activity, but significant differences between alcoholic and control subjects in cesium fluoride-, Gpp (NH)p-, and prostaglandin 1 (PGE1)-stimulated adenylyl cyclase activity, with the alcoholic subjects having lower stimulated adenylyl cyclase activity. At the time of this study, the various isoforms of adenylyl cyclase had not yet been described, but currently, it is known that AC7 is the dominant form of adenylyl cyclase in both platelets and lymphocytes (Hellevuo et al., 1993; Duan et al., 2010). Given the earlier discussion regarding the role of PKC δ in promoting the activation of AC7 by Gs protein, the presence of PKC δ and its significant physiological function in platelets, and the fact that all stimulatory agents used in the study of Tabakoff et al. (1988), were acting *via* the Gs protein to activate adenylyl cyclase, one cannot distinguish the effects as being related to upstream effects involving PKC δ , or to adenylyl cyclase *per se*. An additional observation made in this study, was that the five alcoholic individuals who had abstained for over 12 months, still displayed lower cesium fluoride-stimulated adenylyl cyclase activity. This led to the suggestion that the stimulated adenylyl cyclase activity in platelets may be a “trait” rather than a “state” marker in alcoholism (Tabakoff et al., 1988).

A different conclusion regarding adenylyl cyclase activity measured in lymphocytes of alcoholic and control subjects was provided by Szegedi et al. (1998). These investigators followed the adenylyl cyclase activity in lymphocytes of 73 alcohol-dependent subjects at admission to the clinic while intoxicated, at the time of maximal withdrawal signs, and after detoxification. Lymphocyte adenylyl cyclase activity of the alcohol-dependent subjects was also compared to control subjects. Their findings indicated that there were no differences in lymphocyte adenylyl cyclase activity between the control subjects and the alcohol-dependent subjects at admission, while the dependent subjects were intoxicated, but 2 days later basal, GTP γ S-stimulated, and forskolin-stimulated adenylyl cyclase activity were significantly lower in the alcohol-dependent subjects going through withdrawal. After the withdrawal period, there again was no difference in adenylyl cyclase activity in lymphocytes of the control and alcohol-dependent subjects. The time course of changes in lymphocyte adenylyl cyclase activity in the studies of Szegedi et al. (1998) with humans, mirror the changes described in the striatum (Tabakoff and Hoffman, 1979) and cerebral cortex (Saito et al., 1987) of groups of mice chronically fed ethanol, during the early

withdrawal period, and also several days after withdrawal. The earliest publication to note the differences in adenylyl cyclase activity (decreased adenosine (A₂) receptor-mediated cyclic AMP production) in lymphocytes was that of Diamond et al. (1987). The alcohol-dependent subjects in that study were individuals described as “actively drinking” but having little or no alcohol in blood when blood was taken for isolation of lymphocytes. Thus, these subjects would resemble the “withdrawal” group in the studies of Szegedi et al. (1998). The changes described by Diamond et al. (1987) were evident in both B and T cells in the lymphocyte fraction, and more recent evidence examining the isoform of adenylyl cyclase in T and B cells, as well as macrophages, has identified the major adenylyl cyclase in these cells to be AC7 (Duan et al., 2010). Overall, the measurement of AC7 in lymphocytes may be advantageous for extrapolating to the activity of AC7 in brain of individuals undergoing withdrawal from chronic heavy alcohol consumption. It should be noted that the lower levels of adenylyl cyclase activity in platelets of alcoholics may also be a result of lowering of AC7 expression. But this change of expression would have to take place in the megakaryocytes, which are the precursors of platelets, since platelets do not contain DNA. Thus, at the least, the platelet measures of adenylyl cyclase activity would follow a time course more related to the time course of platelet turnover in blood, rather than a time course for changes in AC7 expression in cells replete with DNA and expression/translation machinery.

The platelet adenylyl cyclase activity measured in alcoholics may be confounded by other variables, particularly by the presence of comorbid MDD (Hoffman et al., 2002). In fact, the platelet adenylyl cyclase activity may be a trait marker for MDD which is in turn confounded by current alcohol use by the depressed subject (Hines and Tabakoff, 2005). The initial studies of platelet adenylyl cyclase activity in depressed subjects indicated that forskolin-stimulated adenylyl cyclase activity was particularly lower in individuals diagnosed with MDD, compared to control subjects (Menninger and Tabakoff, 1997). Since forskolin acts directly on the adenylyl cyclase protein to enhance activity (Seamon et al., 1981), one can surmise that depressed subjects have reduced quantities of adenylyl cyclase protein in platelets, and since there is evidence that the major form of adenylyl cyclase in platelets is AC7, one can go further to consider that depressed subjects have lower levels of AC7 in platelets. This supposition was strengthened by the work of Hines et al. (2006), which also proposed an explanation for the lower levels of AC7 in platelets of humans suffering from depression. Hellevuo et al. (1997) demonstrated that the AC7 gene in humans is characterized by a series of polymorphic repeats in the 3'-UTR. The findings of Hines et al. (2006) indicated that the lowest levels of forskolin-stimulated adenylyl cyclase activity in platelets were in depressed subjects whose DNA in the 3'-UTR harbored the longest stretch (seven repeats) of the tetranucleotide AACA (Hellevuo et al.,

TABLE 2 Microglia were isolated at autopsy from parietal l cortex of 39 human subjects. RNASeq was performed on total RNA extracted from flow cytometry-sorted cells. Values represent median microglia expression levels (RPKM, reads per kilobase of transcript per million reads mapped). Galatro et al., 2017.

Expression levels of adenylyl cyclase	Isoforms in microglia
AC isoform	RPKM
ADCY1	0.071
ADCY2	0.038
ADCY3	1.867
ADCY4	0.619
ADCY5	0.023
ADCY6	2.073
ADCY7	52.570
ADCY8	0
ADCY9	1.219
ADCY10	0.223

1997). Some other observations generated by the work of Hines et al. (2006) were: the most prominent diminution in forskolin-stimulated platelet adenylyl cyclase activity was noted in depressed subjects who also had a family history of depressive illness; females diagnosed with MDD with a family history of depression; and in individuals having a genotype for the seven repeats of AACA.

Through a combination of studies on gene expression and informatics using AC7 TG and WT mice, AC7 was linked to function of the proopiomelanocortin (POMC) system and immune system function. Clearly there is a link between the POMC transcript, stress, and the immune system, since POMC is the precursor to ACTH, and pituitary ACTH release, instigated by CRF, stimulates release of adrenal glucocorticoids, and modulates the activity of the immune system (Leistner and Menke, 2018). Chronic stress, in conjunction with childhood trauma, has been considered a significant contributory factor to the development of major depression (Heim and Nemeroff, 2001). Although the relationship of stress and depression has been considered to arise *via* the activation of corticosteroid receptors in brain (Holsboer, 2000), with polymorphisms in FKBP5 (a co-chaperone for the glucocorticoid receptor) being an important component of this relationship (Binder et al., 2004), the above described function of AC7 in control of CRF-mediated ACTH release (Antoni et al., 2003; Pronko et al., 2010) should also be considered in the etiology of depression. Furthermore, it is now becoming evident that AC7 is the major form of adenylyl cyclase in the immune system, and controls activation of macrophages, as well as B and T lymphocytes (Jiang et al., 2008; Duan et al., 2010). Recent studies also indicate that AC7 is the major form of adenylyl cyclase expressed in mouse and human microglia (Bennett et al., 2016; Galatro et al., 2017).

Microglia are considered the “macrophages” of the CNS, and it is not surprising that AC7 is expressed in microglia. (Table 2 shows the expression levels of the various isoforms of adenylyl cyclase in microglia). Cyclic AMP levels are important for conversion of microglia from the M1 to M2 phenotype (M1 describes a proinflammatory phenotype, and M2 an activated but reparatory phenotype) (Ghosh et al., 2016). The relationship of stress to microglial activation is well summarized in Yirmiya et al. (2015) and these authors propose that some forms of MDD may be a “microglial disease,” dependent on microglia transitioning to the M1 phenotype. In all, the involvement of AC7 in the CRF-mediated release of ACTH from the pituitary, and involvement in microglia activation status, may play an important role in the etiology of depression. Assuming that AC7 is mediating the CRF-stimulated ACTH release, and the stress response is of consequence in the etiology of MDD, the sex differences described earlier in the ACTH and glucocorticoid responses in the WT mice, *versus* those with genetically modified expression of AC7, are notable (Pronko et al., 2010).

Further evidence for the involvement of AC7 in depression emanated from the laboratories of Etienne Sibille (Joeyen-Waldorf et al., 2012). This group used mice lacking the serotonin transporter (SERT^{KO}), which have been considered to be a model for studying depressive behaviors and emotionality (Lira et al., 2003), to assess gene expression in amygdala and cingulate cortex. They then compared the differentially expressed transcripts noted between the SERT^{KO} and WT mice to differentially expressed transcripts noted in postmortem samples of amygdala and cingulate cortex from humans with familial MDD, and matched controls. “Conserved changes” were found for 31 transcripts in the amygdala, and 20 transcripts in cingulate cortex in comparisons of the mouse and human brain samples, and the transcript for AC7 was found to be significantly upregulated in the brain tissue from the SERT^{KO} mice, compared to the WT controls, and in the brain tissue of depressed subjects compared to their matched controls. Their further studies examined (using BOLD (MRI)) threat-related amygdala reactivity in two independent samples of human subjects and its association with a single nucleotide polymorphism in the ADCY7 gene. This SNP (rs1064448) has previously been shown to identify a haplotype including a major portion of the ADCY7 and the 3'UTR containing the tetranucleotide repeats (Hines et al., 2006). In both samples, there was a significant association of rs1064448 with greater threat-related amygdala reactivity (Joeyen-Waldorf et al., 2012). These studies illustrate the possible importance of ADCY7 in fear-related amygdala function, and “conserved changes” in the expression of AC7 transcript in brain tissue from mice used as a model of depressive behavior (Joeyen-Waldorf et al., 2012), and in human subjects diagnosed with MDD, amplify the studies of Hines et al. (2006). The SERT^{KO} mice exhibited higher levels of expression of AC7 in brain tissue, as did the post-mortem tissue of the depressed human subjects, and in the studies of Hines et al.

(2006), it was the genetically manipulated mice with lower levels of AC7 in brain that exhibited the lesser depressive-like behavior in the FST, and the female animals with the higher expression of AC7 showed higher immobility in the FST. It is parsimonious to think that deletion or pharmacologic blockade of SERT is coupled to upregulation of AC7 RNA, but this implication of the relationship of SERT and AC7 expression in development or treatment of depression does not appear straightforward. One has to be careful in making generalizations from the results obtained with the SERT^{KO} mice produced on the 129/SvEv genetic background since the same genetic manipulation produced no effect in the C57BL/6 mice (Lira et al., 2003).

The effect of antidepressants on the activity and possibly the expression of adenylyl cyclase in brain may or may not be reflected in measures of adenylyl cyclase activity in platelets since platelet adenylyl cyclase activity was found to be lower in depressed subjects compared to controls (Hines et al., 2006). A more recent study of platelet adenylyl cyclase activity stimulated by PGE1 (via the GS-coupled prostaglandin EP1 receptor) also demonstrated that subjects diagnosed with MDD had significantly lower PGE1-stimulated platelet adenylyl cyclase activity than control subjects (Targum et al., 2022). This study, however, followed a subset of subjects through a 6-week period of treatment with antidepressants which were primarily inhibitors of SERT (SSRIs). In the subjects that showed significant improvement in their Hamilton Depression Ratings (Ham D₁₇ and Ham D₆), there was also a significant increase in their PGE1-stimulated adenylyl cyclase activity toward levels measured in control subjects. Targum et al. (2022), therefore, replicated the lower adenylyl cyclase activity in platelets of clinically depressed subjects (Hines et al., 2006), but also added the fact that the platelet adenylyl cyclase can be not only a marker for depression, but also for measuring response to antidepressants. Targum et al. (2022) also proposed a mechanism for their observed results to be the sequestration of the Gs protein in lipid rafts (Allen et al., 2009) in the platelets of the depressed subjects and suggested that antidepressant treatment would result in the release of Gs from sequestration to be available for stimulation of adenylyl cyclase. Unfortunately, forskolin-stimulated adenylyl cyclase activity was not measured in the studies of Targum et al. (2022) to distinguish between the proposed mechanism, and the diminution of the adenylyl cyclase protein as proposed in other studies (Hines et al., 2006). There may well be different mechanisms in play which result in higher levels of the RNA for AC7 in brain in conjunction with signs of depression in genetically manipulated mice, and depressed human subjects (Hines et al., 2006; Joeyen-Waldorf et al., 2012), and the lower levels of adenylyl cyclase activity (presumably AC7), activated by various means, in platelets of depressed humans. Although forskolin can enhance adenylyl cyclase activity independent of other factors (Seamon et al., 1981), and forskolin (radioactively labeled), can be used to quantify adenylyl cyclase protein (Insel and Ostrom, 2003),

there is clear evidence that Gsa can further activate adenylyl cyclase catalytic function (Insel and Ostrom, 2003). Thus, the lower levels of adenylyl cyclase activity, stimulated by forskolin or agents acting *via* Gs proteins, in platelets of depressed subjects may be either a result of lower levels of the adenylyl cyclase protein, a sequestration of Gs protein, or both mechanisms. Whether the proposed mechanism involving the sequestration of Gs in platelets (Targum et al., 2022) in depressed subjects extends to brain (Senese and Rasenick, 2021), bears scrutiny.

Summary and consideration of AC7 as a therapeutic target to treat alcoholism and/or depression

AC7 is a member of the sub-family of adenylyl cyclases (Type 2, 4, and 7) whose activity is insensitive to Gia proteins, is potentiated by the $\beta\gamma$ subunits of G proteins in conjunction with Gsa stimulation, and whose responsiveness to Gsa is modulated by the state of phosphorylation catalyzed by PKC δ . This enzyme is also insensitive to calcium in the presence or absence of calmodulin. The distinguishing feature that separates AC7 from the Type 2 and Type 4 adenylyl cyclases is the particularly high level of activation of this enzyme by ethanol when the enzyme activity is also influenced by Gsa. AC7 also has a cellular/tissue distribution that distinguishes it from the other members of its sub-family. Particularly notable is the evidence for its presence in the amygdala, nucleus accumbens, hippocampus, and frontal cortical regions in brains of animals, with evidence for presynaptic and postsynaptic localization (Mons et al., 1998), and its presence in the corticotrophs of the pituitary. The presence of AC7 in the pituitary, and its involvement in the release of ACTH, speaks to the possible importance of AC7 in the hypothalamic/pituitary/adrenocortical response to stress. The presence of AC7 in the amygdala, and possibly in other parts of the striatum, as well as in frontal cortical regions, and its coupling to the CRF1 receptor in the amygdala, as well as in the pituitary, bespeaks a deeper involvement in stress and negative affect. It is, thus, not surprising that associations have been reported between measures of adenylyl cyclase activity in brain, platelets, and lymphocytes of alcoholics, and subjects diagnosed with MDD. This association has been extended to genetic markers which identify the haplotype in which the ADCY7 gene is located.

The significant comorbidity that exists between AUD and MDD is well accepted (Hasin et al., 2018). There are two manifestations of the co-occurrence of depression in individuals who fit the criteria for AUD. In one manifestation, the signs of depression are evident only during the initial period of time that an individual dependent on alcohol tried to abstain (i.e., alcohol withdrawal), and once abstinence has been achieved for some period of time, the signs and symptoms of depression abate (Raimo and Schuckit, 1998). In another manifestation, the

signs of depression become evident during the initial stages of abstinence but continue to persist throughout sobriety (Raimo and Schuckit, 1998). When one considers the time course of changes in brains of animals that have been chronically fed ethanol, and have undergone forced abstinence, one notes that in brain areas such as the cortex, the activity of adenylyl cyclase is within the normal range while the animal is intoxicated, drops below normal levels during the first days of abstinence, and then returns to normal. One wonders whether the lower levels of adenylyl cyclase activity in brain during the initial stages of withdrawal is a contributing factor to the signs of withdrawal (i.e., depression), or simply a byproduct of the withdrawal hyperexcitability syndrome. It is of interest that measures of adenylyl cyclase in platelets of human alcoholics present a picture resembling the time course of fluctuations in adenylyl cyclase activity seen in brains of alcohol dependent and withdrawing animals. Adenylyl cyclase activity in platelets was in the normal range while the individual was actively consuming alcohol, dropped below normal levels during early stages of withdrawal, and then returned to normal after a period of abstinence. It might seem that the stress of abstaining from alcohol may be a factor in diminishing adenylyl cyclase activity during withdrawal. The alcohol withdrawal-induced changes in brain and platelet adenylyl cyclase activity can be classified as a state marker of withdrawal from chronic use of alcohol.

On the other hand, the genetically generated increased expression of adenylyl cyclase in brains of animals is associated with more permanent depressive symptomology. There are a number of missing pieces of evidence that need to be added to assume that increases in mRNA for AC7 are related to higher activity of this enzyme in brain of depressed subjects. Even accurate measures of AC7 protein have not been accomplished (Joeyen-Waldorf et al., 2012).

The differences in adenylyl cyclase activity between depressed human subjects and controls, are related to lower levels of adenylyl cyclase activity in depressed subjects in platelets, and activity of this adenylyl cyclase in response to Gs α is enhanced when the subject is being successfully treated with antidepressants (Targum et al., 2022). Even though the exact relationship between expression and activity of AC7 and MDD is still enigmatic, the development of pharmacological tools for isoform-selective manipulation of AC7 would help resolve the enigmatic features of the relationship and may lead to novel therapeutics for depression and/or AUD.

AC7 as a therapeutic target

A prior review (Price and Brust, 2019) suggested the possibility that AC7 may be “A new target for depression,” but did not propose how to “medicate this target.” An excellent review of molecules that inhibit adenylyl cyclase activity is available (Seifert et al., 2012) including many P-site inhibitors (adenosine analogues) and

substituted nucleotides that act at the catalytic site of the adenylyl cyclases. This review emphasizes the problems encountered in trying to generate inhibitors that interact with the catalytic domains of the adenylyl cyclases, and would also have some substantial selectivity among the nine membrane-bound adenylyl cyclases, and would not have off-target effects on ion channels and glucose transporters. The effects of the large number of compounds developed as catalytic site inhibitors have not been tested for activity and selectivity for AC7. The diterpene alkaloids, such as forskolin, have generally been thought of as activators of adenylyl cyclase (Seamon et al., 1981), however, 1-deoxy-forskolin and 1,9-dideoxy-forskolin have been found to inhibit adenylyl cyclase activity (Seifert et al., 2012). One of the most interesting analogues of forskolin is referred to as BODIPY-FS (Pinto et al., 2008). BODIPY-FS is an activator of Type 1 and 5 adenylyl cyclases, has little effect on Type 3 and 6, but inhibits the activity of the Type 2 adenylyl cyclase (Seifert et al., 2012). The other members of the Type 2 adenylyl cyclase family, i.e., Type 4 and Type 7, have not been explored with regard to their responses to BODIPY-FS.

The search for isoform-specific inhibitors (Brand et al., 2013) or activators of adenylyl cyclases may benefit from a more thorough consideration of structural/regulatory differences. In this regard, peptide analogues designed to correspond to the regions of the Type 2, 4 and 7 adenylyl cyclases that are phosphorylated by PKC may prove valuable modulators of these isoforms, and may even distinguish between these isoforms. Interestingly, a peptide based on the C1b region of AC7 was found to be an inhibitor of this enzyme (Yan et al., 2001). The other sequence that bears attention in trying to modulate the activity of AC7 is the region that binds the β/γ subunits (Diel et al., 2006; Brand, 2015). The sequences in this region of the isoforms responsive to β/γ need to be carefully examined and information should be gathered on the variants of the β and γ subunits that may have selectivity for the particular cyclase isoforms Diel et al. (2006). Such peptide modulators would have an additional advantage (or possible disadvantage) of being coordinate regulators of, for example, AC7 requiring the binding of Gs α , for evidence of their activity (Wang et al., 2005). Development of peptides as drug molecules is a complicated endeavor and as mentioned above, targeting AC7 should be preceded by a clear knowledge of its role in brain function [e.g. opiate tolerance/dependence (Wang et al., 2005), AUD, depression, etc.] as well as in the periphery [e.g. in the immune system (Duan et al., 2010)]. At this point, the evidence for AC7 activity in depression and AUD is tantalizing, but far from definitive. The actions of lithium (a mood stabilizer) as an inhibitor of AC7 (Mann et al., 2008), and the possible upregulation of AC7 by antidepressants such as SSRIs (Targum et al., 2022) should raise interest in the role of this enzyme in mood disorders. On the other hand, the more immediate use of AC7 activity may be as a peripheral state marker in AUD, state or trait marker in depression and a

diagnostic distinguishing MDD from AUD (Tabakoff et al., 1986) or manic-depressive illness (Tabakoff et al., 2010).

Author contributions

All authors listed have made a substantial, direct, and intellectual contribution to the work and approved it for publication.

Acknowledgments

The authors thank NIH for research grant support (Grants R24AA013162; R44AA024905; UG3DA047680), Alexandra Dunbar for assistance with illustrations and Marilyn Sullivan for manuscript preparation.

References

- Agoglia, A. E., and Herman, M. A. (2018). The center of the emotional universe: Alcohol, stress, and CRF1 amygdala circuitry. *Alcohol* 72, 61–73. doi:10.1016/j.alcohol.2018.03.009
- Ahn, N. G., Seger, R., Bratlien, R. L., Diltz, C. D., Tonks, N. K., and Krebs, E. G. (1991). Multiple components in an epidermal growth factor-stimulated protein kinase cascade. *J. Biol. Chem.* 266, 4220–4227. doi:10.1016/s0021-9258(20)64310-1
- Allely, P., Graham, W., McDonnell, M., and Spedding, R. (2006). Alcohol levels in the emergency department: A worrying trend. *Emerg. Med. J.* 23, 707–708. doi:10.1136/emj.2005.034082
- Allen, J. A., Yu, J. Z., Dave, R. H., Bhatnagar, A., Roth, B. L., and Rasenick, M. M. (2009). Caveolin-1 and lipid microdomains regulate Gs trafficking and attenuate Gs/adenylyl cyclase signaling. *Mol. Pharmacol.* 76, 1082–1093. doi:10.1124/mol.109.060160
- Allichon, M. C., Ortiz, V., Pousinha, P., Andrianarivelo, A., Petitbon, A., Heck, N., et al. (2021). Cell-type-specific adaptations in striatal medium-sized spiny neurons and their roles in behavioral responses to drugs of Abuse. *Front. Synaptic Neurosci.* 13, 799274. doi:10.3389/fnsyn.2021.799274
- Antoni, F. A., Sosunov, A. A., Haunso, A., Paterson, J. M., and Simpson, J. (2003). Short-term plasticity of cyclic adenosine 3', 5'-monophosphate signaling in anterior pituitary corticotrope cells: The role of adenylyl cyclase isotypes. *Mol. Endocrinol.* 17, 692–703. doi:10.1210/me.2002-0369
- Bagchi, B. (2005). Water dynamics in the hydration layer around proteins and micelles. *Chem. Rev.* 105, 3197–3219. doi:10.1021/cr020661+
- Bajo, M., Cruz, M. T., Siggins, G. R., Messing, R., and Roberto, M. (2008). Protein kinase C epsilon-mediated release of CRF- and ethanol-induced GABA release in central amygdala. *Proc. Natl. Acad. Sci. U. S. A.* 105, 8410–8415. doi:10.1073/pnas.0802302105
- Bakalyar, H. A., and Reed, R. R. (1990). Identification of a specialized adenylyl cyclase that may mediate odorant detection. *Science* 250, 1403–1406. doi:10.1126/science.2255909
- Beeler, J. A., Yan, S. Z., Bykov, S., Murza, A., Asher, S., and Tang, W. J. (2004). A soluble C1b protein and its regulation of soluble type 7 adenylyl cyclase. *Biochemistry* 43, 15463–15471. doi:10.1021/bi049088+
- Bennett, M. L., Bennett, F. C., Liddelov, S. A., Ajami, B., Zamanian, J. L., Fernhoff, N. B., et al. (2016). New tools for studying microglia in the mouse and human CNS. *Proc. Natl. Acad. Sci. U. S. A.* 113, E1738–E1746. doi:10.1073/pnas.1525528113
- Binder, E. B., and Nemeroff, C. B. (2010). The CRF system, stress, depression and anxiety—insights from human genetic studies. *Mol. Psychiatry* 15, 574–588. doi:10.1038/mp.2009.141
- Binder, E. B., Salyakina, D., Lichtner, P., Wochnik, G. M., Ising, M., Pütz, B., et al. (2004). Polymorphisms in FKBP5 are associated with increased recurrence of depressive episodes and rapid response to antidepressant treatment. *Nat. Genet.* 36, 1319–1325. doi:10.1038/ng1479
- Bjork, K., Terasmaa, A., Sun, H., Sommer, W., and Heilig, M. (2010). Ethanol-induced activation of AKT and DARPP-32 in the mouse striatum mediated by opioid receptors. *Addict. Biol.* 15, 299–303. doi:10.1111/j.1369-1600.2010.00212.x
- Blenkinsopp, J. (2011). Creation, un-creation, Re-creation: A discursive commentary on genesis 1–11. *Clark Int.*
- Boezio, B., Audouze, K., Ducrot, P., and Taboureau, O. (2017). Network-based approaches in Pharmacology. *Mol. Inf.* 36, 1700048. doi:10.1002/minf.201700048
- Brand, C. S., Hocker, H. J., Gorfe, A. A., Cavaotto, C. N., and Dessauer, C. W. (2013). Isoform selectivity of adenylyl cyclase inhibitors: Characterization of known and novel compounds. *J. Pharmacol. Exp. Ther.* 347, 265–275. doi:10.1124/jpet.113.208157
- Brand, C. S. (2015). “Isoform selective regulation of adenylyl cyclase by small molecule inhibitors and gbetagamma protein,” in *The university of Texas MD anderson cancer center UT Health graduate school of biomedical sciences dissertations and theses (open access)*.
- Brand, T. (2019). POPDC proteins and cardiac function. *Biochem. Soc. Trans.* 47, 1393–1404. doi:10.1042/BST20190249
- Brockmann, M. M., Zarebidaki, F., Camacho, M., Grauel, M. K., Trimbuch, T., Südhof, T. C., et al. (2020). A trio of active zone proteins comprised of RIM-BPs, RIMs, and Munc13s governs neurotransmitter release. *Cell Rep.* 32, 107960. doi:10.1016/j.celrep.2020.107960
- Buck, J., Sinclair, M. L., Schapal, L., Cann, M. J., and Levin, L. R. (1999). Cytosolic adenylyl cyclase defines a unique signaling molecule in mammals. *Proc. Natl. Acad. Sci. U. S. A.* 96, 79–84. doi:10.1073/pnas.96.1.79
- Calì, J. J., Zwaagstra, J. C., Mons, N., Cooper, D. M., and Krupinski, J. (1994). Type VIII adenylyl cyclase. A Ca²⁺/calmodulin-stimulated enzyme expressed in discrete regions of rat brain. *J. Biol. Chem.* 269, 12190–12195. doi:10.1016/s0021-9258(17)32700-x
- Chen, B. S., and Roche, K. W. (2007). Regulation of NMDA receptors by phosphorylation. *Neuropharmacology* 53, 362–368. doi:10.1016/j.neuropharm.2007.05.018
- Costa, S. W., Yu, S. C., Liewald, J. F., and Gottschalk, A. (2017). Fast cAMP modulation of neurotransmission via neuropeptide signals and vesicle loading. *Curr. Biol.* 27, 495–507. doi:10.1016/j.cub.2016.12.055
- Cruz, M. T., Bajo, M., Maragnoli, M. E., Tabakoff, B., Siggins, G. R., and Roberto, M. (2011). Type 7 adenylyl cyclase is involved in the ethanol and CRF sensitivity of GABAergic synapses in mouse central amygdala. *Front. Neurosci.* 4, 207. doi:10.3389/fnins.2010.00207
- Desrivieres, S., Pronko, S. P., Lourdasamy, A., Ducci, F., Hoffman, P. L., Wodarz, N., et al. (2011). Sex-specific role for adenylyl cyclase type 7 in alcohol dependence. *Biol. Psychiatry* 69, 1100–1108. doi:10.1016/j.biopsych.2011.01.037
- Devasani, K., and Yao, Y. (2022). Expression and functions of adenylyl cyclases in the CNS. *Fluids Barriers CNS* 19, 23. doi:10.1186/s12987-022-00322-2
- Diamond, I., Wrubel, B., Estrin, W., and Gordon, A. (1987). Basal and adenosine receptor-stimulated levels of cAMP are reduced in lymphocytes from alcoholic patients. *Proc. Natl. Acad. Sci. U. S. A.* 84, 1413–1416. doi:10.1073/pnas.84.5.1413

Conflict of interest

The authors declare that the research was conducted in the absence of any commercial or financial relationships that could be construed as a potential conflict of interest.

Publisher's note

All claims expressed in this article are solely those of the authors and do not necessarily represent those of their affiliated organizations, or those of the publisher, the editors and the reviewers. Any product that may be evaluated in this article, or claim that may be made by its manufacturer, is not guaranteed or endorsed by the publisher.

- Diel, S., Klass, K., Wittig, B., and Kleuss, C. (2006). Gbetagamma activation site in adenylyl cyclase type II. Adenylyl cyclase type III is inhibited by Gbetagamma. *J. Biol. Chem.* 281, 288–294. doi:10.1074/jbc.M511045200
- Donohue, T., Hoffman, P. L., and Tabakoff, B. (2005). Effect of ethanol on DARPP-32 phosphorylation in transgenic mice that express human type VII adenylyl cyclase in brain. *Alcohol. Clin. Exp. Res.* 29, 310–316. doi:10.1097/01.alc.0000156179.22112.0f
- Duan, B., Davis, R., Sadat, E. L., Collins, J., Sternweis, P. C., Yuan, D., et al. (2010). Distinct roles of adenylyl cyclase VII in regulating the immune responses in mice. *J. Immunol.* 185, 335–344. doi:10.4049/jimmunol.0903474
- Feinstein, P. G., Schrader, K. A., Bakalyar, H. A., Tang, W. J., Krupinski, J., Gilman, A. G., et al. (1991). Molecular cloning and characterization of a Ca²⁺/calmodulin-insensitive adenylyl cyclase from rat brain. *Proc. Natl. Acad. Sci. U. S. A.* 88, 10173–10177. doi:10.1073/pnas.88.22.10173
- Fernandez, E., Schiappa, R., Girault, J. A., and Le Novère, N. (2006). DARPP-32 is a robust integrator of dopamine and glutamate signals. *PLoS Comput. Biol.* 2, e176. doi:10.1371/journal.pcbi.0020176
- Fukuoka, H., Shichi, H., Yamamoto, M., and Takahashi, Y. (2020). The mechanisms underlying autonomous adrenocorticotrophic hormone secretion in cushing's disease. *Int. J. Mol. Sci.* 21, 9132. doi:10.3390/ijms21239132
- Galatro, T. F., Holtman, I. R., Lerario, A. M., Vainchtein, I. D., Brouwer, N., Sola, P. R., et al. (2017). Transcriptomic analysis of purified human cortical microglia reveals age-associated changes. *Nat. Neurosci.* 20, 1162–1171. doi:10.1038/nn.4597
- Gao, B., and Gilman, A. G. (1991). Cloning and expression of a widely distributed (type IV) adenylyl cyclase. *Proc. Natl. Acad. Sci. U. S. A.* 88, 10178–10182. doi:10.1073/pnas.88.22.10178
- Gekel, I., and Neher, E. (2008). Application of an Epac activator enhances neurotransmitter release at excitatory central synapses. *J. Neurosci.* 28, 7991–8002. doi:10.1523/JNEUROSCI.0268-08.2008
- Ghosh, M., Xu, Y., and Pearce, D. D. (2016). Cyclic AMP is a key regulator of M1 to M2a phenotypic conversion of microglia in the presence of Th2 cytokines. *J. Neuroinflammation* 13, 9. doi:10.1186/s12974-015-0463-9
- Greener, M. R., and Storr, S. J. (2022). Exploring the role of DARPP-32 in addiction: A review of the current limitations of addiction treatment pathways and the role of DARPP-32 to improve them. *NeuroSci* 3, 494–509. doi:10.3390/neurosci3030035
- Hacker, B. M., Storm, D. R., Wayman, G. A., Sultana, R., Chan, G., Villacrés, E., et al. (1998). Cloning, chromosomal mapping, and regulatory properties of the human type 9 adenylyl cyclase (ADCY9). *Genomics* 50, 97–104. doi:10.1006/geno.1998.5293
- Hasin, D. S., Sarvet, A. L., Meyers, J. L., Saha, T. D., Ruan, W. J., Stohl, M., et al. (2018). Epidemiology of adult DSM-5 major depressive disorder and its specifiers in the United States. *JAMA Psychiatry* 75, 336–346. doi:10.1001/jamapsychiatry.2017.4602
- Heim, C., and Nemeroff, C. B. (2001). The role of childhood trauma in the neurobiology of mood and anxiety disorders: Preclinical and clinical studies. *Biol. Psychiatry* 49, 1023–1039. doi:10.1016/s0006-3223(01)01157-x
- Hellevuo, K., Welborn, R., Menninger, J. A., and Tabakoff, B. (1997). Human adenylyl cyclase type 7 contains polymorphic repeats in the 3' untranslated region: Investigations of association with alcoholism. *Am. J. Med. Genet.* 74, 95–98. doi:10.1002/(sici)1096-8628(19970221)74:1<95:aid-ajmg19>3.0.co;2-m
- Hellevuo, K., Yoshimura, M., Kao, M., Hoffman, P. L., Cooper, D. M., and Tabakoff, B. (1993). A novel adenylyl cyclase sequence cloned from the human erythroleukemia cell line. *Biochem. Biophys. Res. Commun.* 192, 311–318. doi:10.1006/bbrc.1993.1415
- Hellevuo, K., Yoshimura, M., Mons, N., Hoffman, P. L., Cooper, D. M., and Tabakoff, B. (1995). The characterization of a novel human adenylyl cyclase which is present in brain and other tissues. *J. Biol. Chem.* 270, 11581–11589. doi:10.1074/jbc.270.19.11581
- Hines, L. M., Hoffman, P. L., Bhavé, S., Saba, L., Kaiser, A., Snell, L., et al. (2006). A sex-specific role of type VII adenylyl cyclase in depression. *J. Neurosci.* 26, 12609–12619. doi:10.1523/JNEUROSCI.1040-06.2006
- Hines, L. M., and Tabakoff, B. and WHO/ISBRA Study on State and Trait Markers of Alcohol Use and Dependence Investigators (2005). Platelet adenylyl cyclase activity: A biological marker for major depression and recent drug use. *Biol. Psychiatry* 58, 955–962. doi:10.1016/j.biopsych.2005.05.040
- Hoffman, P. L., Glanz, J., and Tabakoff, B. (2002). Platelet adenylyl cyclase activity as a state or trait marker in alcohol dependence: Results of the WHO/ISBRA study on state and trait markers of alcohol use and dependence. *Alcohol. Clin. Exp. Res.* 26, 1078–1087. doi:10.1111/j.1530-0277.2002.tb02642.x
- Hoffman, P. L., Rabe, C. S., Moses, F., and Tabakoff, B. (1989). N-methyl-D-aspartate receptors and ethanol: Inhibition of calcium flux and cyclic GMP production. *J. Neurochem.* 52, 1937–1940. doi:10.1111/j.1471-4159.1989.tb07280.x
- Holsboer, F. (2000). The corticosteroid receptor hypothesis of depression. *Neuropsychopharmacology* 23, 477–501. doi:10.1016/S0893-133X(00)00159-7
- Hucho, T. B., Dina, O. A., and Levine, J. D. (2005). Epac mediates a cAMP-to-PKC signaling in inflammatory pain: An isolectin B4(+) neuron-specific mechanism. *J. Neurosci.* 25, 6119–6126. doi:10.1523/JNEUROSCI.0285-05.2005
- Insel, P. A., and Ostrom, R. S. (2003). Forskolin as a tool for examining adenylyl cyclase expression, regulation, and G protein signaling. *Cell. Mol. Neurobiol.* 23, 305–314. doi:10.1023/a:1023684503883
- Ishikawa, Y., Katsushika, S., Chen, L., Halnon, N. J., Kawabe, J., and Homcy, C. J. (1992). Isolation and characterization of a novel cardiac adenylyl cyclase cDNA. *J. Biol. Chem.* 267, 13553–13557. doi:10.1016/s0021-9258(18)42247-8
- Izumi, Y., Hirai, S., Tamai, Y., Fujise-Matsuoka, A., Nishimura, Y., and Ohno, S. (1997). A protein kinase Cdelta-binding protein SRBC whose expression is induced by serum starvation. *J. Biol. Chem.* 272, 7381–7389. doi:10.1074/jbc.272.11.7381
- Jiang, L. I., Collins, J., Davis, R., Fraser, I. D., and Sternweis, P. C. (2008). Regulation of cAMP responses by the G12/13 pathway converges on adenylyl cyclase VII. *J. Biol. Chem.* 283, 23429–23439. doi:10.1074/jbc.M803281200
- Joeyen-Waldorf, J., Nikolova, Y. S., Edgar, N., Walsh, C., Kota, R., Lewis, D. A., et al. (2012). Adenylate cyclase 7 is implicated in the biology of depression and modulation of affective neural circuitry. *Biol. Psychiatry* 71, 627–632. doi:10.1016/j.biopsych.2011.11.029
- Karlsson, C., Rehman, F., Damadzic, R., Atkins, A. L., Schank, J. R., Gehlert, D. R., et al. (2016). The melanin-concentrating hormone-1 receptor modulates alcohol-induced reward and DARPP-32 phosphorylation. *Psychopharmacol. Berl.* 233, 2355–2363. doi:10.1007/s00213-016-4285-y
- Katsushika, S., Chen, L., Kawabe, J. L., Nilakantan, R., Halnon, N. J., Homcy, C. J., et al. (1992). Cloning and characterization of a sixth adenylyl cyclase isoform: types V and VI constitute a subgroup within the mammalian adenylyl cyclase family. *Proc. Natl. Acad. Sci. U. S. A.* 89, 8774–8778. doi:10.1073/pnas.89.18.8774
- Khasar, S. G., Lin, Y. H., Martin, A., Dadgar, J., McMahon, T., Wang, D., et al. (1999). A novel nociceptor signaling pathway revealed in protein kinase C epsilon mutant mice. *Neuron* 24, 253–260. doi:10.1016/s0896-6273(00)80837-5
- Klemm, W. R. (1998). Biological water and its role in the effects of alcohol. *Alcohol* 15, 249–267. doi:10.1016/s0741-8329(97)00130-4
- Koob, G. F., and Volkow, N. D. (2016). Neurobiology of addiction: A neurocircuitry analysis. *Lancet. Psychiatry* 3, 760–773. doi:10.1016/S2215-0366(16)00104-8
- Kovalovsky, D., Refojo, D., Liberman, A. C., Hochbaum, D., Pereda, M. P., Coso, O. A., et al. (2002). Activation and induction of NUR77/NURR1 in corticotrophs by CRH/cAMP: Involvement of calcium, protein kinase A, and MAPK pathways. *Mol. Endocrinol.* 16, 1638–1651. doi:10.1210/mend.16.7.0863
- Krähling, A. M., Alvarez, L., Debowski, K., Van, Q., Gunkel, M., Irsen, S., et al. (2013). CRIS-A novel cAMP-binding protein controlling spermiogenesis and the development of flagellar bending. *PLoS Genet.* 9, e1003960. doi:10.1371/journal.pgen.1003960
- Krebs, E. G., Love, D. S., Bratvold, G. E., Trayser, K. A., Meyer, W. L., and Fischer, E. H. (1964). Purification and properties of rabbit skeletal muscle phosphorylase B kinase. *Biochemistry* 3, 1022–1033. doi:10.1021/bi00896a003
- Krupinski, J., Coussen, F., Bakalyar, H. A., Tang, W. J., Feinstein, P. G., Orth, K., et al. (1989). Adenylyl cyclase amino acid sequence: Possible channel- or transporter-like structure. *Science* 244, 1558–1564. doi:10.1126/science.2472670
- Krupinski, J., Lehman, P. C., Frankenfield, C. D., Zwaagstra, J. C., and Watson, P. A. (1992). Molecular diversity in the adenylyl cyclase family. Evidence for eight forms of the enzyme and cloning of type VI. *J. Biol. Chem.* 267, 24858–24862. doi:10.1016/s0021-9258(18)35842-3
- Leistner, C., and Menke, A. (2018). How to measure glucocorticoid receptor's sensitivity in patients with stress-related psychiatric disorders. *Psychoneuroendocrinology* 91, 235–260. doi:10.1016/j.psyneuen.2018.01.023
- Lembo, P. M., Grazzini, E., Cao, J., Hubatsch, D. A., Pelletier, M., Hoffert, C., et al. (1999). The receptor for the orexigenic peptide melanin-concentrating hormone is a G-protein-coupled receptor. *Nat. Cell Biol.* 1, 267–271. doi:10.1038/12978
- Lira, A., Zhou, M., Castanon, N., Ansorge, M. S., Gordon, J. A., Francis, J. H., et al. (2003). Altered depression-related behaviors and functional changes in the dorsal raphe nucleus of serotonin transporter-deficient mice. *Biol. Psychiatry* 54, 960–971. doi:10.1016/s0006-3223(03)00696-6
- Lonart, G., Schoch, S., Kaeser, P. S., Larkin, C. J., Südhof, T. C., and Linden, D. J. (2003). Phosphorylation of RIM1alpha by PKA triggers presynaptic long-term potentiation at cerebellar parallel fiber synapses. *Cell* 115, 49–60. doi:10.1016/s0092-8674(03)00727-x

- Luthin, G. R., and Tabakoff, B. (1984). Activation of adenylate cyclase by alcohols requires the nucleotide-binding protein. *J. Pharmacol. Exp. Ther.* 228, 579–587.
- Mann, L., Heldman, E., Shaltiel, G., Belmaker, R. H., and Agam, G. (2008). Lithium preferentially inhibits adenylyl cyclase V and VII isoforms. *Int. J. Neuropsychopharmacol.* 11, 533–539. doi:10.1017/S1461145707008395
- Maruschak, L. (1999). “DWI offenders under correctional supervision,” in *Bureau of justice statistics*. Editor U. S. D. O. JUSTICE.
- Menninger, J. A., and Tabakoff, B. (1997). Forskolin-stimulated platelet adenylyl cyclase activity is lower in persons with major depression. *Biol. Psychiatry* 42, 30–38. doi:10.1016/S0006-3223(96)00245-4
- Miyakawa, T., Yagi, T., Kitazawa, H., Yasuda, M., Kawai, N., Tsuboi, K., et al. (1997). Fyn-kinase as a determinant of ethanol sensitivity: Relation to NMDA-receptor function. *Science* 278, 698–701. doi:10.1126/science.278.5338.698
- Mons, N., Yoshimura, M., Ikeda, H., Hoffman, P. L., and Tabakoff, B. (1998). Immunological assessment of the distribution of type VII adenylyl cyclase in brain. *Brain Res.* 788, 251–261. doi:10.1016/S0006-8993(98)00005-5
- Nakazawa, T., Komai, S., Tezuka, T., Hisatsune, C., Umemori, H., Semba, K., et al. (2001). Characterization of Fyn-mediated tyrosine phosphorylation sites on GluR epsilon 2 (NR2B) subunit of the N-methyl-D-aspartate receptor. *J. Biol. Chem.* 276, 693–699. doi:10.1074/jbc.M008085200
- Nelson, E. J., Hellevuo, K., Yoshimura, M., and Tabakoff, B. (2003). Ethanol-induced phosphorylation and potentiation of the activity of type 7 adenylyl cyclase. Involvement of protein kinase C delta. *J. Biol. Chem.* 278, 4552–4560. doi:10.1074/jbc.M210386200
- Newton, A. C., and Brognard, J. (2017). Reversing the paradigm: Protein kinase C as a tumor suppressor. *Trends Pharmacol. Sci.* 38, 438–447. doi:10.1016/j.tips.2017.02.002
- Nie, Z., Zorrilla, E. P., Madamba, S. G., Rice, K. C., Roberto, M., and Siggins, G. R. (2009). Presynaptic CRF1 receptors mediate the ethanol enhancement of GABAergic transmission in the mouse central amygdala. *ScientificWorldJournal*. 9, 68–85. doi:10.1100/tsw.2009.1
- Nishi, A., Watanabe, Y., Higashi, H., Tanaka, M., Nairn, A. C., and Greengard, P. (2005). Glutamate regulation of DARPP-32 phosphorylation in neostriatal neurons involves activation of multiple signaling cascades. *Proc. Natl. Acad. Sci. U. S. A.* 102, 1199–1204. doi:10.1073/pnas.0409138102
- Olsen, R. W., and Liang, J. (2017). Role of GABA(A) receptors in alcohol use disorders suggested by chronic intermittent ethanol (CIE) rodent model. *Mol. Brain* 10, 45. doi:10.1186/s13041-017-0325-8
- Omori, K., and Kotera, J. (2007). Overview of PDEs and their regulation. *Circ. Res.* 100, 309–327. doi:10.1161/01.RES.0000256354.95791.f1
- Pinto, C., Papa, D., Hübner, M., Mou, T. C., Lushington, G. H., and Seifert, R. (2008). Activation and inhibition of adenylyl cyclase isoforms by forskolin analogs. *J. Pharmacol. Exp. Ther.* 325, 27–36. doi:10.1124/jpet.107.131904
- Premont, R. T., Matsuoka, I., Mattei, M. G., Pouille, Y., Defer, N., and Hanoune, J. (1996). Identification and characterization of a widely expressed form of adenylyl cyclase. *J. Biol. Chem.* 271, 13900–13907. doi:10.1074/jbc.271.23.13900
- Price, T., and Brust, T. F. (2019). Adenylyl cyclase 7 and neuropsychiatric disorders: A new target for depression? *Pharmacol. Res.* 143, 106–112. doi:10.1016/j.phrs.2019.03.015
- Pronko, S. P., Saba, L. M., Hoffman, P. L., and Tabakoff, B. (2010). Type 7 adenylyl cyclase-mediated hypothalamic-pituitary-adrenal axis responsiveness: Influence of ethanol and sex. *J. Pharmacol. Exp. Ther.* 334, 44–52. doi:10.1124/jpet.110.166793
- Rabbani, M., Nelson, E. J., Hoffman, P. L., and Tabakoff, B. (1999). Role of protein kinase C in ethanol-induced activation of adenylyl cyclase. *Alcohol. Clin. Exp. Res.* 23, 77–86. doi:10.1111/j.1530-0277.1999.tb04026.x
- Rabbani, M., and Tabakoff, B. (2001). Chronic ethanol treatment reduces adenylyl cyclase activity in human erythroleukemia cells. *Eur. J. Pharmacol.* 430, 19–23. doi:10.1016/S0014-2999(01)01370-X
- Rabin, R. A. (1990b). Chronic ethanol exposure of PC 12 cells alters adenylate cyclase activity and intracellular cyclic AMP content. *J. Pharmacol. Exp. Ther.* 252, 1021–1027.
- Rabin, R. A. (1990a). Direct effects of chronic ethanol exposure on beta-adrenergic and adenosine-sensitive adenylate cyclase activities and cyclic AMP content in primary cerebellar cultures. *J. Neurochem.* 55, 122–128. doi:10.1111/j.1471-4159.1990.tb08829.x
- Rabin, R. A., and Molinoff, P. B. (1981). Activation of adenylate cyclase by ethanol in mouse striatal tissue. *J. Pharmacol. Exp. Ther.* 216, 129–134.
- Rabin, R. A., Wolfe, B. B., Dibner, M. D., Zahniser, N. R., Melchior, C., and Molinoff, P. B. (1980). Effects of ethanol administration and withdrawal on neurotransmitter receptor systems in C57 mice. *J. Pharmacol. Exp. Ther.* 213, 491–496.
- Raimo, E. B., and Schuckit, M. A. (1998). Alcohol dependence and mood disorders. *Addict. Behav.* 23, 933–946. doi:10.1016/S0306-4603(98)00068-9
- Rao, R. T., and Androulakis, I. P. (2017). Modeling the sex differences and interindividual variability in the activity of the hypothalamic-pituitary-adrenal Axis. *Endocrinology* 158, 4017–4037. doi:10.1210/en.2017-00544
- Reyland, M. E. (2009). Protein kinase C isoforms: Multi-functional regulators of cell life and death. *Front. Biosci.* 14, 2386–2399. doi:10.2741/3385
- Rhee, M. H., Bayewitch, M., Avidor-Reiss, T., Levy, R., and Vogel, Z. (1998). Cannabinoid receptor activation differentially regulates the various adenylyl cyclase isoforms. *J. Neurochem.* 71, 1525–1534. doi:10.1046/j.1471-4159.1998.71041525.x
- Roberto, M., Kirson, D., and Khom, S. (2021). The role of the central amygdala in alcohol dependence. *Cold Spring Harb. Perspect. Med.* 11, a039339. doi:10.1101/cshperspect.a039339
- Robichaux, W. G., 3rd, and Cheng, X. (2018). Intracellular cAMP sensor EPAC: Physiology, pathophysiology, and therapeutics development. *Physiol. Rev.* 98, 919–1053. doi:10.1152/physrev.00025.2017
- Rodbell, M., Birnbaumer, L., Pohl, S. L., and Krans, H. M. (1971a). The glucagon-sensitive adenylyl cyclase system in plasma membranes of rat liver. *J. Biol. Chem.* 246, 1877–1882. doi:10.1016/S0021-9258(18)62390-7
- Rodbell, M., Krans, H. M., Pohl, S. L., and Birnbaumer, L. (1971b). The glucagon-sensitive adenylyl cyclase system in plasma membranes of rat liver. *J. Biol. Chem.* 246, 1872–1876. doi:10.1016/S0021-9258(18)62389-0
- Rodbell, M. (1995). Signal transduction: Evolution of an idea. *Environ. Health Perspect.* 103, 338–345. doi:10.1289/ehp.9510338
- Saito, T., Lee, J. M., Hoffman, P. L., and Tabakoff, B. (1987). Effects of chronic ethanol treatment on the beta-adrenergic receptor-coupled adenylate cyclase system of mouse cerebral cortex. *J. Neurochem.* 48, 1817–1822. doi:10.1111/j.1471-4159.1987.tb05741.x
- Santoro, B., and Shah, M. M. (2020). Hyperpolarization-activated cyclic nucleotide-gated channels as drug targets for neurological disorders. *Annu. Rev. Pharmacol. Toxicol.* 60, 109–131. doi:10.1146/annurev-pharmtox-010919-023356
- Schleifer, L. S., Garrison, J. C., Sternweis, P. C., Northup, J. K., and Gilman, A. G. (1980). The regulatory component of adenylate cyclase from uncoupled S49 lymphoma cells differs in charge from the wild type protein. *J. Biol. Chem.* 255, 2641–2644. doi:10.1016/S0021-9258(19)85780-0
- Scholich, K., Wittpoth, C., Barbier, A. J., Mullenix, J. B., and Patel, T. B. (1997). Identification of an intramolecular interaction between small regions in type V adenylyl cyclase that influences stimulation of enzyme activity by Gsalpha. *Proc. Natl. Acad. Sci. U. S. A.* 94, 9602–9607. doi:10.1073/pnas.94.18.9602
- Scotton, E., Colombo, R., Reis, J. C., Possebon, G. M. P., Hizo, G. H., Valiati, F. E., et al. (2020). BDNF prevents central oxidative damage in a chronic unpredictable mild stress model: The possible role of PRDX-1 in anhedonic behavior. *Behav. Brain Res.* 378, 112245. doi:10.1016/j.bbr.2019.112245
- Seamon, K. B., Padgett, W., and Daly, J. W. (1981). Forskolin: Unique diterpene activator of adenylate cyclase in membranes and in intact cells. *Proc. Natl. Acad. Sci. U. S. A.* 78, 3363–3367. doi:10.1073/pnas.78.6.3363
- Seeber, U., and Kuschinsky, K. (1976). Dopamine-sensitive adenylate cyclase in homogenates of rat striata during ethanol and barbiturate withdrawal. *Arch. Toxicol.* 35, 247–253. doi:10.1007/BF00570266
- Seifert, R., Lushington, G. H., Mou, T. C., Gille, A., and Sprang, S. R. (2012). Inhibitors of membranous adenylyl cyclases. *Trends Pharmacol. Sci.* 33, 64–78. doi:10.1016/j.tips.2011.10.006
- Senese, N. B., and Rasenick, M. M. (2021). Antidepressants produce persistent G_{α_s} -associated signaling changes in lipid rafts after drug withdrawal. *Mol. Pharmacol.* 100, 66–81. doi:10.1124/molpharm.120.000226
- Shen, J. X., Wachten, S., Halls, M. L., Everett, K. L., and Cooper, D. M. (2012). Muscarinic receptors stimulate AC2 by novel phosphorylation sites, whereas G $\beta\gamma$ subunits exert opposing effects depending on the G-protein source. *Biochem. J.* 447, 393–405. doi:10.1042/BJ20120279
- Sossin, W. S. (2007). Isoform specificity of protein kinase Cs in synaptic plasticity. *Learn. Mem.* 14, 236–246. doi:10.1101/lm.469707
- Subramanian, A., Capalbo, A., Iyengar, N. R., Rizzo, R., Di Campli, A., Di Martino, R., et al. (2019). Auto-regulation of secretory flux by sensing and responding to the folded cargo protein load in the endoplasmic reticulum. *Cell* 176, 1461–1476. e23. doi:10.1016/j.cell.2019.01.035

- Südhof, T. C., and Rizo, J. (2011). Synaptic vesicle exocytosis. *Cold Spring Harb. Perspect. Biol.* 3, a005637. doi:10.1101/cshperspect.a005637
- Surmeier, D. J., Ding, J., Day, M., Wang, Z., and Shen, W. (2007). D1 and D2 dopamine-receptor modulation of striatal glutamatergic signaling in striatal medium spiny neurons. *Trends Neurosci.* 30, 228–235. doi:10.1016/j.tins.2007.03.008
- Sutherland, E. W., Rall, T. W., and Menon, T. (1962). Adenyl cyclase. *J. Biol. Chem.* 237, 1220–1227. doi:10.1016/s0021-9258(18)60312-6
- Sutherland, E. W., and Rall, T. W. (1957). The properties of an adenine ribonucleotide produced with cellular particles, ATP, Mg⁺⁺, and epinephrine or glucagon. *J. Biol. Chem.* 403.
- Sutherland, E. W., Robison, G. A., and Butcher, R. W. (1968). Some aspects of the biological role of Adenosine 3',5' mono phosphate (Cyclic AMP). *Circulation* 37, 279–306. doi:10.1161/01.cir.37.2.279
- Szegedi, A., Anghelescu, I., Pauly, T., Dahmen, N., Müller, M. J., Wetzel, H., et al. (1998). Activity of the adenylyl cyclase in lymphocytes of male alcoholic patients is state dependent. *Alcohol. Clin. Exp. Res.* 22, 2073–2079. doi:10.1111/j.1530-0277.1998.tb05918.x
- Tabakoff, B., Cornell, N., and Hoffman, P. L. (1986). Alcohol tolerance. *Ann. Emerg. Med.* 15, 1005–1012. doi:10.1016/s0196-0644(86)80119-6
- Tabakoff, B., and Hoffman, P. L. (1979). Development of functional dependence on ethanol in dopaminergic systems. *J. Pharmacol. Exp. Ther.* 208, 216–222.
- Tabakoff, B., Hoffman, P. L., Lee, J. M., Saito, T., Willard, B., and De Leon-Jones, F. (1988). Differences in platelet enzyme activity between alcoholics and nonalcoholics. *N. Engl. J. Med.* 318, 134–139. doi:10.1056/NEJM198801213180302
- Tabakoff, B., Martinez, L., Saba, L., and Hoffman, P. L. 2010. Genetic diagnosis of depression. In: DEPRESSION, U. P. A. F. G. D. O. (ed.). US Patent 20100273153.
- Tabakoff, B., Munoz-Marcus, M., and Fields, J. Z. (1979). Chronic ethanol feeding produces an increase in muscarinic cholinergic receptors in mouse brain. *Life Sci.* 25, 2173–2180. doi:10.1016/0024-3205(79)90089-4
- Tabakoff, B., Whelan, J. P., Ovchinnikova, L., Nhamburo, P., Yoshimura, M., and Hoffman, P. L. (1995). Quantitative changes in G proteins do not mediate ethanol-induced downregulation of adenylyl cyclase in mouse cerebral cortex. *Alcohol. Clin. Exp. Res.* 19, 187–194. doi:10.1111/j.1530-0277.1995.tb01491.x
- Tang, W. J., Krupinski, J., and Gilman, A. G. (1991). Expression and characterization of calmodulin-activated (type I) adenylylcyclase. *J. Biol. Chem.* 266, 8595–8603. doi:10.1016/s0021-9258(18)93016-4
- Targum, S. D., Schappi, J., Koutsouris, A., Bhaumik, R., Rapaport, M. H., Rasgon, N., et al. (2022). A novel peripheral biomarker for depression and antidepressant response. *Mol. Psychiatry* 27, 1640–1646. doi:10.1038/s41380-021-01399-1
- Tesmer, J. J., Sunahara, R. K., Gilman, A. G., and Sprang, S. R. (1997). Crystal structure of the catalytic domains of adenylyl cyclase in a complex with G α .GTP γ S. *Science* 278, 1907–1916. doi:10.1126/science.278.5345.1907
- Valverius, P., Hoffman, P. L., and Tabakoff, B. (1989). Brain forskolin binding in mice dependent on and tolerant to ethanol. *Brain Res.* 503, 38–43. doi:10.1016/0006-8993(89)91700-9
- Van Der Horst, J., Greenwood, I. A., and Jepps, T. A. (2020). Cyclic AMP-dependent regulation of Kv7 voltage-gated potassium channels. *Front. Physiol.* 11, 727. doi:10.3389/fphys.2020.00727
- Walsh, D. A., Perkins, J. P., and Krebs, E. G. (1968). An adenosine 3', 5'-monophosphate-dependant protein kinase from rabbit skeletal muscle. *J. Biol. Chem.* 243, 3763–3765. doi:10.1016/s0021-9258(19)34204-8
- Wang, H. Y., Friedman, E., Olmstead, M. C., and Burns, L. H. (2005). Ultra-low-dose naloxone suppresses opioid tolerance, dependence and associated changes in mu opioid receptor-G protein coupling and Gbetagamma signaling. *Neuroscience* 135, 247–261. doi:10.1016/j.neuroscience.2005.06.003
- Wang, X.-T., Zhou, L., Xu, F.-X., Wang, D.-J., Cai, X.-Y., Wang, Y., et al. (2022a). cAMP–EPAC–PKC ϵ –RIM1 α signaling regulates presynaptic long-term potentiation and motor learning. *bioRxiv*, 2022.06.15.496308.
- Watson, P. A., Krupinski, J., Kempinski, A. M., and Frankenfield, C. D. (1994). Molecular cloning and characterization of the type VII isoform of mammalian adenylyl cyclase expressed widely in mouse tissues and in S49 mouse lymphoma cells. *J. Biol. Chem.* 269, 28893–28898. doi:10.1016/s0021-9258(19)61991-5
- Yaka, R., Phamluong, K., and Ron, D. (2003). Scaffolding of Fyn kinase to the NMDA receptor determines brain region sensitivity to ethanol. *J. Neurosci.* 23, 3623–3632. doi:10.1523/jneurosci.23-09-03623.2003
- Yan, S. Z., Beeler, J. A., Chen, Y., Shelton, R. K., and Tang, W. J. (2001). The regulation of type 7 adenylyl cyclase by its C1b region and *Escherichia coli* peptidylprolyl isomerase, SlyD. *J. Biol. Chem.* 276, 8500–8506. doi:10.1074/jbc.M010361200
- Yan, S. Z., Hahn, D., Huang, Z. H., and Tang, W. J. (1996). Two cytoplasmic domains of mammalian adenylyl cyclase form a Gs α - and forskolin-activated enzyme *in vitro*. *J. Biol. Chem.* 271, 10941–10945. doi:10.1074/jbc.271.18.10941
- Yirmiya, R., Rimmerman, N., and Reshef, R. (2015). Depression as a microglial disease. *Trends Neurosci.* 38, 637–658. doi:10.1016/j.tins.2015.08.001
- Yoshimura, M., and Cooper, D. M. F. (1992). Cloning and expression of a Ca²⁺ inhibitable adenylyl cyclase from NCB-20 cells. *Proc. Natl. Acad. Sci. U. S. A.* 89, 6716–6720. doi:10.1073/pnas.89.15.6716
- Yoshimura, M., and Cooper, D. M. (1993). Type-specific stimulation of adenylylcyclase by protein kinase C. *J. Biol. Chem.* 268, 4604–4607. doi:10.1016/s0021-9258(18)53439-6
- Yoshimura, M., Ikeda, H., and Tabakoff, B. (1996). mu-Opioid receptors inhibit dopamine-stimulated activity of type V adenylyl cyclase but enhance dopamine-stimulated activity of type VII adenylyl cyclase. *Mol. Pharmacol.* 50, 43–51.
- Yoshimura, M., Pearson, S., Kadota, Y., and Gonzalez, C. E. (2006). Identification of ethanol responsive domains of adenylyl cyclase. *Alcohol. Clin. Exp. Res.* 30, 1824–1832. doi:10.1111/j.1530-0277.2006.00219.x
- Yoshimura, M., and Tabakoff, B. (1999). Ethanol's actions on cAMP-mediated signaling in cells transfected with type VII adenylyl cyclase. *Alcohol. Clin. Exp. Res.* 23, 1457–1461. doi:10.1097/0000374-199909000-00006
- Yoshimura, M., and Tabakoff, B. (1995). Selective effects of ethanol on the generation of cAMP by particular members of the adenylyl cyclase family. *Alcohol. Clin. Exp. Res.* 19, 1435–1440. doi:10.1111/j.1530-0277.1995.tb01004.x
- Yoshimura, M., Wu, P. H., Hoffman, P. L., and Tabakoff, B. (2000). Overexpression of type 7 adenylyl cyclase in the mouse brain enhances acute and chronic actions of morphine. *Mol. Pharmacol.* 58, 1011–1016. doi:10.1124/mol.58.5.1011
- Zaccolo, M., Zerio, A., and Lobo, M. J. (2021). Subcellular organization of the cAMP signaling pathway. *Pharmacol. Rev.* 73, 278–309. doi:10.1124/pharmrev.120.000086
- Zhang, D., and Heaney, A. P. (2020). 9. Cells, E900. doi:10.3390/cells9040900Nuclear receptors as regulators of pituitary corticotroph pro-opiomelanocortin transcriptionCells
- Zhang, T. A., Maldve, R. E., and Morrisett, R. A. (2006). Coincident signaling in mesolimbic structures underlying alcohol reinforcement. *Biochem. Pharmacol.* 72, 919–927. doi:10.1016/j.bcp.2006.04.022



OPEN ACCESS

EDITED BY
Rennolds S. Ostrom,
Chapman University, United States

REVIEWED BY
Giovanni Hernandez,
McGill University, Canada
Ming Zhang,
Kunming Medical University, China

*CORRESPONDENCE

Mark M. Rasenick,
raz@uic.edu
Jeffrey M. Schappi,
jschap3@uic.edu

†These authors have contributed equally
to this work and share senior authorship

SPECIALTY SECTION

This article was submitted to
Neuropharmacology,
a section of the journal
Frontiers in Pharmacology

RECEIVED 05 August 2022
ACCEPTED 31 October 2022
PUBLISHED 18 November 2022

CITATION

Schappi JM and Rasenick MM (2022),
 $G\alpha_s$, adenylyl cyclase, and their
relationship to the diagnosis and
treatment of depression.
Front. Pharmacol. 13:1012778.
doi: 10.3389/fphar.2022.1012778

COPYRIGHT

© 2022 Schappi and Rasenick. This is an
open-access article distributed under
the terms of the [Creative Commons
Attribution License \(CC BY\)](#). The use,
distribution or reproduction in other
forums is permitted, provided the
original author(s) and the copyright
owner(s) are credited and that the
original publication in this journal is
cited, in accordance with accepted
academic practice. No use, distribution
or reproduction is permitted which does
not comply with these terms.

$G\alpha_s$, adenylyl cyclase, and their relationship to the diagnosis and treatment of depression

Jeffrey M. Schappi^{1,2*†} and Mark M. Rasenick^{1,3,2,4*†}

¹Departments of Physiology and Biophysics, University of Illinois at Chicago, Chicago, IL, United States, ²Jesse Brown VAMC, Chicago, IL, United States, ³Department of Psychiatry, University of Illinois at Chicago, Chicago, IL, United States, ⁴Pax Neuroscience, Glenview, IL, United States

The relationship between depression, its etiology and therapy, and the cAMP signaling system have been studied for decades. This review will focus on cAMP, G proteins and adenylyl cyclase and depression or antidepressant action. Both human and animal studies are compared and contrasted. It is concluded that there is some synteny in the findings that cAMP signaling is attenuated in depression and that this is reversed by successful antidepressant therapy. The G protein that activates adenylyl cyclase, $G\alpha_s$, appears to have diminished access to adenylyl cyclase in depression, and this is rectified by successful antidepressant treatment. Unfortunately, attempts to link specific isoforms of adenylyl cyclase to depression or antidepressant action suffer from discontinuity between human and animal studies.

KEYWORDS

GPCR, cAMP, lipid rafts, cytoskeleton, depression, antidepressant

Introduction

The World Health Organization states that major depressive disorder (MDD) is the most common cause of disability worldwide. The medical and non-medical costs of MDD in the US are now estimated at nearly \$300B. The current COVID-19 pandemic is likely to exacerbate this. Treatment of MDD also poses significant obstacles. Despite undergoing multiple treatment regimes, about one-third of patients never achieve remission, and it is this “treatment-resistant” group who are at the greatest risk of suicide. Thus, there remains a pressing need for novel compounds that are effective in this nonresponsive population. New antidepressant drugs are needed, and in order to develop them, greater insight is needed into the biology of depression and antidepressant response. Additionally, diagnosis of depression is both difficult, imprecise, and based on subjective inventories. Both diffusely-targeted therapy and imprecise diagnosis are a result of our failure to understand the molecular and cellular biology of depression. Discovery and verification of cellular hallmarks (biomarkers) for both depression and antidepressant response is a pressing need.

cAMP, BDNF, and depression

No common mechanism has emerged to link the activities of the diverse compounds used in therapy for depression. Although not necessarily linked to therapeutic action, most antidepressants elevate cAMP production and evoke a cascade of events resulting from sustained increase in cAMP (e.g. increased P-CREB and BDNF) (Donati and Rasenick, 2003). Antidepressant treatment also causes a shift in the localization of the heterotrimeric G protein, G_{α_s} , from lipid rafts to more “fluid” membrane regions, facilitating G_{α_s} activation of adenylyl cyclase (AC). Both diminished G_{α_s} -adenylyl cyclase coupling and an increase in the proportion of G_{α_s} in lipid rafts are seen in depression (post-mortem and peripheral tissue) (Donati et al., 2008; Singh et al., 2020; Targum et al., 2022), and this is consistent with the augmentation of cAMP production by antidepressants. There are also compounds, such as ketamine, and, perhaps psychedelics, that appear to exert more rapid effects on depression, acting in hours rather than weeks for traditional antidepressants. Ketamine shows similar, but more rapid, effects on G_{α_s} and cAMP compared to traditional antidepressants (Wray et al., 2018).

Several studies (*vide infra*) indicate that chronic antidepressant treatment increases physical coupling between G_{α_s} and adenylyl cyclase, resulting in increased cAMP generation. This is consistent with the observation that chronic treatment with antidepressants results in long-term increases in cellular cAMP (Malberg and Blendy, 2005). Consistent with this, depressed subjects show decreased ^{11}C rolipram binding that recovers with successful antidepressant treatment (Fujita et al., 2016). Furthermore, increasing cAMP with inhibitors of phosphodiesterase have showed a promising antidepressant-adjuvant properties in a recent clinical study (Zhao et al., 2003; El-Haggar et al., 2018).

The initial studies showing that CREB knockout blocks the behavioral response to antidepressants date back at least 20 years (Conti et al., 2002) and more recent papers target serotonergic and noradrenergic neurons in achieving this effect (Rafa-Zablocka et al., 2017). BDNF and TrkB knockout also ablated antidepressant effects in mice (Björkholm and Monteggia, 2016). Both humans and mice with the BDNF val66met allele are more vulnerable to stress-induced anxiety and depression, but this is variable with age and sex (Hwang et al., 2006) (Verhagen et al., 2010). A polymorphism in the regulatory region of the human *BDNF* gene, which reduces BDNF expression and release, is also associated with depression (Björkholm and Monteggia, 2016).

Activated by phosphorylation, pCREB in combination with coactivator CPB (CREB binding protein) is able to act as a transcription factor at CRE (cAMP response element), promoting transcription of cAMP-regulated genes, particularly BDNF (brain-derived neurotrophic factor) (Blendy, 2006; Dwivedi and Pandey, 2008). Animal models of stress and depression-like behavior have revealed decreased BDNF

expression, as well as loss of synaptic plasticity, particularly in the hippocampus (Duman et al., 1999), as well as restoration of BDNF expression with extended antidepressant treatment (Fujimaki et al., 2000; Coppel et al., 2003; Foubert et al., 2004). Likewise, human postmortem samples show decreases in BDNF expression in depression (Dunham et al., 2009; Castrén and Monteggia, 2021), and increases with antidepressant treatment (Chen et al., 2001). BDNF itself may be required for the action of antidepressants (Adachi et al., 2008), including ketamine (Autry et al., 2011). The decreased expression of BDNF in stress models and in depression, and restoration of BDNF expression with antidepressant treatment, could be linked by the cAMP changes in depression, and with antidepressant treatment, noted above.

Antidepressants and cAMP

Monoamine centric antidepressants

The majority of extant antidepressants are targeted at monoamine reuptake and metabolism; particularly, inhibition of these. More recently, drugs targeting melatonergic (agomelatine) (Kennedy and Eisfeld, 2007) and glutamatergic (rapid acting antidepressant ketamine) (Matveychuk et al., 2020) systems have been developed or approved for use in depression. Nonetheless, reuptake inhibitors acting at various combinations of SERT, NET, and DAT (serotonin, norepinephrine, and dopamine reuptake transporters) remain the predominant antidepressant class in clinical use. Reuptake inhibitors have shown, collectively, relevant affinities at numerous sites, including reuptake transporters, their canonical targets, as well as monoamine and cholinergic receptors. Despite 60 + years of research, no clear direct mechanism of action has emerged to link their activities. In the case of serotonin, perhaps the most widely implicated neurotransmitter in depression in lay and scientific press alike, a recent review found no clear association between serotonin and depression and also cited several studies demonstrating decreased serotonin content in human and animal subjects post-antidepressant treatment (Moncrieff et al., 2022).

Sulser and his colleagues suggested that one role of extended treatment with tricyclic antidepressants was desensitization of the β -adrenergic receptor and a generalized dampening of cAMP signaling (Sulser et al., 1984). This was contradicted, in part, by results of Menkes et al., showing augmented cAMP signaling in multiple rat brain regions (but not other tissues) after 3 weeks of antidepressant treatment (including ECS) in rats (Menkes et al., 1983). The apparent controversy was resolved through the use of a cellular model system for antidepressant activity, where the time required for an antidepressant response was 3 days (vs 3 weeks in rats and 8 weeks in humans). In this system, antidepressant exposure desensitized the β -receptor on a much faster timescale (24 h) that required for augmented G_{α_s} -activation of AC (Chen and Rasenick, 1995b).

Model systems for determining antidepressant action

We have tested a variety of cell lines including C6 glioma, PC12 pheochromocytoma, SK-N-SH neuroblastoma, as well as patient stem cell-derived neural and glial cell lines, for G protein-based antidepressant response. All compounds with antidepressant activity elicited translocation of G_{α_s} out of lipid rafts, enhanced G_{α_s} -mediated cAMP generation, and slowed FRAP (fluorescence recovery after photobleaching) of GFP- G_{α_s} . Collectively, antidepressant actions on G_{α_s} and adenylyl cyclase are summarized in Figure 1.

Antidepressants from all functional and chemical classes tested, promoted movement of G_{α_s} out of lipid rafts, and enhanced stimulation of adenylyl cyclase promoting increased cAMP production. Total cellular G_{α_s} content is unchanged; the shift out of lipid rafts represents a redistribution of G_{α_s} . Furthermore, G proteins G_{α_i} , G_{α_o} , and G_{α_q} are unaffected. The redistribution of G_{α_s} out of lipid rafts occurs in a dose- and time-dependent fashion, with maximal effect occurring after approximately 3 days of antidepressant treatment, perhaps mirroring the delayed onset of effects in human subjects (which typically requires several weeks of treatment). Notably, the “rapid acting antidepressant”, ketamine, also produces these effects, and on an accelerated timeline, matching the rapid effects seen in humans.

The above findings have consistently been seen in cells of neural/glial character, either cell lines (such as C6 glioma, PC12 pheochromocytoma, and SK-N-SH neuroblastoma, or induced neural stem cells (Yu et al., 2021), while the effect has not been seen in cell lines of non-neural origin such as HEK293 and COS7. This has also raised the question of why cell lines, which cannot be considered to be “depressed” (though the tissue from which they were generated may be from a depressed subject, as in our patient stem cell-derived lines), nonetheless show an “antidepressant response.” This is a consistent empirical finding in the antidepressant responsive cell lines. Likewise, “normal” rodents respond to antidepressant administration in many behavioral tests. Selected studies reflecting the above findings are presented below.

Chen and Rasenick examined in C6 glioma the effect of chronic tricyclic antidepressant desipramine treatment for 1–5 days at 5 and 10 μ M (note: 50 mM was also tested but was deleterious to cells) on membrane cAMP production in response to stimulation with nonhydrolyzable GTP analog Gpp (NH)p (direct G protein activator) or isoproterenol (Chen and Rasenick, 1995b). Membrane cAMP production was significantly enhanced in a dose- and time-dependent fashion. This effect was not seen in membranes treated acutely (at the time of assay) with desipramine. The effect of desipramine treatment on total membrane content (lipid rafts were not considered at this point) of G_{α_s} , G_{α_i} , G_{α_o} , and $G\beta$ was assessed by western blot, and no difference was

found, compared to control. A similar contemporaneous study in rats, also by Chen and Rasenick, showed findings consistent with those in C6 glioma (Chen and Rasenick, 1995a). Here, rats treated with tricyclic antidepressants amitriptyline and desipramine were assessed for cortical membrane cAMP production and G protein disposition, as well as G_{α_s} /adenylyl cyclase interaction *via* co-immunoprecipitation. Also tested were amphetamine (which elevates synaptic norepinephrine and serotonin (Berman et al., 2009), the canonical mechanism of action of most extant antidepressants, but without recognized clinical antidepressant activity) and ECT (electroconvulsive therapy). As in C6 glioma, treatment of rats with antidepressant drugs resulted in enhanced membrane cAMP production in response to Gpp (NH)p or forskolin stimulation, compared to controls. Unlike C6 glioma, no effect was seen with 1-day treatment; 21-day treatment was required, which is more similar to the extended treatment period required for clinical effects in humans. ECT (11 sessions) produced similar effects, and no effect was seen with amphetamine. These findings were consistent with an earlier study in rats, which also found increased cAMP in cortical and hippocampal membranes post chronic, but not acute, antidepressant or ECT treatment (Menkes et al., 1983). Additionally, antidepressant treatment and ECT resulted in increased adenylyl cyclase activity immunoprecipitated with G_{α_s} as measured by assay of the immunoprecipitated complex. Again consistent with the results in C6 glioma, total membrane content of G_{α_s} , G_{α_i} , G_{α_o} (as well as adenylyl cyclase 1 and 2) were unchanged by antidepressant or ECT treatments.

While the above studies revealed enhancement of cAMP production by antidepressant treatment (and ECT), without change in total G protein content, further studies noted an enhancement by antidepressant treatment upon detergent extractability of G_{α_s} , bringing lipid rafts into this scheme. Toki et al. (Toki et al., 1999) treated C6 glioma for 3 days with antidepressants iprindole, amitriptyline, and fluoxetine, as well as chlorpromazine (antipsychotic drug, structurally similar to tricyclics and without clinical antidepressant activity). Membrane proteins were sequentially extracted with Triton X-100 and Triton X-114, with Triton X-100 acting upon less hydrophobic membrane regions, and Triton X-114 acting upon more hydrophobic regions (Regula et al., 1986) (now considered as nonraft and lipid raft domains) and allowing differential separation of proteins from these membrane domains. While drug treatments again did not affect total G_{α_s} content, G_{α_s} extraction by Triton X-100 was increased, and extraction by Triton X-114 decreased, by all antidepressant treatments, suggesting a change in the membrane environment of G_{α_s} subsequent to antidepressant treatment—in contemporary parlance, a redistribution of G_{α_s} from lipid raft to nonraft membrane fractions. In contrast, G_{α_i} was unaffected and

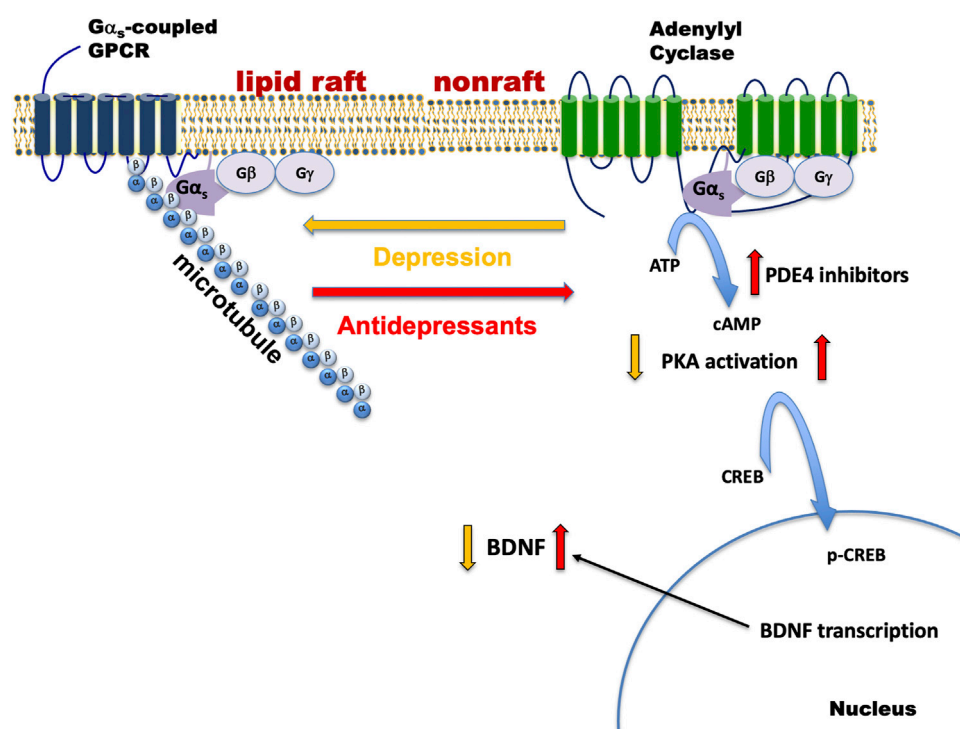


FIGURE 1

Depression and antidepressant effects on $G\alpha_s$ plasma membrane localization. $G\alpha_s$ is normally distributed between non-raft regions of the membrane where it moves freely and promotes neurotransmitter-activated adenylyl cyclase activity and a specialized region of the membrane rich in cholesterol (lipid raft), where the movement/adenylyl cyclase activation of $G\alpha_s$ is impaired. During depression, $G\alpha_s$ is enriched in the lipid raft region and it is anchored there by the structural protein, tubulin (α/β). Antidepressant treatment changes $G\alpha_s$ such that it exits from the raft and moves to the non-raft region where it completes the process of neurotransmitter action by activating the enzyme, adenylyl cyclase. Increased $G\alpha_s$ -mediated adenylyl cyclase activity results in increased generation of cAMP, PKA activation, phosphorylation of CREB, and increases in BDNF transcription and translation. cAMP phosphodiesterase (e.g., PDE4) is another point of regulation for cAMP and inhibition here will also result in increased cAMP activity. $G\alpha_s$ -coupled GPCRs that may be relevant to depression include receptors for corticotropin releasing factor (CRF 1&2), serotonin (5-HT_{4,6,7}), dopamine (D1), and β -adrenergic receptors. Antidepressant treatment also causes some $G\alpha_s$ to be released from the plasma membrane, where it associates with microtubules and modifies their dynamic behavior.

treatment with non-antidepressant chlorpromazine had no effect on $G\alpha_s$. Cortical membranes from antidepressant-treated rats also showed similar redistribution of $G\alpha_s$. C6 glioma membranes were additionally fractionated *via* sucrose density gradient, and consecutive fractions assayed for forskolin-stimulated cAMP production. Membrane fractions from antidepressant-treated cells showing increased $G\alpha_s$ content had significant increases in cAMP production, compared to controls. Collectively, the above studies illustrate a cellular response to chronic antidepressant treatment specifically targeting $G\alpha_s$, but not other G proteins, with redistribution of $G\alpha_s$ out of lipid rafts into nonraft membrane fractions, and enhanced association with adenylyl cyclase/increased cAMP production.

Creation of a fluorescent GFP-tagged $G\alpha_s$ construct with normal membrane expression and adenylyl cyclase activation (Yu and Rasenick, 2002) and stable C6 GFP- $G\alpha_s$ cell line allowed development of a higher-throughput assay utilizing FRAP (Czys et al., 2015). Treatment with antidepressants and resulting redistribution of $G\alpha_s$ out of lipid rafts results in

slower lateral membrane mobility of $G\alpha_s$, seen as a slower recovery of GFP- $G\alpha_s$ fluorescence after photobleaching, presumably due to increased interaction between GFP- $G\alpha_s$ and the larger, more slowly moving adenylyl cyclase molecule. Again, treatment with numerous antidepressants from varied classes resulted in significantly slowed GFP- $G\alpha_s$ mobility (i.e., longer half-time of recovery), while psychiatric drugs lacking antidepressant activity did not alter GFP- $G\alpha_s$ mobility. Among notable findings were the contrasting results of currently popular antidepressant escitalopram (S-citalopram) and its clinically inactive stereoisomer R-citalopram. While escitalopram showed the antidepressant-characteristic slowing of GFP- $G\alpha_s$ mobility, R-citalopram had no effect, which is consistent with traditional biochemical assays of the two drugs (Zhang and Rasenick, 2010). Also consistent with past findings were the dose- and time-dependence of antidepressant-induced $G\alpha_s$ redistribution, as well as restriction of this effect to $G\alpha_s$ and not other G protein types.

PDE4 inhibitors

Phosphodiesterases (PDEs) regulate the activity of cyclic nucleotides cAMP and cGMP by catalyzing their degradation into adenosine- and guanosine-5' monophosphate, respectively. They comprise 11 isoforms, with a growing catalog of subtypes with varied subcellular localization (Delhay and Bardoni, 2021). They display varying selectivity for cAMP and cGMP, with some targeting both (PDE1,2,3,10,11), some cGMP-selective (PDE5,6,9), and others cAMP-selective (PDE4,7,8) (Azevedo et al., 2014). Inhibitors of cAMP-targeted phosphodiesterases, particularly PDE4, have been investigated as potential antidepressants.

Rolipram (ZK 62711) was identified in the 1970s as an inhibitor of phosphodiesterase (and later, as a PDE4-specific inhibitor), elevating cAMP, but not cGMP, concentrations in rat brain tissue homogenates and slices (Schwabe et al., 1976). Early studies of rolipram in rodents as a potential antidepressant examined the drug's (and other cAMP-selective PDE inhibitors) ability to reverse reserpine-induced hypothermia and hypokinesia (reserpine inhibits vesicular monoamine transporters, depleting synaptic monoamines) and potentiate yohimbine-induced toxicity (Wachtel, 1983). Other rodent studies identified rolipram's ability to suppress avoidance of foot shock in a rat model of depression ("Flinders sensitive line") (Overstreet et al., 1989). Zhang et al. examined the behavioral phenotype of heterozygous and homozygous PDE4D-subtype mouse knockouts (Zhang et al., 2002). Both knockouts showed significantly reduced immobility in tail suspension- and forced swim tests, an antidepressant-like effect, with the strongest effect seen in the heterozygous knockouts. The antidepressant effect of rolipram in the forced swim test was significantly blunted in the knockout mice, suggesting subtype PDE4D may be responsible for these effects. Additional PDE4 inhibitors Ro 20-1724, ICI 63,197, and CP 67,593 have also shown antidepressant-like effects in rats (O'Donnell, 1993). Interestingly, this study also examined the effect of forskolin, which broadly activates adenylyl cyclase isoforms, increasing cellular cAMP (Insel and Ostrom, 2003; Pinto et al., 2008), finding it to lack antidepressant activity. This could reflect a requirement for a microdomain-specific enhancement of cAMP, rather than an overall increase in cellular cAMP.

Numerous clinical studies evaluated the antidepressant activity of rolipram in humans, finding it efficacious (Zeller et al., 1984), comparable to tricyclic imipramine (Bertolino et al., 1988), but less effective than tricyclic amitriptyline (Scott et al., 1991). However, clinical use of rolipram has been limited by side effects, particularly nausea and sedation (O'Donnell and Zhang, 2004).

Other antidepressants

More recently, HDAC6 (histone deacetylase) inhibitors have been suggested as a possible new antidepressant class (Jochims et al.,

2013). Unlike other HDACs, which are targeted at nuclear histones, HDAC6 acts outside of the nucleus, particularly at Lys40 of α -tubulin in microtubules and inhibiting deacetylation of this residue (Hubbert et al., 2002). Singh et al. compared the effects of HDAC6 inhibitor tubastatin A to traditional antidepressants SSRI escitalopram and tricyclic imipramine in C6 glioma (Singh et al., 2018). While all drugs promoted the typical redistribution of G_{α_s} out of lipid rafts and increased expression of downstream cAMP effectors phospho-CREB and BDNF, only tubastatin A promoted tubulin acetylation. So while the three compounds ultimately converge upon G_{α_s} and G_{α_s} signaling, tubulin acetylation is not a shared mechanism of action. It is also notable that Lys40 is located in the microtubule interior on α -tubulin (Janke and Montagnac, 2017), while G_{α_s} interacts with β -tubulin (Layden et al., 2008), suggesting acetylation does not directly interfere with G_{α_s} binding. Also notable in this regard is the recent finding that postmortem brain from depressed subjects shows decreased acetylation of membrane-associated tubulin (typically associated with lipid rafts) (Singh et al., 2020), compared to controls, as well as increased G_{α_s} localized to lipid rafts (Donati et al., 2008)).

Nasal esketamine (S-ketamine) has recently been approved for depression and, in contrast to traditional antidepressants which take weeks to manifest clinical effects, esketamine (as well as racemic ketamine given intravenously or sub-lingually) has almost immediate effects lasting up to a week (Yavi et al., 2022). While ketamine's canonical target/mechanism is antagonism of the NMDA glutamate receptor, racemic ketamine metabolite (2R,6R)-hydroxynorketamine has been suggested to possess antidepressant activity in animal models, and that its antidepressant activity, as well as those of ketamine, are independent of NMDAR activity (Zanos et al., 2016). Wray et al. examined the effect of ketamine upon G_{α_s} membrane disposition and signaling of ketamine and (2R,6R)-hydroxynorketamine in C6 glioma or primary astrocytes, as well as the effect of other NMDA antagonists (Wray et al., 2018). A single ketamine treatment produced rapid (within 15 min) translocation of G_{α_s} out of lipid rafts, persisting at least 12 h and returning to baseline within 24 h, as well as enhanced cAMP production compared to control. FRAP assay also showed the characteristic slowing of GFP- G_{α_s} membrane mobility. In contrast, NMDA antagonists memantine, AP5, and MK-801 had no effect on G_{α_s} membrane localization or mobility, suggesting NMDA antagonism is insufficient to explain ketamine's effects in this system. Likewise, knockdown of NMDA subunit GluN1 (i.e., NR1) did not inhibit ketamine's potentiation of cAMP production. The ketamine metabolite, (2R, 6R)-hydroxynorketamine also potentiated cAMP production and slowed GFP- G_{α_s} mobility. Together, these results suggest that ketamine shares traditional antidepressants' effects upon G_{α_s} , though in a highly accelerated fashion, mirroring ketamine's clinical timeline, and that these effects are NMDA receptor-independent (Wray et al., 2018).

Studies with human tissue

The human data in this area are derived from studies on peripheral tissue, such as various blood cells, from living subjects, studies on postmortem brain tissue from deceased subjects, as well as noninvasive imaging studies on living subjects.

Postmortem studies

In a series of papers, Trevor Young's group examined changes in cAMP, CREB, and BDNF in postmortem samples from depressed patients. Dowlatshahi et al. found significantly decreased CREB immunoreactivity in temporal cortex samples from nonmedicated depressed subjects, compared to control, while depressed subjects receiving antidepressant treatment were significantly higher than the nonmedicated and did not differ from healthy control subjects (Dowlatshahi et al., 1998). Chen et al. examined postmortem hippocampus from depressed, bipolar, and schizophrenic subjects, comparing BDNF expression in unmedicated and medicated (antidepressant) subjects (Chen et al., 2001). Overall, subjects receiving antidepressants displayed significantly increased BDNF immunoreactivity across several hippocampal regions, compared to subjects not receiving antidepressants. When depressed subjects were considered separately, these hippocampal regions showed increased BDNF expression in the medicated, but did not reach significance. A third related study examined temporal/occipital cortical brain tissue from postmortem mood disorder subjects for G protein content, cAMP production, and CREB expression (Dowlatshahi et al., 1999). While G protein (G_{α_s} and G_{α_i}) content did not differ among controls and depressed and bipolar subjects, forskolin-stimulated cAMP production was decreased in the depressed and bipolar samples, though not reaching significance. CREB expression did not differ among the three groups overall; however suicide subjects did have significant reductions in CREB expression compared to nonsuicide subjects.

Donati et al. examined prefrontal cortex and cerebellum of postmortem suicide subjects and found differences in detergent extractability (Triton X-100/Triton X-114) of G_{α_s} , suggesting altered membrane localization of G_{α_s} in depressed suicide subjects (Donati et al., 2008). Sequential detergent extractions of cellular membranes from both brain regions showed an increased fraction of G_{α_s} localized to lipid raft vs. nonraft membrane, where it is less able to activate adenylyl cyclase (Chen and Rasenick, 1995a), consistent with the above findings in Dowlatshahi (Dowlatshahi et al., 1999).

Blood studies

Alterations in cAMP signaling are perhaps the oldest specific biomarker of depression and response to antidepressant treatment,

and these changes are seen in varied cell types. Studies reporting reduced cAMP production in samples from depressed patients extend back to the 1970s. Alterations in platelets in depression have also noted for many years, and due to their short lifespan may serve as a better model, particularly for antidepressant response, than other circulating cells. While red blood cells persist for approximately 120 days (Thiagarajan et al., 2021), and lymphocytes for at least several months (Westera et al., 2013; Jones et al., 2015), platelet lifespan is approximately 7–10 days (Josefsson et al., 2020). Because of this, platelets may be better positioned to reflect any early changes in cellular behavior as a consequence of antidepressant treatment.

An early study on platelets from depressed patients found no significant difference in platelet cAMP production in response to PGE1 and norepinephrine stimulation, compared to controls (Wang et al., 1974). However, subsequent studies have shown decreased cAMP production in platelets from depressed subjects, as well as increased cAMP production in subjects successfully treated with antidepressants. Hines and Tabakoff examined unstimulated and agonist-stimulated (CsF, forskolin, GppNHp) cAMP production in platelets from depressed subjects, finding significantly decreased cAMP production in platelets from depressed subjects (Hines and Tabakoff, 2005). Furthermore, significance increased as subjects with history of various recent drug use (drugs of abuse, analgesics, antidepressants) were excluded from the analysis due to these drugs' effects on adenylyl cyclase activity. Overall, subjects with the lowest platelet cAMP production had a 2–6X risk of depression compared to subjects with the greatest cAMP production. Likewise, Mooney et al. examined cAMP production in mononuclear leukocytes and platelets from depressed subjects (Mooney et al., 2013). Their results revealed two subgroups of depressed patients whose demographics and medical histories were not substantially different. One depressed group ("DP-1") showed significant differences in cAMP production compared to controls as well as the other depressed subgroup ("DP-2"), which did not significantly differ from each other: in mononuclear leukocytes, cAMP production in response to fluoride (AlF) stimulation was significantly lower, and the ratio of GTP γ S/AlF-stimulated cAMP was significantly higher; for platelets, fluoride, PGE2, and PGD2 stimulation produced significantly lower cAMP, while PGE2/AlF ratio was significantly higher. G_{α_i} activity was assessed in the three groups and did not significantly differ.

More recently, Targum et al. (2022) have examined platelet PGE1-stimulated cAMP from depressed subjects before and after antidepressant treatment, with subjects stratified into "responder" or "nonresponder" groups based on HAMD₁₇ (Hamilton Depression Rating Scale) rating post-treatment (Targum et al., 2022). Consistent with Hines and Tabakoff, and Mooney et al., depressed subjects had lower PGE1-stimulated cAMP production compared to normal controls at the start of treatment. Post-treatment, responders and nonresponders differed significantly, with responders showing increased PGE1-stimulated cAMP relative to basal, compared to pre-treatment values, while this

value actually decreased in nonresponders. This is notable because it suggests that restoration of cAMP production is a function of clinical improvement, rather than antidepressant exposure *per se*, and as such is promising as a marker of successful antidepressant response. Because of the short platelet lifetime/high turnover, these changes may be evidenced in advance of clinical improvement and serve to guide antidepressant selection and drug changes early in treatment.

Imaging

An interesting series of experiments approximating direct visualization of altered brain cAMP content in depressed patients, and patients treated for depression, was done by the groups of Zarate and Innis. These experiments utilized PET detection of ^{11}C -labeled PDE4 inhibitor rolipram as a proxy for cAMP concentration. Briefly, PDE4 isoenzyme PDE4D3 activity is regulated by cAMP as a target of PKA phosphorylation on two serine residues, Ser⁵⁴ and Ser¹³, with Ser⁵⁴ phosphorylation upregulating phosphodiesterase activity. PDE4D3 activated *via* serine phosphorylation shows both increased sensitivity to rolipram inhibition (MacKenzie et al., 2002) as well as increased affinity for rolipram binding (Hoffmann et al., 1998). Expression of PDE4 isoenzymes is also enhanced by increased cellular cAMP levels (Ye et al., 2002) (Campos-Toimil et al., 2008). Thus, both expression and activity of PDE4 are regulated by cAMP. The PET-detectable binding of ^{11}C -labeled rolipram provided the basis for the following studies. Fujita et al. (Fujita et al., 2012) showed consistent decreases in ^{11}C -rolipram binding across 10 brain regions in unmedicated depressed patients compared to healthy controls, suggesting corresponding decreases in cAMP in these regions, reflected as decreased PDE4 expression or activity. This study was followed by Fujita et al. (Fujita et al., 2016), which examined the effect of antidepressant treatment on ^{11}C -labeled rolipram binding. Again, depressed patients demonstrated decreased labeled rolipram binding in these brain regions compared to controls. After the initial PET scan, the depressed patients were treated for 2 months with SSRI antidepressants citalopram, escitalopram, or sertraline and subjected to a second PET scan. Sertraline treatment produced significant and consistent increases in ^{11}C -labeled rolipram binding in the depressed patients, but the increases in rolipram binding did not correlate with improvement of depressive symptoms. These studies support the theory of cAMP changes in depression and with antidepressant treatment, and provide a technique whereby brain cAMP can be assessed *in vivo*, but also reflect the uncertainty of cAMP's specific role in depression pathology and treatment.

Note also advances in cellular imaging related to GPCR signaling and adenylyl cyclase. Irannejad et al. (Irannejad et al., 2013) have used conformation-sensitive nanobodies to identify intracellular activation of G α_s . Senese and Rasenick (Senese and Rasenick, 2021) have used fluorescent cAMP

reporters targeted to different cellular and membrane domains to illustrate sustained action of certain antidepressants.

Adenylyl cyclase isoforms and neuropsychiatric disease

Several studies exist for genetic association in humans and genetic manipulation in mice. Few human neurological or psychiatric diseases are associated with mutations in adenylyl cyclase, with only AC5 specifically implicated. Sporadic mutations in *ADCY5* result in dyskinesia (Chen D.-H. et al., 2015; Ferrini et al., 2021). Several mutations have been identified; the number of established cases is very small (<500). There is no mechanism linking *ADCY5* mutations to the exaggerated muscle movements seen in this disorder. Likewise, AC5 knockout mice display Parkinsonian-type movement disorders (Iwamoto et al., 2003). In contrast, mouse models with AC5 disruption through knockout or small molecule inhibitors show protective cardiovascular or metabolic effects (Okumura et al., 2003, 2007; Zhang et al., 2018) and tend to be “health-promoting,” with increased lifespan and reduced age-related degeneration (Yan et al., 2007). The beneficial cardioprotective effects of AC5 disruption are particularly curious, given the reported predominance of AC5 (and AC6) in cardiomyocytes (Sadana and Dessauer, 2009). Studies on adenylyl cyclase isoforms and depression are summarized in Table 1.

Depression and adenylyl cyclases regulated by Ca²⁺

Numerous studies have examined the role of Ca²⁺-regulated AC isoforms in the context of depression and other mood disorders, both singly and in combination. Rodent models allow genetic experimental manipulation, which is not possible in human subjects. Therefore, the most “direct” studies of AC isoform effect upon behavior have been done in rodents, typically through knockdown studies, though overexpression studies have also been done (as with AC7, *vide infra*).

Krishnan et al. contrasted the behavioral effects of AC1/8 double knockouts to that of AC5 knockouts (Krishnan et al., 2008). First, the two knockout models displayed differences in locomotor habituation, which developed later in the testing period (>60 min), as well as sex-based differences. While female mice did not show a statistical difference compared to wild type in either knockout model, male AC5 knockouts mice displayed significantly increased locomotion, while male AC1/8 double knockout mice displayed significantly decreased locomotion. Further behavioral tests including elevated plus maze, dark-light, and forced swim tests. Elevated plus maze and dark-light tests showed clear differences between the two knockout models: for both males and females, the AC5 knockout

TABLE 1 Animal and human studies of AC and depression.

AC isoform	Finding	References
AC1/8 double knockout (mice)	Mixed results; overall depression-like	Krishnan et al., 2008
AC3 knockout (mice)	Depression- and anxiety-like behaviors	Chen et al., 2015b; Yang et al., 2021; Liu et al., 2020
AC3 (Human)	Decreased blood AC3 transcript in depressed subjects	Redei et al., 2014
AC4 (Human)	Temporal cortex from suicide subjects shows decreased AC4 immunoreactivity and forskolin-stimulated cAMP compared to controls	Reiach et al., 1999
AC5 knockout (mice)	Mixed results; overall decreased anxiety- and depression-like behaviors	Krishnan et al., 2008
AC5 (Human)	ADCY5 related dyskinesia, not directly related to depression	Chen et al., 2015a; Ferrini et al., 2021
AC7 knockout and overexpression (mice)	Heterozygous knockdown reduced depression-like behavior (females); Overexpression increased depression-like behaviors (females); no effect in males Upregulation of AC7 mRNA in amygdala in mouse SERT knockout depression model	Hines et al., 2006; Joeyen-Waldorf et al., 2012
AC7 (Human)	Hines et al. identified depression-associated tandem repeat and haplotype in females; Joeyen-Waldorf et al. showed upregulation of AC7 in amygdala in depressed subjects (only males tested) and identified G to T SNP associated with increased threat-related amygdala reactivity, though G allele is found in depression associated-haplotype identified in Hines et al.	Hines et al., 2006; Joeyen-Waldorf et al., 2012
AC9 (Human)	AC9 genetic polymorphisms identified, not associated with depression	Toyota et al., 2002

Studies on adenylyl cyclase in depression demonstrate no clear or consistent role of the enzyme. Though studies of depression identify decreases in cAMP in depressed subjects, both human and animal, animal knockout studies have shown depressive, antidepressive, or no effect, depending on the study as well as the specific behavioral tests employed in the study. Likewise, human studies have associated depression with both increased and decreased expression of adenylyl cyclase, with genetic polymorphisms showing varied effect as well.

model showed a less anxiety-like phenotype, while the AC1/8 double knockout mice did not differ from wild type. In the forced swim test, AC5 knockout females showed significantly less immobility (i.e., a less “despondent” phenotype), while AC1/8 double knockout males showed a similar effect. Sucrose preference tests showed no significant effect of AC5 knockout, with significantly decreased sucrose preference (“anhedonia”) for AC1/8 double knockout males and females. Finally, social interaction tests showed decreased sociability among the AC5 knockout (males only), while both males and females showed increased sociability in the context of the AC1/8 double knockout. Overall, AC5 knockout mice displayed a less anxiety- or anti-depressive-like behavioral phenotype, while AC1/8 knockout mice displayed a more anxiety- or depressive-like behavioral phenotype, with some curious exceptions as noted above. The authors suggest that the knockouts may have divergent effects on different behaviors, such as sociability. Biochemical analysis of several brain regions was notable for decreased BDNF and TrkB (BDNF receptor) in the amygdala of AC5, but not AC1/8 knockouts, while AC1/8 knockouts showed increased BDNF signaling in the nucleus accumbens, which is also previously reported by the authors in the context of mice in a social defeat paradigm (Krishnan et al., 2007). Others (Govindarajan et al., 2006) have reported divergent effects in a transgenic mouse model overexpressing BDNF in the amygdala and hippocampus. There, mice showed increased anxiety-like behavior in open field and elevated plus tests, while showing an antidepressant-like effect in the forced swim test. Although brain cAMP was not measured in the Krishnan et al. study, simply knocking out adenylyl cyclase isoforms clearly does not lead to depression, which is characterized by decreased cAMP in the

brain globally (Fujita et al., 2012, 2016), as illustrated in the divergent behavioral effects seen in the two knockout models, as well as the apparent behavioral inconsistencies noted above. Krishnan et al. (Krishnan et al., 2008) is the first of numerous studies presented herein which illustrate this “contradiction,” perhaps better viewed as the complexity of associating specific genetic variations with specific behavioral phenotypes.

AC3

Numerous studies in rodents as well as humans have implicated AC3 in depression. Chen et al. evaluated in global, forebrain, and forebrain-targeted inducible AC3 knockouts, depressive behavioral phenotypes (Chen X. et al., 2015). Constitutive AC3 knockouts demonstrated a collection of depressive behaviors in behavioral assessments including forced swim, tail suspension, novelty-suppressed feeding/drinking, grooming, 3-chamber sociability, and nest quality. Sleep patterns were disrupted. Total brain and hippocampal volume were reduced, a finding also associated with human depression (Sapolsky, 2001). Reductions in hippocampal neural activity and long-term potentiation were also noted, as were deficits in spatial navigation/learning. Forebrain AC3 knockouts displayed a similar depressive-like phenotype in behavioral tests (though tests of anxiety such as elevated plus maze and 3-chamber sociability did not differ from wild-type) and also shared deficits memory and navigation. To rule out developmental deficits due to AC3 ablation, an inducible AC3 forebrain knockout was also considered. Again, a depression-like behavioral phenotype was observed. Together, their findings implicate AC3 as a factor in depression.

Yang and others ablated, in a mouse model, AC3 in somatostatin- and parvalbumin-expressing interneurons (Yang et al., 2021). Here, deletion of AC3 resulted in a variety of depressive- or anxious-like behaviors, but only through deletion in somatostatin-expressing interneurons. The authors note other studies implicating somatostatin interneurons in depression, including Douillard-Guilloux et al., who showed significantly diminished number of somatostatin interneurons in postmortem amygdala of depressed female subjects (Douillard-Guilloux et al., 2017). The connection to AC3, however, is unclear.

AC3 is highly expressed in olfactory cilia, and loss of AC3 results in anosmia (Wong et al., 2000) (Wang et al., 2006). Depressive (but also anxiolytic) behaviors have been reported (Ahn et al., 2016, 2018) in mouse models of anosmia chemically induced by application of zinc sulfate solution (McBride et al., 2003). Liu et al. examined behavior in mouse AC3 knockouts, olfactory epithelium-targeted AC3 knockouts, and zinc sulfate-induced anosmia mice (Liu et al., 2020). Consistent with other studies of AC3 knockouts, mice displayed increased depressive- and anxious-like behaviors compared to controls. Interestingly, the olfactory epithelium AC3 knockouts displayed similar depressive- and anxiety-like behaviors, while the zinc sulfate anosmic mice displayed primarily depressive behaviors. All three models also showed decreases in dopaminergic and glutaminergic pathways in the hippocampus, with reductions in mRNA or expressed protein for tyrosine hydroxylase, various dopamine receptors, and glutamate receptor subunit GluN2B. Again, it is unclear how AC3 ablation affects the above parameters, or how chemically-induced anosmia results in a similar behavioral and biochemical profile.

In human subjects, Redei et al. have examined blood RNA biomarkers of depression in a depressed population undergoing cognitive behavioral therapy (Redei et al., 2014). *ADCY3* expression was found to be significantly decreased in the depressed population compared to nondepressed subjects, and this difference normalized after the completion of the therapy period (although all patients did not achieve full remission). Targum et al. used platelet PGE1 stimulated cAMP production as a blood biomarker of depression as well as antidepressant response, finding significant decreases in depressed subjects compared to healthy controls, as well as increases in platelet cAMP, but only in subjects who achieved remission post-antidepressant treatment (Targum et al., 2022). This is relevant in the context of AC3, because AC3 has been reported as the primary adenylyl cyclase isoform expressed in platelets (Katsel et al., 2009). Still, questions remain regarding the relevance of AC3 for human depression (Rasenick, 2016).

Adenylyl cyclases not regulated by Ca^{2+}

AC4

Reiach and others have compared adenylyl cyclase expression (AC1, AC4, AC5/6) in postmortem brain

(temporal cortex) from suicide, bipolar, and nondepressed control subjects *via* western blot (Reiach et al., 1999). While no difference was seen in bipolar vs normal subjects, the suicide group showed a significant decrease in AC4 immunoreactivity compared to control. Membranes from these tissues were also assayed for basal, forskolin, and GTP γ S-stimulated cAMP production. Forskolin-stimulated cAMP relative to basal was significantly decreased in the suicide group compared to controls. This is consistent with others' findings in depression, but the relevance of cAMP changes attributable to any given isoform to the overall clinical phenotype is unclear. Furthermore, antibodies available for adenylyl cyclase isoforms are of notoriously poor quality, rendering quantitation difficult.

AC7

A role for AC7 in depression, as well as sex-based differences, has been identified through human gene array analysis and studies of genetically altered mice. Hines et al. examined mice overexpressing AC7, as well as heterozygous AC7 knockout mice in forced swim and tail suspension tests (Hines et al., 2006). In forced swim tests, female mice overexpressing AC7 had a longer period of immobility compared to their wild-type counterparts, suggesting a depressive-like phenotype, while female heterozygous knockouts had a shorter period of immobility, suggesting an anti-depressive-like phenotype. In tail suspension tests, female mice overexpressing AC7 displayed longer immobility compared to wild type, with no effect of the heterozygous knockout. However, the performance of male mice in both behavioral tests was unaffected by either genetic manipulation. These results suggest overexpression of AC7 as promoting a depression-like phenotype, with reduced expression promoting the opposite effect, but only in female mice. The same study also examined polymorphisms in *ADCY7*, specifically a variable tetranucleotide (AACA) repeat, in the 3' UTR of human populations in relation to depression. In particular, a seven-fold repeat of (AACA) was associated with depression in humans. The study considered separately, "family history of depression" (history of depression in a first degree relative) as well as "familial depression" (depressed subject, plus history of depression in a first-degree relative). The (AACA)₇ repeat was significantly associated with family history of depression in females, but not in males, or females and males grouped together. For familial depression, (AACA)₇ was significantly associated with depression in females as well as females plus males grouped together, and nearly significant for males alone ($p = 0.08$). Finally, the authors examined a series of SNPs in *ADCY7* and found no association of depression with any particular SNP, but identified a particular haplotype (TG7AT) associated with increased depression risk, and significant in females.

Joeyen-Waldorf et al. examined AC7 expression and polymorphisms in the context of human depression, as well as a SERT knockout mouse depression model (Joeyen-Waldorf

et al., 2012). Both postmortem tissue from humans, as well as mouse SERT knockout mice, showed significant changes in expression of a large number of genes, with an increase of AC7 transcript seen in the amygdala in both mice and humans (note, only male humans were tested in this part of the study). The second part of the study assessed threat-related amygdala activity *via* fMRI in a population of human males plus females, in the context of rs1064448, a G to T SNP in the region of the female depression-associated haplotype identified above in Hines (Hines et al., 2006). Carriers of the T allele showed significant elevation of amygdala reactivity, compared to G homozygotes; no sex difference was observed. Interestingly, the authors note that while the T allele was associated with increased threat-related amygdala reactivity in this study, the G allele is represented in the female depression-associated TG7AT haplotype identified in Hines et al., and suggest that this apparent contradiction may be due to the difficulties in extrapolating clinical phenotypes from genetic polymorphisms, *versus* the more consistent associations seen between genetics and more “proximate” biological findings, such as the fMRI imaging data obtained in this study. Another possibility is that variety of depression phenotypes seen clinically may be associated with a variety of genetic polymorphisms.

Also notable for both studies is the association of increased AC7 expression with depression. While Joeyen-Waldorf et al. examined only mRNA, Hines et al. additionally examined AC7 protein expression and AC7-specific cAMP production, finding protein and cAMP highest for AC7 overexpression, lowest for heterozygous knockouts, and intermediate for wild-type mice. Given the large number of studies identifying decreased cAMP in brain and other cell types such as platelets in depression, as well as downstream targets of cAMP, it is counterintuitive that increased AC7 expression and cAMP production are associated with depression. Others such as Krishnan et al. have found similar results, with AC1/8 double knockout mice showing a depressive-like phenotype, and AC5 knockouts showing an anti-depressive-like phenotype (Krishnan et al., 2008). Perhaps this apparent contradiction again reflects the complexity of the combined effect of a variety of cyclase isoforms, or regional effects in cyclase isoform regulation. Finally, Price and Brust have reviewed AC7 and neuropsychiatric disorders and this review may be of interest to the reader (Price and Brust, 2019).

AC9

Toyota et al. examined polymorphisms in *ACDY9* in a depressed (unipolar and bipolar) population of males and females, compared to non-depressed controls (Toyota et al., 2002). Seven SNPs and one tandem repeat of (TTTA)₄ or ₅ in the 3' UTR were identified, with one SNP (2316A>G; Ile772Met) constituting a missense mutation. The tandem repeat and missense mutation were selected for further study due to their potential for altered regulation or function. In both cases, the polymorphism was not associated with depression, compared to

controls, and no difference was seen when unipolar and bipolar depression were considered separately or together. The functional consequences of the missense mutation were later examined in Small et al. through expression in HEK293 and the polymorphism demonstrated altered sensitivity to β_2 adrenergic stimulation *via* isoproterenol (Small et al., 2003). While EC50 did not differ between the two variants, isoproterenol was significantly less efficacious in stimulating cAMP production from the Met variant. Significantly diminished efficacy was also observed upon stimulation with fluoride (direct activator of G_{α_s}) as well as Mn^{2+} (direct activator of adenylyl cyclase).

Conclusion

Consistently inconsistent, is the term best describing the studies described above on depression and adenylyl cyclase. This underscores the difficulty of translating alterations in the activity of a given adenylyl cyclase isoform to the development of a clinically significant phenotype.

While a great deal has been published on adenylyl cyclase and depression, it is difficult to develop a viable framework to house these myriad results. While it does appear that cAMP is lower in depression and that antidepressants increase overall cAMP, there is no evidence linking this to the etiology of depression or mechanism of antidepressant action. While the association between G_{α_s} and adenylyl cyclase seems relevant for depression and antidepressant therapy, the identity of the isoforms involved is yet to be determined. Further complications could be distribution of adenylyl cyclase isoforms in the many types of cells resident in the human brain and the possibility that those isoforms are unequally distributed amongst membrane microdomains (e.g. lipid rafts). Further complicating this is that this differential distribution may differ in mouse and human. Nonetheless, techniques developed with support from the BRAIN Initiative have permitted rapid advances in identifying circuitry in the brains of both mice and humans. Hopefully, a resolution will accompany the development of improved tools (e.g. opto- and chemogenetics and sophisticated fluorescent reporters) for investigation of adenylyl cyclase, its distribution, and its regulation.

Author contributions

JMS and MMR wrote and edited the manuscript.

Funding

This research was supported by the VA Merit BX00149 (MMR). MMR is a VA Research Career Scientist BX004475.

Conflict of interest

MMR is a founder of Pax Neuroscience, Inc. and has a financial interest in that concern.

The remaining author, JMS, declares that the research was conducted in the absence of any commercial or financial relationships that could be construed as a potential conflict of interest.

References

- Adachi, M., Barrot, M., Autry, A. E., Theobald, D., and Monteggia, L. M. (2008). Selective loss of brain-derived neurotrophic factor in the dentate gyrus attenuates antidepressant efficacy. *Biol. Psychiatry* 63, 642–649. doi:10.1016/j.biopsych.2007.09.019
- Ahn, S., Choi, M., Kim, H., Yang, E., Mahmood, U., Kang, S.-I., et al. (2018). Transient anosmia induces depressive-like and anxiolytic-like behavior and reduces amygdalar corticotropin-releasing hormone in a ZnSO₄-induced mouse model. *Chem. Senses* 43, 213–221. doi:10.1093/chemse/bjy008
- Ahn, S., Shin, H.-W., Mahmood, U., Khalmuratova, R., Jeon, S.-Y., Jin, H. R., et al. (2016). Chronic anosmia induces depressive behavior and reduced anxiety via dysregulation of glucocorticoid receptor and corticotropin-releasing hormone in a mouse model. *Rhinology* 54, 80–87. doi:10.4193/Rhin15.209
- Autry, A. E., Adachi, M., Nosyreva, E., Na, E. S., Los, M. F., Cheng, P., et al. (2011). NMDA receptor blockade at rest triggers rapid behavioural antidepressant responses. *Nature* 475, 91–95. doi:10.1038/nature10130
- Azevedo, M. F., Faucz, F. R., Bimpaki, E., Horvath, A., Levy, I., Alexandre, R. B. de, et al. (2014). Clinical and molecular genetics of the phosphodiesterases (PDEs). *Endocr. Rev.* 35, 195–233. doi:10.1210/er.2013-1053
- Berman, S. M., Kuczenski, R., McCracken, J. T., and London, E. D. (2009). Potential adverse effects of amphetamine treatment on brain and behavior: A review. *Mol. Psychiatry* 14, 123–142. doi:10.1038/mp.2008.90
- Bertolino, A., Crippa, D., Dio, S. D., Fichte, K., Musmeci, G., Porro, V., et al. (1988). Risperidone versus imipramine in inpatients with major, "minor" or atypical depressive disorder: A double-blind double-dummy study aimed at testing a novel therapeutic approach. *Int. Clin. Psychopharmacol.* 3, 245–253. doi:10.1097/00004850-198807000-00006
- Björkholm, C., and Monteggia, L. M. (2016). Bdnf - a key transducer of antidepressant effects. *Neuropharmacology* 102, 72–79. doi:10.1016/j.neuropharm.2015.10.034
- Blendy, J. A. (2006). The role of CREB in depression and antidepressant treatment. *Biol. Psychiatry* 59, 1144–1150. doi:10.1016/j.biopsych.2005.11.003
- Campos-Toimil, M., Keravis, T., Orallo, F., Takeda, K., and Lugnier, C. (2008). Short-term or long-term treatments with a phosphodiesterase-4 (PDE4) inhibitor result in opposing agonist-induced Ca²⁺ responses in endothelial cells. *Br. J. Pharmacol.* 154, 82–92. doi:10.1038/bjp.2008.56
- Castrén, E., and Monteggia, L. (2021). Brain-derived neurotrophic factor signaling in depression and antidepressant action. *Biol. Psychiatry* 90, 128–136. doi:10.1016/j.biopsych.2021.05.008
- Chen, B., Dowlathshahi, D., MacQueen, G. M., Wang, J.-F., and Young, L. T. (2001). Increased hippocampal BDNF immunoreactivity in subjects treated with antidepressant medication. *Biol. Psychiatry* 50, 260–265. doi:10.1016/s0006-3223(01)01083-6
- Chen, D.-H., Méneret, A., Friedman, J. R., Korvatska, O., Gad, A., Bonkowski, E. S., et al. (2015a). ADCY5-related dyskinesia: Broader spectrum and genotype-phenotype correlations. *Neurology* 85, 2026–2035. doi:10.1212/wnl.0000000000002058
- Chen, J., and Rasenick, M. M. (1995a). Chronic antidepressant treatment facilitates G protein activation of adenylyl cyclase without altering G protein content. *J. Pharmacol. Exp. Ther.* 275, 509–517.
- Chen, J., and Rasenick, M. M. (1995b). Chronic treatment of C6 glioma cells with antidepressant drugs increases functional coupling between a G protein (gs) and adenylyl cyclase. *J. Neurochem.* 64, 724–732. doi:10.1046/j.1471-4159.1995.64020724.x
- Chen, X., Luo, J., Leng, Y., Yang, Y., Zweifel, L. S., Palmiter, R. D., et al. (2015b). Ablation of type III adenylyl cyclase in mice causes reduced neuronal activity, altered sleep pattern, and depression-like phenotypes. *Biol. Psychiatry* 80, 836–848. doi:10.1016/j.biopsych.2015.12.012
- Conti, A. C., Cryan, J. F., Dalvi, A., Lucki, I., and Blendy, J. A. (2002). cAMP response element-binding protein is essential for the upregulation of brain-derived neurotrophic factor transcription, but not the behavioral or endocrine responses to antidepressant drugs. *J. Neurosci.* 22, 3262. doi:10.1523/JNEUROSCI.22-08-03262.2002
- Coppell, A. L., Pei, Q., and Zetterström, T. S. C. (2003). Bi-phasic change in BDNF gene expression following antidepressant drug treatment. *Neuropharmacology* 44, 903–910. doi:10.1016/s0028-3908(03)00077-7
- Czys, A. H., Schappi, J. M., and Rasenick, M. M. (2015). Lateral diffusion of Gα_s in the plasma membrane is decreased after chronic but not acute antidepressant treatment: Role of lipid raft and non-raft membrane microdomains. *Neuropsychopharmacology* 40, 766–773. doi:10.1038/npp.2014.256
- Delhaye, S., and Bardoni, B. (2021). Role of phosphodiesterases in the pathophysiology of neurodevelopmental disorders. *Mol. Psychiatry* 26, 4570–4582. doi:10.1038/s41380-020-00997-9
- Donati, R. J., Dwivedi, Y., Roberts, R. C., Conley, R. R., Pandey, G. N., and Rasenick, M. M. (2008). Postmortem brain tissue of depressed suicides reveals increased gs localization in lipid raft domains where it is less likely to activate adenylyl cyclase. *J. Neurosci.* 28, 3042–3050. doi:10.1523/jneurosci.5713-07.2008
- Donati, R. J., and Rasenick, M. M. (2003). G protein signaling and the molecular basis of antidepressant action. *Life Sci.* 73, 1–17. doi:10.1016/s0024-3205(03)00249-2
- Douillard-Guilloux, G., Lewis, D., Seney, M. L., and Sibille, E. (2017). Decrease in somatostatin-positive cell density in the amygdala of females with major depression. *Depress. Anxiety* 34, 68–78. doi:10.1002/da.22549
- Dowlathshahi, D., MacQueen, G. M., Wang, J. F., and Young, L. T. (1998). Increased temporal cortex CREB concentrations and antidepressant treatment in major depression. *Lancet* 352, 1754–1755. doi:10.1016/s0140-6736(05)79827-5
- Dowlathshahi, D., MacQueen, G. M., Wang, J., Reisch, J. S., and Young, L. T. (1999). G protein-coupled cyclic AMP signaling in postmortem brain of subjects with mood disorders: Effects of diagnosis, suicide, and treatment at the time of death. *J. Neurochem.* 73, 1121–1126. doi:10.1046/j.1471-4159.1999.0731121.x
- Duman, R. S., Malberg, J., and Thome, J. (1999). Neural plasticity to stress and antidepressant treatment. *Biol. Psychiatry* 46, 1181–1191. doi:10.1016/s0006-3223(99)00177-8
- Dunham, J. S., Deakin, J. F. W., Miyajima, F., Payton, A., and Toro, C. T. (2009). Expression of hippocampal brain-derived neurotrophic factor and its receptors in Stanley consortium brains. *J. Psychiatr. Res.* 43, 1175–1184. doi:10.1016/j.jpsychires.2009.03.008
- Dwivedi, Y., and Pandey, G. N. (2008). Adenylyl cyclase-cyclicAMP signaling in mood disorders: Role of the crucial phosphorylating enzyme protein kinase A. *Neuropsychiatr. Dis. Treat.* 4, 161–176. doi:10.2147/ndt.s2380
- El-Haggar, S. M., Eissa, M. A., Mostafa, T. M., El-Attar, K. S., and Abdallah, M. S. (2018). The phosphodiesterase inhibitor pentoxifylline as a novel adjunct to antidepressants in major depressive disorder patients: A proof-of-concept, randomized, double-blind, placebo-controlled trial. *Psychother. Psychosom.* 87, 331–339. doi:10.1159/000492619
- Ferrini, A., Steel, D., Barwick, K., and Kurian, M. A. (2021). An update on the phenotype, genotype and neurobiology of ADCY5-related disease. *Mov. Disord.* 36, 1104–1114. doi:10.1002/mds.28495
- Foubert, G. de, Carney, S. L., Robinson, C. S., Destexhe, E. J., Tomlinson, R., Hicks, C. A., et al. (2004). Fluoxetine-induced change in rat brain expression of brain-derived neurotrophic factor varies depending on length of treatment. *Neuroscience* 128, 597–604. doi:10.1016/j.neuroscience.2004.06.054

Publisher's note

All claims expressed in this article are solely those of the authors and do not necessarily represent those of their affiliated organizations, or those of the publisher, the editors and the reviewers. Any product that may be evaluated in this article, or claim that may be made by its manufacturer, is not guaranteed or endorsed by the publisher.

- Fujimaki, K., Morinobu, S., and Duman, R. S. (2000). Administration of a cAMP phosphodiesterase 4 inhibitor enhances antidepressant-induction of BDNF mRNA in rat Hippocampus. *Neuropsychopharmacology* 22, 42–51. doi:10.1016/s0893-133x(99)00084-6
- Fujita, M., Hines, C. S., Zoghbi, S. S., Mallinger, A. G., Dickstein, L. P., Liow, J. S., et al. (2012). Downregulation of brain phosphodiesterase type IV measured with ¹¹C-(R)-Rolipram positron emission tomography in major depressive disorder. *Biol. Psychiatry* 72, 548–554. doi:10.1016/j.biopsych.2012.04.030
- Fujita, M., Richards, E. M., Nicu, M. J., Ionescu, D. F., Zoghbi, S. S., Hong, J., et al. (2016). cAMP signaling in brain is decreased in unmedicated depressed patients and increased by treatment with a selective serotonin reuptake inhibitor. *Mol. Psychiatry* 22, 754–759. doi:10.1038/mp.2016.171
- Govindarajan, A., Rao, B. S. S., Nair, D., Trinh, M., Mawjee, N., Tonegawa, S., et al. (2006). Transgenic brain-derived neurotrophic factor expression causes both anxiogenic and antidepressant effects. *Proc. Natl. Acad. Sci. U. S. A.* 103, 13208–13213. doi:10.1073/pnas.0605180103
- Hines, L. M., Hoffman, P. L., Bhawe, S., Saba, L., Kaiser, A., Snell, L., et al. (2006). A sex-specific role of type VII adenylyl cyclase in depression. *J. Neurosci.* 26, 12609–12619. doi:10.1523/jneurosci.1040-06.2006
- Hines, L. M., and Tabakoff, B. (2005). Platelet adenylyl cyclase activity: A biological marker for major depression and recent drug use. *Biol. Psychiatry* 58, 955–962. doi:10.1016/j.biopsych.2005.05.040
- Hoffmann, R., Wilkinson, I. R., McCallum, J. F., Engels, P., and Houslay, M. D. (1998). cAMP-specific phosphodiesterase HSPDE4D3 mutants which mimic activation and changes in rolipram inhibition triggered by protein kinase A phosphorylation of Ser-54: generation of a molecular model. *Biochem. J.* 333, 139–149. doi:10.1042/bj3330139
- Hubbert, C., Guardiola, A., Shao, R., Kawaguchi, Y., Ito, A., Nixon, A., et al. (2002). HDAC6 is a microtubule-associated deacetylase. *Nature* 417, 455–458. doi:10.1038/417455a
- Hwang, J.-P., Tsai, S.-J., Hong, C.-J., Yang, C.-H., Lin, J.-F., and Yang, Y.-M. (2006). The Val66Met polymorphism of the brain-derived neurotrophic-factor gene is associated with geriatric depression. *Neurobiol. Aging* 27, 1834–1837. doi:10.1016/j.neurobiolaging.2005.10.013
- Insel, P. A., and Ostrom, R. S. (2003). Forskolin as a tool for examining adenylyl cyclase expression, regulation, and G protein signaling. *Cell. Mol. Neurobiol.* 23, 305–314. doi:10.1023/a:1023684503883
- Irannejad, R., Tomshine, J. C., Tomshine, J. R., Chevalier, M., Mahoney, J. P., Steyaert, J., et al. (2013). Conformational biosensors reveal GPCR signalling from endosomes. *Nature* 495, 534–538. doi:10.1038/nature12000
- Iwamoto, T., Okumura, S., Iwatsubo, K., Kawabe, J.-I., Ohtsu, K., Sakai, I., et al. (2003). Motor dysfunction in type 5 adenylyl cyclase-null mice. *J. Biol. Chem.* 278, 16936–16940. doi:10.1074/jbc.c300075200
- Janke, C., and Montagnac, G. (2017). Causes and consequences of microtubule acetylation. *Curr. Biol.* 27, R1287–R1292. doi:10.1016/j.cub.2017.10.044
- Jochims, J., Boulden, J., Lee, B. G., Blendy, J. A., Jarpe, M., Mazitschek, R., et al. (2013). Antidepressant-like properties of novel HDAC6-selective inhibitors with improved brain bioavailability. *Neuropsychopharmacology* 39, 389–400. doi:10.1038/npp.2013.207
- Joeyen-Waldorf, J., Nikolova, Y. S., Edgar, N., Walsh, C., Kota, R., Lewis, D. A., et al. (2012). Adenylate cyclase 7 is implicated in the biology of depression and modulation of affective neural circuitry. *Biol. Psychiatry* 71, 627–632. doi:10.1016/j.biopsych.2011.11.029
- Jones, D. D., Wilmore, J. R., and Allman, D. (2015). Cellular dynamics of memory B cell populations: IgM+ and IgG+ memory B cells persist indefinitely as quiescent cells. *J. Immunol.* 195, 4753–4759. doi:10.4049/jimmunol.1501365
- Josefsson, E. C., Vainchenker, W., and James, C. (2020). Regulation of platelet production and life span: Role of bcl-xL and potential implications for human platelet diseases. *Int. J. Mol. Sci.* 21, 7591. doi:10.3390/ijms21207591
- Katsel, P. L., Tagliente, T. M., Schwarz, T. E., Craddock-Royal, B. D., Patel, N. D., and Maayani, S. (2009). Molecular and biochemical evidence for the presence of Type III adenylyl cyclase in human platelets. *Platelets* 14, 21–33. doi:10.1080/0953710021000062905
- Kennedy, S. H., and Eisfeld, B. S. (2007). Agomelatine and its therapeutic potential in the depressed patient. *Neuropsychiatr. Dis. Treat.* 3, 423–428.
- Krishnan, V., Graham, A., Mazei-Robison, M. S., Lagace, D. C., Kim, K.-S., Birnbaum, S., et al. (2008). Calcium-sensitive adenylyl cyclases in depression and anxiety: Behavioral and biochemical consequences of isoform targeting. *Biol. Psychiatry* 64, 336–343. doi:10.1016/j.biopsych.2008.03.026
- Krishnan, V., Han, M.-H., Graham, D. L., Berton, O., Renthal, W., Russo, S. J., et al. (2007). Molecular adaptations underlying susceptibility and resistance to social defeat in brain reward regions. *Cell* 131, 391–404. doi:10.1016/j.cell.2007.09.018
- Layden, B. T., Saengsawang, W., Donati, R. J., Yang, S., Mulhearn, D. C., Johnson, M. E., et al. (2008). Structural model of a complex between the heterotrimeric G protein, Gα₁₂, and tubulin. *Biochim. Biophys. Acta* 1783, 964–973. doi:10.1016/j.bbamcr.2008.02.017
- Liu, X., Zhou, Y., Li, S., Yang, D., Jiao, M., Liu, X., et al. (2020). Type 3 adenylyl cyclase in the main olfactory epithelium participates in depression-like and anxiety-like behaviours. *J. Affect. Disord.* 268, 28–38. doi:10.1016/j.jad.2020.02.041
- MacKenzie, S. J., Baillie, G. S., McPhee, I., MacKenzie, C., Seamons, R., McSorley, T., et al. (2002). Long PDE4 cAMP specific phosphodiesterases are activated by protein kinase A-mediated phosphorylation of a single serine residue in Upstream Conserved Region 1 (UCR1). *Br. J. Pharmacol.* 136, 421–433. doi:10.1038/sj.bjp.0704743
- Malberg, J. E., and Blendy, J. A. (2005). Antidepressant action: To the nucleus and beyond. *Trends Pharmacol. Sci.* 26, 631–638. doi:10.1016/j.tips.2005.10.005
- Matveychuk, D., Thomas, R. K., Swanson, J., Khullar, A., MacKay, M.-A., Baker, G. B., et al. (2020). Ketamine as an antidepressant: Overview of its mechanisms of action and potential predictive biomarkers. *Ther. Adv. Psychopharmacol.* 10, 2045125320916657. doi:10.1177/2045125320916657
- McBride, K., Slotnick, B., and Margolis, F. L. (2003). Does intranasal application of zinc sulfate produce anosmia in the mouse? An olfactory and anatomical study. *Chem. Senses* 28, 659–670. doi:10.1093/chemse/bjg053
- Menkes, D. B., Rasenick, M. M., Wheeler, M. A., and Bitensky, M. W. (1983). Guanosine triphosphate activation of brain adenylate cyclase: Enhancement by long-term antidepressant treatment. *Science* 219, 65–67. doi:10.1126/science.6849117
- Moncrieff, J., Cooper, R. E., Stockmann, T., Amendola, S., Hengartner, M. P., and Horowitz, M. A. (2022). The serotonin theory of depression: A systematic umbrella review of the evidence. *Mol. Psychiatry* 14, 1. doi:10.1038/s41380-022-01661-0
- Mooney, J. J., Samson, J. A., McHale, N. L., Pappalardo, K. M., Alpert, J. E., and Schildkraut, J. J. (2013). Increased gsa within blood cell membrane lipid microdomains in some depressive disorders: An exploratory study. *J. Psychiatr. Res.* 47, 706–711. doi:10.1016/j.jpsychires.2013.02.005
- O'Donnell, J. M. (1993). Antidepressant-like effects of rolipram and other inhibitors of cyclic adenosine monophosphate phosphodiesterase on behavior maintained by differential reinforcement of low response rate. *J. Pharmacol. Exp. Ther.* 264, 1168–1178.
- O'Donnell, J. M., and Zhang, H.-T. (2004). Antidepressant effects of inhibitors of cAMP phosphodiesterase (PDE4). *Trends Pharmacol. Sci.* 25, 158–163. doi:10.1016/j.tips.2004.01.003
- Okumura, S., Takagi, G., Kawabe, J., Yang, G., Lee, M.-C., Hong, C., et al. (2003). Disruption of type 5 adenylyl cyclase gene preserves cardiac function against pressure overload. *Proc. Natl. Acad. Sci. U. S. A.* 100, 9986–9990. doi:10.1073/pnas.1733772100
- Okumura, S., Vatner, D. E., Kurotani, R., Bai, Y., Gao, S., Yuan, Z., et al. (2007). Disruption of type 5 adenylyl cyclase enhances desensitization of cyclic adenosine monophosphate signal and increases Akt signal with chronic catecholamine stress. *Circulation* 116 (16), 1776–1783. doi:10.1161/CIRCULATIONAHA.107.698662
- Overstreet, D. H., Double, K., and Schiller, G. D. (1989). Antidepressant effects of rolipram in a genetic animal model of depression: Cholinergic supersensitivity and weight gain. *Pharmacol. Biochem. Behav.* 34, 691–696. doi:10.1016/0091-3057(89)90260-8
- Pinto, C., Papa, D., Hubner, M., Mou, T. C., Lushington, G. H., and Seifert, R. (2008). Activation and inhibition of adenylyl cyclase isoforms by forskolin analogs. *J. Pharmacol. Exp. Ther.* 325, 27–36. doi:10.1124/jpet.107.131904
- Price, T., and Brust, T. F. (2019). Adenylyl cyclase 7 and neuropsychiatric disorders: A new target for depression? *Pharmacol. Res.* 143, 106–112. doi:10.1016/j.phrs.2019.03.015
- Rafa-Zablocka, K., Kreiner, G., Bagińska, M., Kuśmierczyk, J., Parlato, R., and Nalepa, I. (2017). Transgenic mice lacking CREB and CREM in noradrenergic and serotonergic neurons respond differently to common antidepressants on tail suspension test. *Sci. Rep.* 7, 13515. doi:10.1038/s41598-017-14069-6
- Rasenick, M. M. (2016). Depression and adenylyl cyclase - sorting out the signals. *Biol. Psychiatry* 80, 812–814. doi:10.1016/j.biopsych.2016.09.021
- Redei, E. E., Andrus, B. M., Kwasny, M. J., Seok, J., Cai, X., Ho, J., et al. (2014). Blood transcriptomic biomarkers in adult primary care patients with major depressive disorder undergoing cognitive behavioral therapy. *Transl. Psychiatry* 4, e442. doi:10.1038/tp.2014.66
- Regula, C. S., Sager, P. R., and Berlin, R. D. (1986). Membrane tubulin. *Ann. N. Y. Acad. Sci.* 466, 832–842. doi:10.1111/j.1749-6632.1986.tb38466.x

- Reiach, J. S., Li, P. P., Warsh, J. J., Kish, S. J., and Young, L. T. (1999). Reduced adenylyl cyclase immunolabeling and activity in postmortem temporal cortex of depressed suicide victims. *J. Affect. Disord.* 56, 141–151. doi:10.1016/s0165-0327(99)00048-8
- Sadana, R., and Dessauer, C. W. (2009). Physiological roles for G protein-regulated adenylyl cyclase isoforms: Insights from knockout and overexpression studies. *Neurosignals* 17, 5–22. doi:10.1159/000166277
- Sapolsky, R. M. (2001). Depression, antidepressants, and the shrinking hippocampus. *Proc. Natl. Acad. Sci. U. S. A.* 98, 12320–12322. doi:10.1073/pnas.231475998
- Schwabe, U., Miyake, M., Ohga, Y., and Daly, J. W. (1976). 4-(3-Cyclopentyl-4-methoxyphenyl)-2-pyrrolidone (ZK 62711): A potent inhibitor of adenosine cyclic 3', 5'-monophosphate phosphodiesterases in homogenates and tissue slices from rat brain. *Mol. Pharmacol.* 12, 900–910.
- Scott, A. I. F., Perini, A. F., Shering, P. A., and Whalley, L. J. (1991). In-patient major depression: Is rolipram as effective as amitriptyline? *Eur. J. Clin. Pharmacol.* 40, 127–129. doi:10.1007/bf00280065
- Senese, N. B., and Rasenick, M. M. (2021). Antidepressants produce persistent α_1 -associated signaling changes in lipid rafts after drug withdrawal. *Mol. Pharmacol.* 100, 66–81. MOLPHARM-AR-2020-000226. doi:10.1124/molpharm.120.000226
- Singh, H., Chmura, J., Bhaumik, R., Pandey, G. N., and Rasenick, M. M. (2020). Membrane-associated α -tubulin is less acetylated in postmortem prefrontal cortex from depressed subjects relative to controls: Cytoskeletal dynamics, HDAC6, and depression. *J. Neurosci.* 40, 4033–4041. doi:10.1523/jneurosci.3033-19.2020
- Singh, H., Wray, N., Schappi, J. M., and Rasenick, M. M. (2018). Disruption of lipid-raft localized α -tubulin is less acetylated in postmortem prefrontal cortex from depressed subjects relative to controls: Cytoskeletal dynamics, HDAC6, and depression. *J. Neurosci.* 40, 4033–4041. doi:10.1523/jneurosci.3033-19.2020
- Singh, H., Wray, N., Schappi, J. M., and Rasenick, M. M. (2018). Disruption of lipid-raft localized α -tubulin is less acetylated in postmortem prefrontal cortex from depressed subjects relative to controls: Cytoskeletal dynamics, HDAC6, and depression. *J. Neurosci.* 40, 4033–4041. doi:10.1523/jneurosci.3033-19.2020
- Small, K. M., Brown, K. M., Theiss, C. T., Seman, C. A., Weiss, S. T., and Liggett, S. B. (2003). An Ile to Met polymorphism in the catalytic domain of adenylyl cyclase type 9 confers reduced beta2-adrenergic receptor stimulation. *Pharmacogenetics* 13, 535–541. doi:10.1097/00008571-200309000-00002
- Sulser, F., Gillespie, D. D., Mishra, R., and Manier, D. H. (1984). Desensitization by antidepressants of central norepinephrine receptor systems coupled to adenylyl cyclase. *Ann. N. Y. Acad. Sci.* 430, 91–101. doi:10.1111/j.1749-6632.1984.tb14500.x
- Targum, S. D., Schappi, J., Koutsouris, A., Bhaumik, R., Rapaport, M. H., Rasgon, N., et al. (2022). A novel peripheral biomarker for depression and antidepressant response. *Mol. Psychiatry* 27, 1640–1646. doi:10.1038/s41380-021-01399-1
- Thiagarajan, P., Parker, C. J., and Prchal, J. T. (2021). How do red blood cells die? *Front. Physiol.* 12, 655393. doi:10.3389/fphys.2021.655393
- Toki, S., Donati, R. J., and Rasenick, M. M. (1999). Treatment of C6 glioma cells and rats with antidepressant drugs increases the detergent extraction of G(s) from plasma membrane. *J. Neurochem.* 73, 1114–1120. doi:10.1046/j.1471-4159.1999.0731114.x
- Toyota, T., Hattori, E., Meerabux, J., Yamada, K., Saito, K., Shibuya, H., et al. (2002). Molecular analysis, mutation screening, and association study of adenylyl cyclase type 9 gene (ADCY9) in mood disorders. *Am. J. Med. Genet.* 114, 84–92. doi:10.1002/ajmg.10117
- Verhagen, M., Meij, A. van der, Deurzen, P. A. M. van, Janzing, J. G. E., Arias-Vásquez, A., Buitelaar, J. K., et al. (2010). Meta-analysis of the BDNF Val66Met polymorphism in major depressive disorder: Effects of gender and ethnicity. *Mol. Psychiatry* 15, 260–271. doi:10.1038/mp.2008.109
- Wachtel, H. (1983). Potential antidepressant activity of rolipram and other selective cyclic adenosine 3', 5'-monophosphate phosphodiesterase inhibitors. *Neuropharmacology* 22, 267–272. doi:10.1016/0028-3908(83)90239-3
- Wang, Y.-C., Pandey, G. N., Mendels, J., and Frazer, A. (1974). Platelet adenylyl cyclase responses in depression: Implications for a receptor defect. *Psychopharmacologia* 36, 291–300. doi:10.1007/bf00422561
- Wang, Z., Sindreu, C. B., Li, V., Nudelman, A., Chan, G. C.-K., and Storm, D. R. (2006). Pheromone detection in male mice depends on signaling through the type 3 adenylyl cyclase in the main olfactory epithelium. *J. Neurosci.* 26, 7375–7379. doi:10.1523/jneurosci.1967-06.2006
- Westera, L., Drylewicz, J., Braber, I. den, Mugwagwa, T., Maas, I. van der, Kwast, L., et al. (2013). Closing the gap between T-cell life span estimates from stable isotope-labeling studies in mice and humans. *Blood* 122, 2205–2212. doi:10.1182/blood-2013-03-488411
- Wong, S. T., Trinh, K., Hacker, B., Chan, G. C. K., Lowe, G., Gaggari, A., et al. (2000). Disruption of the type III adenylyl cyclase gene leads to peripheral and behavioral anosmia in transgenic mice. *Neuron* 27, 487–497. doi:10.1016/s0896-6273(00)00060-x
- Wray, N. H., Schappi, J. M., Singh, H., Senese, N. B., and Rasenick, M. M. (2018). NMDAR-independent, cAMP-dependent antidepressant actions of ketamine. *Mol. Psychiatry* 24, 1833–1843. doi:10.1038/s41380-018-0083-8
- Yan, L., Vatner, D. E., O'Connor, J. P., Ivessa, A., Ge, H., Chen, W., et al. (2007). Type 5 adenylyl cyclase disruption increases longevity and protects against stress. *Cell* 130, 247–258. doi:10.1016/j.cell.2007.05.038
- Yang, X.-Y., Ma, Z.-L., Storm, D. R., Cao, H., and Zhang, Y.-Q. (2021). Selective ablation of type 3 adenylyl cyclase in somatostatin-positive interneurons produces anxiety- and depression-like behaviors in mice. *World J. Psychiatry* 11, 35–49. doi:10.5498/wjpv.v11.i2.35
- Yavi, M., Lee, H., Henter, I. D., Park, L. T., and Zarate, C. A. (2022). Ketamine treatment for depression: A review. *Discov. Ment. Health* 2, 9. doi:10.1007/s44192-022-00012-3
- Ye, Y., Conti, M., Houslay, M. D., Farooqui, S. M., Chen, M., and O'Donnell, J. M. (2002). Noradrenergic activity differentially regulates the expression of rolipram-sensitive, high-affinity cyclic AMP phosphodiesterase (PDE4) in rat brain. *J. Neurochem.* 69, 2397–2404. doi:10.1046/j.1471-4159.1997.69062397.x
- Yu, J.-Z., and Rasenick, M. M. (2002). Real-time visualization of a fluorescent G(alpha)(s): Dissociation of the activated G protein from plasma membrane. *Mol. Pharmacol.* 61, 352–359. doi:10.1124/mol.61.2.352
- Yu, J.-Z., Wang, J., Sheridan, S. D., Perlis, R. H., and Rasenick, M. M. (2021). N-3 polyunsaturated fatty acids promote astrocyte differentiation and neurotrophin production independent of cAMP in patient-derived neural stem cells. *Mol. Psychiatry* 26, 4605–4615. doi:10.1038/s41380-020-0786-5
- Zanos, P., Moaddel, R., Morris, P. J., Georgiou, P., Fischell, J., Elmer, G. I., et al. (2016). NMDAR inhibition-independent antidepressant actions of ketamine metabolites. *Nature* 533, 481–486. doi:10.1038/nature17998
- Zeller, E., Stief, H., Pflug, B., and Sastre-y-Hernández, M. (1984). Results of a phase II study of the antidepressant effect of rolipram. *Pharmacopsychiatry* 17, 188–190. doi:10.1055/s-2007-1017435
- Zhang, H.-T., Huang, Y., Jin, S.-L. C., Frith, S. A., Suvana, N., Conti, M., et al. (2002). Antidepressant-like profile and reduced sensitivity to rolipram in mice deficient in the PDE4D phosphodiesterase enzyme. *Neuropsychopharmacology* 27, 587–595. doi:10.1016/s0893-133x(02)00344-5
- Zhang, J., Levy, D., Oydanich, M., Bravo, C., Yoon, S., Vatner, D. E., et al. (2018). A novel adenylyl cyclase type 5 inhibitor that reduces myocardial infarct size even when administered after coronary artery reperfusion. *J. Mol. Cell. Cardiol.* 121, 13–15. doi:10.1016/j.yjmcc.2018.05.014
- Zhang, L., and Rasenick, M. M. (2010). Chronic treatment with escitalopram but not R-citalopram translocates galpha(s) from lipid raft domains and potentiates adenylyl cyclase: A 5-hydroxytryptamine transporter-independent action of this antidepressant compound. *J. Pharmacol. Exp. Ther.* 332, 977–984. doi:10.1124/jpet.109.162644
- Zhao, Y., Zhang, H.-Ti., and O'Donnell, J. M. (2003). Antidepressant-induced increase in high-affinity rolipram binding sites in rat brain: Dependence on noradrenergic and serotonergic function. *J. Pharmacol. Exp. Ther.* 307, 246–253. doi:10.1124/jpet.103.053215

Frontiers in Pharmacology

Explores the interactions between chemicals and living beings

The most cited journal in its field, which advances access to pharmacological discoveries to prevent and treat human disease.

Discover the latest Research Topics

[See more →](#)

Frontiers

Avenue du Tribunal-Fédéral 34
1005 Lausanne, Switzerland
frontiersin.org

Contact us

+41 (0)21 510 17 00
frontiersin.org/about/contact



Frontiers in Pharmacology

